

**Interferon-induced alteration of the cellular splicing machinery  
and its influence on HIV-1 replication**

**Durch Interferone hervorgerufene Änderung des zellulären  
Spleißapparates und der Einfluss auf die Replikation von HIV-1**

Inaugural-Dissertation  
zur  
Erlangung des Doktorgrades  
Dr. rer. nat.

der Fakultät für Biologie  
an der  
Universität Duisburg-Essen

vorgelegt von

**Helene Sertznig**

aus Grevenmacher

November 2021

# DuEPublico

Duisburg-Essen Publications online

UNIVERSITÄT  
DUISBURG  
ESSEN

*Offen im Denken*

ub | universitäts  
bibliothek

Diese Dissertation wird via DuEPublico, dem Dokumenten- und Publikationsserver der Universität Duisburg-Essen, zur Verfügung gestellt und liegt auch als Print-Version vor.

**DOI:** 10.17185/duepublico/76157

**URN:** urn:nbn:de:hbz:465-20221017-110246-9

Alle Rechte vorbehalten.

Die der vorliegenden Arbeit zugrundeliegenden Experimente wurden am Institut für Virologie der Universität Duisburg-Essen durchgeführt.

1. Gutachter: Prof. Dr. Ulf Dittmer

2. Gutachter: Prof. Dr. Karl Sebastian Lang

Vorsitzender des Prüfungsausschusses: Prof. Dr. Dominik Boos

Tag der mündlichen Prüfung: 13.04.2022

---

## Table of Contents

<b>1.</b>	<b>Introduction .....</b>	<b>1</b>
<b>1.1.</b>	<b>The Human Immunodeficiency Virus Type 1 .....</b>	<b>1</b>
1.1.1.	Classification, Morphology and Genomic structure .....	1
1.1.2.	HIV-1 replication cycle .....	3
1.1.3.	HIV-1 alternative splicing .....	6
1.1.4.	Splicing regulatory elements.....	10
1.1.5.	Host Dependency Factors.....	11
1.1.5.1.	Serine/arginine-rich splicing factors.....	12
1.1.5.1.1.	Serine/arginine-rich splicing factor 1.....	13
1.1.5.2.	Heterogeneous nuclear ribonucleoproteins.....	15
1.1.5.2.1.	Heterogeneous nuclear ribonucleoprotein A0.....	17
1.1.6.	Host Restriction Factors.....	18
<b>1.2.</b>	<b>Innate immune sensing of HIV-1 .....</b>	<b>18</b>
1.2.1.	Interferons.....	19
1.2.2.	Type I interferons .....	20
1.2.2.1.	Type I IFN induced signaling pathways.....	21
1.2.3.	Type II interferons .....	23
1.2.3.1.	Type II IFN induced signaling pathways.....	23
1.2.4.	Restriction of HIV-1 infection .....	24
1.2.4.1.	IFN-stimulated genes .....	25
1.2.4.2.	IFN-repressed genes.....	28
<b>1.3.</b>	<b>Aim of this thesis .....</b>	<b>28</b>
<b>2.</b>	<b>Material .....</b>	<b>30</b>
2.1.	Chemicals and reagents .....	30
2.2.	Kits .....	33
2.3.	Cell lines .....	33
2.4.	Oligo nucleotides.....	34
2.5.	Plasmids .....	35
2.6.	Antibodies.....	37

---

2.7.	Enzymes .....	37
2.8.	Buffers and solutions.....	38
2.9.	Bacteria Cells .....	39
2.10.	Viruses.....	40
2.11.	Material.....	40
2.12.	Instruments.....	41
2.13.	Software.....	42
<b>3.</b>	<b>Methods .....</b>	<b>43</b>
<b>3.1.</b>	<b>Cell culture .....</b>	<b>43</b>
3.1.1.	Maintenance of human cell lines .....	43
3.1.2.	Differentiation of THP-1 monocytes.....	43
3.1.3.	Stimulation of cells with interferon (IFN).....	44
3.1.4.	Infection of cells.....	44
3.1.5.	Transient Transfection .....	44
3.1.6.	siRNA gene silencing .....	45
3.1.7.	Isolation of peripheral blood mononuclear cells (PBMCs) .....	45
<b>3.2.</b>	<b>Methods in molecular biology .....</b>	<b>46</b>
3.2.1.	RNA isolation.....	46
3.2.2.	cDNA synthesis from total cellular and viral RNA .....	46
3.2.3.	Semi-quantitative PCR analysis (RT-PCR) .....	47
3.2.4.	Separation of DNA fragments by polyacrylamide (PAA) gel electrophoresis	48
3.2.5.	Quantitative real-time PCR analysis (RT-qPCR) .....	48
3.2.6.	One Step quantitative real-time PCR analysis (One-Step RT-qPCR).....	49
3.2.7.	Western Blot analysis.....	50
3.2.8.	Cloning.....	51
3.2.8.1.	Polymerase Chain Reaction (PCR) .....	51
3.2.8.2.	DNA purification.....	52
3.2.8.3.	Ligation .....	52
3.2.8.3.1.	NEB PCR Cloning Kit.....	52
3.2.8.3.2.	T4 DNA Ligase .....	52
3.2.8.4.	Restriction enzyme digest.....	53

---

3.2.8.5.	Separation of DNA fragments by agarose gel electrophoresis.....	53
3.2.8.6.	DNA extraction from agarose gels.....	53
3.2.8.7.	Sanger sequencing .....	53
3.2.8.8.	Construction of an hnRNP A0 expression plasmid .....	54
3.2.9.	4sU-tagging .....	56
<b>3.3.</b>	<b>Methods in microbiology.....</b>	<b>57</b>
3.3.1.	Transformation of bacteria .....	57
3.3.2.	Plasmid DNA isolation from bacteria for restriction analysis .....	57
3.3.3.	Plasmid DNA isolation from bacteria for preparation .....	58
3.3.4.	Preparation of glycerol stocks.....	58
3.3.5.	Production of LB agar plates.....	59
<b>3.4.</b>	<b>Methods in virology .....</b>	<b>59</b>
3.4.1.	Preparation of virus stocks.....	59
3.4.2.	Viral titer determination via TCID <sub>50</sub> .....	59
3.4.3.	Calculation of multiplicity of infection (MOI) for infection experiments .....	60
3.4.4.	Determination of viral infectivity via TZM-bl assay.....	60
3.4.5.	HIV-1 p24-capsid Enzyme Linked Immunosorbent Assay (ELISA).....	61
3.4.6.	Viral RNA isolation .....	61
<b>4.</b>	<b>Results.....</b>	<b>63</b>
<b>4.1.</b>	<b>SRSF transcript levels are lower upon HIV-1 infection.....</b>	<b>64</b>
4.1.1.	<i>SRSF1</i> expression is lower in HIV-1 infected individuals .....	66
4.1.2.	The degree of <i>SRSF1</i> repression is IFN $\alpha$ subtype dependent.....	69
4.1.3.	<i>SRSF1</i> is differentially regulated in HIV-1 target cells upon IFN-stimulation .....	71
4.1.4.	Alteration in <i>SRSF1</i> gene expression occurs on transcriptional level.....	76
4.1.5.	Knockdown of <i>SRSF1</i> levels affects HIV-1 post integration steps .....	78
4.1.6.	Overexpression of <i>SRSF1</i> levels affects HIV-1 post integration steps .....	84
4.1.7.	HIV-1 affects the IFN-mediated regulation of <i>SRSF1</i> .....	89
<b>4.2.</b>	<b><i>hnRNP</i> transcript levels are lower upon HIV-1 infection .....</b>	<b>92</b>
4.2.1.	Specific <i>hnRNPs</i> are repressed upon IFN-stimulation in macrophages .....	94
4.2.2.	<i>hnRNP A0</i> expression is lower in HIV-1 infected individuals.....	95

---

4.2.3.	<i>hnRNP A0</i> is differentially regulated in HIV-1 target cells upon IFN-stimulation .....	98
4.2.4.	Alteration in <i>hnRNP A0</i> gene expression occurs on transcriptional level ...	102
4.2.5.	Knockdown of <i>hnRNP A0</i> levels affects HIV-1 post integration steps.....	103
4.2.6.	Overexpression of <i>hnRNP A0</i> levels affects HIV-1 post integration steps..	109
4.2.7.	HIV-1 affects the IFN-mediated regulation of <i>hnRNP A0</i> .....	114
<b>5.</b>	<b>Discussion.....</b>	<b>117</b>
5.1.	<i>SRSF1</i> and <i>hnRNP A0</i> mRNA expression is predominantly type I IFN-regulated.....	117
5.2.	<i>SRSF1</i> and <i>hnRNP A0</i> mRNA expression is regulated through an autoregulatory feedback loop.....	124
5.3.	Altered expression levels of <i>SRSF1</i> decisively affect HIV-1 post integration steps .....	126
5.4.	Altered expression levels of <i>hnRNP A0</i> decisively affect HIV-1 post integration steps .....	134
5.5.	Balanced levels of <i>SRSF1</i> and <i>hnRNP A0</i> are required for efficient HIV-1 LTR transcription, alternative splicing and virus production .....	139
5.6.	<i>SRSF1</i> and <i>hnRNP A0</i> are potential targets for antiviral therapy.....	142
<b>6.</b>	<b>Conclusion.....</b>	<b>144</b>
<b>7.</b>	<b>Summary.....</b>	<b>145</b>
7.1.	Summary .....	145
7.2.	Zusammenfassung.....	146
<b>8.</b>	<b>References.....</b>	<b>148</b>
<b>9.</b>	<b>Appendix.....</b>	<b>177</b>
9.1.	List of abbreviations .....	177
9.2.	List of figures .....	185
9.3.	List of tables.....	187

---

9.4.	Supplementary Figures .....	188
9.5.	Acknowledgements .....	190
9.6.	Curriculum Vitae .....	191
9.7.	Declarations.....	193



---

## 1. Introduction

### 1.1. The Human Immunodeficiency Virus Type 1

The history of the human immunodeficiency virus type 1 started in the early 1980's, as a novel retrovirus was identified as the causative agent of the acquired immunodeficiency syndrome (AIDS) (32; 156). In 2020, 37.7 million people worldwide were living with an HIV-1 infection, of which 1.5 million people became newly infected. 680,000 deaths were associated with AIDS-related illnesses in 2020 (462). Extensive research since the 1980's has led to the development of antiretroviral therapy (ART), which involves taking a combination of different antiretroviral drugs in order to slow down the disease progression (33). However, only 27.5 million people (72.9 %) were accessing ART treatment by the end of 2020 (462). The introduction of ART had widespread implementations for the treatment of HIV-1 infected individuals, drastically increasing their life expectancy and avoiding millions of AIDS-related deaths (79). Despite ART changing AIDS from a fatal to a chronic disease by depleting HIV-1 below detectable levels, the virus cannot be completely eradicated, leaving HIV-1 infected individuals in need of a lifelong treatment (79; 104). Alongside the side effects caused by ART-treatment, 20 to 30 % of the patients are still prone to develop other diseases like the HIV-associated neurocognitive disorder (81; 248; 472). Furthermore, the high genetic variability of the virus, which originates from a high error rate of the viral reverse transcriptase, leads to the emergence of drug-resistant strains (3; 158; 295; 389). Thus, further understanding of the regulation of the viral life cycle and the molecular mechanisms involved is crucial for the development of novel therapeutic strategies.

#### 1.1.1. Classification, Morphology and Genomic structure

HIV-1 belongs to the family of *Retroviridae* (genus: lentivirus) and is grouped into the Baltimore classification group VI, which includes positive-sensed and single-stranded (ss) RNA viruses replicating via reverse transcription (28). The virus contains two copies of the RNA genome, which are associated with nucleocapsid proteins (p7) and enclosed by a conical capsid, consisting of capsid proteins (p24). The linker protein (p6) links the capsid to the envelope, which consists of a host cell derived lipid bilayer. The transmembrane glycoprotein (gp41) and surface envelope protein (gp120) build trimers on the surface of the envelope, while the matrix protein (p17) covers the inner layer. Furthermore, the viral enzymes reverse transcriptase (RT), integrase (IN) and protease

(PR), as well as the viral accessory proteins Vif (viral infectivity factor), Vpr (viral protein R) and Nef (negative effector) are located within the capsid (145; 146; 161; 489).

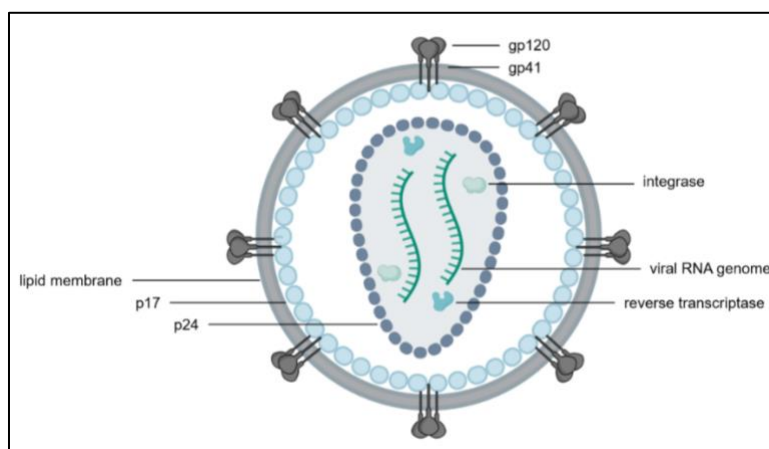


**Figure 1-1: Structure of a mature HIV-1 particle.** HIV-1 virions are enveloped by a host cell derived lipid bilayer. The trimers built by the transmembrane (gp41) and surface envelope glycoprotein (gp120) are anchored to the envelope. The inner layer of the envelope is covered by matrix proteins (p17). The conical capsid formed by the capsid protein (p24) contains two copies of the viral (+)-sensed ssRNA genome as well as the viral enzymes reverse transcriptase and integrase (145; 146; 161; 489). Created with BioRender.com.

The linear HIV-1 genome is 9.7 kb in size and contains densely packed open reading frames (ORF) for at least 18 proteins and polyprotein-isoforms (480). Furthermore, the genome contains a 7-methylguanylate cap structure at the 5'-end and a poly-(A)-tail at the 3'-end. At both ends of the genome, long terminal repeats (LTR) are localized featuring U3 (Unique 3), R (Repeated) and U5 (Unique 5) regions. Further elements on the HIV-1 genome include the primer binding site (PBS), where binding of a tRNA initiates the process of reverse transcription, polypurine tracts (cPPT, PPT), which are involved in cDNA synthesis and a packaging signal ( $\psi$ ), which is involved in incorporating the viral RNA into the capsid. The Rev-responsive element (RRE) is bound by the viral protein Rev and involved in the nuclear export of unspliced and intron-containing mRNAs (136; 146). Binding of Tat to the trans-activation response element (TAR) recruits pTEF-b (transcription elongation factor b), which hyperphosphorylates the C-terminal domain of RNA polymerase II (RNAPII) and increases transcriptional elongation (347). In order to extract all the genetic information from the partially overlapping sequences of several ORFs, the HIV-1 primary transcript undergoes excessive alternative splicing (375; 410; 435) (Chapter 1.1.3).

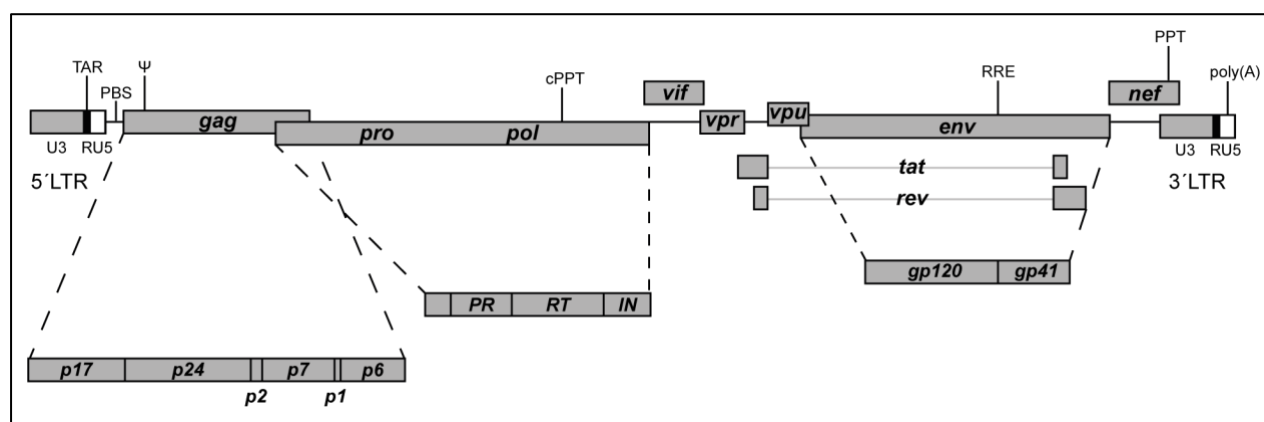


**Figure 1-2: Illustration of the HIV-1 genomic structure.** The HIV-1 open reading frames (ORFs) *gag-pol*, *vif*, *vpr*, *vpu*, *env*, *tat*, *rev* and *nef* are indicated by grey boxes. The long terminal repeats flanking the HIV-1 genome at the 5'- and 3'-end are depicted in a three-color-code: U3 (grey), R (black) and U5 (white). The position on the HIV-1 genome of TAR (trans-activation response element), PBS (primer binding site),  $\psi$  (RNA packaging signal), cPPT (PPT located at the center of the HIV-1 genome), RRE (Rev-responsive element), PPT (polypurine tract) and poly(A) signal are depicted. The Gag-Pol precursor polyprotein is cleaved by the usage of multiple cleavage sites to release the matrix protein (p17), the capsid protein (p24), the spacer peptide 2 (p2), the nucleocapsid protein (p7), the spacer peptide 1 (p1) and p6-gag. Furthermore, the viral enzymes protease (PR), reverse transcriptase (RT) and integrase (IN) are also cleaved from the Gag-Pol polyprotein by ribosomal frame-shifting. The Env precursor polyprotein (gp160) is cleaved into the surface glycoprotein (gp120) and the transmembrane glycoprotein (gp41). The regulatory HIV-1 proteins Tat and Rev, as well as the accessory proteins Vif, Vpr, Vpu and Nef are translated from multiply spliced mRNA isoforms (146). This illustration was modified according to (485).

### 1.1.2. HIV-1 replication cycle

HIV-1 specifically targets cells expressing the cell surface receptor CD4, which is expressed on the surface of mononuclear cells like CD4<sup>+</sup> T-cells, macrophages or dendritic cells (DCs). For viral entry however, which happens through glycoprotein-mediated membrane fusion, a second chemokine co-receptor (CCR5 or CXCR4) is required in addition to the CD4 receptor (72; 80; 146). The tropism of a specific HIV-1 strain is determined via the variable loop 3 (V3 loop) of gp120. Viral strains binding to the CCR5 co-receptor are referred to as R5-tropic, while variants binding to the CXCR4 co-receptor are referred to as X4-tropic. Strains with the ability to bind to either one of the co-receptors are termed dual-tropic (80; 146; 370).

During infection, the viral surface protein gp120 interacts with the CD4 receptor, resulting in a conformational change of the glycoprotein, which exposes binding sites for the interaction with the respective co-receptor. Binding of the V3 loop of gp120 to the co-receptor then results in gp41-mediated membrane fusion of viral and host membrane via

Clathrin-dependent endocytosis (80; 125; 146; 332; 488). The process of uncoating after the release of the conical nucleocapsid into the host cell cytoplasm is still under debate (451). Early models suggest, that cytoplasmic uncoating occurs rapidly after viral entry (133; 146; 309; 329). Other models propose a disassembly at the nuclear pore after docking to the nuclear pore complex (18; 144; 195; 380). However, despite the capsid being approximately 60 nm wide (53; 319) and the nuclear pore complexes being roughly 40 nm in diameter (473), increasing evidence suggests that the capsid enters the nucleus before uncoating (58; 108; 520). The viral enzyme RT transcribes the ssRNA genome into a double stranded (ds) DNA molecule. A packaged host cell tRNA binds to the PBS to initiate minus-strand DNA synthesis. The RT is a bifunctional enzyme that, in addition to the synthesis of DNA from RNA templates, has an RNase H function, enabling the cleavage of RNA/DNA complexes. This function of the RT is particularly important, as the process of reverse transcription relies on two inter- and intramolecular jumps of DNA intermediates (125; 146; 201). Also, the RT does not feature a proof reading capacity, thus resulting in a high error rate during reverse transcription ( $1.2 \times 10^{-5}$  to  $6.7 \times 10^{-4}$  mutations per base per replication cycle). This high variability leads to the development of drug-resistant mutations and so-called quasispecies (158; 313). Since it is not yet fully elucidated, when and where the viral capsid is uncoated, the exact location and time of reverse transcription are still unknown. Early models, suggesting uncoating of the viral capsid in the cytoplasm, propose the reverse transcription in the cytoplasm. After synthesis of the positive-strand DNA, the dsDNA molecule is associated with viral and cellular proteins forming the pre-integration complex (PIC), which is transported into the nucleus, where the imported DNA is integrated as a provirus into the host cell genome by the viral enzyme integrase (56; 146; 372). More recent models, however, show that the integration of the capsid into the nucleus precedes the completion of reverse transcription (108). The viral DNA is then transcribed by the RNA polymerase II (RNAPII), and the resulting pre-mRNAs are spliced, capped and polyadenylated. Initial transcription efficiency is low and requires transactivation by the trans-activator of transcription (Tat) protein (146; 244; 347). The recruitment of pTEF-b by Tat upon binding to the TAR region within the HIV-1 LTR promoter results in the hyperphosphorylation of the C-terminal domain of RNAPII and in turn significantly enhances the transcription elongation efficiency (281; 347; 408). The primary full-length pre-mRNA undergoes extensive alternative splicing, resulting in a timely equilibrium of spliced and unspliced mRNAs, necessary for

efficient viral replication (86; 254; 375; 435). The viral mRNAs can be classified into three major classes, the unspliced 9 kb mRNAs, the intron-containing 4 kb mRNAs and the multiply spliced 2 kb mRNAs and will be described in more detail in (Chapter 1.1.3.) (375). The unspliced 9 kb mRNA serves as genomic RNA for progeny virions and gets encapsidated by recognition of the RNA packaging signal ( $\psi$ ) (146; 147). New virions are assembled at the membrane of the host cell, where they exit the cell by budding of the host's plasma membrane. Maturation occurs after the release of the virus, through an auto-cleavage cascade of the Gag-Pol precursor protein and through a morphologic change within the immature viral particle, where the capsid proteins form the conical shape of the viral capsid (125; 146; 147).

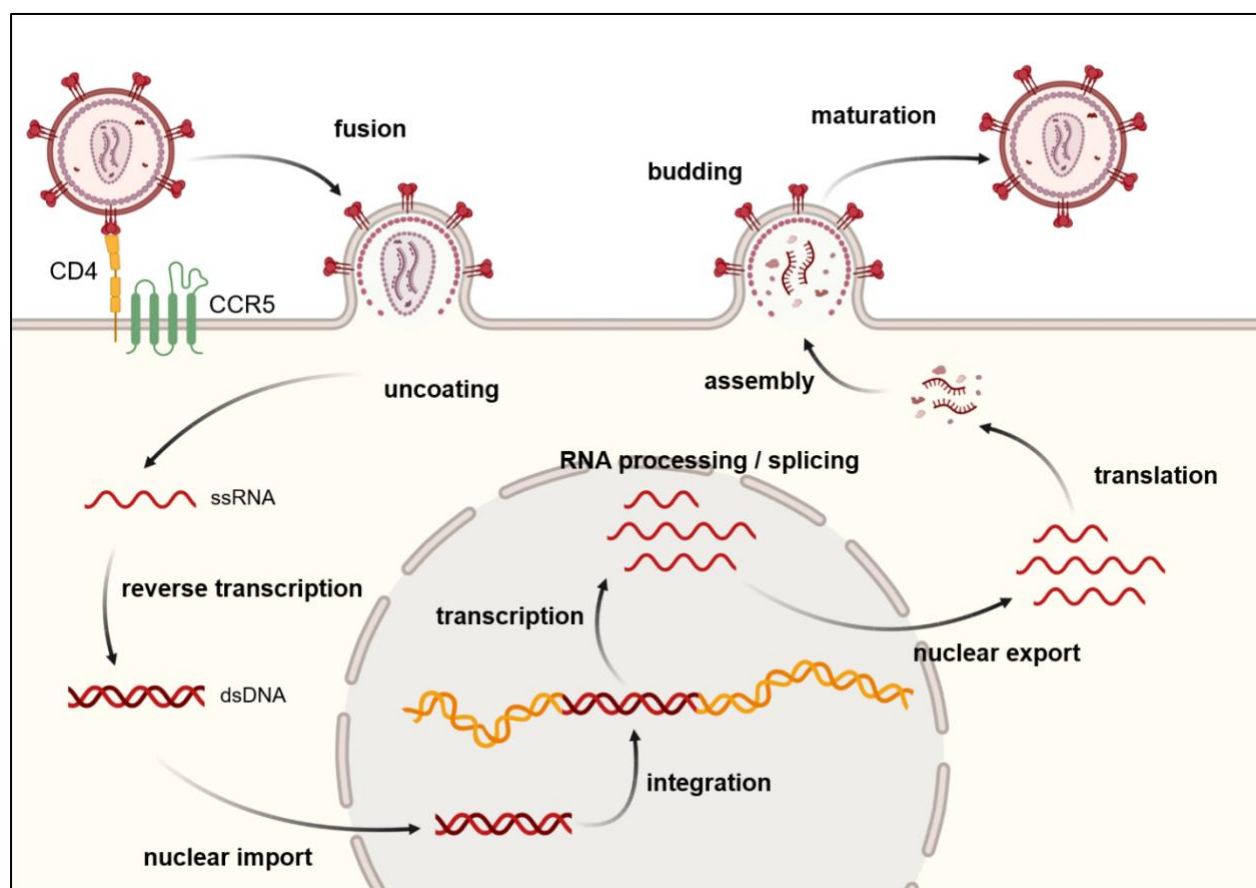


**Figure 1-3: Schematic and simplified drawing of the HIV-1 replication cycle.** After binding of the viral surface glycoprotein gp120 to the cellular CD4 receptor, a conformational change of the glycoprotein results in the binding of transmembrane glycoprotein gp41 to the chemokine receptor CCR5 (or CXCR4, not shown). Subsequently, HIV-1 enters the host cell through glycoprotein-mediated membrane fusion (72; 80; 125; 146; 332; 488). The conical nucleocapsid is released and uncoated into the cytoplasm (125; 146), where the genomic ssRNA gets reverse transcribed into a dsDNA molecule and imported into the nucleus (125; 146; 201). The viral DNA is randomly

---

integrated into the host cell genome, followed by transcription of the RNA polymerase II (RNAPII) (56; 372). Excessive splicing of the primary full-length pre-mRNA results in the formation of spliced and intron-containing mRNAs, which are then translated into all viral proteins (86; 254; 375; 435). The virus is assembled at the host cell plasma membrane and exits the cell by budding, followed by maturation of the virus (125; 146; 147). Figure adapted from “HIV replication cycle” by BioRender.com (2021). Retrieved from <https://app.biorender.com/biorender-templates>.

### 1.1.3. HIV-1 alternative splicing

The protein coding sequences of eukaryotic genes are often interspersed with introns (342; 475; 490; 491). These non-coding segments are removed from the messenger RNA precursor (pre-mRNA) to generate a mature mRNA. This essential process of intron excision and exon ligation is termed pre-mRNA splicing. While for constitutively spliced genes, the intron sequence is removed from each pre-mRNA, alternatively spliced genes can lead to the formation of different transcripts (reviewed in (475; 490; 491)). 95 % of the approximately 20,000 protein-coding human genes are alternatively spliced, thereby vastly expanding the number of proteins expressed from a limited number of genes (198; 342; 350; 461; 476).

Many pathogenic viruses, such as HIV-1, use alternative splicing to extract the full genetic content of their short and compact genome (254; 257; 375). The full-length HIV-1 transcript harbors eight ORFs including *gag-pol*, *env*, *vif*, *vpr*, *vpu*, *tat*, *rev* and *nef* (146; 244). Since eukaryotic translation is initiated via binding of the 43S ribosomal subunit to the 5'-cap followed by ribosomal scanning for an efficient AUG codon (220), this would result in the sole translation of the *gag-pol* ORF. Thus, HIV-1 exploits the cellular splicing apparatus to remove translational inhibitory upstream AUGs and transfer downstream ORFs into proximity of the 5'-cap in order to increase their translational efficiency (66; 375; 409; 435). The sole exception is the bi-cistronic *vpu/env* mRNA, which permits efficient translation at the downstream AUG due to discontinuous ribosome scanning (15; 269). More than 50 alternatively spliced mRNA isoforms emerge from the variable usage of four different 5'-splice donor sites (SD1, SD2, SD3 and SD4) and eight different 3'-splice acceptor sites (SA1, SA2, SA3, SA4cab, SA5 and SA7) (375; 410; 435). According to their size, the resulting transcripts can be classified into the unspliced 9 kb mRNAs, the intron-containing 4 kb mRNAs and the multiply spliced 2 kb mRNAs (66; 375). Furthermore, an additional minor transcript class of 1 kb mRNAs was identified by next generation sequencing (NGS) (345).

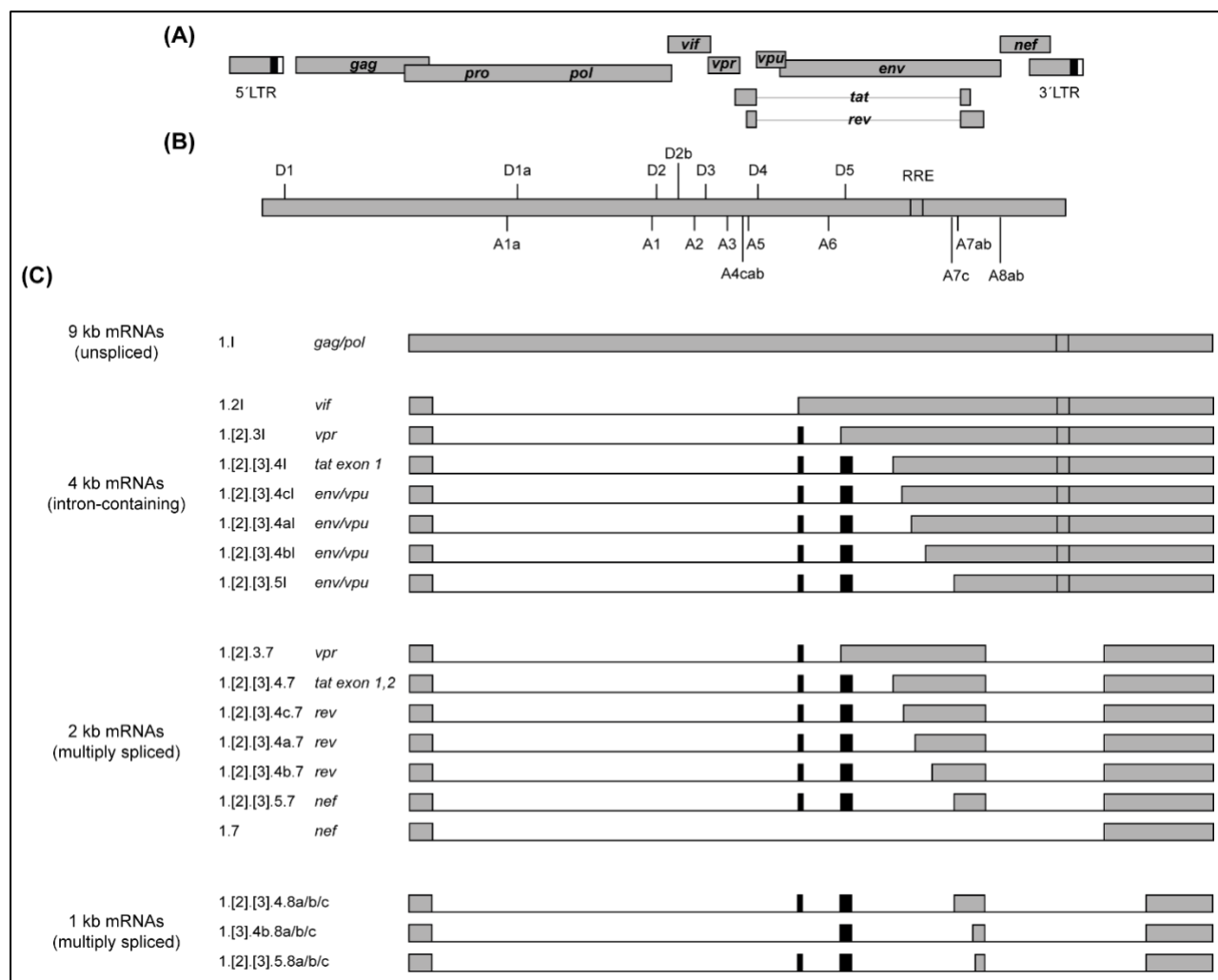


**Figure 1-4: Schematic representation of the HIV-1 mRNA classes. (A)** The HIV-1 ORFs *gag-pol*, *vif*, *vpr*, *vpu*, *env*, *tat*, *rev* and *nef* are indicated by grey boxes. LTRs are depicted at both ends of the viral genome in a three-color-code: U3 (grey), R (black) and U5 (white) (146). **(B)** Positions of the 5'- and 3'-splice sites on the viral pre-mRNA are shown. The RRE is involved in the nuclear export of intron-containing mRNAs (9 kb and 4 kb class). **(C)** The full-length 9 kb viral pre-mRNA is expressed from the 5'-LTR promoter and serves either as genomic RNA or codes for the Gag-Pol polyprotein precursor. The non-coding leader exon 1 is present in all viral transcript isoforms. Non-coding leader exons 2 and 3 (depicted as black boxes) are alternatively spliced and give rise to a large number of mRNAs. The nomenclature of each transcript indicates the exons which are included in the respective mRNA. Transcripts containing at least one intron are marked with an "l". The transcript isoforms that show the non-coding leader exons 2 and 3 in brackets exist in both variants, with and without exon 2 and 3. The 2 kb mRNA class is defined by additional splicing between splice donor (SD) 4 and splice acceptor (SA) 7. The 1 kb mRNA class is formed through usage of the alternative SA8. This illustration was modified according to (435) and supplemented with information from (345).

The timely expression of the viral mRNA classes is tightly regulated. In the early phase of viral gene expression, mRNA transcripts of the multiply spliced 2 kb class are generated,

coding for the regulatory proteins Tat and Rev and the accessory proteins Nef and Vpr (375). Both accessory proteins Nef and Vpr prevent the infected cell from immune cell recognition (258; 275; 496). Tat engages in the activation of the LTR promoter (97; 470), whereas Rev binds to the Rev-responsive element (RRE), localized in the env-coding sequence, to allow the nuclear export of late phase viral mRNAs via CRM1 (Chromosomal Maintenance 1) receptor-mediated export into the cytoplasm (89; 308; 369; 438). The accessory and structural proteins Vif, Vpu and Env derive from intron-containing 4 kb mRNAs and are expressed during the late phase of viral gene expression (435). The full-length primary transcript is exported into the cytoplasm and used either for the translation of Gag-Pol or as genomic RNA for progeny virions (146).

Exon definition requires functional cross-exon interactions between the 5'-SD and the upstream 3'-SA (100; 317). Binding of the U1 small nuclear ribonucleoprotein (snRNP) to the 5'-SD activates the upstream 3'-SA, which results in the binding of U2 snRNP to the BPS. Interactions between U1 and U2 snRNPs establish a molecular bridge across the exon, leading to the formation of the exon-definition complex. However, since splicing occurs across the intron, the exon-definition complex must undergo a transition into an intron-definition complex, where interactions between U1 and U2 snRNPs form an intron-spanning molecular bridge (100; 317; 385; 514). Thus, the decision which splice sites are paired together is determined by two consecutive processes, which are recognition and pairing.

5'-ss are defined via their consensus sequence consisting of the 11 nucleotides (nt) CAG/GURAGUNN (R = purine, N = purine or pyrimidine, / = exon/intron border) and are referred to as splice donors (SD). The highly conserved dinucleotide GU at the positions +1 and +2 at the 5'-end of an intron is indispensable for most splicing reactions. The intrinsic strength of a SD is defined via the complementarity between the 11 nt consensus sequence of the SD and the 5'-end of the spliceosomal U1 small nuclear RNA (snRNA), which is a component of the U1 snRNP (67; 100; 151; 236; 475). 3'-ss are defined via an intron-mapping consensus sequence CAG/G (/ = intron/exon border), a branch point sequence YNYURAY (Y = pyrimidine, N = purine or pyrimidine, R = purine) recognized by the U2 snRNA and a poly-pyrimidine tract (PPT) of 10-20 pyrimidine nucleotides (Y). Here, the conserved dinucleotide AG at the positions -2 and -1 at the 3'-end of an intron is essential for most splicing reactions (67; 317; 426; 475). While minor degeneracies were observed in the consensus sequence of the HIV-1 5'-SDs (67; 100; 415; 475), the



HIV-1 3'-SA consensus motifs were shown to be highly degenerated (94; 119; 435). Splice sites with highly degenerated consensus sequences are defined as intrinsically weak, thus enabling alternative splice site usage. The production of balanced ratios of HIV-1 mRNAs depends, in addition to the intrinsic strength of the 5'- and 3'-ss, on the presence of *cis*-acting splicing regulatory elements (SREs), which are bound by *trans*-acting factors and thus modulate splice site usage (410). Both together are referred to as the 'splicing code' (31; 478). Binding of splicing regulatory proteins to SREs can enhance or silence the usage of a specific splice site depending on their binding position (127) and will be discussed in more detail in (Chapter 1.1.4.). Hence, alternative splicing is the key for HIV-1 to maintain efficient viral replication by extracting the full genetic content of the relatively short and compact genome.

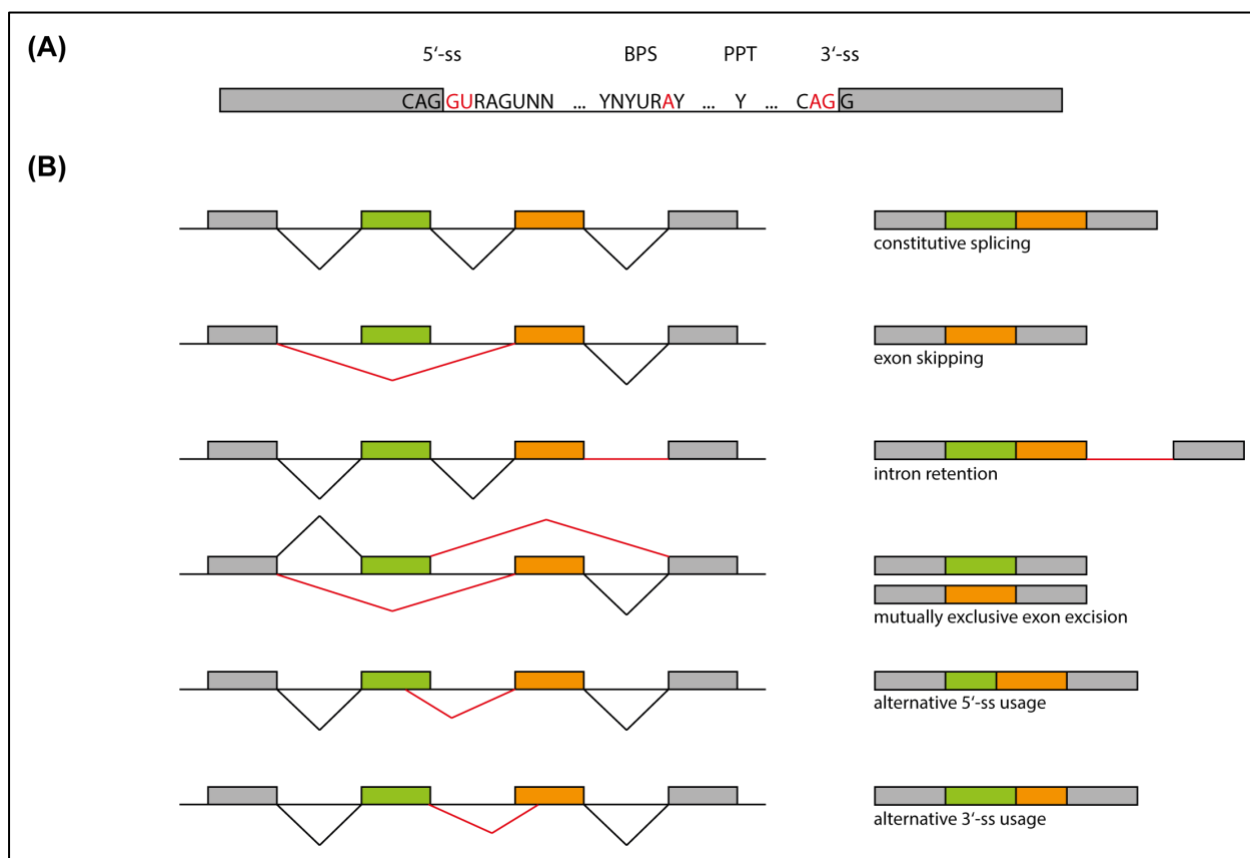


**Figure 1-5: Schematic representation of splice site recognition and alternatively spliced transcripts.** **(A)** Two exons, depicted by grey boxes, are interspersed by an intron. The consensus sequences for the 5'- and 3'-ss, the branch point sequence (BPS) and the polypyrimidine tract (PPT) are illustrated. (Y = pyrimidine, N = purine or pyrimidine, R = purine). Highly conserved nucleotides for the 5'- and 3'-ss and for the BPS are marked in red. **(B)** Different forms of alternative splicing are illustrated. In addition to constitutive splicing, exons can be excluded (exon skipping) or excised in a mutually exclusive manner (mutually exclusive exon excision). The

---

retention of introns into mRNAs (intron retention) represents a further element of alternative splicing, as well as the usage of alternative 5'- or 3'-splice sites. This illustration was modified according to (67).

#### **1.1.4. Splicing regulatory elements**

Splicing regulatory elements (SREs) are dispersed throughout the viral pre-mRNA and represent binding sites for *trans*-acting cellular RNA-binding proteins such as the serine/arginine-rich splicing factors (SRSF) and the heterogeneous nuclear ribonucleoproteins (hnRNP) (162; 312). SREs can be located in exonic or intronic sequences and categorized into four categories: exonic splicing enhancer (ESE), exonic splice silencer (ESS), intronic splicing enhancer (ISE) and intronic splice silencer (ISS). It has been shown, that the position of the SRE relative to the splice site determines whether they act as enhancer or silencer for the usage of a specific splice site (40; 44; 127; 153; 317; 318; 342). The consensus sequence of many splice sites is highly degenerated, thus SREs are particularly important to regulate alternative splice site usage (31; 171; 478).

HIV-1 alternative splicing crucially depends on the interplay between the intrinsic strength of the viral 5'- and 3'-ss and the interactions of cellular *trans*-acting splicing regulatory proteins with the SREs localized on the viral pre-mRNA. Mutations within the SREs on the HIV-1 pre-mRNA have been shown to affect virus replication (126; 131; 306; 483; 485; 486). While SRSF proteins enhance splicing from an exonic position and exhibit an inhibitory effect when binding an SRE from an intronic position, hnRNP proteins display opposing functionalities (127). Splice site activation occurs via increased recognition in the early steps of spliceosomal formation, while repression of a splice site results from the formation of non-productive complexes that inhibit spliceosome assembly (127). A large number of SREs on the HIV-1 genome have been identified so far (410). Computational algorithms such as the hexamer based algorithm termed HEXplorer (129) or ESEfinder (69) further allow the prediction of potential new SREs on the HIV-1 pre-mRNA.

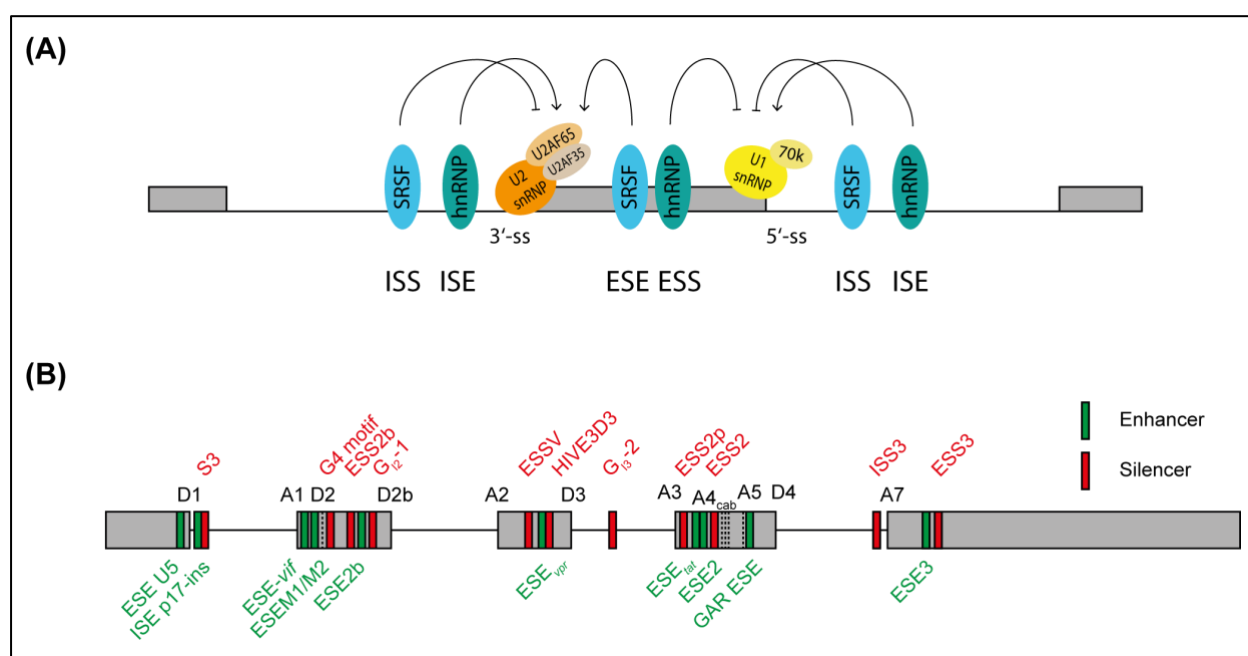


**Figure 1-6: Splicing regulatory elements (SREs) regulate cellular and viral splice site usage.** (A) Three exons (grey) are interspersed with two introns (black lines). SREs on the HIV-1 genome are bound by SRSF and hnRNP proteins, which enhances or silences the recognition of a specific splice site in a position-dependent manner. ESE: exonic splicing enhancer; ESS: exonic splicing silencer; ISE: intronic splicing enhancer; ISS: intronic splicing silencer. This illustration was modified according to (478). (B) Positions of SREs within the HIV-1 genome. Exons are depicted as grey boxes, while introns are shown as black lines. Splicing enhancers are colored in green, while splicing silencers are colored in red. This illustration was modified according to (410).

### 1.1.5. Host Dependency Factors

The short genome of HIV-1 only encodes for approximately 18 protein isoforms. The virus hijacks and exploits specific host cell factors for efficient viral replication, which are termed host dependency factors (HDFs). HDFs are, by definition, essential for HIV-1 replication, but not lethal to the host cell when their expression is silenced (51; 260; 337; 515; 518). Based on siRNA screens, which identified a large number of HDFs, HDFs are commonly associated with the spliceosome and splicing regulatory proteins (51; 260; 337; 515). Cellular splicing factors, such as hnRNP F, hnRNP H, hnRNP U, SRSF2 or SRSF6, were identified as HDFs (51; 260; 515; 518). The protein families of SRSF and hnRNP are the most prominent mediators of constitutive and alternative splice site regulation (59). Since HIV-1 crucially relies on alternative splicing and balanced binding of splicing regulatory proteins to the *cis*-regulatory elements on the pre-mRNA, cellular splicing factors are particularly important for efficient HIV-1 replication (244; 410; 435). Thus, the protein

families of SRSF (Chapter 1.1.5.1.) and hnRNP (Chapter 1.1.5.2.) will be discussed in more detail below.

### 1.1.5.1. Serine/arginine-rich splicing factors

SR proteins were discovered in the early 1990s and represent a large family of RNA-binding proteins (RBPs) (16; 49; 152; 177). The highly conserved SR proteins all feature two main structural characteristics, the protein-interacting RS-domain, which is rich in serine and arginine (SR) dipeptides, and the RNA recognition motif (RRM) (228; 414). While the RRM enables the interaction of SR proteins with pre-mRNAs, the RS-domain mediates protein-protein-interactions (228; 317; 414). The activity and subcellular localization of SRSF proteins is regulated via post-transcriptional modification, such as phosphorylation (240), methylation (296; 418; 508) and acetylation (78). The twelve human SR proteins were renamed to serine/arginine-rich splicing factors (SRSF) 1-12 by Manley and colleagues (311).

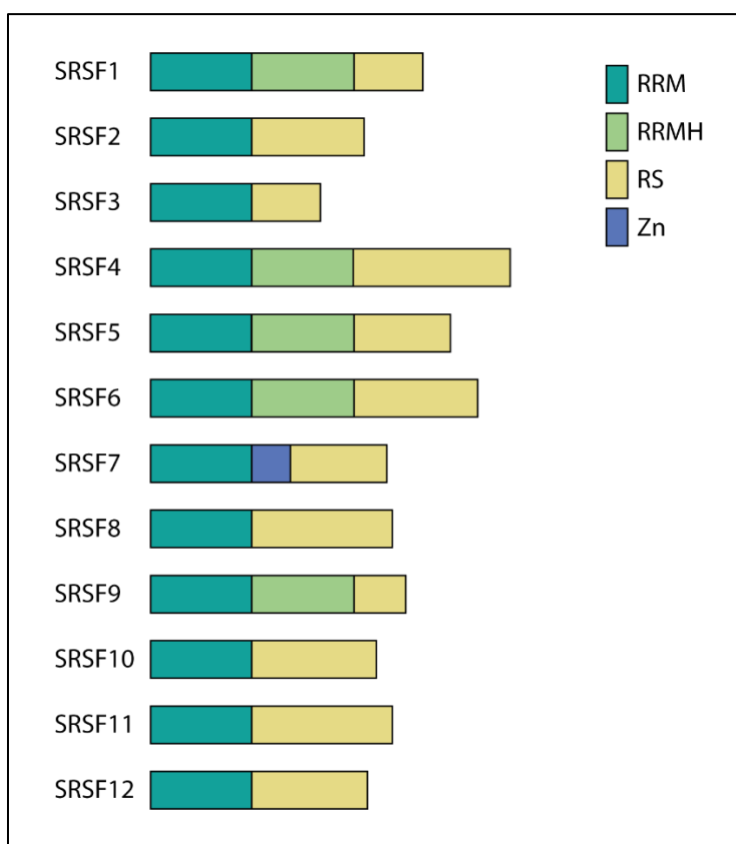


**Figure 1-7: Structural organization of the SRSF proteins.** The domain structures of the human SRSF proteins are depicted. RRM: RNA recognition motif; RS: arginine/serine-rich domain;

---

RRMH: RRM homology domain; Zn: Zinc knuckle. This illustration was modified according to (517).

Splicing of mRNA precursors (pre-mRNA) is an indispensable process in mammalian gene expression to excise introns. In addition to the spliceosome, which is involved in splice site selection, intron removal and exon ligation, splicing factors such as SRSF proteins are crucial for the regulation of splice site usage (16). Several SRSFs were also described to regulate alternative splice site usage in HIV-1 gene regulation. When binding to a SRE in an exonic position upstream of a 5'-ss, SRSF proteins have been shown to enhance recruitment of the U1 snRNP and thus splice site recognition (76; 127; 154; 294). SRSF1 and SRSF5 were described to enhance the recruitment of U1 snRNP to the 5'-SD4 through the binding of guanosine-adenosine-rich (GAR) ESE (63). Facilitated recognition of 5'-SD2 is promoted via the binding of SRSF1 to ESE M1/M2 (237), whereas binding of SRSF4 to ESE Vif resulted in increased inclusion of exon 2 (131). Furthermore, binding of SRSF proteins to a SRE surrounding a 3'-ss can facilitate the recognition of intrinsically weak splice sites through the stabilization of the spliceosome complex (44; 177; 450; 479; 500). Binding of SRSF1 to ESE3, which is located downstream of SA7, resulted in enhanced recruitment of the U2 snRNP associated U2 auxiliary factor 65 kDa subunit (U2AF65) to the 3'-SA (446), while binding of SRSF2 and SRSF6 to ESE<sub>lat</sub> and ESE2 respectively, promoted the activation of 3'-ss SA3 (126). However, when binding to a SRE in an intronic position, SRSF proteins can inhibit splice site usage due to steric hindrance or other mechanisms that have not been completely elucidated yet (194; 209; 241).

In addition to their role as regulators in alternative splicing, SRSF proteins are involved in many other steps of gene expression. SRSF1 and SRSF3 were shown to interact with interphase chromatin (299), SRSF2 has been shown to be involved in transcriptional regulation (229; 398), and SRSF3 and SRSF7 act as export adaptors in nuclear mRNA export (202; 203). SRSF proteins are further involved in the regulation of translation and mRNA decay (204; 373).

#### **1.1.5.1.1. Serine/arginine-rich splicing factor 1**

Serine/arginine-rich splicing factor 1 (SRSF1) was one of the founding members of the SRSF protein family. The protein formerly known as SRp30a or ASF/SF2 (311), was identified in the early 1990s to promote spliceosomal assembly and pre-mRNA splicing in

HeLa cells and to regulate alternative splicing of the SV40 pre-mRNA in HEK293 cells (160; 266). “SELEX” (selected evolution of ligands through exponential enrichment), which is based on the selection of high-affinity binding sites from randomized pools of RNA sequences, identified purine-rich sequences as the high affinity binding sites for SRSF1 (441; 458). In the transcriptome of HEK293T cells, 23,632 binding sites for SRSF1 were detected performing CLIP-seq (cross-linking immunoprecipitation and high-throughput sequencing). 83 % of the binding sites featured purine-rich sequences and were in close proximity to splice sites (397).

Alongside the crucial role in cellular pre-mRNA splicing (517), SRSF1 has been shown to regulate translation, either through the activation of translation initiation or the repression of its own mRNA (328; 396; 439). Furthermore, SRSF1 can induce the nonsense-mediated mRNA decay (NMD) (23; 512) or regulate genome stability (288). Lack of SRSF1 gene expression resulted in G2 cell cycle arrest and subsequent programmed cell death (289). SRSF1 has also been shown to play a role in tumorigenesis and was described as proto-oncogene, since the splicing factor regulates alternative splicing of many cancer-related genes (228; 230; 245).

Gene expression and RNA processing of HIV-1 are tightly regulated by SRSF1 (63; 237; 433; 446). SRSF1 has been shown to compete with Tat for a binding site within the hairpin structure of the TAR region on the LTR promoter, significantly impeding Tat transactivated HIV-1 LTR transcription (355; 356). Furthermore, several SREs on the HIV-1 pre-mRNA are bound by SRSF1, which results in facilitated spliceosome assembly and the recruitment of core spliceosomal components (99). Binding of SRSF1 to ESE M1/M2, which is located in proximity of the 5'-SD2, promotes exon 2 recognition via cross-exon interactions between SD2 and SA1 (237), while binding of SRSF1 to the bidirectional GAR ESE results in enhanced binding of U1 snRNP to the 5'-SD4 and thus increases splicing frequency at the upstream 3'-SA5 and 3'-SA4cab (63). The SRSF-1 targeted ESE3 is located downstream of SA7 and promotes binding of the U2 snRNP associated U2AF65 to the 3'-SA, thereby increasing splice site usage (433). Knockdown of SRSF1 was shown to generally induce an increase in total viral mRNA levels, while overexpression suppressed viral transcription (219; 221; 387). Thus, SRSF1 represents a key regulator for efficient HIV-1 post integration steps.

Subcellular localization and functions of SRSF1 are regulated through post-translational modifications. Phosphorylation of the RS-domain serves as nuclear localization signal

---

(NLS) (388; 517). While SR specific protein kinases 1 and 2 (SRPK) or CDC-like kinase 1 (Clk1) phosphorylate Ser residues within the RS domain (85; 181; 259; 339), dephosphorylation occurs through protein phosphatases 1 and 2A (PP1 and PP2A) (205; 330; 343; 395). Partially phosphorylated SRSF1 was shown to bind with high affinity to RNA target sequences. However, unphosphorylated or fully phosphorylated SRSF1 did not have a high affinity for its target RNA sequence (107). Furthermore, several Arg residues within the RRM region were shown to be methylated, thus modulating SRSF1 nuclear-cytoplasmic shuttling (423).

#### **1.1.5.2. Heterogeneous nuclear ribonucleoproteins**

Heterogeneous nuclear ribonucleoproteins (hnRNPs) are also part of the large family of RBPs (117; 162; 185). The hnRNP proteins feature multiple RNA-binding domains (RBDs) and auxiliary domains, such as the RRM, the quasi-RRM, the glycine-rich RGG-box and the K-homology (KH) domain (57). The RRM enables the interaction with pre-mRNAs (173), while the qRRM (113; 393) and KH domain (227) represent further RNA-binding domains, expanding the RNA-binding specificity. The RGG-box enables homologous or heterologous interactions with hnRNPs and other proteins and is often seen as an auxiliary domain (68). The highly divergent auxiliary domains usually consist of proline-, glycine- or acid-rich domains (116) and determine various biological functions, such as protein-protein-interactions or nuclear localization (38). The combination of these domains gives rise to a high functional diversity within the hnRNP family (162).

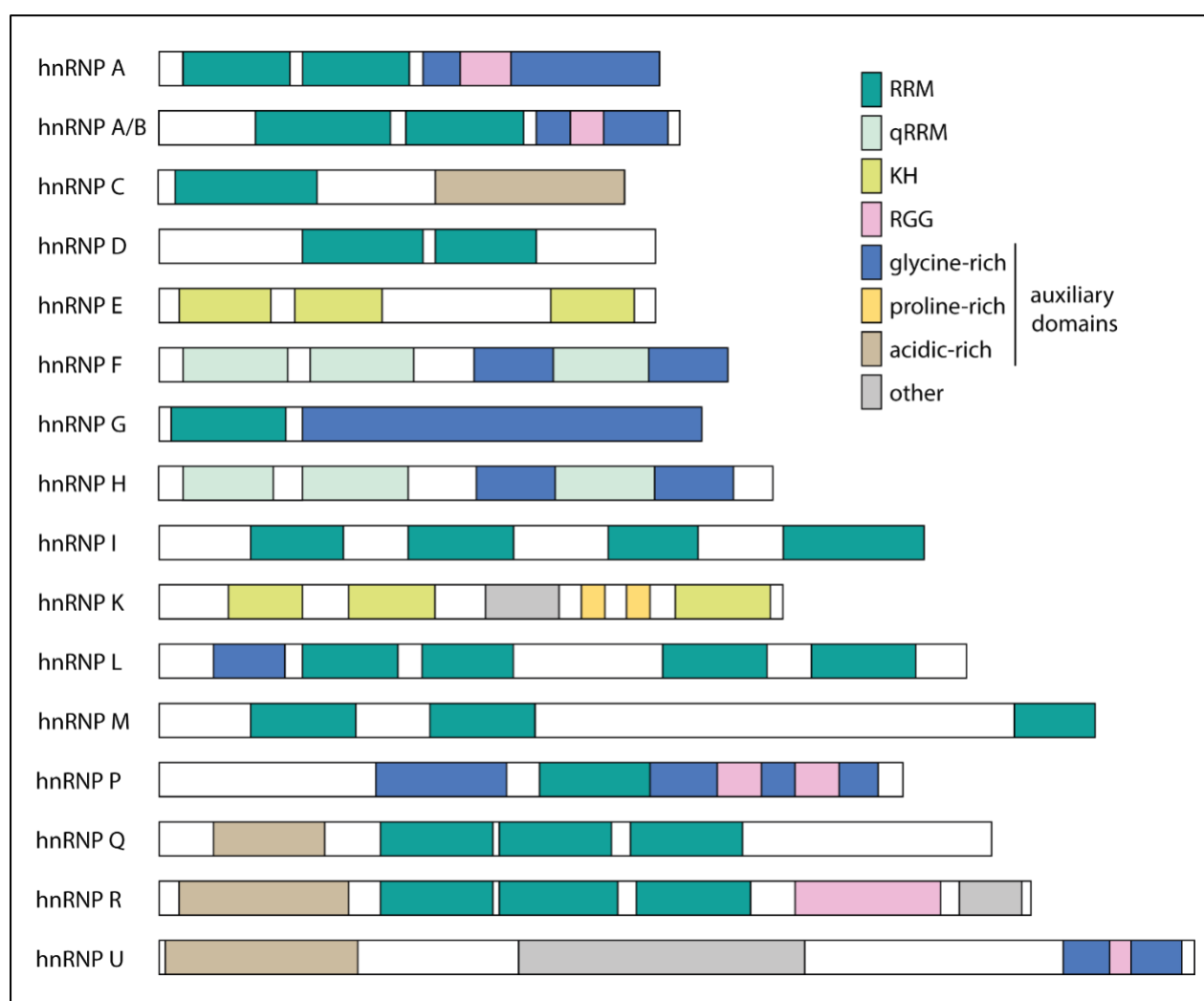


**Figure 1-8: Structural organization of the hnRNP proteins.** The domain structures of the human hnRNP proteins are depicted. RRM: RNA recognition motif; qRRM: quasi-RNA recognition motif; KH: K-homology domain; RGG: glycine-rich RGG-box. This illustration was modified according to (162).

The hnRNP protein family can be classified into different subfamilies, which include hnRNP A/B (hnRNP A0, hnRNP A1, hnRNP A2B1 and hnRNP A3), hnRNP C (hnRNP C1 and hnRNP C2), hnRNP D, hnRNP E (hnRNP E1, hnRNP E2, hnRNP E3 and hnRNP E4), hnRNP F/H (hnRNP F and hnRNP H), hnRNP G, hnRNP I/L (hnRNP I and hnRNP L), hnRNP K, hnRNP M/Q (hnRNP M and hnRNP Q), hnRNP P2 and hnRNP R/U (hnRNP R and hnRNP U) (162). The subfamilies differ in their composition and functional properties (162). Among other post-translational modifications, phosphorylation of serine and threonine residues and methylation of arginine residues regulate the activity and subcellular localization of hnRNP proteins (117; 172; 367). hnRNPs can form homo- or



heteromers with each other, thus further increasing their complexity and functional properties (253).

In addition to the SRSF family, members of the hnRNP family are the main types of *trans*-acting splicing factors (59). Thousands of cellular alternative splicing events are regulated by hnRNPs, which, in a position-dependent manner, activate or repress exon inclusion (117; 162; 185; 207; 267). In comparison to SRSF proteins, hnRNP proteins function inversely. Thus, when binding upstream of a 5'-ss, hnRNPs exhibit an inhibitory effect, but when binding downstream of a 5'-ss, they facilitate splice site recognition (127; 477). The subfamilies hnRNP A/B (hnRNP A0, hnRNP A1, hnRNP A2B1 and hnRNP A3), hnRNP D and hnRNP F/H (hnRNP F and hnRNP H) have been described to regulate splicing of several HIV-1 genes (as reviewed in (40; 207; 315; 317; 410)). Binding of hnRNP A1 to ISS, which is located upstream of 3'-SA7, sterically hinders the recruitment of U2 snRNP, thereby inhibiting splice site usage at SA7 (445). Interaction between ESS2, localized 70 nt downstream of 3'-SA3, and hnRNP A1 prevents the binding of spliceosomal components to the pre-mRNA (182; 509). Binding of hnRNP F/H and hnRNP A2B1 to the intronic G-run G<sub>13-2</sub> was suggested to inhibit binding of U1 snRNP to SD3 (486). G<sub>12-1</sub>, a further G-run targeted by hnRNP F/H, was shown to decrease recruitment of U1 snRNP to the 5'-SD2b and thus preventing exon 2b recognition (485). Competitive binding of hnRNP H with the U1 snRNP for a sequence of the silencer element G4 (GGGG) within SD2 resulted in decreased splicing events at SD2 (131).

In addition to the regulation of splice site usage, the functional diversity of hnRNP proteins include telomere biogenesis, RNA editing, mRNA stabilization, nuclear export and translation (as reviewed in (162; 185; 267)).

#### **1.1.5.2.1. Heterogeneous nuclear ribonucleoprotein A0**

The hnRNP A/B subfamily includes hnRNP A0, hnRNP A1, hnRNP A2B1 and hnRNP A3 (162; 185). While hnRNP A1, hnRNP A2B1 and hnRNP A3 have been largely described as cellular and HIV-1 splicing factors (40; 225; 315; 317; 410), little is known about the specific role of hnRNP A0. The low abundant member of the hnRNP protein family hnRNP A0 was identified unexpectedly by Myer and colleagues (338). hnRNP A0 has been linked to post-transcriptional mRNA regulation of the transcription factors TNF- $\alpha$ , COX-2 and MIP-2 (390). Furthermore, hnRNP A0 has been identified as a substrate of the checkpoint kinase MK2, regulating cell cycle arrest and cellular resistance to DNA damaging

chemotherapy (62). It was shown that hnRNP A0 is also strongly involved in the regulation of cancer cell growth in pancreatic, lung, esophageal and gastric cancer (62; 262).

The target sequence of hnRNP A0 are adenylate-uridylate (AU)-rich elements (AREs), which are often located in 3'-UTRs of mRNAs (74; 338; 390; 507). The most common consensus motif is the pentamer AUUUA, which is bound by hnRNP A0 (390), and also hnRNP A1 (183), with high affinity. Binding affinity of hnRNP A0 is regulated via phosphorylation at Ser-84 through MAPKAP-K2 (390). While no direct targets of hnRNP A0 on the HIV-1 pre-mRNA are known, many AREs are dispersed throughout the viral genome (404).

### **1.1.6. Host Restriction Factors**

Host cells have evolved intrinsic resistance factors to suppress viral replication and propagation. Host restriction factors (HRF) are components of the innate immune system induced by interferons (IFNs), which provide an early line of defense against viral infections including HIV-1. HRFs thus belong to the family of IFN-stimulated genes (ISGs) and inhibit distinct stages of the viral replication cycle. In addition to the intrinsic antiviral effects, HRFs were shown to modulate the cellular adaptive immunity (as reviewed in (135; 141; 163; 307; 521)). However, HIV-1 has evolved various mechanisms to evade the intrinsic HRFs, mainly by the use of its accessory proteins Vif, Vpr, Vpu and Nef (422; 521). The antiviral mechanisms of the HRFs as well as the counter-restrictions induced by viral proteins will be described in more detail in (Chapter 1.2.4.1.).

## **1.2. Innate immune sensing of HIV-1**

Pathogen-associated molecular patterns (PAMPs), which are evolutionary conserved structures of pathogens, are recognized through pattern-recognition receptors (PRRs). PRRs include the family of Toll-like receptors (TLRs), NOD-like receptors (NLRs), retinoic acid-inducible gene I (RIG-I), melanoma differentiation-associated gene 5 (MDA-5) and cyclic GMP-AMP [cGAMP] synthase (cGAS) (271; 333; 444). Upon recognition of a foreign molecular structure, PRRs activate a variety of intracellular signaling pathways (7). Ultimately, the induced signaling cascade leads to the gene expression of transcription factors like nuclear factor  $\kappa$ -light-chain-enhancer of activated B-cells (NF- $\kappa$ B) or myeloid differentiation primary response 88 (MyD88), which in turn induce the production of pro-inflammatory cytokines such as type I IFNs (216).

The family of TLRs represents an extensively studied class of PRRs and can be divided into subfamilies based on their recognition pattern (8). TLRs are widely expressed on cells of the innate immune system, such as DCs, macrophages or B-cells (217). TLRs 3, 7, 8 and 9 are localized in endosomes and are involved in viral recognition (333). Specifically, TLR 7 and 8 recognize guanosine-uridine-rich ssRNA molecules such as the HIV-1 genome, while TLR 3 binds to dsRNA molecules (142; 191; 304; 421). Since TLR 7 and 8 recognize the HIV-1 genome as ssRNA molecule, they can also trigger an immune response in cells that have not been productively infected (140; 238). After stimulation, TLRs form a homo- or heterodimer, which recruit adaptor molecules such as MyD88 to the TLR and activates a range of signaling cascades. The activation of the transcription factor NF- $\kappa$ B induces the production of pro-inflammatory cytokines (36; 249; 325; 351; 449). However, the production of IFN depends on the interferon-regulatory factor (IRF) 7, which is phosphorylated by NF- $\kappa$ B before shuttling to the nucleus and inducing the expression of type I IFNs (8; 249). Furthermore, binding of adaptor protein TIR-domain-containing adapter-inducing interferon- $\beta$  (TRIF) to dimerized TLR 3 results in the phosphorylation of IRF3 and the subsequent expression of IFN $\beta$  (36; 506).

Alongside the TLRs, which are membrane proteins, a range of cytosolic PRRs are also involved in the recognition of viral structures. NLRs are involved in the induction of proinflammatory gene expression through the binding of virus-associated PAMPs (216). RIG-I and MDA-5 are RNA helicases that can recognize cytoplasmic dsRNA molecules. Since the viral genome is encapsidated in the cytosol except for the short duration of reverse transcription, recognition of viral RNA is impeded heavily (216; 246; 333). Another soluble factor binding to dsDNA during the short process of reverse transcription is cGAS. After binding to dsDNA, cGAS produces cyclic guanosine monophosphate-adenosine monophosphate (cGAMP), which can in turn bind to stimulator of IFN genes (STING). Subsequently, IRF3 and IRF7 are activated via phosphorylation and the expression of type I IFNs and other proinflammatory cytokines is induced (1; 157).

### **1.2.1. Interferons**

In 1957, soluble macromolecules were described, which were able to 'interfere' with virus replication in cell culture and were thus termed interferons (IFNs) (213). IFNs are cytokines released by host cells in response to viral or microbial infection (394; 443). Human IFNs have been classified into three different families, based on sequence

homology and the receptor they bind to. The type I IFNs, including IFN $\alpha$ , IFN $\beta$ , IFN $\epsilon$ , IFN $\kappa$  and IFN $\omega$ , have antiproliferative, antiviral and immunomodulatory properties. The type II IFNs with their sole member IFN $\gamma$  are a crucial link between innate and adaptive immune response. The type III IFNs, including IFN $\lambda$ 1, IFN $\lambda$ 2, IFN $\lambda$ 3 and IFN $\lambda$ 4, have antiviral and immunomodulatory properties similar to the type I IFNs (362; 443; 467). Each IFN family binds to a specific receptor, which are the IFN $\alpha/\beta$ -receptor (IFNAR) for type I IFNs, the IFN $\gamma$ -receptor (IFNGR) for type II IFNs and the IFN $\lambda$ -receptor for type III IFNs (280; 282; 368).

### 1.2.2. Type I interferons

Type I IFN secretion is induced in response to the stimulation of PRRs as described in (Chapter 1.2.) and represents an early line of defense against viral infections. Type I IFN mainly refers to IFN $\alpha$  subtypes, which are mainly expressed by plasmacytoid dendritic cells (pDCs), but also by other immune cells (419). There are 13 different genes on chromosome 9 coding for the individual subtypes of IFN $\alpha$ . Since IFN $\alpha$ 1 and IFN $\alpha$ 13 share an identical sequence, the number of individual IFN $\alpha$  subtypes is set to 12 (186; 482). Even though all IFN $\alpha$  subtypes share a high sequence homology and bind the same receptor, the IFN $\alpha/\beta$ -receptor (IFNAR), they induce different biological responses (164; 165; 186; 193). While it has not yet been fully elucidated why IFN $\alpha$  subtypes possess distinct biological functions, several mechanisms have been proposed. It was shown, that IFN $\alpha$  subtypes have different binding affinities to the IFNAR receptor subunits, which can result in the activation of different downstream signaling pathways (88; 223; 279). Furthermore, tissue-specific expression of different IFN $\alpha$  subtypes and also the IFNAR receptor could influence the stimulated pattern of ISGs (335).

Viral infections induce a unique expression pattern of IFN $\alpha$  subtypes (25; 121). Upon HIV-1 infection, a generally enhanced IFN $\alpha$  expression was detected. IFN $\alpha$ 4, IFN $\alpha$ 5, IFN $\alpha$ 7 and IFN $\alpha$ 14 were the most abundantly expressed subtypes in acutely infected HIV-1 patients, while during chronic HIV-1 infection subtypes IFN $\alpha$ 2 and IFN $\alpha$ 16 were strongly expressed in addition (290).

Induction of type I IFNs and particularly IFN $\alpha$  stimulates the expression of hundreds of IFN-stimulated genes (ISGs), such as HIV-1 restriction factors with direct antiviral functions, or other factors involved in inflammation or immunomodulation (101; 406). The specific functions of ISGs and particularly HIV-1 host restriction factors will be described

in more detail in (Chapter 1.2.4.1.). In addition to ISG-stimulation, type I IFNs also induce the downregulation of specific genes, which are termed IRepGs and will be discussed further in (Chapter 1.2.4.2.) (324; 455). The upregulation of type I IFNs was suggested to increase differentiation of pDCs into myeloid-derived DCs, thereby increasing T-cell activation (522). The induction of CC-chemokine ligand 2 (CCL2) secretion by type I IFNs was shown to recruit inflammatory monocytes to the site of infection, where they stimulate immune cell antiviral functions and differentiate into macrophages (211; 283). The recruitment and activation of natural killer (NK) cells, which in response induce IFN $\gamma$ , was also shown to be regulated by type I IFNs (291; 466). Thus, type I IFNs establish an antiviral state in the host and bystander cells and modulate the innate immune response upon viral infection.

#### **1.2.2.1. Type I IFN induced signaling pathways**

All type I IFN bind to the same receptor, the IFN $\alpha/\beta$ -receptor (IFNAR). The heterodimeric receptor consists of the subunits IFNAR1 and IFNAR2 and is present on almost all cell types (102; 193; 214). The first signaling pathway which was discovered was the Janus activated kinase/signal transducer and activator of transcription (JAK/STAT) pathway. This signaling pathway is active in almost all cell types. Both subunits of IFNAR constitutively bind a receptor-associated tyrosine kinase at their cytoplasmic domain, which are tyrosine kinase 2 (TYK2) for IFNAR1 and Janus kinase 1 (JAK1) for IFNAR2. Binding of type I IFN to the extracellular IFNAR domain leads to dimerization and autophosphorylation, which activates TYK2. Phosphorylation of tyrosine residues at the cytoplasmic domain of IFNAR exposes a binding site for src-homology 2 (SH2)-containing signaling molecules STAT-1 and STAT-2. Binding of STAT-1 and STAT-2 molecules leads to phosphorylation of tyrosine residues Y7101 (STAT-1) and Y690 (STAT-2), which is followed by the dimerization of STAT-1 and STAT-2. Interferon regulatory factor 9 (IRF9) then binds to the heterodimer, thus forming the interferon stimulated gene factor 3 (ISGF3) complex. ISGF3 then translocates into the nucleus and acts as transcription factor, binding specifically to its consensus sequence on the IFN-stimulated response element (ISRE), thus inducing the transcription of ISGs (102; 193; 214; 368).

Alongside the typical STAT-1 and STAT-2 phosphorylation, the JAK/STAT-pathway can be induced by the phosphorylation of other STATs such as STAT-1, STAT-3 or STAT-5. STAT-4 and STAT-6 have also been shown to be phosphorylated upon type I IFN

stimulation, although with restriction to specific cell types. The phosphorylation of these STAT molecules can lead to the formation of homo- or heterodimers, which can also act as transcription factors, inducing the transcription of different regulatory sequences such as IFN $\gamma$ -activated sites (GAS) (193; 214; 368).

Next to the JAK/STAT signaling pathway, further signaling pathways can be induced by type I IFNs such as the mitogen activated protein kinase (MAPK) pathway, the phosphoinositide 3-kinase (PI3K) pathway, the v-crk sarcoma virus CT10 oncogene homolog (avian)-like (CRKL) pathway or the nuclear factor 'kappa-light-chain-enhancer' of activated B-cells (NF- $\kappa$ B) pathway (193; 214; 368).

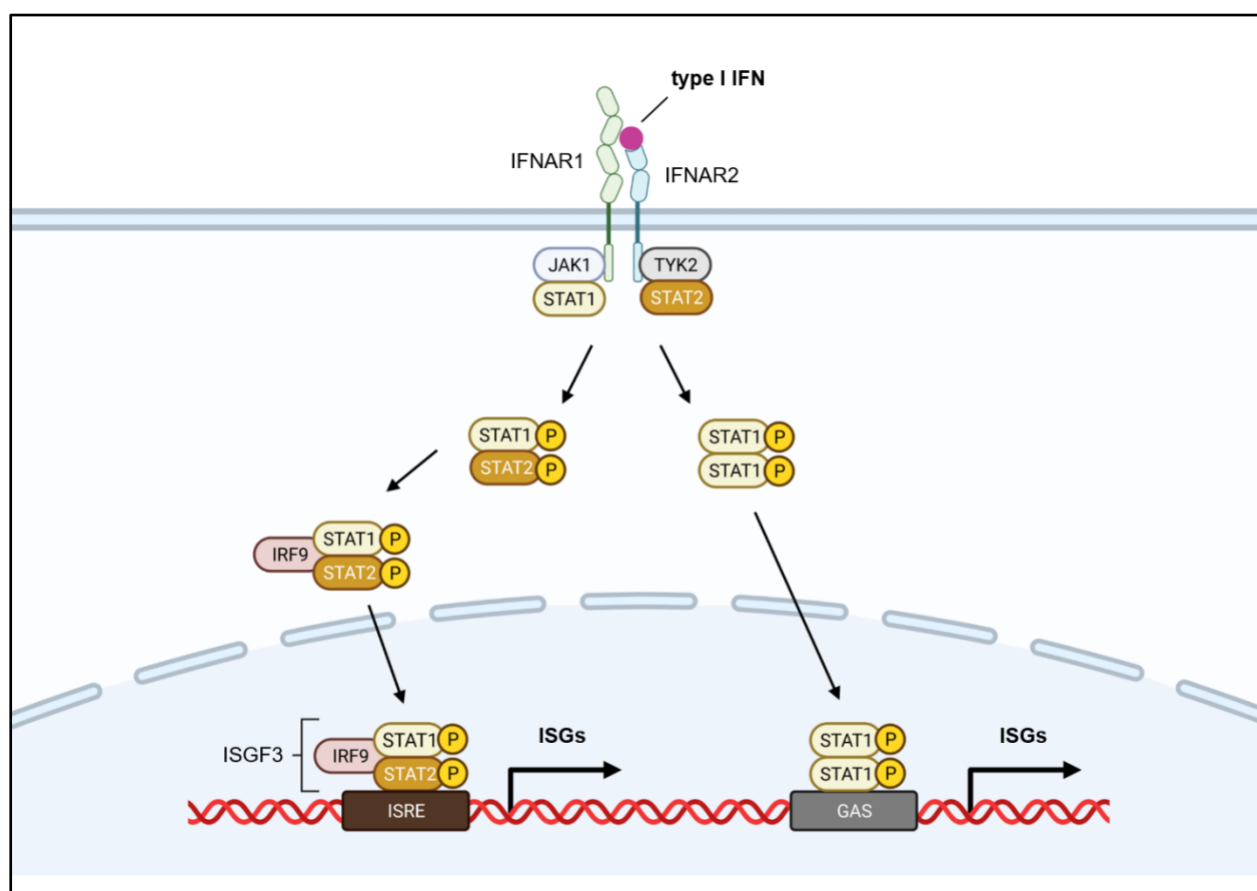


**Figure 1-9: Type I IFN signaling pathway.** Upon binding of type I IFN to the IFN $\alpha/\beta$ -receptor IFNAR receptor, Janus kinase 1 (JAK1) and tyrosine kinase 2 (TYK2) are activated. Conformational change then enables the recruitment of STAT-1 and STAT-2. After phosphorylation, STAT-1 and STAT-2 dimerize and bind IFN-regulatory factor 9 (IRF9). The resulting IFN-stimulated gene factor 3 (ISGF3) complex then translocates to the nucleus and binds to ISRE elements, thus inducing the transcription of antiviral genes (102; 193; 214; 368). Furthermore, homodimers of phosphorylated STAT-1 can directly translocate to the nucleus and bind to IFN $\gamma$ -activated site (GAS) elements (193; 214; 368). Figure adapted from "Interferon

---

Pathway” by BioRender.com (2021). Retrieved from <https://app.biorender.com/biorender-templates>.

### **1.2.3. Type II interferons**

IFN $\gamma$  is the sole member of the type II IFN family and has no structural homologies to type I IFNs. The gene coding for IFN $\gamma$  is located on chromosome 12 (340). IFN $\gamma$ , though binding to a different signaling receptor than the type I IFNs, also has antiviral and immunomodulatory functions (37; 282; 368). NK cells predominantly express IFN $\gamma$  upon stimulation with type I IFN or different interleukins (ILs) (166; 283; 358). Furthermore, CD4<sup>+</sup> T-helper cell type 1 (Th1) lymphocytes, B cells and other antigen-presenting cells (APCs) have also been shown to produce IFN $\gamma$  (24; 407). IFN $\gamma$  thus has a crucial function as linker between the innate and adaptive immune response (471).

#### **1.2.3.1. Type II IFN induced signaling pathways**

IFN $\gamma$  binds in the active form of a homodimer to the IFN $\gamma$ -receptor (IFNGR), which includes the subunits IFNGR1 and IFNGR2 (363; 484). Conformational changes within the transmembrane domain of the receptor allow the subsequent binding of JAK1 and JAK2. Autophosphorylation of JAK2 in turn phosphorylates JAK1 (45; 55; 120). The phosphorylation of specific residues on the IFNGR by the activated JAK2 further enables binding of the transcription factor STAT-1 (210). STAT1 in turn gets phosphorylated at the tyrosine residue Y701 and forms a homodimer. After translocation of the STAT-1 homodimer to the nucleus, the transcription factor binds IFN $\gamma$ -activated sites (GAS) elements to initiate transcription of ISGs (96; 103; 179; 407). Binding of the STAT1 homodimer to IRF9 prior to nuclear translocation also allows the transcriptional activation of specific ISRE elements (178).

Like type I IFNs, IFN $\gamma$  can also induce alternative pathways such as the extracellular-signal regulated kinase 1/2 (ERK1/2) pathway or the v-crk sarcoma virus CT10 oncogene homolog (avian)-like (CRKL) pathway (9; 429). Furthermore, IFN $\gamma$  can activate STAT-3, which leads to the formation of a phosphorylated homodimer, translocation to the nucleus and transactivation of GAS-elements (376; 468).

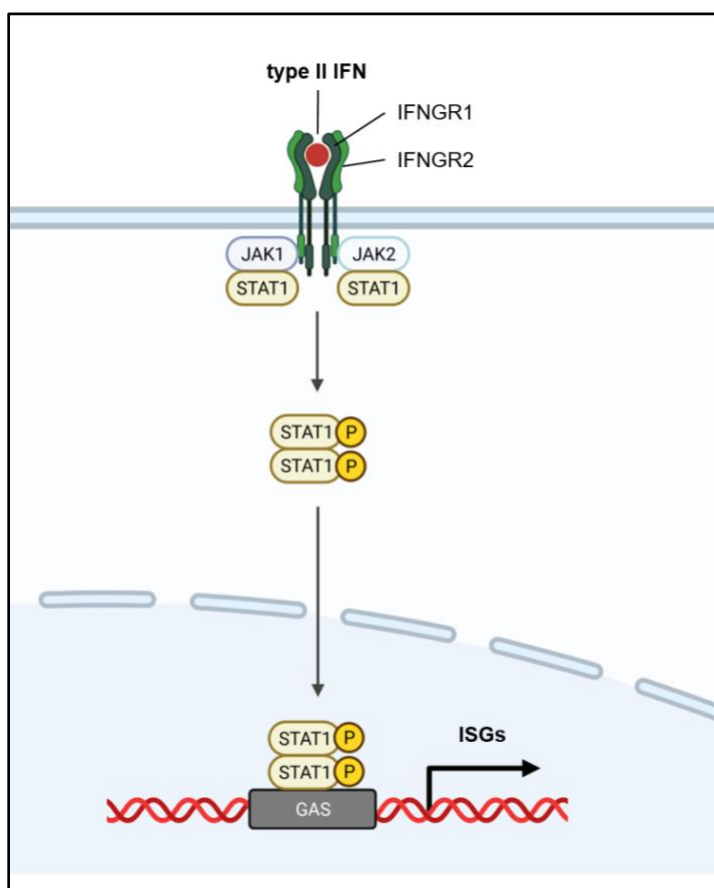


**Figure 1-10: Type II IFN signaling pathway.** Upon binding of IFN $\gamma$  to the IFN $\gamma$ -receptor (IFNGR), JAK1 and JAK2 are phosphorylated and in turn phosphorylate STAT-1. STAT-1 forms a homodimer and translocated to the nucleus. The transcription factor then binds IFN $\gamma$ -activated sites (GAS) elements to initiate transcription of ISGs (45; 55; 96; 103; 120; 179; 210; 363; 407; 484). Figure adapted from “Interferon Pathway” by BioRender.com (2021). Retrieved from <https://app.biorender.com/biorender-templates>.

#### 1.2.4. Restriction of HIV-1 infection

HIV-1 must pass several barriers in order to establish a systemic infection. Alongside the transition from the donor’s body fluid to the genital tract compartment and the survival of the virus within the transmission fluid, a further physical barrier is the crossing of the mucosa in the recipient’s genital tract (235; 243; 411). The virus needs to pass the multi-layered epithelium and infect sub-epithelial mononuclear CD4<sup>+</sup> cells in the lamina propria (235; 243; 413). Additional donor effects affecting the transmission of HIV-1 are the viral load within the transmission fluid and a concomitant viral or bacterial infection (235). Whether a systemic infection is established, further depends on the viral fitness. Transmission selects for viruses with a high replication rate and a pronounced interferon IFN $\alpha$ -resistance (235).



Thus, there is strong evidence, that only specifically adapted viral variants are able to overcome the barriers of HIV-1 transmission, which are defined as transmitted founder viruses (TFV). HIV-1 infection typically results from the transmission of a single viral variant (250). An HIV-1 genome study, focusing on the HIV-1 glycoprotein Env, revealed that in a patient cohort of 102 subjects, 76 % showed evidence of a productive clinical infection caused by a single virus, while the other 24 % showed evidence of a productive clinical infection caused by five viruses at most (250). TFV are generally CCR5-tropic (98 %), possess fewer potential N-linked glycosylation sites and have a higher viral fitness and replication capacity (20; 135; 243; 250; 353). Interestingly, TFV are relatively resistant to IFN $\alpha$ , which induce the production of host restriction factors and thus constitute an early defense against viral infections (20; 135; 353). To escape the strong selective pressure by the host's immune system, HIV-1 thus has to circumvent these host restriction factors.

#### **1.2.4.1. IFN-stimulated genes**

IFNs induce the stimulation of hundreds of ISGs, including host restriction factors, which induce an antiviral state within the host cell, but also in neighboring cells. Many ISGs have broad antiviral activities, which are not limited to a specific pathogen (297). The  $\gamma$ -IFN inducible protein 16 (IFI16) has been described to recognize dsDNA from DNA viruses as well as ssDNA from RNA viruses such as HIV-1. IFI16 promotes the transcription of further antiviral cytokines and RIG-I (110; 231). It was also shown that IFI16 is able to inhibit HIV-1 replication without a concomitant ISG induction (199). The IFN-induced protein 44 (IFI44) is induced by type I IFN (256). While the exact antiviral mechanism has not yet been elucidated, it was shown that IFI44 shuttles to the nucleus and inhibits HIV-1 LTR promoter activity (374). 2',5'-oligoadenylate-synthetase 1 (OAS1) senses dsRNA molecules and constitutes an RNA decay pathway together with RNaseL (392; 420). Protein kinase R (PKR) is constitutively expressed in all tissues as an inactive kinase. Upon activation by the sensing of viral RNA, PKR stimulates the transcription initiation factor 2a (eIF2a), which blocks the translation of mRNA and thus the synthesis of viral and cellular proteins (392; 492). IFN-stimulated gene 15 (ISG15) is one of the most abundant ISGs to be induced by type I IFNs. ISG15 forms conjugates with hundreds of proteins in a reversible process termed ISGylation, similar to the process of ubiquitination. The exact functional consequences of ISGylation are not completely understood so far (336; 392; 511). ISG15 inhibits the release of HIV-1 virions during the process of budding (346; 365).

The myxovirus resistance 2 (Mx2) is a member of the guanosine triphosphatase (GTPase) family. Mx2 accumulates at the intracellular cell membrane. Upon binding of viral components, such as the HIV-1 capsid protein, Mx2 initiates their degradation (175; 239). IFN-regulatory factor 1 (IRF1) acts as a transcription factor and has been described to inhibit the replication of different RNA viruses (65). Furthermore, IRF1 is suggested to be a key regulator of innate immunity by regulating several signaling cascades and antiviral responses (134). The interferon-induced transmembrane proteins 1-3 (IFITM1-3) inhibit the cellular entry of different viruses including HIV-1 and have also been shown to inhibit translation of viral proteins (284; 301). The viral protein Nef has been suggested to counteract the IFITM-mediated suppression of HIV-1 virus production (284). The exact mechanism of action, however, is still unclear. As many ISGs individually only exhibit moderate viral suppression, it is suggested that an orchestration of ISG activities is necessary to establish an efficient antiviral state (297).

Several ISGs specifically inhibit distinct stages of the HIV-1 replication cycle. However, HIV-1 has adapted and evolved strategies to evade the antiviral activity of the HRFs. The viral accessory proteins Vif, Vpr, Vpu and Nef allow HIV-1 to overcome the barriers of intrinsic immunity during infection (141; 307). The DNA deaminase APOBEC3G is widely expressed in hematopoietic cells (261; 384) and incorporates into newly assembled virions through the interaction with the nucleocapsid protein p6 (403; 494; 510). Upon infection of a target cell, APOBEC3G inserts C → U mutations during the synthesis of the (-)-strand cDNA via the deamination of deoxycytidine to deoxyuridine. The resulting G → A hypermutations result in mutations within the protein sequences or in premature stop codons, which render the produced virions replication incompetent (348; 383; 412; 494). A further antiviral mechanism of APOBEC3G includes the inhibition of tRNA processing, which results in aberrant DNA ends defective for (+)-strand transfer and thus integration (320; 321). The HIV-1 accessory protein Vif counteracts APOBEC3G through binding to CBFβ and the subsequent polyubiquitinylation finally leads to the degradation of the host protein (383; 436; 494). Thus, HIV-1 virions lacking Vif protein can only replicate in permissive cells, which, amongst other HRFs, do not express APOBEC3G (188; 412). In non-permissive, APOBEC3G-expressing cells, *vif*-deficient HIV-1 strains fail to replicate (412; 485). The transmembrane glycoprotein tetherin anchors budding virions on the surface of the cell and blocks their release via interaction with the viral envelope (341; 361). Tetherin is antagonized by the HIV-1 protein Vpu by inducing proteasomal

degradation and by reducing tetherin expression on the cellular surface (215; 331; 341; 361; 469). The Deoxynucleotide triphosphohydrolase SAMHD1 depletes the pool of cellular dNTPs by hydrolyzing dNTPs into deoxynucleosides and inorganic triphosphates, thereby impeding HIV-1 reverse transcription (200; 273; 274). SAMHD1 is counteracted by the accessory proteins Vpr and Vpx, which target SAMHD1 for proteasomal degradation via the interaction with the C-terminal domain (5; 149; 200; 273). However, Vpx is only present in HIV-2 and SIV strains (273; 292). The E3-ligase TRIM5 $\alpha$  recognizes motifs within the capsid proteins, thereby impeding the uncoating process and preventing reverse transcription and the nuclear import of the viral genome (124; 378). The tRNA-binding protein SLFN11 selectively inhibits the translation of viral proteins at the late stage of HIV-1 replication by exploiting the codon bias towards A/T nucleotides (222; 286; 382). No viral proteins have so far been described to antagonize the antiviral activity of TRIM5 $\alpha$  or SLFN11.

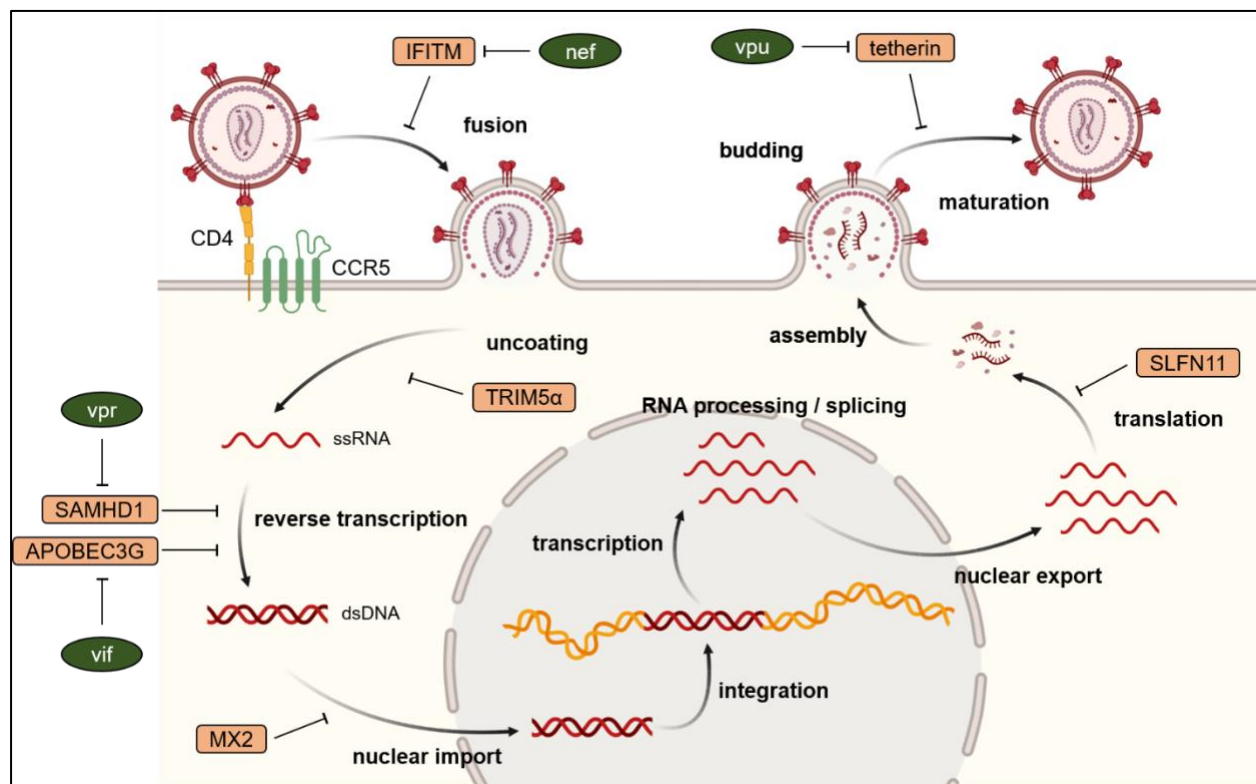


**Figure 1-11: IFN-induced HIV-1 restriction factors.** Host restriction factors (HRF) are induced by IFNs to inhibit distinct stages of the viral replication cycle. Interferon-induced transmembrane proteins (IFITM) inhibit viral entry of the cell. Tripartite motif-containing protein 5  $\alpha$  (TRIM5 $\alpha$ ) interferes with the uncoating process after cellular entry. Sterile alpha motif and HD domain-containing protein 1 (SAMHD1), which depletes the intracellular dNTP pool in the cytoplasm, and apolipoprotein B mRNA editing enzyme 3G (APOBEC3G), which inserts G  $\rightarrow$  A

hypermutations into the HIV-1 genome during reverse transcription, both inhibit the process of reverse transcription. Myxovirus 2 (MX2) prevents nuclear import of viral DNA. tRNA-binding protein SLFN11 (Schlafen 11) inhibits the translation of viral proteins. Tetherin blocks the release of assembled viral particles from the cell surface. The viral proteins Vpr, Vif and Vpu antagonize the HRFs SAMHD1, APOBEC3G and tetherin respectively (115; 141; 307). Figure adapted from “HIV replication cycle” by BioRender.com (2021). Retrieved from <https://app.biorender.com/biorender-templates>.

#### **1.2.4.2. IFN-repressed genes**

Alongside the upregulation of a large number of genes, IFNs also induce the repression of a subset of genes, which are termed IFN-repressed genes (IRepGs). 4-thiouridine-tagging was used to identify negatively regulated genes upon IFN-treatment, as this method enables the analysis of newly synthesized mRNAs. The repression of IRepGs has been shown to be STAT1-dependent (324; 455). As for the ISG stimulation patterns, the patterns of IRepGs also differ between type I and II IFNs (324). It was observed that several translation factors belong to the group of IRepGs, which suggests that IRepGs can restrict cellular and viral translation. Furthermore, fatty acid synthase (FASN), which is required for the replication of dengue virus or hepatitis C virus, was downregulated by IFNs (324). Several genes that have previously shown to be essential for the replication of HIV-1 (60), could also be identified as IRepGs (324). The exact function of IFN-mediated gene repression and their role in antiviral, antibacterial and immunomodulatory function has yet to be determined.

### **1.3. Aim of this thesis**

Upon viral infection, type I IFNs induce the expression of hundreds of ISGs, thus establishing an antiviral state within host and bystander cells. Furthermore, IFNs also induce the repression of specific genes, termed IRepGs. Several of these IRepGs were identified as HDFs, which are essential for viral replication. HIV-1 exploits the cellular transcription and RNA processing machinery for viral replication. In particular, alternative splicing plays a crucial role in the viral life cycle and is regulated by a complex network of SREs, which are localized in the vicinity of viral splice sites and bound by cellular splicing factors. Members of the SRSF and hnRNP protein families were identified as HDFs and shown to regulate HIV-1 alternative splice site usage. This work aims to investigate, whether *SRSF* and *hnRNP* transcript levels are altered upon HIV-1 infection, possibly due to IFN induction and the concomitant inflammation. HIV-1 target cells will be stimulated

---

with different IFN $\alpha$  subtypes to examine, whether the expression of specific *SRSFs* and *hnRNPs* is type I IFN-regulated. It will be evaluated, whether the potential modulation of *SRSF1* and *hnRNP A0* expression levels upon IFN stimulation might be a part of the type I IFN-induced antiviral activity. In addition, the effect of altered expression levels of *SRSF1* and *hnRNP A0* on HIV-1 post integration steps will be examined at the level of LTR transcription, alternative splicing and virus production. Thus, the importance of balanced levels of *SRSF1* and *hnRNP A0* for efficient HIV-1 replication will be investigated.

## 2. Material

### 2.1. Chemicals and Reagents

**Table 2-1:** Chemicals and reagents.

<b>Chemical/Reagent</b>	<b>Manufacturer</b>
Acrylamide/bis 30 %	Bio-Rad, Feldkirchen
Amersham ECL WB Detection Reagent	GE Healthcare Life Sciences, Buckinghamshire (UK)
Agarose	FMC, Stade
Ampicillin	Roth, Karlsruhe
APS	Roth, Karlsruhe
Beetle juice Firefly substrate	p.j.k., Kleinblittersdorf
2x Beetle-Lysis juice	p.j.k., Kleinblittersdorf
Bicoll separation medium	VWR, Darmstadt
Biotin-HPDP	Thermo Scientific, Schwerte
$\beta$ -mercaptoethanol	Sigma Aldrich, Darmstadt
Bromophenol blue	Sigma Aldrich, Darmstadt
Bovine serum albumin (BSA)	Thermo Scientific, Schwerte
Chloroform	Sigma Aldrich, Darmstadt
5x Colorless GoTaq buffer	Promega, Mannheim
Complete™ Protease Inhibitor Cocktail	Roche, Mannheim
CSPD® Substrate (Sapphire II)	Thermo Scientific, Schwerte
CutSmart buffer	NEB, Frankfurt a. M.
DNase buffer	NEB, Frankfurt a. M.
dNTP mix	Promega, Mannheim
DMEM medium	Thermo Scientific, Schwerte
DMSO	Sigma Aldrich, Darmstadt
DPBS	Thermo Scientific, Schwerte co
DTT	Roth, Karlsruhe
EDTA	Fluka, Bucks (Switzerland)
10x ELISA-Light Assay buffer	Thermo Scientific, Schwerte
Empigen	Sigma Aldrich, Darmstadt
Ethanol	AppliChem, Darmstadt

FCS	Thermo Scientific, Schwerte
Formaldehyde	Sigma Aldrich, Darmstadt
5x First Strand Buffer	Thermo Scientific, Schwerte
Gelatin solution	Sigma Aldrich, Darmstadt
Glutaraldehyde	Sigma Aldrich, Darmstadt
Glycerol	Merck, Darmstadt
Glycogen	Thermo Scientific, Schwerte
5x Green GoTaq buffer	Promega, Mannheim
IFN $\gamma$	PBL Assay Science, Piscataway, NJ (US)
IMDM medium	Thermo Scientific, Schwerte
Isopropanol	Merck, Darmstadt
K <sub>3</sub> [Fe(CN) <sub>6</sub> ]	Sigma Aldrich, Darmstadt
K <sub>4</sub> [Fe(CN) <sub>6</sub> ]	Roth, Karlsruhe
1 kb Plus DNA ladder	NEB, Frankfurt a. M.
LB Agar	Roth, Karlsruhe
LB Medium	Roth, Karlsruhe
Leupeptin	Roth, Karlsruhe
Lipofectamine™ 2000 transfection reagent	Thermo Scientific, Schwerte
2-log ladder	NEB, Frankfurt a. M.
Methanol	J.T. Baker, Phillipsburg, NJ (US)
MgCl <sub>2</sub>	Roth, Karlsruhe
Midori Green Advance	Nippon Genetics Europe, Düren
Na <sub>3</sub> VO <sub>4</sub>	AppliChem, Darmstadt
NaCl	AppliChem, Darmstadt
Na-deoxycholate	Roth, Karlsruhe
NaF	Roth, Karlsruhe
Non-fat dried milk powder	AppliChem, Darmstadt
NP-40	Sigma Aldrich, Darmstadt
Nuclease-free H <sub>2</sub> O	Braun, Melsungen
Oligo dT(23) VN	NEB, Frankfurt a. M.
Opti-MEM	Thermo Scientific, Schwerte

PBS	Thermo Scientific, Schwerte
Penicillin/Streptavidin	Thermo Scientific, Schwerte
Pepstatin	Roth, Karlsruhe
Phenol	Sigma Aldrich, Darmstadt
PMSF	Roth, Karlsruhe
Protein marker IV	PeqLab, Erlangen
Purple loading dye	NEB, Frankfurt a. M.
Recombinant HIV-1 p24	Aalto, Dublin (Irland)
RNAse Inhibitor, Human Placenta	NEB, Frankfurt a. M.
Roti-Quant	Roth, Karlsruhe
RPMI medium	Thermo Scientific, Schwerte
SDS 10 %	AppliChem, Darmstadt
siRNA hnRNP A0 (s21545)	Thermo Scientific, Schwerte
siRNA negative control No. 2	Thermo Scientific, Schwerte
siRNA SRSF1 (s12727)	Thermo Scientific, Schwerte
Streptavidin MicroBeads	Miltenyi Biotec, Bergisch Gladbach
10x TBE	Thermo Scientific, Schwerte
TEMED	AppliChem, Darmstadt
4-thiouridine	Sigma Aldrich, Darmstadt
TPA	Sigma Aldrich, Darmstadt
TransIT <sup>®</sup> -LT1 transfection reagent	Mirus Bio LLC, Madison, WI (US)
Tris-glycine (10x)	Bio-Rad, Feldkirchen
Tris-HCl, pH 6.8, 0.5 M	Bio-Rad, Feldkirchen
Tris-HCl, pH 8.8, 1.5 M	Bio-Rad, Feldkirchen
TRIzol	Zymo Research, Freiburg
Trypan blue	Thermo Scientific, Schwerte
Trypsin-EDTA 0.05 %	Thermo Scientific, Schwerte
Tween-20	AppliChem, Darmstadt
X-Gal	Sigma Aldrich, Darmstadt



## 2.2. Kits

**Table 2-2:** Commercially available Kits.

Kit	Manufacturer
ELISA-Light™ Immunoassay System	Thermo Scientific, Schwerte
HIV-1 p24 ELISA Kit	Aalto, Dublin (Irland)
Luna® Universal qPCR Master Kit	NEB, Frankfurt a. M.
Luna® Universal One-Step RT-qPCR Kit	NEB, Frankfurt a. M.
Monarch® DNA Gel Extraction Kit	NEB, Frankfurt a. M.
Monarch® PCR&DNA Cleanup Kit	NEB, Frankfurt a. M.
Monarch® Plasmid Miniprep Kit	NEB, Frankfurt a. M.
NEB® PCR Cloning Kit	NEB, Frankfurt a. M.
ProtoScript® II First Strand cDNA Synthesis Kit	NEB, Frankfurt a. M.
QIAamp Viral RNA Mini Kit	Qiagen, Hilden
QIAGEN RNeasy Mini Kit	Qiagen, Hilden
QIAshredder	Qiagen, Hilden
ZymoPURE™ II Plasmid Midiprep Kit	Zymo Research, Freiburg

## 2.3. Cell lines

**Table 2-3:** Cell lines.

Cell line	Features
<b>HEK293T</b>	HEK293T cells derive from primary human embryonic kidney cells and have been transformed with adenovirus type 5 DNA. They express the SV40 large T-antigen to enable replication of SV40 origin of replication plasmids. (ATCC CRL-3216).
<b>TZM-bl</b>	TZM-bl cells are HeLa derived cells generated from JC.53 cells, which express surface receptor CD4 and co-receptors CXCR4 and CCR5. These cells harbor both a firefly luciferase and a $\beta$ -galactosidase cassette under the control of the HIV-1 LTR promoter and thus allow quantitative analysis of an HIV-1 infection. (HIV Reagent Program ARP-8129)

<b>THP-1</b>	THP-1 cells are monocytic cells derived from an acute monocytic leukemia. Differentiation into macrophage-like cells using TPA renders the cell line susceptible to HIV-1 infection. (ATCC TIB-202)
<b>Jurkat</b>	Jurkat cells are T lymphocyte cells derived from an acute T-cell leukemia and susceptible to infection with HIV-1. This cell line is used as model system for HIV-1 infection in T-cells. (ATCC TIB-152)
<b>RPE-ISRE-luc</b>	RPE-ISRE-luc cells are human retinal pigment epithelial cells (RPE), stably transfected with a plasmid harboring the firefly luciferase gene under the control of the IFN-stimulated response element (ISRE) (277).

## 2.4. Oligonucleotides

**Table 2-4:** Oligonucleotides used for cloning, RT-qPCR and RT-PCR.

<u>Primer</u>	<u>Primer Sequence (5'-3')</u>	<u>Target</u>
MW_1001	CATCGAGCAC GGCATCGTCA	ACTB fwd
MW_1002	TAGCACAGCC TGGATAGCAA C	ACTB rev
MW_1003	TGCACCACCA ACTGCTTA	GAPDH fwd
MW_1004	GGATGCAGGG ATGATGTTC	GAPDH rev
MW_1005	GAGAGGCAGC GAACTCATCT	ISG15 fwd
MW_1006	AGGGACACCT GGAATTCGTT	ISG15 rev
MW_1007	TTTGTATCGG CCTGTGTGAA TG	IRF1 fwd
MW_1008	AAGCATGGCT GGGACATCA	IRF1 rev
MW_1009	GAGATGGCAC TGGTGTCTGTG	SRSF1 fwd
MW_1010	TGCGACTCCT GCTGTTGCTT C	SRSF1 rev
MW_1092	GGTAACGGCT TCGGCGGCTT	hnRNP A0 fwd
MW_1093	ATAGCCACCC CCACCGCCAT	hnRNP A0 rev
MW_1246	AACGATAACG GCGGCGACGG	hnRNP A0 complete CDS fwd
MW_1247	TGACCCCACT TGGGCTGTTG	hnRNP A0 complete CDS rev
MW_1248	GGTTCTGGAT CCGAGAATTC TCAGTTGTGT AA	hnRNP A0 w/ restriction sites fwd
MW_1249	TCTAGACTCG AGTTAGAAGG AGCTGCCTC	hnRNP A0 w/ restriction sites rev
MW_0001	CGCAAATGGG CGGTAGGCGTG	CMV fwd
MW_0010	TAGAAGGCAC AGTCGAGG	BGH rev
MW_3380	CAATACTACT TCTTGTGGGT TGG	HIV-1 4 kb mRNA class
MW_3384	CTTGAAAGCG AAAGTAAAGC	HIV-1 2 kb-, 4 kb-, tat mRNA class

MW_3323	CTGAGCCTGG GAGCTCTCTG GC	HIV-1 exon 1 fwd
MW_3324	GGGATCTCTA GTTACCAGAG	HIV-1 exon 1 rev
MW_3387	TTGCTCAATG CCACAGCCAT	HIV-1 exon 7 fwd
MW_3388	TTTGACCACT TGCCACCCAT	HIV-1 exon 7 rev
MW_3389	TTCTTCAGAG CAGACCAGAG C	HIV-1 unspliced mRNA fwd
MW_3390	GCTGCCAAAG AGTGATCTGA	HIV-1 unspliced mRNA rev
MW_3391	TCTATCAAAG CAACCCACCT C	HIV-1 multiply spliced mRNA fwd
MW_3392	CGTCCCAGAT AAGTGCTAAG G	HIV-1 2 kb mRNA class HIV-1 multiply spliced mRNA rev
MW_3395	GGCGACTGGG ACAGCA	HIV-1 vif mRNA fwd HIV-1 tat2 mRNA fwd HIV-1 exon 2 inclusion mRNA fwd
MW_3396	CCTGTCTACT TGCCACAC	HIV-1 vif mRNA rev
MW_3397	CGGCGACTGA ATCTGCTAT	HIV-1 vpr mRNA fwd HIV-1 tat3 mRNA fwd HIV-1 exon 3 inclusion mRNA fwd
MW_3398	CCTAACACTA GGCAAAGGTG	HIV-1 vpr mRNA rev
MW_3381	CGGCGACTGA ATTGGGTGT	HIV-1 tat1 mRNA fwd
MW_3382	TGGATGCTTC CAGGGCTC	HIV-1 tat1 mRNA rev HIV-1 tat3 mRNA rev HIV-1 tat mRNA class
MW_3393	CCGCTTCTTC CTTGTTATGT C	HIV-1 exon 3 inclusion mRNA rev
MW_3385	CCGCTTCTTC CTTCCAGAG G	HIV-1 exon 2 inclusion mRNA rev
MW_3386	ACCCAATTCT TTCCAGAGG	HIV-1 tat2 mRNA rev

All oligonucleotides were purchased from Metabion (Planegg). Positions of the primers on the HIV-1 genome are indicated in (Supplementary Figure 1)

## 2.5. Plasmids

**Table 2-5:** Plasmids used for transfection or cloning.

Plasmid	Features
pMiniT 2.0	This plasmid contains an origin of replication, an ampicillin-resistance cassette and a toxic minigene cloning site. This vector was used as a cloning vector. (NEB #N0312AVIAL)
pMiniT2.0-hnRNP A0	This plasmid contains the coding sequence for hnRNP A0 cloned into the pMiniT 2.0 backbone (see Chapter 3.2.8.8.).

pMiniT2.0-hnRNP A0 CDS w/ restriction sites	This plasmid contains the coding sequence for hnRNP A0 flanked by restriction sites for BamHI and XhoI cloned into the pMiniT 2.0 backbone (see Chapter 3.2.8.8.).
pcDNA3.1(+)	This mammalian expression vector contains an origin of replication, a multiple cloning site, an ampicillin- and neomycin-resistance cassette and a CMV promoter. This plasmid was used as empty vector to normalize DNA amounts during transfection and as a cloning vector. (Invitrogen #V79020)
pcDNA-FLAG-SF2	This plasmid contains the coding sequence for SRSF1 cloned into the pcDNA3.1(+)-backbone, including a FLAG-tag at the N-terminus. This plasmid was a gift from Honglin Chen. (Addgene # 99021)
pcDNA-hnRNPA0	This plasmid contains the coding sequence for hnRNP A0 cloned into the pcDNA3.1(+)-backbone, including an NLS- and a FLAG-tag at the N-terminus (see Chapter 3.2.8.8.).
pNL4-3	This plasmid codes for the full-length genome of the replication competent and infectious HIV-1 molecular clone NL4-3 (subtype B). The virus is X4-tropic. (HIV Reagent Program ARP-114)
pNL4-3 PI952	This plasmid codes for the full-length genome of the replication competent and infectious HIV-1 molecular clone NL4-3. The V3 loop sequence of NL4-3 was exchanged with the V3 loop sequence of the primary isolate PI952. The virus is dual-tropic (370).
pNL4-3 (AD8)	This plasmid codes for the full-length genome of the replication competent and infectious HIV-1 molecular clone NL4-3. In the gp41 region, a 1.7 kb fragment was exchanged with the corresponding sequence from the AD8 clone. The virus is R5-tropic. (HIV Reagent Program ARP-11346)
pNL4-3 eGFP	This plasmid codes for the full-length genome of the replication competent and infectious HIV-1 molecular clone

NL4-3. The sequence of eGFP was inserted into the *nef* open reading frame, resulting in a Nef-eGFP fusion protein (487).

## 2.6. Antibodies

**Table 2-6:** Antibodies used for Western Blot or ELISA.

<u>Antibody</u>	<u>Host</u>	<u>Dilution</u>	<u>Manufacturer</u>
<b>Primary antibodies</b>			
$\alpha$ -GAPDH (ab181602)	rabbit	1:50,000	abcam, Cambridge (UK)
$\alpha$ -hnRNP A0 (ab197023)	rabbit	1:1,000	abcam, Cambridge (UK)
$\alpha$ -SRSF1 (AB_2533079)	mouse	1:500	Invitrogen, Darmstadt
$\alpha$ -p24 (D7320)	sheep	1:1,300	Aalto Bio Reagents, Dublin (Ireland)
<b>Secondary antibodies</b>			
$\alpha$ -mouse (315-035-048)	rabbit	1:10,000	Jackson ImmunoResearch
$\alpha$ -rabbit (ab97051)	goat	1:10,000	abcam, Cambridge (UK)
$\alpha$ -p24 (BC 1071-AP)	mouse	1:5,000	Aalto Bio Reagents, Dublin (Ireland)

## 2.7. Enzymes

**Table 2-7:** Enzymes used for restriction digest, DNA digest, RT-PCR, RT or ligation.

<u>Enzyme</u>	<u>Manufacturer</u>
BamHI-HF	NEB, Frankfurt a. M.
DNase I	NEB, Frankfurt a. M.
HindIII	NEB, Frankfurt a. M.
GoTaq G2 DNA Polymerase	Promega, Mannheim
Platinum Taq DNA Polymerase	Invitrogen, Darmstadt
ProtoScript II Reverse Transcriptase	NEB, Frankfurt a. M.
StuI	NEB, Frankfurt a. M.
SuperScript III Reverse Transcriptase	Thermo Scientific, Schwerte
T4 DNA Ligase	NEB, Frankfurt a. M.

Xbal	NEB, Frankfurt a. M.
XhoI-HF	NEB, Frankfurt a. M.

## 2.8. Buffers and solutions

**Table 2-8:** Buffers and solutions.

<u>Solution</u>	<u>Components</u>
10x biotinylation buffer	100 mM Tris, pH 7.4 10 mM EDTA H <sub>2</sub> O
Blocking buffer	5 % non-fat dried milk powder TBS-T
Blotting buffer	1x Tris-glycine 20 % MeOH H <sub>2</sub> O
Coating buffer	100 mM NaHCO <sub>3</sub> , pH 8.5 H <sub>2</sub> O
10x ELISA-Light Assay buffer	200 mM Tris, pH 9.8 10 mM MgCl <sub>2</sub> H <sub>2</sub> O
Fixation solution (X-Gal assay)	0.25 % glutaraldehyde 0.9 % formaldehyde PBS
RIPA buffer	50 mM Tris-HCl, pH 7.5 150 mM NaCl 0.2 mM PMSF 0.1 mM Na <sub>3</sub> VO <sub>4</sub> 1 µg/ml Pepstatin 1 µg/ml Leupeptin 50 mM NaF 1 % NP-40 1 % Na-deoxycholate

	0.1 % SDS 1 mM DTT 2x Complete™ Protease Inhibitor Cocktail H <sub>2</sub> O
SDS-PAGE buffer	1x Tris-glycine 0.1 % SDS H <sub>2</sub> O
5x SDS sample buffer	60 mM Tris-HCl, pH 6.8 24 % glycerol 1 % bromophenol blue 14.4 mM β-mercaptoethanol
Staining solution (X-Gal assay)	4 mM K <sub>3</sub> [Fe(CN) <sub>6</sub> ] 4 mM K <sub>4</sub> [Fe(CN) <sub>6</sub> ] 2 mM MgCl <sub>2</sub> 0.4 mg/ml X-Gal PBS
10x TBE	1 M Tris 0.9 M boric acid 0.01 M EDTA H <sub>2</sub> O
TBS	50 mM Tris 150 mM NaCl H <sub>2</sub> O
TBS-T	1x TBS 0.1 % Tween-20 H <sub>2</sub> O

## 2.9. Bacteria Cells

The *Escherichia coli* (*E. coli*) strain NEB® 10-beta Competent *E. coli* (NEB) was used for transformation and amplification of plasmid DNA. This bacteria strain has the genotype  $\Delta(ara-leu) 7697 araD139 fhuA \Delta lacX74 galK16 galE15 e14- \phi 80dlacZ\Delta M15 recA1 relA1$

*endA1 nupG rpsL (Str<sup>R</sup>) rph spoT1 Δ(mrr-hsdRMS-mcrBC)*. Bacteria were stored at -80 °C.

## 2.10. Viruses

For information about the viruses used for infection experiments in this work, please refer to the respective plasmids pNL4-3, pNL4-3 PI952, pNL4-3 (AD8) and pNL4-3 eGFP, which are described in (Chapter 2.5.).

## 2.11. Material

**Table 2-9:** Material.

<u>Material</u>	<u>Manufacturer</u>
Amersham™ Protran® 0.45 µm Nitrocellulose Blotting Membrane	Merck, Darmstadt
Beakers (50, 100, 250 ml)	Schott, Mainz
Cell culture dishes (10 cm)	Greiner Bio One, Frickenhausen
Cell culture flasks (T25, T75, T175)	Greiner Bio One, Frickenhausen
Cell culture plates (6-well, 12-well, 96-well)	Greiner Bio One, Frickenhausen
Centrifuge tubes (15, 50 ml)	Greiner Bio One, Frickenhausen
Cryo tubes (2 ml)	Greiner Bio One, Frickenhausen
Erlenmeyer flasks (250 , 500 ml)	Schott, Mainz
Gloves Vasco Nitril	Braun, Melsungen
Laboratory Bottles (0.5, 1 l)	Schott, Mainz
LeucoSEP tubes	Greiner Bio One, Frickenhausen
MACS® MultiStand	Miltenyi Biotec, Bergisch Gladbach
MACS® SmartStrainers (30 µm)	Miltenyi Biotec, Bergisch Gladbach
Microcentrifugation tubes (1.5, 2 ml, Safe-Lock)	Eppendorf, Hamburg
Mr. Frosty™	Thermo Scientific, Schwerte
Nunc™ 96-well cell culture plate (white)	Thermo Scientific, Schwerte
Parafilm	Bemis Company, Amsterdam (Netherlands)
PCR tubes (0.2 ml, PP)	Sarstedt, Nümbrecht
Pipette tips (10, 100, 200, 1,000 µl)	StarLab, Ahrensberg



ROTILABO® single-use cuvettes (UV-permeable)	Roth, Karlsruhe
Rotor-Gene® Style 4-Strip tubes and Caps (0.1 ml, PP)	StarLab, Ahrensberg
Serological pipettes (5, 10, 25 ml)	Greiner Bio One, Frickenhausen
µMACS™ columns	Miltenyi Biotec, Bergisch Gladbach
Whatman paper	Roth, Karlsruhe

## 2.12. Instruments

**Table 2-10:** Instruments.

<u>Instrument</u>	<u>Manufacturer</u>
ADVANCED Fluorescence and ECL Imager	Intas, Göttingen
BioPhotometer Plus	Eppendorf, Hamburg
Centrifuge 5415R	Eppendorf, Hamburg
Centrifuge 5417R	Eppendorf, Hamburg
Centrifuge 5424	Eppendorf, Hamburg
Centrifuge 5810R	Eppendorf, Hamburg
Digital Vortex Mixer	VWR, Darmstadt
GloMax®-Multi Detection System	Promega, Mannheim
Heraeus Megafuge 3.0R	Thermo Scientific, Schwerte
HERAcell® 240 CO <sub>2</sub> Incubator	Thermo Scientific, Schwerte
HERAcell® 240i CO <sub>2</sub> Incubator	Thermo Scientific, Schwerte
Leica DM IL LED	Leica, Wetzlar
Liebherr Comfort freezer -20 °C	Liebherr, Bulle (Switzerland)
M2000 RealTime System	Abbott, Wiesbaden
Max Q 6000 Incubator	Thermo Scientific, Schwerte
Mini Protean® Tetra Vertical Electrophoresis Cell	Bio-Rad, Feldkirchen
Mini Trans-Blot® Cell	Bio-Rad, Feldkirchen
MJ MINI Personal Thermal Cycler	Bio-Rad, Feldkirchen
NanoDrop™ 2000/2000c Spectrophotometer	Thermo Scientific, Schwerte
Neubauer cytometer	Marienfeld Superior
Nikon TMS Inverted Phase Microscope	Nikon, Düsseldorf

Eppendorf Research® plus pipettes	Eppendorf, Hamburg
RotorGene Q	Qiagen, Hilden
Spark® Multimode Reader	Tecan, Crailsheim
Thermo Herasafe™ Safety Workbench	Thermo Scientific, Schwerte
Thermomixer comfort	Eppendorf, Hamburg
Thermo Scientific Forma -86°C Series 900	Thermo Scientific, Schwerte
Water bath	Julabo, Seelbach
Zeiss Primo Vert	Zeiss, Oberkochen

### 2.13. Software

**Table 2-11:** Software.

<u>Software</u>	<u>Developer</u>
Adobe Illustrator CC 2019	Adobe Systems, San José, CA (US)
Excel 2013	Microsoft, Redmond, WA (US)
Geneious Pro 5.1.7.	Biomatters, Auckland (New Zealand)
GraphPad Prism 6	GraphPad Software, San Diego, CA (US)
ImageJ 1.52n	NIH, Bethesda, MD (US)
PowerPoint 2013	Microsoft, Redmond, WA (US)
Q-Rex 1.1.0.4.	Qiagen, Hilden
Word 2013	Microsoft, Redmond, WA (US)

---

### **3. Methods**

#### **3.1. Cell culture**

##### **3.1.1. Maintenance of human cell lines**

HEK293T, TZM-bl and RPE-ISRE-luc reporter cells were maintained in Dulbecco's modified Eagle medium (DMEM) supplemented with 10 % (v/v) heat-inactivated fetal calf serum (FCS) and 1 % (v/v) Penicillin/Streptomycin (P/S, 10,000 U/ml). THP-1 and Jurkat cells were maintained in Roswell Park Memorial Institute 1640 medium (RPMI) supplemented with 20 % (THP-1) or 10 % (Jurkat) (v/v) heat-inactivated FCS and 1 % (v/v) P/S. All cell lines were maintained at 37 °C and 5 % CO<sub>2</sub>.

Adherent cell lines were kept in T75-flasks (75 cm<sup>2</sup>). For passaging, the medium was discarded and cells were washed with Dulbecco's phosphate buffered saline (PBS). Cells were coated with 2 ml of Trypsin-EDTA and incubated for 5 min at 37 °C. 10 ml of fresh medium was added to the flask to inactivate Trypsin and detached cells were washed off the surface. 1 ml of the cell suspension was added to a newly prepared flask with 12 ml of fresh medium and incubated for further use. Passaging of adherent cells was performed every three to four days.

Suspension cells were kept in T25-flasks (25 cm<sup>2</sup>). For passaging, the cell suspension was transferred to a 50 ml tube and spun down for 5 min at 500 rcf. The supernatant was discarded and 10 ml of PBS were added. After 5 min of centrifugation at 500 rcf, the supernatant was again discarded and the cells were resuspended in 10 ml of fresh medium. 2 ml of cell suspension were added to a newly prepared flask with 12 ml of fresh medium and incubated for further use. Passaging of suspension cells was performed every three to four days.

##### **3.1.2. Differentiation of THP-1 monocytes**

THP-1 monocytes were seeded at 500,000 cells per well in 6-well plates. 12-O-tetradecanoylphorbol-13-acetate (TPA) was added at a concentration of 100 nM and cells were incubated for 5 days at 37 °C and 5 % CO<sub>2</sub>. Differentiation into macrophage-like cells was monitored via cell morphology and adhesion (Figure 3-1).

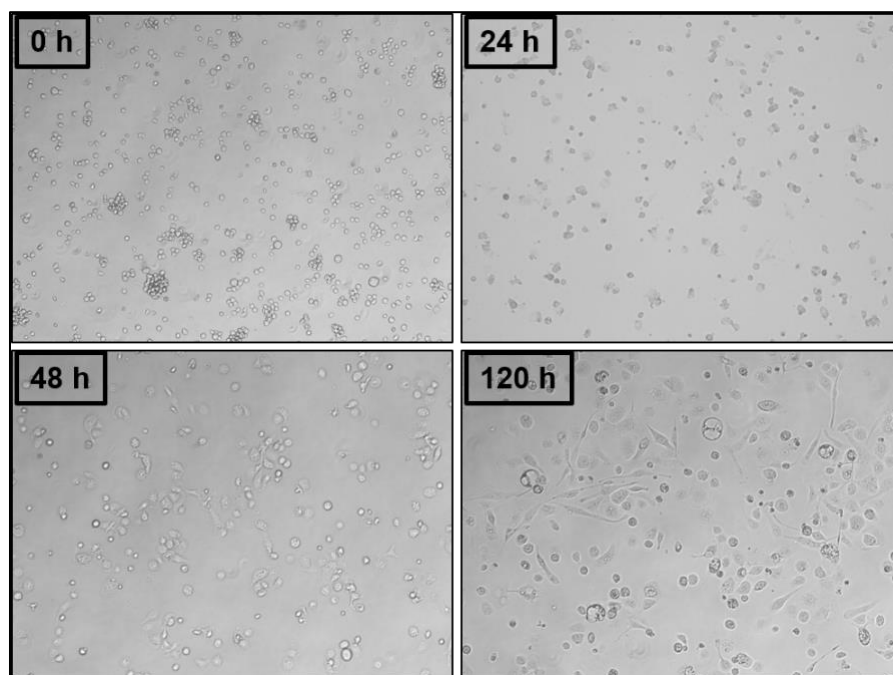


**Figure 3-1: Differentiation of THP-1 monocytic cells.** THP-1 cells were differentiated for 120 h at a final concentration of 100 nM 12-*O*-tetradecanoylphorbol-13-acetate (TPA).

### 3.1.3. Stimulation of cells with interferon (IFN)

IFN $\alpha$  subtypes were produced as described elsewhere (277) and provided by PD Dr. Kathrin Sutter (Institute for Virology, University Hospital Essen, Essen). IFN $\gamma$  was purchased from PBL assay science (Piscataway, US). IFN was added in fresh medium at a final concentration of 10 ng/ml to the cells. Cells were incubated at 37 °C and 5 % CO<sub>2</sub> for the indicated amount of time before being harvested.

### 3.1.4. Infection of cells

Cells were seeded 24 h prior to infection and incubated at 37 °C. THP-1 cells were differentiated prior to infection as indicated (Chapter 3.1.2.). Cells were infected with the respective virus stock or mock-infected with a spin-inoculation for 2 h at 1,500x g. An MOI of 1 was used to statistically infect every cell. After the spin-inoculation, cells were incubated at 37 °C until they were harvested. All indicated treatments were carried out 16 h post infection.

### 3.1.5. Transient transfection

Cells were counted using trypan blue stain (0.4 % (v/v)) and a Neubauer hemocytometer. For transient transfection,  $2.5 \times 10^5$  cells were seeded per well in 2 ml of the respective

medium in 6-well plates and incubated overnight at 37 °C and 5 % CO<sub>2</sub>. The next day, cells were transfected with the indicated expression plasmids using TransIT<sup>®</sup>-LT1 (Mirus Bio LLC). Plasmids were added to 250 µl OptiMEM serum-free medium before adding TransIT<sup>®</sup>-LT1 transfection reagent at a ratio of 2:1 to the DNA. The transfection mixture was incubated for 20 min at room temperature before being added dropwise to the cells. Plates were gently shaken and incubated at 37 °C and 5 % CO<sub>2</sub> before being harvested at the indicated time point.

### **3.1.6. siRNA gene silencing**

HEK293T or RPE-ISRE-luc cells were counted using trypan blue stain (0.4 % (v/v)) and a Neubauer hemocytometer.  $2.5 \times 10^5$  cells were seeded per well in 2 ml of the respective medium in 6-well plates and incubated overnight at 37 °C and 5 % CO<sub>2</sub>. The next day, cells were transiently co-transfected with the indicated expression plasmid and siRNA at a final concentration of 8 nM using Lipofectamine 2000 (Thermo Scientific). Lipofectamine 2000 transfection reagent, plasmid and siRNA were added separately to OptiMEM serum-free medium. Then, all reagents were combined and the mixture was incubated for 5 min before being added dropwise to the cells. Plates were gently shaken and incubated at 37 °C and 5 % CO<sub>2</sub> before being harvested at the indicated time point. The following siRNAs were used in this work: Silencer Select Negative Control No. 2 siRNA (Thermo Scientific) as control siRNA, s12727 (Thermo Scientific) as SRSF1-specific siRNA and s21545 (Thermo Scientific) as hnRNP A0-specific siRNA.

### **3.1.7. Isolation of peripheral blood mononuclear cells (PBMCs)**

Peripheral blood mononuclear cells (PBMCs) were isolated from whole blood samples by Ficoll density gradient centrifugation. This method enables the separation by density of erythrocytes, granulocytes and lymphocytes.

For the isolation of PBMCs, LeucoSEP tubes were used, which contain a polyethylene-separation disc. 15 ml of Bicol separation medium was added to the tube and centrifuged for 1 min at 1,000 rcf until the separation medium passed the separation disc. Next, 15 ml of whole blood were added to the tube and centrifuged for 15 min at 1,000 rcf while disabling the brake function of the centrifuge. The blood components were separated via density gradient. While the upper phase consisted of plasma, the interphase contained

the PBMCs. Below the separation disc, the cell pellet consisted of granulocytes and erythrocytes. After carefully removing the upper phase, the PBMC-containing interphase was transferred to a fresh tube and washed with 30 ml PBS for 5 min at 1,000 rcf. After removing the supernatant, another wash step was carried out. The cell pellet was lysed using buffer RLT and total RNA was isolated as described in (Chapter 3.2.1.). Plasma viral load was determined using the RealTime HIV-1 m2000 test system (Abbott) according to the manufacturer's instructions.

PBMCs were provided from PD Dr. med. Stefan Esser (Clinic for Dermatology, HPSTD, University Hospital Essen, Essen). Isolation of the PBMCs was performed by Dr. Carina Elsner (Institute for Virology, University Hospital Essen, Essen). This study has been approved by the Ethics Committee of the Medical Faculty of the University of Duisburg-Essen (14-6155-BO, 16-7016-BO, 19-8909-BO). Form of consent was not obtained since the data were analyzed anonymously.

## **3.2. Methods in molecular biology**

### **3.2.1. RNA isolation**

Total cellular RNA was extracted using RNeasy® Mini Kit (Qiagen). Cells incubated in 6-well plates were washed with PBS and lysed in 350 µl buffer RLT with 1 % β-mercaptoethanol. The lysate was homogenized using QIAshredder spin columns (Qiagen) and centrifugation at 14,000 rcf for 2 min. 1 Volume of ethanol (70 %) was added to the lysate, mixed well and transferred to RNeasy Mini spin columns. Centrifugation steps were carried out at 10,000 rcf for 30 s. The sample was subsequently washed with 700 µl buffer RW1 and twice with 500 µl buffer RPE. Finally, RNA was eluted into a fresh RNase-free tube with 30 µl of RNase-free water after 1 min of incubation on column. RNA concentration and quality was monitored via photometric measurement using NanoDrop2000c. RNA was stored at -80 °C.

### **3.2.2. cDNA synthesis from total cellular and viral RNA**

For reverse transcription, 1 µg total RNA was digested with 2 U of DNase I for 20 min at 37 °C. This step ensured the removal of contaminating traces of plasmid DNA. DNase was then heat inactivated at 70 °C for 5 min.

All samples containing HIV-1 viral RNA were reverse transcribed using SuperScript III Reverse Transcriptase (Thermo Scientific). 500 ng (5  $\mu$ l) of DNase-digested RNA were pre-incubated for 5 min at 65 °C with 1  $\mu$ l of Oligo d(T)23 VN (50  $\mu$ M), 4  $\mu$ l of deoxyribonucleotide triphosphate Mix (10 mM each) and 3  $\mu$ l of RNase-free water. After cooling down on ice for 1 min, 4  $\mu$ l 5x First Strand Buffer (250 mM Tris-HCl, 375 mM KCl, 15 mM MgCl<sub>2</sub>), 1  $\mu$ l dithiothreitol (DTT, 100 mM), 1  $\mu$ l RNase Inhibitor Human Placenta (40 U) and 1  $\mu$ l SuperScript III Reverse Transcriptase (200 U) were added. cDNA synthesis was performed at 50 °C for 60 min and 72 °C for 15 min.

For all other samples, reverse transcription was performed using ProtoScript II First Strand cDNA synthesis kit (NEB). 500 ng (5  $\mu$ l) of DNase-digested RNA were pre-incubated for 5 min at 65 °C with 2  $\mu$ l of Oligo d(T)23 VN (50  $\mu$ M) and 1  $\mu$ l of RNase-free water. After cooling down on ice for 1 min, 10  $\mu$ l 2x ProtoScript II Reaction Mix and 2  $\mu$ l 10x ProtoScript II Enzyme Mix were added. cDNA synthesis was performed at 42 °C for 60 min and 80 °C for 5 min.

### 3.2.3. Semi-quantitative PCR analysis (RT-PCR)

Qualitative analysis of HIV-1 mRNAs was performed using GoTaq G2 DNA Polymerase (Promega). 2  $\mu$ l cDNA were used as template for semi-quantitative PCR reactions. The reaction mixture included 10  $\mu$ l 5x Green GoTaq Reaction buffer, 1  $\mu$ l deoxyribonucleotide triphosphate Mix (10 mM each), 1  $\mu$ l of the respective forward and reverse primer (10  $\mu$ M), 0.25  $\mu$ l GoTaq G2 DNA Polymerase (1.25 U) and 34.75  $\mu$ l nuclease-free water. The samples were incubated in a MJ Mini Personal thermal cycler (Bio-Rad) with the following program:

	Initial denaturation	2 min	95°C
X Cycles	[	Denaturation	1 min 95 °C
		Annealing	0.5 min X °C
		Elongation	1 min 72 °C
		Final elongation	5 min 72 °C
	Cool down		4 °C

For the PCR reaction using GAPDH or HIV-1 exon 7 specific primers, the annealing temperature was set to 56 °C and 28 cycles were run. For all PCR reactions analyzing

HIV-1 2 kb-, 4 kb- and *tat* specific mRNA classes, the annealing temperature was set to 53 °C and 35 cycles were run. The evaluation of the PCR reactions occurred via DNA separation on 12 % polyacrylamide gels (Chapter 3.2.4.).

### 3.2.4. Separation of DNA fragments by polyacrylamide (PAA) gel electrophoresis

PCR products were separated on non-denaturing polyacrylamide (PAA) gels (12 %). The gels were prepared according to the recipe (Table 3-1) and run in 1 x TBE running buffer for 1-4 h (depending on the sample) at 130 V using the Mini-PROTEAN® Tetra Vertical Electrophoresis Cell (Bio-Rad).

**Table 3-1: Recipe for one 12 % polyacrylamide (PAA) gel used for DNA separation.**

<u>Reagent</u>	<u>Volume</u>
10 x TBE	0.75 ml
Polyacrylamide (PAA)	3.125 ml
10 % APS	60 µl
TEMED	4 µl
H <sub>2</sub> O	3.75 ml

The gels were then stained for 10 min with Midori green Advanced DNA stain (Nippon Genetics) and visualized with ADVANCED Fluorescence and ECL Imager (Intas Science Imaging).

### 3.2.5. Quantitative real-time PCR analysis (RT-qPCR)

Quantitative real-time SYBR green PCR (RT-qPCR) was performed using Luna® Universal qPCR Master Mix (NEB). 1 µl of cDNA was used as template and added to 10 µl 2x Luna® Universal qPCR Master Mix, 0.5 µl of the respective forward and reverse primer (10 µM) and 8 µl nuclease-free water. The RT-qPCR was performed with the Qiagen RotorGene Q (Qiagen) using the following standard program:



	Initial denaturation	60 s	95°C	
45 Cycles	[	Denaturation	15 s	95 °C
		Annealing / Extension	30 s	60 °C
	Melting Curve	90 s	60 °C - 95 °C (4 s / 1 °C)	

Fluorescence acquisition occurred during each cycle at the extension step. Product specificity was determined via melting curve. All data was normalized to  $\beta$ -actin or GAPDH expression, which were used as housekeeping genes, to enable relative comparison between samples. Expression levels of the target genes were calculated using the  $2^{(-\Delta\Delta CT)}$  method, where the cycle threshold (CT) represents the value at which the fluorescent signal exceeds a defined baseline (364).

### 3.2.6. One-Step quantitative real-time PCR analysis (One-Step RT-qPCR)

Since SRSF1 is very low abundant, One-Step quantitative real-time PCR analysis (One-Step RT-qPCR) was performed for reverse transcription and subsequent DNA amplification using Luna<sup>®</sup> Universal One-Step RT-qPCR Kit (NEB). In a total volume of 20  $\mu$ l, 500 ng RNA were added to 10  $\mu$ l 2x Luna Universal One-Step reaction mix, 1  $\mu$ l 20x Luna WarmStart<sup>®</sup> RT Enzyme Mix and 0.8  $\mu$ l of the respective forward and reverse primer (10  $\mu$ M). The One-Step RT-qPCR was performed with the Qiagen RotorGene Q (Qiagen) using the following standard program:

	Reverse Transcription	10 min	55 °C	
	Initial denaturation	60 s	95°C	
45 Cycles	[	Denaturation	10 s	95 °C
		Annealing / Extension	30 s	60 °C
	Melting Curve	90 s	60 °C - 95 °C (4 s / 1 °C)	

Fluorescence acquisition occurred during each cycle at the extension step. Melt curves were analyzed to ensure specificity of the product. All data was normalized to  $\beta$ -actin or GAPDH expression, which were used as housekeeping genes, to enable relative comparison between samples. Expression levels of the target genes were calculated

using the  $2^{(-\Delta\Delta CT)}$  method, where the cycle threshold (CT) represents the value at which the fluorescent signal exceeds a defined baseline (364).

### 3.2.7. Western Blot analysis

Adherent cells were detached from the plate using Trypsin-EDTA and transferred into a fresh tube. After washing the cells with PBS and centrifuging for 5 min at 500 rcf, 100  $\mu$ l RIPA buffer (50 mM Tris-HCl pH 7.5, 150 mM NaCl, 0.2 mM PMSF, 0.1 mM  $\text{Na}_3\text{VO}_4$ , 1  $\mu$ g/ml pepstatin, 1  $\mu$ g/ml leupeptin, 50 mM NaF, 1 % NP-40, 1 % Na-deoxycholate, 0.1 % SDS, 1 mM DTT, 2x Complete Protease Inhibitor Cocktail in  $\text{H}_2\text{O}$ ) were added to up to  $1 \times 10^6$  cells and mixed by pipetting. After centrifugation of the lysate for 20 min at 14,000 rcf and 4  $^\circ\text{C}$ , the supernatant was transferred to a fresh tube. The protein concentration was determined by Bradford assay for the normalization of the samples (50). 5x SDS sample buffer (60 mM Tris-HCl pH 6.8, 24 % glycerol, 2 % SDS, 14.4 mM  $\beta$ -mercaptoethanol, 1 % bromophenol blue) was added to the samples before incubation at 95  $^\circ\text{C}$  for 10 min.

Protein separation and immunoblot were performed with the Mini-PROTEAN<sup>®</sup> Tetra Vertical Electrophoresis Cell (Bio-Rad) and the Mini Trans-Blot<sup>®</sup> Module (Bio-Rad). Proteins were separated under denaturing conditions (272) using 12 % SDS-polyacrylamide gels according to the recipe (Table 3-2).

**Table 3-2: Recipe for four 12 % SDS-polyacrylamide gels used for protein separation.**

<u>Reagent</u>	<u>Stacking gel (4 %)</u>	<u>Separating gel (12 %)</u>
30 % Acrylamide	1.32 ml	8 ml
0.5 M Tris-HCl pH 6.8	2.52 ml	-
1.5 M Tris-HCl pH 8.8	-	5 ml
10 % SDS	100 $\mu$ l	200 $\mu$ l
10 % APS	50 $\mu$ l	100 $\mu$ l
TEMED	10 $\mu$ l	10 $\mu$ l
$\text{H}_2\text{O}$	6 ml	6.72 ml

After the polymerization was complete, the gels were placed into the electrophoresis chamber and covered in SDS-PAGE running buffer (10 % Tris-glycine, 0.1 % SDS). Protein samples

and ladder were applied to the gel and protein separation was performed at 120 V for 2 h. peqGOLD protein marker IV (VWR, 10 – 170 kDa) was used as a protein standard.


The separated proteins were then transferred onto a nitrocellulose membrane using the Mini Trans-Blot® Module (Bio-Rad). 10 % Tris-glycine (20 % methanol) was used as transfer buffer and blotting was performed for 1 h at 300 mA. The membrane was blocked for 1 h with 5 % non-fat dried milk powder in TBS-T at room temperature and under agitation. The primary antibody was added at the indicated concentration (Chapter 2.6.) in 0.5 % non-fat dried milk powder in TBS-T and incubated overnight under agitation at 4 °C. The next day, the membrane was washed 5 times for 12 min in TBS-T under agitation at room temperature. The secondary antibody was added at the indicated concentration (Chapter 2.6.) in 0.5 % non-fat dried milk powder in TBS-T and incubated for 1 h under agitation at room temperature. The membrane was washed again 5 times for 12 min in TBS-T under agitation at room temperature. The membrane was finally incubated with Amersham ECL Western Blotting Detection Reagent (GE Healthcare Life Sciences) and wrapped into transparent film, before readout of the chemiluminescent signal with the ADVANCED Fluorescence and ECL Imager (Intas).

### **3.2.8. Cloning**

#### **3.2.8.1. Polymerase Chain Reaction (PCR)**

Specific DNA fragments required for cloning were amplified from cDNA of untreated HEK293T cells or plasmid DNA. PCR reaction was performed using GoTaq G2 DNA Polymerase (Promega) with 2 µl of cDNA or plasmid DNA as template. The reaction mixture included 10 µl 5x Colorless GoTaq Reaction buffer, 1 µl deoxyribonucleotide triphosphate Mix (10 mM each), 1 µl of the respective forward and reverse primer (10 µM), 0.25 µl GoTaq G2 DNA Polymerase (1.25 U) and 34.75 µl nuclease-free water. The samples were incubated in a MJ Mini Personal thermal cycler (Bio-Rad) with the following program:

---

	Initial denaturation	2 min	95°C
35 Cycles		Denaturation	1 min 95 °C
		Annealing	0.5 min 56 °C
		Elongation	1 min 72 °C
	Final elongation	5 min	72 °C
	Cool down		4 °C

The evaluation of the PCR amplicons occurred via DNA separation on 12 % PAA gels (Chapter 3.2.4.).

### 3.2.8.2. DNA purification

PCR products were purified using Monarch<sup>®</sup> PCR & DNA Cleanup Kit (NEB). Therefore, PCR samples were diluted 1:5 with DNA Cleanup binding buffer before transferring the mixture to the column. Centrifugation steps were carried out at 13,000 rcf for 1 min. After washing the spin column twice with 200 µl DNA wash buffer, the column was transferred to a fresh tube. DNA was eluted into a fresh nuclease-free tube with 10 µl of DNA elution buffer after 1 min of incubation on column.

### 3.2.8.3. Ligation

#### 3.2.8.3.1. NEB PCR Cloning Kit

PCR products were cloned into the pMiniT 2.0 vector (NEB) using the NEB PCR Cloning Kit (NEB) according to the manufacturer's instructions. This vector allows the cloning of blunt-ended or single-base overhang PCR products. The total reaction volume of 10 µl included 1 µl (25 ng) linearized pMiniT 2.0 vector, 2 µl insert (cleaned PCR product), 4 µl Cloning Mix 1, 1 µl Cloning Mix 2 and 2 µl H<sub>2</sub>O. The ligation mixture was incubated for 15 min at room temperature and transformed immediately (Chapter 3.3.1.).

#### 3.2.8.3.2. T4 DNA Ligase

Digested PCR product and pcDNA3.1(+) (Invitrogen) backbone with complementary ends were ligated using T4 DNA Ligase (NEB). The total reaction volume of 20 µl included 2 µl T4 DNA Ligase Buffer, 1 µl T4 DNA Ligase, 50 ng vector DNA and 37.5 ng insert (approximate molar ratio of 1:3). The ligation reaction was incubated overnight at 16 °C.

---

The next day, the ligase was heat-inactivated for 10 min at 65 °C and the ligation mixture was used for bacterial transformation (Chapter 3.3.1.).

#### **3.2.8.4. Restriction enzyme digest**

Plasmids and PCR products were digested by restriction enzymes according to the manufacturer's instructions. The restriction digest mixture included 1 µg of the respective plasmid or 10 µl of the PCR product (Chapter 3.2.8.1.), 1 µl of each restriction enzyme and 2 µl of CutSmart Buffer in a total volume of 20 µl. The mixture was incubated at 37 °C for 2 h. If applicable, restriction enzymes were inactivated following restriction digest.

#### **3.2.8.5. Separation of DNA fragments by agarose gel electrophoresis**

To separate the digested DNA fragments, samples were loaded on a 1 % low melting agarose gel. The gels were run for 2 h at 110 V using 1 x TBE as running buffer. Staining with Midori green Advanced DNA stain (Nippon Genetics) was used for visualization by UV-light (320 nm). Respective bands were cut out from the gel and purified for further use (Chapter 3.2.8.6.).

#### **3.2.8.6. DNA extraction from agarose gels**

DNA fragments were excised and purified from an agarose gel using the Monarch<sup>®</sup> DNA Gel Extraction Kit (NEB). Therefore, respective bands were cut out from the gel using a scalpel and transferred to a clean microcentrifuge tube. 4 volumes of Monarch Gel Dissolving Buffer were added to the gel slice and the mixture was incubated at 50 °C until the gel slice was completely dissolved. Next, the mixture was loaded onto the column. Centrifugation steps were carried out at 13,000 rcf for 1 min. The column was washed twice with 200 µl DNA Wash Buffer and transferred to a clean tube. DNA was eluted with 6 µl of DNA elution buffer after 1 min of incubation on column. DNA concentration and quality was monitored via photometric measurement using NanoDrop2000c.

#### **3.2.8.7. Sanger sequencing**

Sequence validation of the plasmid DNA and PCR products was performed using Sanger sequencing. Samples were prepared according to instructions and send to GATC. The resulting sequences were analyzed using Geneious Pro 5.1.7..

### **3.2.8.8. Construction of an hnRNP A0 expression plasmid**

The genomic sequence of hnRNP A0, including the complete coding sequence (CDS) (918 base pairs (bp)), was amplified by polymerase chain reaction (PCR) from cDNA of untreated HEK293T cells. Therefore, primers were designed with the forward primer binding 65 bp upstream of the CDS and the reverse primer binding 66 bp downstream of the CDS. The resulting PCR product was separated on a 1 % agarose gel and purified. The purified amplicon was inserted into the pMiniT 2.0 (NEB) backbone (pMiniT2.0-hnRNP A0).

A further primer pair was designed covering the complete CDS of hnRNP A0 and flanked by the restriction sites for BamHI and XhoI, respectively. A PCR was conducted using the newly designed primer pair and pMiniT 2.0-hnRNP A0 as target. The PCR product was again separated on a 1 % agarose gel and purified. The resulting amplicon contained the complete CDS of hnRNP A0 with restriction sites for BamHI and XhoI at the ends. The purified amplicon was again inserted into the pMiniT 2.0 (NEB) backbone (pMiniT 2.0-hnRNP A0 CDS w/ restriction sites).

A restriction digest of pMiniT 2.0-hnRNP A0 CDS w/ restriction sites was performed with BamHI and XhoI. The digested fragment was purified and ligated into the pcDNA3.1-(+) (Invitrogen) backbone using T4 DNA ligase (NEB) resulting in plasmid pcDNA3.1-hnRNP A0 (Figure 3-2 A). Plasmid was amplified using bacterial transformation and verified via restriction digest with StuI or HindIII/XbaI (Figure 3-2 B). Finally, Sanger sequencing was performed to verify nucleotide sequence (Figure 3-2 C).

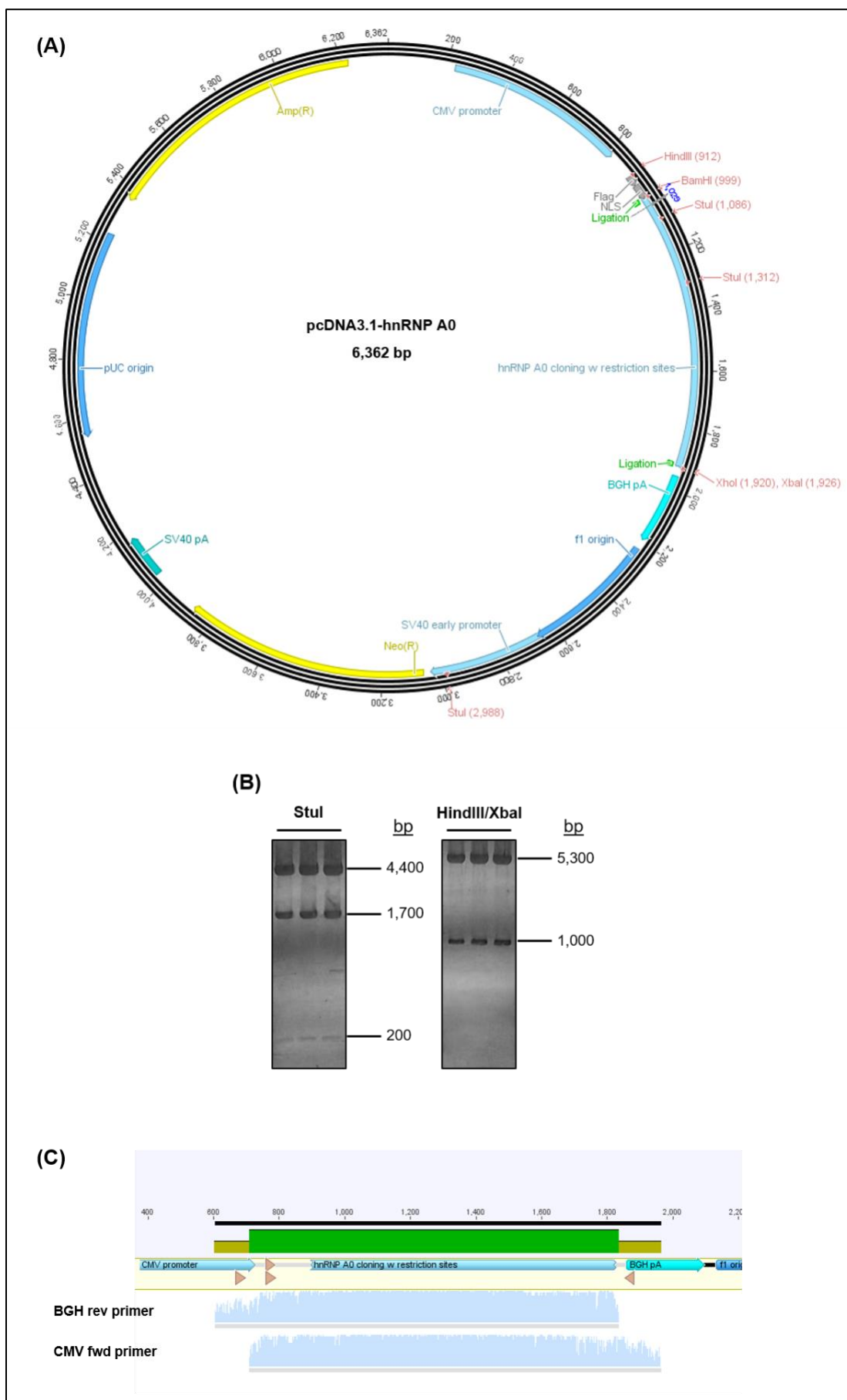


**Figure 3-2: Expression vector pcDNA3.1-hnRNP A0. (A)** Vector map of pcDNA3.1-hnRNP A0. **(B)** Restriction digest of pcDNA3.1-hnRNP A0 using *Stu*I or *Hind*III/*Xba*I. 1 µg of plasmid was digested for 2 h at 37 °C and separated on a 1 % agarose gel. **(C)** Results from Sanger sequencing of pcDNA3.1-hnRNP A0 using primers located within the CMV promoter (CMV fwd) or the BGH poly (A) signal (BGH rev).

### 3.2.9. 4sU-tagging

THP-1 cells were seeded at  $6 \times 10^6$  cells in 10 cm dishes and differentiated as explained above (Chapter 3.1.2.). IFN was added in fresh medium at a final concentration of 10 ng/ml to the cells. Cells were then incubated at 37 °C and 5 % CO<sub>2</sub> for the indicated amount of time. 30 min prior to cell harvest, 4-thiouridine (4sU) was added in fresh medium for metabolic labeling of the newly synthesized RNA to the cells at a final concentration of 500 µM. Cells were washed with PBS and lysed in 1 ml of TRIZol™ reagent, before being frozen at -80 °C overnight. The next day, lysates were thawed, 200 µl of chloroform were added and mixture was vortexed for 20 s. After centrifugation for 15 min at full speed and 4 °C, the clear upper phase was transferred to a clean tube. An equal volume of isopropanol was added and the mixture was vortexed again for 10 s, followed by centrifugation for 1 h at full speed and 4 °C. The supernatant was fully removed and the pellet washed with 800 µl EtOH (75 %). After centrifugation for 10 min at full speed and 4 °C, EtOH was removed and pellet was dried for a maximum of 5 min at 50 °C. Following the addition of 60 µl RNase-free H<sub>2</sub>O, the pellet was incubated for 1 min at 50 °C, resuspended and stored at -80 °C overnight. After thawing, RNA concentration and quality was monitored using NanoDrop2000c. For biotinylation, 100 µg RNA were added to 2 µl biotin-HPDP and 1 µl 10x biotinylation buffer per µg RNA in a total volume of 1 ml. The mixture was rotated for 2 h at room temperature in the dark. Following the biotinylation reaction, 1 ml of a phenol/chloroform solution (1:1) was added and the mixture was vortexed for 20 s. After phase separation for 3 min, the mixture was centrifuged for 5 min at 8 °C and the upper phase was transferred to a clean tube. After addition of 1/10 volume of 5 M NaCl and 1 volume isopropanol, the mixture was inverted and mixed well before centrifugation for 20 min at full speed and 8 °C. The supernatant was fully removed and the pellet washed with 1 ml EtOH (75 %). After centrifugation for 10 min at full speed and 8 °C, EtOH was removed and 100 µl RNase-free H<sub>2</sub>O were added to the pellet. The RNA was heated for 10 min at 65 °C before cooling on ice for 5 min. 100 µl of streptavidin-beads were added and the mixture was rotated for 15 min at room temperature. The



$\mu$ macs columns were placed into the magnetic stand and equilibrated with 900  $\mu$ l washing buffer. Bead-bound RNA was then applied to the column and washed subsequently three times with 900  $\mu$ l washing buffer at 65 °C and three times with 900  $\mu$ l washing buffer at room temperature. The labeled RNA was eluted using 100  $\mu$ l 100 mM DTT, followed by a second dilution with 100  $\mu$ l 100 mM DTT after 5 min. 500  $\mu$ l EtOH (100 %) and 10  $\mu$ g glycogen were added to the eluted RNA, before precipitating the RNA overnight at -20 °C. The sample was centrifuged for 15 min at full speed and 4 °C and the supernatant was removed. The pellet was washed with 1 ml EtOH (75 %) before centrifugation for 5 min at 4 °C. After complete removal of the supernatant, 20  $\mu$ l RNase-free H<sub>2</sub>O were added to the pellet. RNA concentration and quality was monitored using NanoDrop2000c.

### **3.3. Methods in microbiology**

#### **3.3.1. Transformation of bacteria**

To amplify plasmid DNA, NEB<sup>®</sup> 10-beta Competent *E. coli* (NEB) were used. 0.5  $\mu$ l of a purified plasmid DNA or 5  $\mu$ l of a ligation reaction (Chapter 3.2.8.3.) were added to 50  $\mu$ l of bacteria cell suspension and the mixture was incubated for 30 min on ice. After heat-shocking at 42 °C for 60 s, the bacteria were cooled on ice for 5 min. 950  $\mu$ l of LB medium were added before incubating for 1 h and 20 min at 37 °C and 200 rpm. Transformed bacteria were then streaked on LB agar plates containing ampicillin (100  $\mu$ g/ml) and incubated overnight at 37 °C.

#### **3.3.2. Plasmid DNA isolation from bacteria for restriction analysis**

5 ml LB medium containing ampicillin (100  $\mu$ g/ml) was inoculated with a single colony from an LB agar plate and incubated overnight at 37 °C under agitation.

Plasmid DNA was isolated using the Monarch<sup>®</sup> Plasmid Miniprep Kit (NEB). Therefore, 2 ml of the bacterial overnight culture was centrifuged at 16,000 rcf for 1 min. The supernatant was discarded and the bacterial pellet was resuspended in 200  $\mu$ l of resuspension buffer. For bacterial cell rupture, 200  $\mu$ l of lysis buffer were added and the tube was inverted 6 times. After incubating for 1 min at room temperature, 400  $\mu$ l of neutralization buffer was added and the tube was inverted until the neutralization was complete. The mixture was incubated for 2 min at room temperature and centrifuged at 16,000 rcf for 3 min. Next, the supernatant was transferred to a spin column, followed by

centrifugation at 16,000 rcf for 1 min. After washing the spin column with 200  $\mu$ l wash buffer 1 and 400  $\mu$ l wash buffer 2, with centrifugation steps of 16,000 rcf for 1 min, the column was transferred to a clean tube. Plasmid DNA was eluted at 10,000 rcf for 1 min using 30  $\mu$ l of elution buffer. Concentration and purity of the plasmid DNA was monitored at the NanoDrop2000c.

### **3.3.3. Plasmid DNA isolation from bacteria for preparation**

150 ml LB medium containing ampicillin (100  $\mu$ g/ml) was inoculated with 50  $\mu$ l of plasmid-containing bacteria from a pre-culture (Chapter 3.3.2.) or with 5  $\mu$ l of a glycerol stock (Chapter 3.3.4.) and incubated overnight at 37 °C under agitation. Plasmid DNA was isolated using the ZymoPure™ Plasmid Midiprep Kit (Zymo Research). Therefore, the bacterial overnight culture was centrifuged at 6,000 rcf for 10 min. The supernatant was discarded and the bacterial pellet was resuspended in 8 ml of ZymoPure™ P1. For bacterial cell rupture, 8 ml of ZymoPure™ P2 was added and the tube was inverted 6 times. After incubating for 3 min at room temperature, 8 ml of ZymoPure™ P3 was added and the tube was inverted until the neutralization was complete. The mixture was loaded into the ZymoPure™ Syringe Filter and incubated for 5 min until the precipitate floats to the top. The clear solution is pushed through the ZymoPure™ Syringe Filter until 20 ml of lysate is recovered. Next, 8 ml of ZymoPure™ Binding Buffer was added to the lysate and the tube was inverted 8 times. The mixture was transferred to the ZymoSpin™ III-P Column Assembly and pulled through the column by vacuum suction. After washing the column with 800  $\mu$ l ZymoPure™ Wash 1 and twice with 800  $\mu$ l ZymoPure™ Wash 2, the column was placed in a 1.5 ml tube and centrifuged at 16,000 rcf for 1 min to remove any remaining washing buffer. The column was then transferred to a clean tube and plasmid DNA was eluted with 200  $\mu$ l ZymoPure™ Elution Buffer at 10,000 rcf for 1 min. Concentration and purity of the plasmid DNA was monitored at the NanoDrop2000c.

### **3.3.4. Preparation of glycerol stocks**

For long-time storage of transformed *E. coli*'s, cryo stocks were prepared. Therefore, 500  $\mu$ l of a transformed bacteria culture was added to 500  $\mu$ l glycerol (86 %), mixed well by pipetting and stored at -80 °C.

### **3.3.5. Production of LB agar plates**

40 g of LB agar was added to 1 l of H<sub>2</sub>O and autoclaved. After cooling down the medium to around 50 °C, ampicillin was added at a final concentration of 100 µg/ml. Sterile Petri dishes were filled with LB agar medium and cooled down at room temperature until polymerization was complete. To avoid condensation water, plates were turned upside-down and let sit at room temperature for another 6 h. LB agar plates were stored at 4 °C and used up to 4 weeks.

## **3.4. Methods in virology**

### **3.4.1. Preparation of virus stocks**

For the preparation of virus stocks,  $6.5 \times 10^6$  HEK293T cells were seeded in T175-flasks (175 cm<sup>2</sup>) coated with 0.1 % gelatin solution and incubated overnight at 37 °C. Cells were then transiently transfected with 19 µg of the respective proviral plasmid DNA using TransIT<sup>®</sup>-LT1 transfection reagent (Mirus Bio LLC) as explained in (Chapter 3.1.4.). 24 h post transfection, the medium was changed to Iscove's Modified Dulbecco's Medium (IMDM) supplemented with 10 % (v/v) FCS and 1 % (v/v) P/S and incubated again overnight at 37 °C. The next day, the virus containing supernatant was centrifuged at 1,500 rcf for 10 min to remove residual cells and purified by filtration through 0.30 µm MACS SmartStrainers. Virus stocks were aliquoted into cryo tubes and stored at -80 °C.

### **3.4.2. Viral titer determination via TCID<sub>50</sub>**

Viral titers of the virus stocks were determined using TZM-bl cells. TZM-bl reporter cells harbor a luciferase and a β-galactosidase expression cassette under the control of the HIV-1 LTR promoter, which are activated upon infection with HIV-1 due to the expression of the HIV-1 trans-activator of transcription (Tat) (505). Since HIV-1 does not induce a countable cytopathic effect, the number of infectious particles is measured indirectly by determining the TCID<sub>50</sub> via X-Gal staining of infected TZM-bl cells (505). Thus, TZM-bl cells were seeded at 4,000 cells per well in 96-well plates and incubated overnight at 37 °C. Virus stocks were then added to the cells in a serial dilution, with a starting dilution of 1:50 and a subsequent dilution of 1:5. Each dilution was added to the cells in eight replicas. The infected cells were then incubated for 48 h. Next, the supernatant was removed and the cells were washed with 200 µl PBS. 100 µl of pre-cooled fixation solution

(0.06 % glutaraldehyde, 0.9 % formaldehyde in PBS) was added to the cells and incubated for 10 min at 4 °C. Cells were washed twice with 200 µl of PBS before 100 µl of staining solution was added (400 mM K<sub>3</sub>[Fe(CN)<sub>6</sub>], 400 mM K<sub>4</sub>[Fe(CN)<sub>6</sub>], 100 mM MgCl<sub>2</sub> and 20 mg/ml X-Gal in PBS). After incubation overnight at 37 °C, the staining solution was removed and cells were overlaid with 50 % glycerol. Readout was performed optically using light-microscopy. Each well with at least one infected cell was defined as positive. The TCID<sub>50</sub> was calculated using the Spearman-Kärber algorithm (242; 379; 432).

### 3.4.3. Calculation of the multiplicity of infection (MOI) for infection experiments

The average number of virus particles infecting each cell is defined as multiplicity of infection (MOI). Every cell is statistically expected to be infected by one viral particle at an MOI of 1. To calculate the MOI, the plaque forming units (PFU), which are a mean of infectious viral particles, have to be determined. Since a standard plaque assay is not applicable to HIV-1, as the virus does not induce a countable cytopathic effect, the number of infectious particles is indirectly measured via TCID<sub>50</sub> (Chapter 3.4.2.) (118). TCID<sub>50</sub> and PFU are related based on the Poisson distribution as PFU / ml = 0.7 x TCID<sub>50</sub> / ml. Thus, the MOI can be determined using the TCID<sub>50</sub> via the following equation:

$$MOI = \frac{0.7 * TCID_{50}}{\text{number of cells}}$$

### 3.4.4. Determination of viral infectivity via TZM-bl assay

For the determination of viral infectivity, the TZM-bl assay was used (505). Therefore, TZM-bl cells were seeded at 4,000 cells per well in 96-well plates and incubated overnight at 37 °C. 100 µl of cellular supernatant was added to the cells and the plates were incubated for 48 h. For readout via X-Gal staining, TZM-bl cells were washed and stained as explained above (Chapter 3.4.2.). For readout via luciferase assay, cells were washed with PBS before 50 µl of lysis juice (p.j.k.) was added. The plate was shaken for 15 min at room temperature and then frozen for at least 1.5 h at -80 °C before being thawed. The lysates were resuspended and transferred to a white Nunc 96 MicroWell plate. 100 µl beetle juice was added per well and luminescence was measured with the Spark<sup>®</sup> Microplate Reader (Tecan) at an integration time of 2 s.

### **3.4.5. HIV-1 p24-capsid Enzyme Linked Immunosorbent Assay (ELISA)**

For quantification of HIV-1 p24-capsid (CA) in the cellular supernatant, a twin-site sandwich ELISA was performed. 75 µl of the anti-HIV-1-p24 gag polyclonal antibody (D7320, Aalto Bio Reagents) were diluted in 10 ml bicarbonate coating buffer (NaHCO<sub>3</sub>, 100 mM, pH 8.5) and added to a Nunc 96 MicroWell plate with 100 µl per well. The plate was sealed with adhesive foil and incubated overnight at room temperature. The next day, the antibody-containing solution was removed and the plate was washed twice with TBS and blocked with 100 µl of 2 % non-fat dried milk powder for 1 h at room temperature. Following the blocking procedure, plates could be stored at -20 °C for several weeks or used immediately.

For sample preparation, samples were diluted 1:5 in TBS containing 1 % Empigen zwitterionic detergent and incubated at 56 °C for 30 min for virus inactivation. Recombinant HIV-1 p24 gag protein was treated equally and used for the generation of a calibration curve. After inactivation of the samples and recombinant protein, serial dilutions were prepared with a final concentration of 0.1 % Empigen. After removal of the blocking buffer, 100 µl was added per well to the prepared antibody-coated 96-well plate. The plate was sealed with adhesive foil and incubated for 3 h at room temperature.

The serial dilutions were removed and 100 µl of the secondary antibody solution (2 % non-fat dried milk powder, 20 % FCS, 0.5 % Tween-20 in TBS), containing an alkaline phosphatase-coupled anti-HIV-1-p24 gag monoclonal antibody (BC1071 AP, Aalto Bio Reagents), was added to the wells. The plate was sealed again with adhesive foil and incubated for 1 h at room temperature.

The plate was washed with TBS (0.1 % Empigen) four times, followed by washing with 1x ELISA-Light Wash Buffer twice. 50 µl of CSPD™ substrate with Sapphire-II™ was added per well and the plate was incubated at room temperature in the dark for 20 min. Readout was performed using the Spark® Microplate Reader (Tecan), measuring the absorbance at 492 nm.

### **3.4.6. Viral RNA isolation**

Viral RNA from cellular supernatant was isolated using QIAamp Viral RNA Mini Kit (Qiagen). 140 µl of virus-containing supernatant was added to 560 µl buffer AVL containing carrier RNA followed by pulse-vortexing for 15 s. Samples were then incubated for 10 min at room temperature. After addition of 560 µl Ethanol (100 %), samples were

---

pulse-vortexed again for 15 s. The mixture was transferred in two steps to the QIAamp Mini column. Centrifugation steps were carried out at 6,000 rcf for 1 min. The columns were washed subsequently with 500 µl buffer AW1 and 500 µl buffer AW2. To remove residual washing buffer, columns were centrifuged for 3 min at 20,000 rcf after the final wash step. Finally, viral RNA was eluted into a fresh RNase-free tube with 60 µl buffer AVE after 1 min of incubation on column. RNA concentration and quality was monitored via photometric measurement using NanoDrop2000c. RNA was stored at -80 °C.

#### 4. Results

After innate sensing of HIV-1, type I IFNs are induced to trigger the antiviral immune response. Previous studies have demonstrated the induction of the 12 IFN $\alpha$  subtypes, IFN $\beta$  and other type I IFNs upon HIV-1 infection (109; 290). Although all type I IFNs bind to the IFNAR receptor, distinct biological activities are induced, resulting in different antiviral potencies against HIV-1 (277; 447). HIV-1 replication is restricted through various mechanisms such as immunomodulatory regulation and the stimulation of IFN-stimulated genes (ISGs), thus inducing an antiviral state in both infected and bystander cells (247; 282). It was shown that HIV-1 restriction factors (HRF), which are ISGs, such as APOBEC3G, Tetherin, TRIM22 or MX2 were strongly elevated upon chronic HIV-1 infection (109; 290).

While HRFs are host cell proteins inhibiting HIV-1 replication at different stages of the viral life cycle (307), host dependency factors (HDFs) are host cell proteins hijacked by the virus, which are indispensable for efficient HIV-1 replication (410). Based on siRNA screenings, HDFs are defined as crucial factors for HIV-1 replication, but not lethal to the host cell when their gene expression is silenced. Among others, distinct members of the SRSF and hnRNP protein families have been identified as HIV-1 HDFs (51; 260; 337; 515; 518). Both protein families are known to be crucially involved in cellular and HIV-1 RNA processing (99; 162; 312; 375; 410; 435). However, whether an HIV-1 infection and the subsequent stimulation of IFNs might alter the expression of SRSF and hnRNP family members, and in turn possibly affect HIV-1 replication, was so far unclear.

Thus, the focus of this work was to investigate the impact of IFN $\alpha$  subtypes on *SRSF* and *hnRNP* expression and their functional relevance for HIV-1 post integration steps and RNA processing. The expression of *SRSF1* and *hnRNP A0* has been analyzed in more detail, as these two HDFs were identified as IFN-regulated genes. *SRSF1* has previously been shown to be involved in HIV-1 post integration steps (63; 219; 221; 237; 355; 356; 387; 410; 433; 446), while *hnRNP A0* has not yet been described in the context of HIV-1 RNA processing. However, *hnRNP A0* is a member of the *hnRNP A/B* family, which is known to play an important role in HIV-1 RNA processing (93; 410; 486; 509).

---

#### 4.1. *SRSF* transcript levels are lower upon HIV-1 infection

To investigate, whether the expression levels of *SRSFs* are significantly altered upon HIV-1 infection, gene transcript levels were quantified in lamina propria mononuclear cells (LPMCs) from the gut of chronically HIV-1 infected patients, either treatment naïve or under antiretroviral therapy (ART) and compared to those of healthy individuals. LPMCs reside within the lamina propria and are the first cells which are encountered by HIV-1 upon entry via the gastrointestinal tract (46; 427; 519). In collaboration with Mario Santiago (Department of Medicine, University of Colorado Denver, USA), RNA-sequencing data from a previous publication was reanalyzed for the gene expression of all *SRSF* family members (109). Elevated levels of several ISGs (Tetherin, APOBEC3G and MX2) upon HIV-1 infection due to the IFN signature confirmed chronic inflammation (109).

As shown in (Figure 4-1 A), significantly lower levels of mRNA transcripts were detected for *SRSF1* (1.8-fold), *SRSF3* (1.3-fold), *SRSF7* (1.4-fold) and *SRSF10* (1.2-fold) in chronically HIV-1 infected patients when compared to healthy individuals. The expression levels of *SRSF2* (1.4-fold) and *SRSF8* (1.1-fold) were also lower, albeit with no statistical significance (Figure 4-1 A).



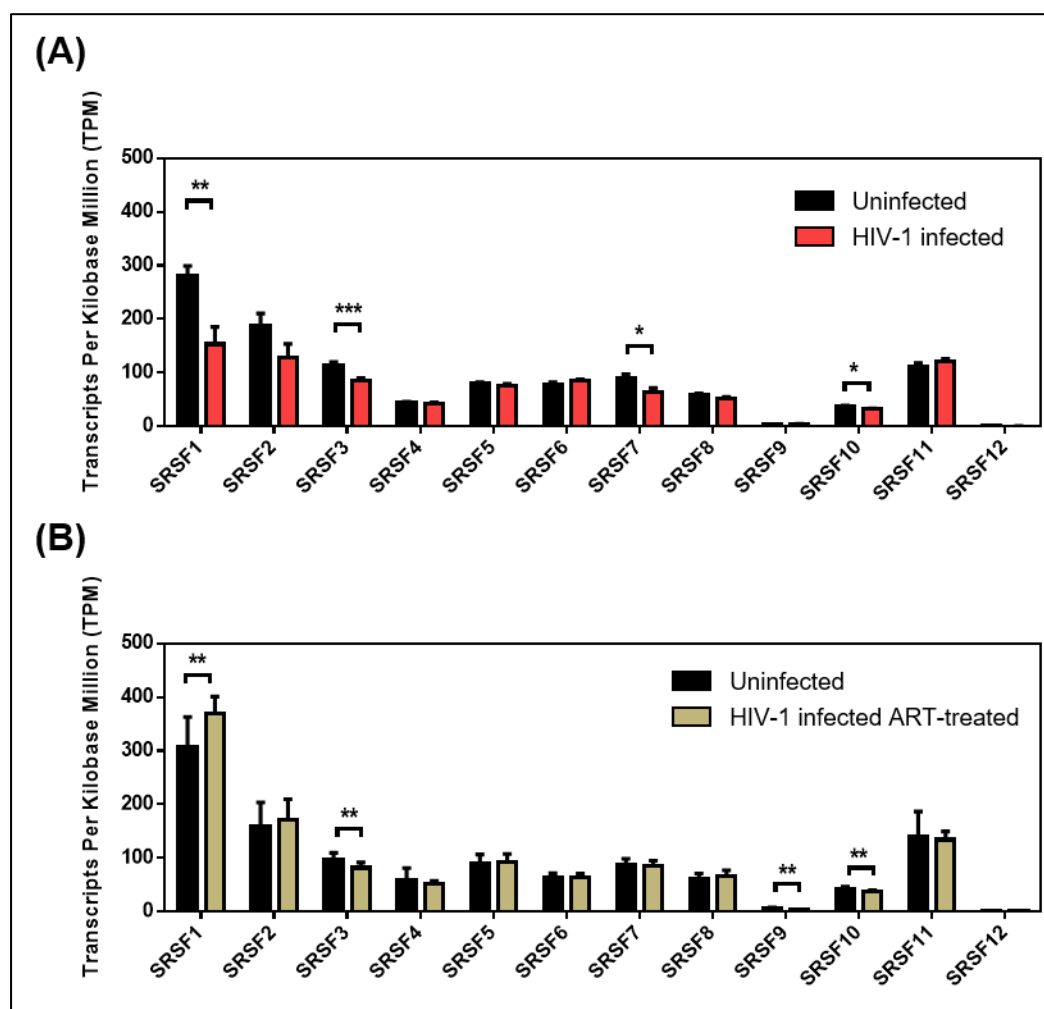


**Figure 4-1: Gene expression levels of *SRSFs* in treatment naïve or ART-treated HIV-1 infected individuals.** Transcript levels of *SRSF* genes were measured in lamina propria mononuclear cells (LPMCs) using RNA-sequencing analysis. Comparison of transcript levels from **(A)** treatment naïve HIV-1 infected and healthy individuals and **(B)** ART-treated HIV-1 infected and healthy individuals. TPM are depicted as mean (+ SD) for **(A)** 19 HIV-1 infected and 13 uninfected individuals and **(B)** 14 ART-treated and 11 uninfected individuals. Unpaired two-tailed t-tests were calculated to determine statistical significance between the groups (\*  $p < 0.05$ , \*\*  $p < 0.01$  and \*\*\*  $p < 0.001$ ).

In the cohort of ART-treated patients, gene expression of *SRSF2*, *SRSF7* and *SRSF8* was comparable with the group of healthy donors. *SRSF3* (1.2-fold) and *SRSF10* (1.1-fold) were expressed at a lower level upon ART-treatment when compared to uninfected individuals (Figure 4-1 B). Remarkably, the transcript levels of *SRSF1* were significantly higher (1.2-fold) in HIV-1 infected patients under ART-treatment when compared to healthy donors (Figure 4-1 B). Notably, HIV-1 infection and ART-treatment generally invoked opposite effects on the gene expression of *SRSFs* when compared to healthy

donors. No significant difference in expression upon HIV-1 infection, either treatment naïve or under ART-treatment was observed for *SRSF4*, *SRSF5*, *SRSF6* and *SRSF11* in comparison to uninfected donors. Transcript levels of *SRSF9* were not different upon HIV-1 infection when compared to healthy individuals, but were significantly lower in patients under ART-treatment (1.6-fold). *SRSF12* transcript levels were only marginally above the limit of detection in all patient groups (Figure 4-1). Since the transcript levels of many members of the *SRSF* family were lower upon HIV-1 infection in comparison to uninfected individuals, a direct or indirect interaction between HIV-1 infection and the expression of *SRSFs* was indicated. The induction of IFNs in response to an HIV-1 infection, which results in chronic inflammation, could be a potential link.

As the most significant alteration in gene expression upon HIV-1 infection was observed for *SRSF1* and since this factor has already been described to be involved in the regulation of HIV-1 post integration steps (219; 356), this member of the *SRSF* family was chosen for further investigation.

#### **4.1.1. *SRSF1* expression is lower in HIV-1 infected individuals**

*SRSF1* has previously been described to be crucially involved in HIV-1 post integration steps (219; 356). As this gene was the most significant of the *SRSF* family to be differentially expressed in LPMCs of HIV-1-infected patients when compared to healthy donors (Figure 4-1 A), the expression profile of *SRSF1* was further analyzed in peripheral blood mononuclear cells (PBMCs) of HIV-1 positive individuals at different phases of infection. PBMCs were isolated from whole blood samples of HIV-1 infected patients during acute (Fiebig I-V) or chronic phase of infection (Fiebig VI) (138), either treatment naïve or under ART-treatment, as well as from HIV-1 negative donors (as described in Chapter 3.1.7.). Total RNA was isolated and subjected to RT-qPCR analysis. Since it has previously been described that ISG expression levels are stimulated upon HIV-1 infection in PBMCs (290), *ISG15* mRNA expression levels were determined as surrogate marker for IFN signature to verify the cohort as representative. To analyze a potential correlation between ISG-induction and the repression of *SRSF1*, patients with no measurable induction in *ISG15* mRNA levels were excluded from the statistical analysis and are marked accordingly in (Figure 4-2).

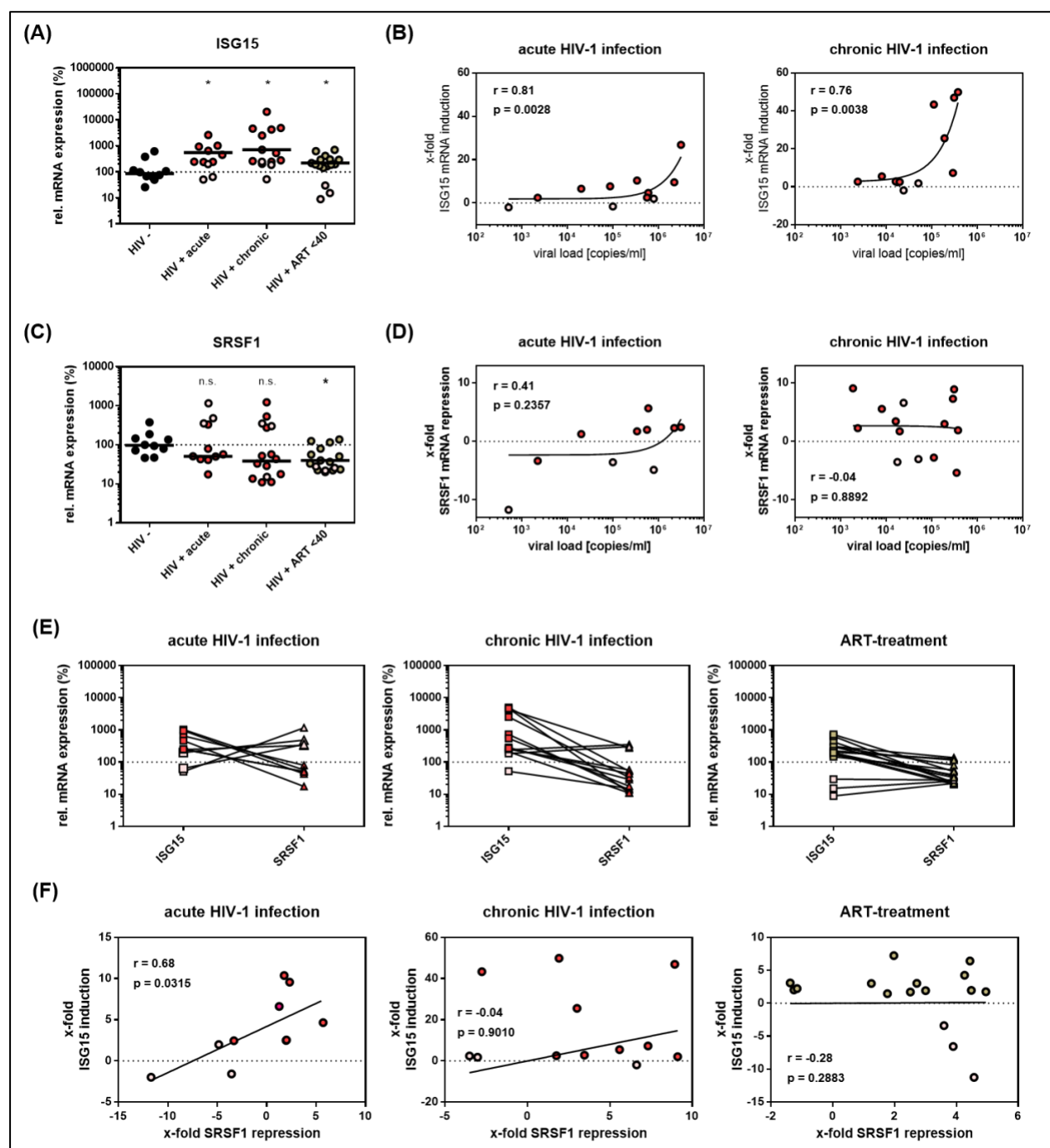


**Figure 4-2: *SRSF1* and *ISG15* expression levels inversely correlate upon HIV-1 infection.** **(A)** and **(C)** RT-qPCR determined the relative mRNA expression levels of **(A)** *ISG15* and **(C)** *SRSF1* in PBMCs from acutely and chronically HIV-1 infected patients, either naïve or under ART-treatment as well as healthy donors. ACTB was used for normalization. Unpaired one-tailed t-tests were calculated to determine whether the difference between the group of samples reached the level of statistical significance (\*  $p < 0.05$ ). **(B)** and **(D)** Correlation between plasma viral load of HIV-1 infected individuals and *ISG15* and *SRSF1* mRNA expression. Plasma viral load was quantified as described in (Chapter 3.1.7.). RT-qPCR analysis was performed to determine *ISG15* and *SRSF1* mRNA expression. Pearson correlation was calculated between plasma viral load and **(B)** *ISG15* or **(D)** *SRSF1* expression for acutely and chronically HIV-1 infected patients. Pearson

correlation coefficient ( $r$ ) and  $p$ -value ( $p$ ) are indicated. **(E)** Comparison of relative *ISG15* and *SRSF1* mRNA levels for individual patients. **(F)** Calculated correlation between  $x$ -fold repression of *SRSF1* mRNA levels and  $x$ -fold induction of *ISG15* mRNA levels for all patient groups. Pearson correlation coefficient ( $r$ ) and  $p$ -value ( $p$ ) are indicated. Data points from healthy donors were depicted in black, while data points from treatment naïve HIV-1 infected individuals were shown in red. ART-treated patients are colored in green. Patients with no or low *ISG15* mRNA induction upon HIV-1 infection were considered as low responders without IFN signature and were thus excluded from statistical analysis. Data points of these patients are depicted in light pink. This patient cohort included 10 uninfected donors, 8 acutely HIV-1 infected patients, 11 chronically HIV-1 infected patients and 13 HIV-1 infected patients under ART-treatment.

Higher levels of 5.6-fold and 7.3-fold in *ISG15* mRNA expression were detected upon both acute and chronic HIV-1 infection respectively when compared to healthy donors (Figure 4-2 A). *ISG15* mRNA levels were lower in patients under ART-treatment when compared to HIV-1 infected and treatment naïve individuals, but still 2.2-fold higher when compared to HIV-1 negative donors (Figure 4-2 A). Comparing gene expression of *ISG15* with the plasma viral load of each patient revealed a virus induced IFN signature proportional to the viral load for the groups of acutely and chronically HIV-1 infected patients (Figure 4-2 B). To investigate whether the repression of *SRSF1* might correlate with the IFN signature in HIV-1 infected individuals, *SRSF1* mRNA expression levels were determined via RT-qPCR. In acutely and chronically HIV-1 infected patients the mRNA levels of *SRSF1* were lower by 2- and 2.6-fold respectively when compared to healthy individuals, while patients under ART-treatment had 2.6-fold lower levels (Figure 4-2 C). While most HIV-1 infected treatment naïve patients had lower expression levels of *SRSF1* mRNA, *SRSF1* expression was higher for some patients when compared to uninfected individuals (Figure 4-2 C). Most of the patients with elevated mRNA levels of *SRSF1* also had no or only marginally induced levels of *ISG15* and were thus excluded from statistical analysis. No significant correlation could be found between the level of *SRSF1* repression and the plasma viral load of the patients (Figure 4-2 D). Comparing IFN signature and *SRSF1* repression in single individuals, a high induction of *ISG15* mRNA levels was generally concomitant with a strong downregulation of *SRSF1* mRNA levels. Patients with no or low induction of *ISG15* levels were defined as low responders and are marked accordingly (see color code in Figure 4-2). In all patient groups, individuals with low induction of *ISG15* mRNA levels simultaneously had elevated mRNA levels of *SRSF1* (Figure 4-2 E). To assess, whether a direct correlation existed between the induction of ISGs and the repression of *SRSF1*, Pearson correlation coefficients were determined

(Figure 4-2 F). A significant correlation was found for the group of acutely HIV-1 infected patients (Figure 4-2 F). Since chronically HIV-1 infected individuals generally represent a heterogeneous cohort with respect to infection phase and possible other viral infections and co-morbidities, it was not surprising that no significant correlation was determined due to a high dispersion of the expression values.

In conclusion, the induction of ISGs seems to be concomitant with a repression of *SRSF1* in HIV-1 infected individuals. These findings indicate a possible link between IFN signature and the downregulation of *SRSF1*, thus suggesting that *SRSF1* might potentially act as an IFN-repressed gene (IRepG) in the early immune response to HIV-1.

#### **4.1.2. The degree of *SRSF1* repression is IFN $\alpha$ subtype dependent**

Type I IFNs include 12 different IFN $\alpha$  subtypes, which exert different biological functions and play a crucial role in the innate immune defense against HIV-1 (187; 277). To investigate, whether the observed correlation between ISG-induction and *SRSF1*-repression in the early immune response to an HIV-1 infection was induced by the IFN signature, the effect of IFN $\alpha$  subtypes on the mRNA expression level of *SRSF1* was analyzed. To this end, THP-1 macrophages were stimulated with all 12 IFN $\alpha$  subtypes ( $\alpha$ 1,  $\alpha$ 2,  $\alpha$ 4,  $\alpha$ 5,  $\alpha$ 6,  $\alpha$ 7,  $\alpha$ 8,  $\alpha$ 10,  $\alpha$ 14,  $\alpha$ 16,  $\alpha$ 17 and  $\alpha$ 21). For quality control, a luciferase reporter cell line (RPE-ISRE luc) harboring the firefly luciferase gene downstream of the IFN-inducible ISRE promoter (277) was used to verify the biological activity of the different subtypes before each experiment (data not shown).

THP-1 monocytic cells were differentiated into macrophage-like cells by 5 days of incubation with phorbol 12-myristate 13-acetate (PMA) prior to IFN-stimulation as described in (Chapter 3.1.2.). While THP-1 monocytic cells restrict the infection and replication of HIV-1, differentiated THP-1 macrophage-like cells are susceptible to HIV-1 infection (263; 327). Thus, differentiated THP-1 cells have been established as a robust model system to study the interactions between HIV-1 and macrophages. Macrophages are, alongside the CD4<sup>+</sup> T-cells, the main target cells of HIV-1. While it is still under debate, whether macrophages play an important role in the transmission of a HIV-1 infection, they have been shown to contribute to the spreading of the virus into different tissues of the body due to their ability to migrate. Furthermore, they have been described to contribute to viral persistence and the formation of the viral reservoir (268; 401).

To monitor the IFN signature, the induction of ISGs was analyzed using *ISG15* as a surrogate marker. Stimulation with subtypes IFN $\alpha$ 1 (5.4-fold), IFN $\alpha$ 7 (3.4-fold) and IFN $\alpha$ 8 (1.9-fold) only led to a weak induction in *ISG15* mRNA expression, while stimulation with IFN $\alpha$ 5 (32.3-fold), IFN $\alpha$ 10 (62.1-fold), IFN $\alpha$ 16 (17.1-fold), IFN $\alpha$ 17 (47.0-fold) and IFN $\alpha$ 21 (18.5-fold) led to a moderate increase in *ISG15* expression when compared to the untreated control (Figure 4-3 A). The strongest induction of *ISG15* mRNA levels was observed upon stimulation with subtypes IFN $\alpha$ 2 (124.7-fold), IFN $\alpha$ 4 (223.4-fold), IFN $\alpha$ 6 (106.2-fold) and IFN $\alpha$ 14 (94.5-fold) (Figure 4-3 A). These findings were generally in agreement with previously published data, which showed the induction of other ISGs (MX2, SAMHD1, Tetherin or TRIM22) upon stimulation with IFN $\alpha$  subtypes (290).

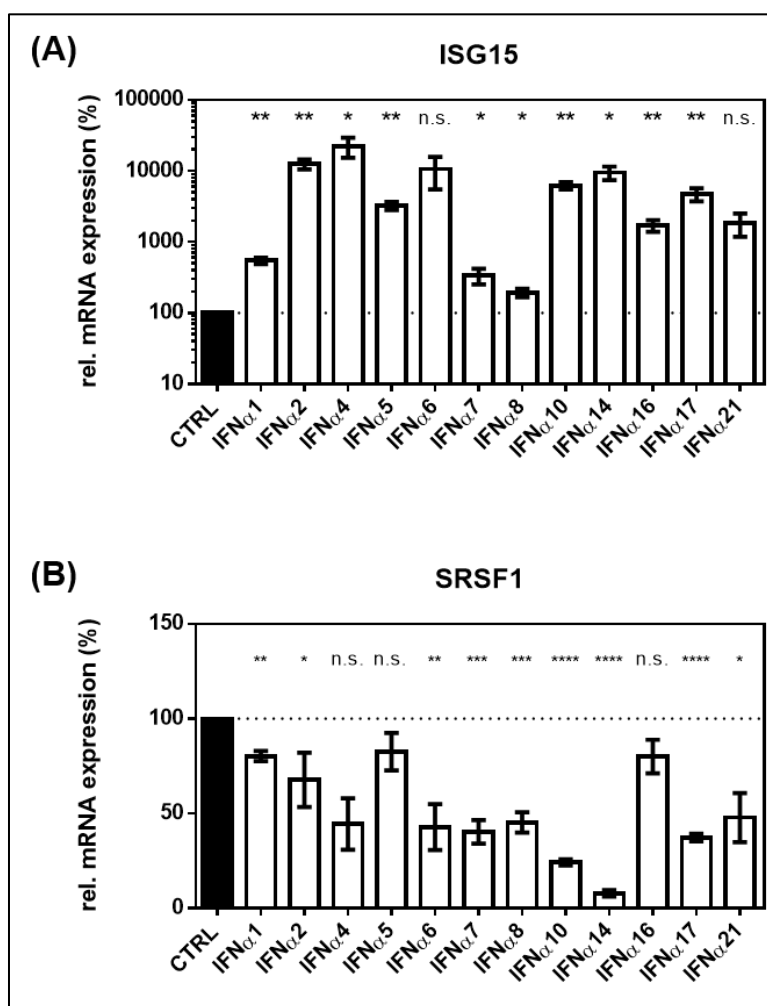


**Figure 4-3: *SRSF1* expression upon stimulation with IFN $\alpha$  subtypes. (A) – (B)** Differentiated THP-1 cells were treated with the indicated IFN subtype [10 ng/ml]. 24 h post treatment, cells were harvested, RNA isolated and subjected to RT-qPCR for measurement of relative (A) *ISG15* and (B) *SRSF1* mRNA expression levels. Statistical significance was analyzed performing unpaired

two-tailed t-tests (\*  $p < 0.05$ , \*\*  $p < 0.01$ , \*\*\*  $p < 0.001$  and \*\*\*\*  $p < 0.0001$ ). Mean (+ SEM) of  $n = 3$  biological replicates is depicted.

Next, a possible repression of *SRSF1* upon IFN-stimulation was tested, revealing a weak downregulation for the subtypes IFN $\alpha$ 1 (1.3-fold), IFN $\alpha$ 2 (1.5-fold), IFN $\alpha$ 5 (1.2-fold) and IFN $\alpha$ 16 (1.3-fold), while subtypes IFN $\alpha$ 4 (2.3-fold), IFN $\alpha$ 6 (2.3-fold), IFN $\alpha$ 7 (2.5-fold), IFN $\alpha$ 8 (2.2-fold), IFN $\alpha$ 17 (2.7-fold) and IFN $\alpha$ 21 (2.1-fold) induced a moderate downregulation of *SRSF1* mRNA expression levels (Figure 4-3 B). The strongest repression was induced after stimulation with IFN $\alpha$ 10 (4.2-fold) and IFN $\alpha$ 14 (12.5-fold) (Figure 4-3 B). Interestingly, not all subtypes showed an inverse correlation between ISG induction and *SRSF1* repression. Stimulation with the subtypes IFN $\alpha$ 2, IFN $\alpha$ 4 and IFN $\alpha$ 6 induced a strong upregulation in *ISG15* mRNA levels but a comparatively weak downregulation of *SRSF1* mRNA, while IFN $\alpha$ 14 induced a disproportionately strong downregulation of *SRSF1* mRNA expression compared to the induction of *ISG15* mRNA (Figure 4-3).

In conclusion, in accordance to previous publications, the extent of *ISG15* mRNA induction was IFN $\alpha$  subtype dependent, suggesting distinct biological activities (164; 165; 186; 193). Furthermore, stimulation with all IFN $\alpha$  subtypes resulted in the repression of *SRSF1* mRNA expression levels, substantiating the assumption of *SRSF1* acting as an IRepG. While the magnitude of the repression differed in a subtype dependent manner, IFN $\alpha$ 10 and IFN $\alpha$ 14 were the most potent subtypes for the downregulation of *SRSF1* mRNA.

#### **4.1.3. *SRSF1* is differentially regulated in HIV-1 target cells upon IFN-stimulation**

To further investigate the hypothesis of *SRSF1* acting as an IRepG, *SRSF1* mRNA expression levels were analyzed in HIV-1 target cells upon IFN stimulation in a time-course experiment. Based on the results from the previous chapter (Chapter 4.1.2.), the subtypes IFN $\alpha$ 2 and IFN $\alpha$ 14 were included. IFN $\alpha$ 14 was shown to induce the strongest repression of *SRSF1* expression levels of all IFN $\alpha$  subtypes in THP-1 macrophages (Figure 4-3 B). Furthermore, IFN $\alpha$ 14 has previously been shown to be the most potent IFN $\alpha$  subtype against HIV-1 (277). The subtype IFN $\alpha$ 2 was also included, as this subtype is already in clinical use for the treatment of other viruses like hepatitis B (17).

In THP-1 macrophages, stimulation with both IFN $\alpha$ 2 and IFN $\alpha$ 14 induced a strong 100- to 1,000-fold induction of *ISG15* mRNA expression levels, indicating an IFN signature (Figure 4-4 A and B, left panel). Both subtypes induced a 13-fold downregulation of *SRSF1* mRNA expression. Upon stimulation with IFN $\alpha$ 2, *SRSF1* expression levels were repressed by 13-fold after 12 h, while gene expression was recovered to a less than 2-fold reduction after 24 and 48 h (Figure 4-4 A, right panel). Stimulation with IFN $\alpha$ 14 led to a 13-fold reduction in *SRSF1* mRNA expression after 24 h and induced a long-lasting effect with a remaining 6-fold repression after 48 h (Figure 4-4 B, right panel). Interestingly, upon stimulation with both subtypes, a 2.2- and 1.7-fold increase in *SRSF1* mRNA expression for IFN $\alpha$ 2 and IFN $\alpha$ 14 respectively was observed 4 h post stimulation, albeit with no statistical significance (Figure 4-4 A and B, right panel).



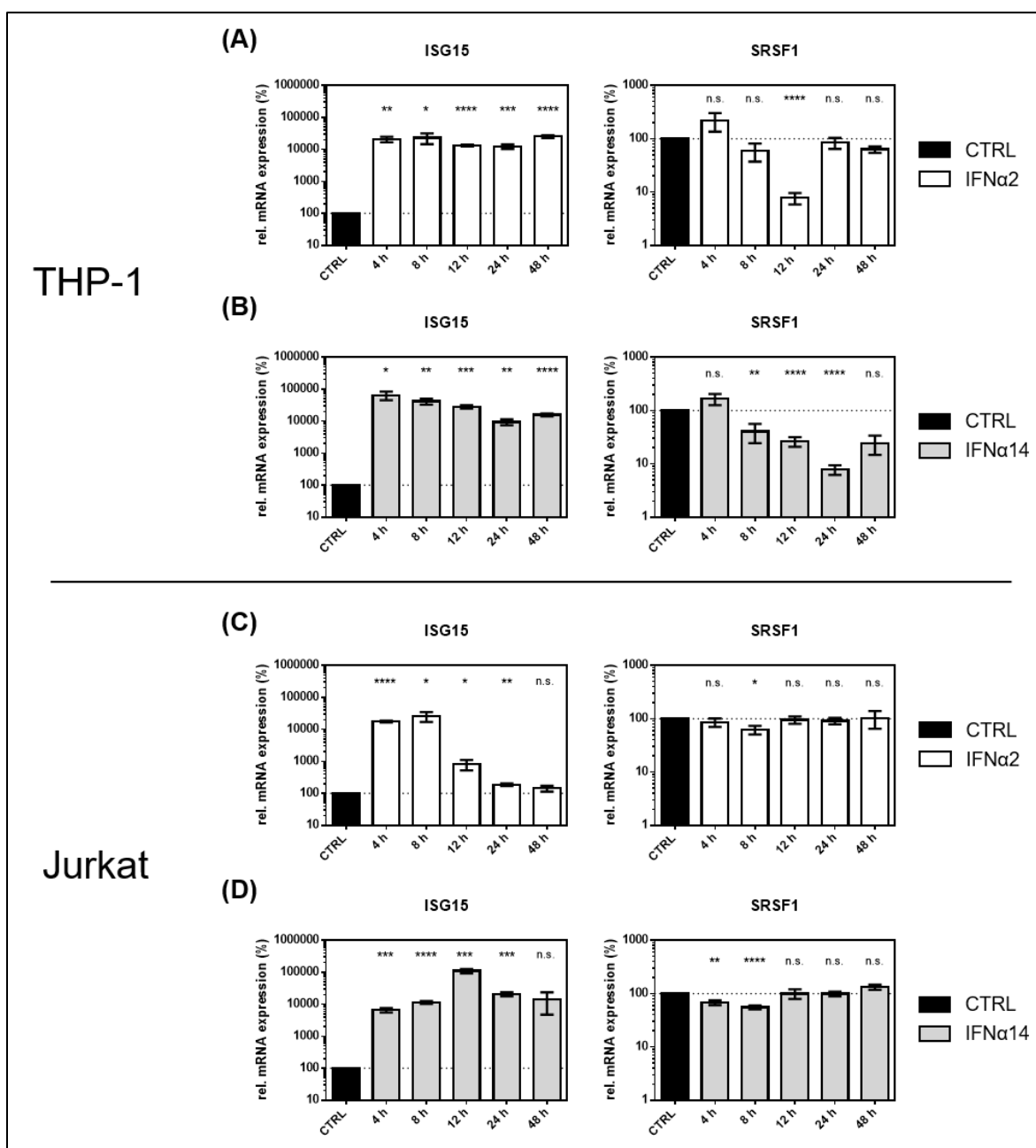


**Figure 4-4: *SRSF1* mRNA levels are differentially regulated upon stimulation of HIV-1 target cells with IFNα2 or IFNα14.** Differentiated THP-1 macrophages and Jurkat T-cells were treated with IFNα2 (white) or IFNα14 (grey) [10 ng/ml] over a period of 48 h before cells were harvested and RNA was isolated. Relative mRNA expression levels were measured via RT-qPCR analysis. **(A) – (B)** Relative mRNA expression levels of *ISG15* and *SRSF1* upon stimulation with **(A)** IFNα2 or **(B)** IFNα14 in THP-1 cells. **(C) – (D)** Relative mRNA expression levels of *ISG15* and *SRSF1* upon stimulation with **(C)** IFNα2 or **(D)** IFNα14 in Jurkat cells. ACTB was used as house-keeping gene for normalization. Unpaired two-tailed t-tests were calculated to determine whether the difference between the group of samples reached the level of statistical significance (\*  $p < 0.05$ , \*\*  $p < 0.01$ , \*\*\*  $p < 0.001$  and \*\*\*\*  $p < 0.0001$ ). Mean (+ SEM) of  $n = 4$  biological replicates is shown.

In Jurkat cells, which are used as a model system for HIV-1 target T-cells, stimulation with IFN $\alpha$ 2 led to 100-fold increased expression of *ISG15* mRNA levels. However, already 12 h post IFN $\alpha$ 2 stimulation, *ISG15* levels were only 10-fold higher, while after 24 to 48 h the levels were comparable to the untreated control (Figure 4-4 C, left panel). Stimulation with IFN $\alpha$ 14 induced a 100- to 1,000-fold induction in *ISG15* mRNA levels throughout the course of the experiment (Figure 4-4 D, left panel). Hence, ISG induction was generally less pronounced in Jurkat T-cells than THP-1 macrophages. IFN $\alpha$ 2 induced a significant 1.6-fold downregulation of *SRSF1* mRNA levels after 8 h, while IFN $\alpha$ 14 induced a significant downregulation of 1.5- and 2-fold after 4 and 8 h respectively. For both subtypes, *SRSF1* mRNA levels were restored 12 h after the stimulation (Figure 4-4 C and D, right panel).

In both macrophages and T-cells, stimulation with IFN $\alpha$ 2 and IFN $\alpha$ 14 induced a time-dependent and significant repression of *SRSF1* mRNA levels. However, the downregulation of *SRSF1* was much more pronounced in differentiated THP-1 macrophages than in Jurkat T-cells, indicating a cell-type specific effect. Furthermore, the expression levels of *SRSF1* mRNA differ upon stimulation with IFN $\alpha$ 2 and IFN $\alpha$ 14 in THP-1 cells. While treatment with IFN $\alpha$ 2 induced *SRSF1* repression at an earlier time point than IFN $\alpha$ 14, treatment with IFN $\alpha$ 14 resulted in a longer-lasting downregulation of *SRSF1*. The magnitude of *SRSF1* mRNA repression, however, was similar for both subtypes.

Thus, *SRSF1* could potentially represent an IRepG in HIV-1 target cells, particularly in macrophages. However, the slight increase in *SRSF1* mRNA expression 4 h post stimulation with both IFN $\alpha$ 2 and IFN $\alpha$ 14 in THP-1 macrophages could also potentially indicate a role of *SRSF1* as ISG, which, after a short period of induction, is repressed through negative autoregulation. The latter seems plausible, as homeostatic levels of *SRSF1* have been described to be maintained via an autoregulatory feedback loop (99; 111; 169).

To confirm the IFN-induced repression of *SRSF1* on protein level, Western Blot analysis was performed. Stimulation of THP-1 macrophages with both IFN $\alpha$  subtypes led to decreased *SRSF1* protein levels after 36 to 42 h (Figure 4-5 A). In agreement with the results on the mRNA level, stimulation with IFN $\alpha$ 14 induced a stronger downregulation in *SRSF1* levels than stimulation with IFN $\alpha$ 2. Compared to the repression of *SRSF1* on the mRNA level, protein levels of *SRSF1* were reduced with a timely delay of 12 to 24 h.

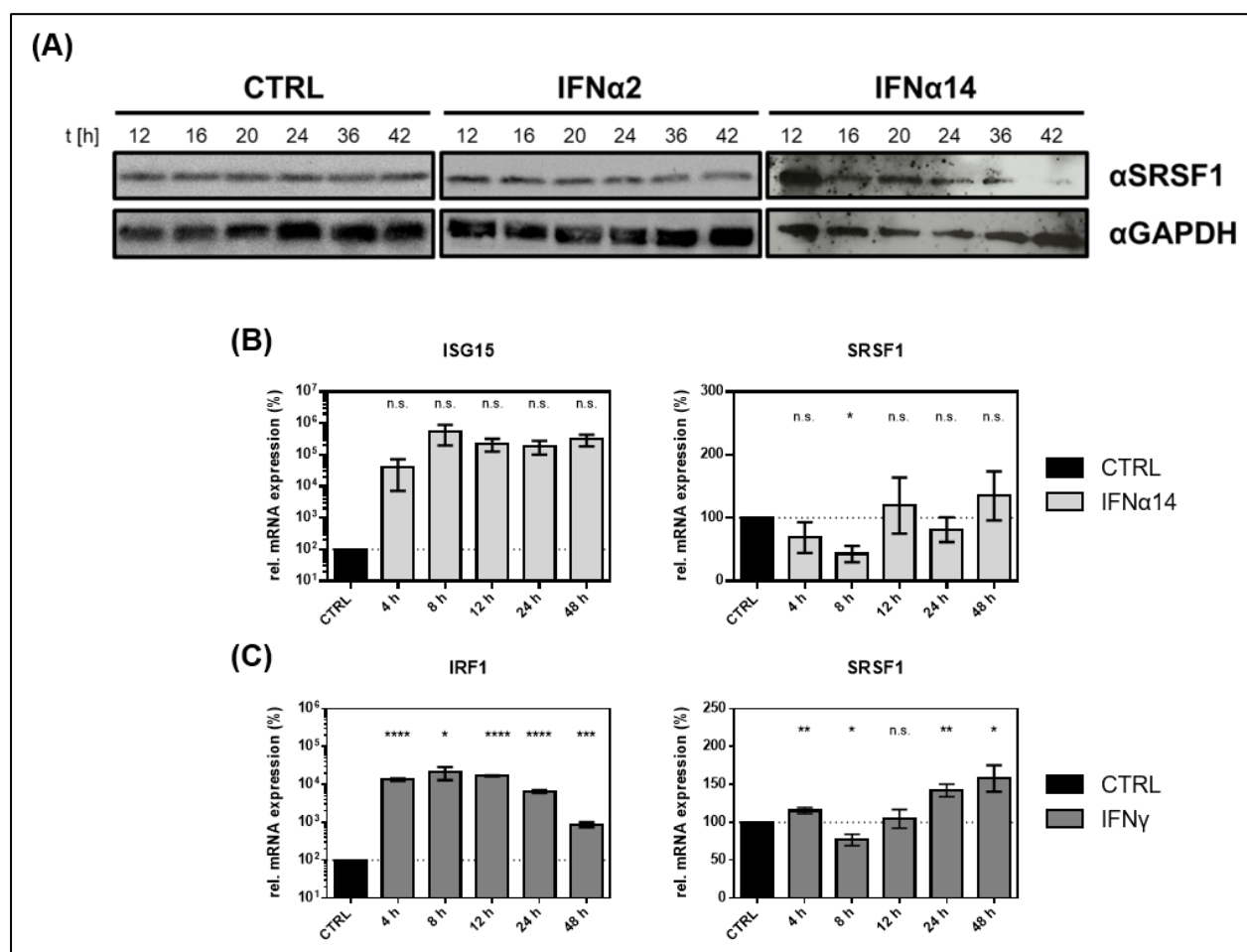


**Figure 4-5: SRSF1 mRNA and protein levels are differentially regulated upon treatment of macrophages with IFNs.** **(A)** Differentiated THP-1 macrophages were treated with IFN $\alpha$ 2 or IFN $\alpha$ 14 [10 ng/ml] for the indicated amount of time before cells were harvested and proteins were isolated. Proteins were separated by SDS-PAGE, blotted, and analyzed with an antibody specific to SRSF1. GAPDH was used as loading control. **(B)** Monocyte-derived macrophages (MDMs) were treated for 48 h with 10 ng/ml of IFN $\alpha$ 14. After harvesting the cells, RNA was extracted and subjected to RT-qPCR. Relative mRNA expression levels of *ISG15* and *SRSF1* are shown. Expression levels were normalized to GAPDH. Time points 24 h and 48 h only include two biological replicates. **(C)** Differentiated THP-1 cells were stimulated with IFN $\gamma$  [10 ng/ml] for 48 h before cells were harvested and RNA was isolated. Relative mRNA expression levels of *IRF1* and *SRSF1* were measured via RT-qPCR. GAPDH was used as house-keeping gene for normalization. Unpaired t-tests were calculated to determine whether the difference between the group of samples reached the level of statistical significance (\*  $p < 0.05$ , \*\*  $p < 0.01$ , \*\*\*  $p < 0.001$  and \*\*\*\*  $p < 0.0001$ ). Mean (+ SEM) of  $n = 4$  biological replicates is shown for **(B)** and **(C)**.

To assess whether the downregulation of SRSF1 upon IFN stimulation in cell culture model systems could also be validated in primary human cells, primary monocyte-derived macrophages (MDMs) were stimulated with IFN $\alpha$ 14 in collaboration with Fabian Roesmann (AG Widerra, Institute for Medical Virology, University Hospital Frankfurt,

Frankfurt am Main). *ISG15* mRNA expression was induced 50- to 500-fold upon stimulation, verifying IFN signature (Figure 4-5 B, left panel). *SRSF1* mRNA levels were significantly reduced by 2.4-fold after 8 h of treatment, thus supporting the role of *SRSF1* as a potential IFN-regulated gene in primary human cells (Figure 4-5 B, right panel). When compared to the effect of IFN $\alpha$ 14 stimulation on THP-1 macrophages, the repression of *SRSF1* mRNA levels in MDMs was less pronounced. The expression pattern was generally different, as *SRSF1* levels were comparable to the untreated control in MDMs after 12 to 48 h, whereas in THP-1 macrophages, IFN $\alpha$ 14 induced a long-lasting repression in *SRSF1* mRNA expression. Furthermore, no increase in *SRSF1* mRNA could be observed after 4 h of treatment.

To assess whether the repression of *SRSF1* was type I IFN specific, *SRSF1* mRNA expression levels were also analyzed in THP-1 macrophages upon stimulation with IFN $\gamma$ . As the sole member of the type II IFN family, IFN $\gamma$  activates a distinct signaling pathway than the type I IFNs after binding to the IFN $\gamma$  receptor (IFNGR) (37; 39). Thus, the IFN-regulatory factor 1 (IRF1) was chosen as a surrogate marker for type II IFN specific activation of the IFN $\gamma$  activation site (GAS) regulated promoter (366). *IRF1* mRNA expression was strongly induced by 50- to 100-fold upon IFN $\gamma$  stimulation after 4 to 24 h. 48 h post treatment, *IRF1* mRNA induction was only 9-fold (Figure 4-5 C, left panel). However, *SRSF1* mRNA expression was only slightly reduced by 1.3-fold after 8 h of stimulation. Interestingly, an additional time-dependent upregulation in *SRSF1* mRNA expression was detected between 12 to 48 h, resulting in significantly increased expression levels after 24 and 48 h. Similar to stimulation with IFN $\alpha$ 2 and IFN $\alpha$ 14, a slight upregulation (1.2-fold) in *SRSF1* mRNA levels was observed after 4 h (Figure 4-5 C, right panel). Generally, the IFN-mediated repression of *SRSF1* seems to be a preferentially type I IFN specific effect.

#### **4.1.4. Alteration in *SRSF1* gene expression occurs on transcriptional level**

The expression of *SRSF1* mRNA was differentially regulated upon IFN-stimulation in HIV-1 target cells (Chapter 4.1.3.). However, the mechanistic mode, in which this IFN-mediated regulation might function was still unknown. To investigate, whether the IFN-mediated regulation of *SRSF1* occurred on the transcriptional level, the 4-thiouridine (4sU)-tagging method was applied. The use of 4sU enables metabolic labeling of newly synthesized RNA and allows the subsequent isolation and separation of freshly

transcribed RNA from pre-existing RNA. Thus, 4sU-tagging allows the study of RNA synthesis, degradation, and stability, as well as transcription factor activities, unbiased from RNA synthesis or decay rates in total RNA (159; 377; 455; 493).

THP-1 macrophages were treated with IFN $\alpha$ 14 for 4, 8 or 24 h before adding 4sU 30 min prior to cell harvest. After biotinylation of the incorporated 4sU, streptavidin-coated magnetic beads were used to separate the freshly transcribed RNA from the untagged RNA. Changes in gene expression were measured via RT-qPCR. IFN stimulation was analyzed using *ISG15* as surrogate marker. Stimulation with IFN $\alpha$ 14 induced a 300-, 70- and 440-fold increase in *ISG15* mRNA expression after 4, 8 and 24 h (Figure 4-6 A).

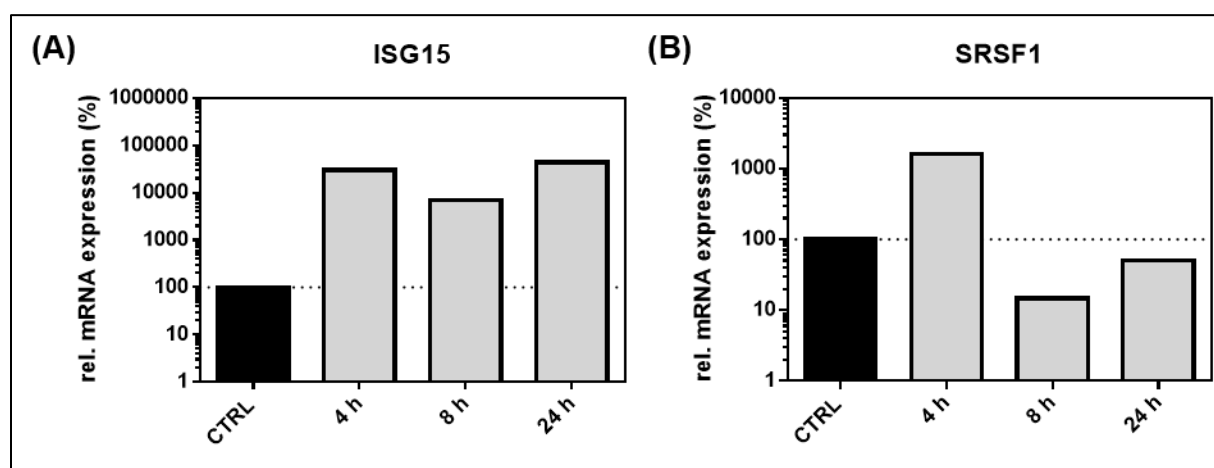


**Figure 4-6: IFN $\alpha$ 14-mediated changes in newly transcribed *SRSF1* mRNA. (A) – (B)** THP-1 macrophages were stimulated with IFN $\alpha$ 14 [10 ng/ml]. 4-thiouridine (4sU) was added 30 min before harvesting the cells at the indicated time points in order to label newly synthesized RNA. After separation and isolation of the freshly synthesized RNA, RT-qPCR was performed to measure relative mRNA expression levels of (A) *ISG15* and (B) *SRSF1*. GAPDH was used as house-keeping gene for normalization. Due to low yields of 4sU-labeled RNA, two biological replicates were pooled for RT-qPCR analysis.

Interestingly, when analyzing the expression levels of *SRSF1*, a 16-fold increase in 4sU-labeled mRNA expression was detected 4 h after IFN treatment. However, 8 h post IFN-stimulation, the levels of *SRSF1* mRNA were reduced by 10-fold, while 24 h post IFN-stimulation, *SRSF1* mRNA expression was recovered, but still 2-fold reduced when compared to the untreated control (Figure 4-6 B).

Hence, IFN-mediated alteration of *SRSF1* mRNA expression likely occurred on the transcriptional level. The expression profile in newly synthesized, 4sU-labeled *SRSF1* mRNA, which revealed a biphasic pattern with an early increase in expression prior to a

strong downregulation, was in accordance with the expression profile of *SRSF1* mRNA analyzing total RNA (Figure 4-4 A and B, right panel) and supports the potential role of *SRSF1* as an ISG. This expression pattern indicated the concatenation of several regulatory instances, with both positive and negative effects on *SRSF1* mRNA expression. The initial upregulation of *SRSF1* upon IFN $\alpha$ 14 stimulation is thus possibly counteracted by an autoregulatory mechanism, which has been described to be regulated through a negative feedback loop (99; 111; 169).

#### **4.1.5. Knockdown of SRSF1 levels affect HIV-1 post integrations steps**

*SRSF1* has been shown to be crucially involved in HIV-1 post integration steps, as several binding sites of *SRSF1* on the viral pre-mRNA have been identified (63; 446). Furthermore, *SRSF1* competes with the viral protein Tat for a sequence on TAR, thus affecting HIV-1 LTR transcription (356). As shown in Figure 4-4, stimulation with type I IFNs was shown to alter the expression profile of *SRSF1* mRNA in HIV-1 target cells, revealing a strong time-dependent repression in THP-1 macrophages (Figure 4-4). An inverse correlation was also detected between the repression of *SRSF1* and the IFN signature in the early immune response to HIV-1 (Chapter 4.1.1.).

Thus, to analyze the effect of depleted levels of *SRSF1*, as induced by IFN-stimulation or during the early immune response to HIV-1 infection, on HIV-1 post integration steps, *SRSF1* expression was transiently silenced using a siRNA-mediated knockdown approach. Therefore, HEK293T cells were transiently co-transfected with a plasmid expressing the HIV-1 laboratory strain NL4-3 PI952 (pNL4-3 PI952) (371) and a siRNA specifically targeting *SRSF1* or a siRNA negative control. Cells were incubated for 72 h, before cells and virus-containing supernatant were harvested. One-Step RT-qPCR was performed to quantify *SRSF1* gene knockdown efficiency. The siRNA-based approach induced a knockdown of *SRSF1* gene expression of 85 % when compared to the negative control siRNA (Figure 4-7 A).

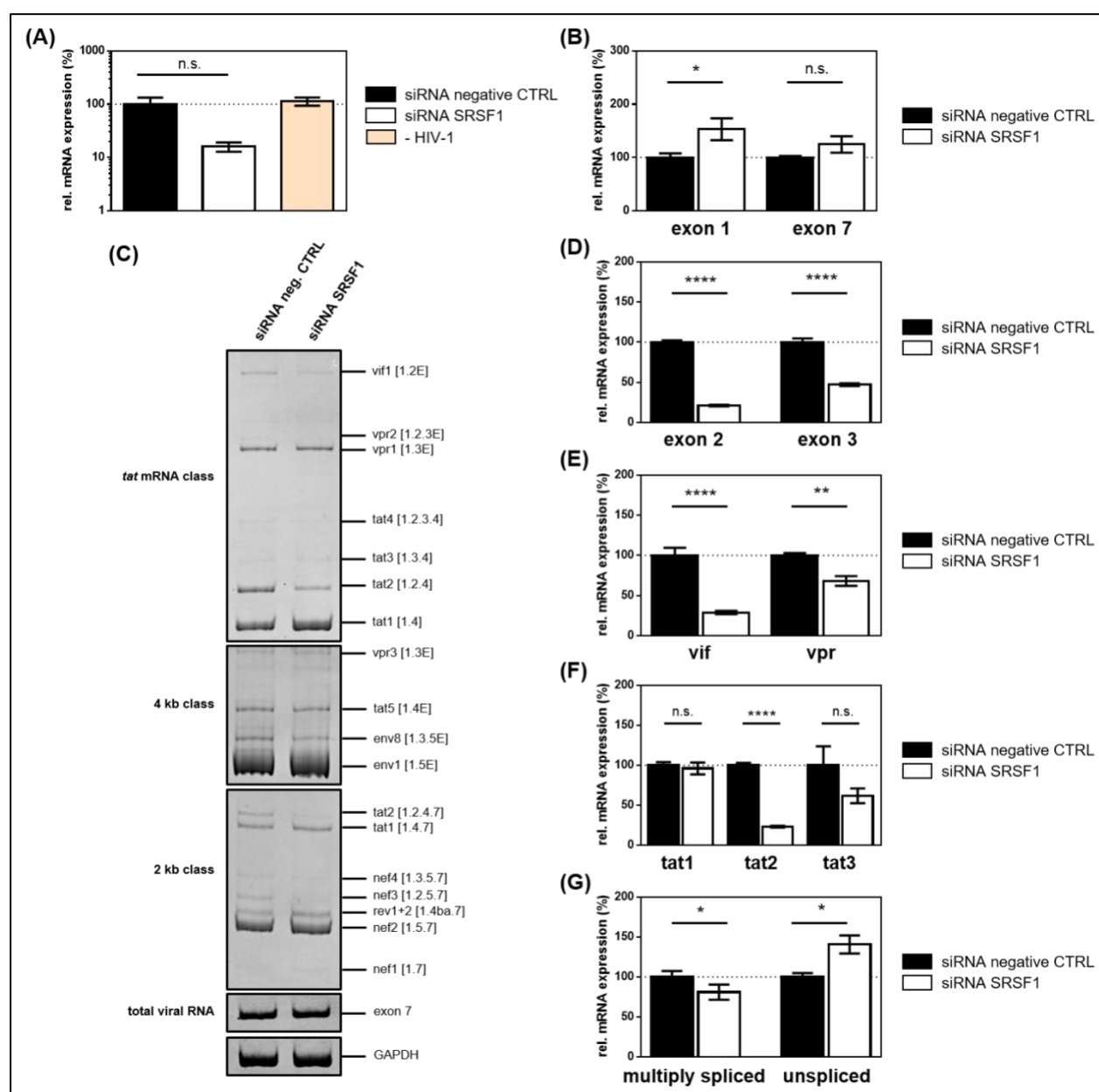


**Figure 4-7: siRNA-mediated knockdown of SRSF1 affects HIV-1 LTR transcription and splice site usage.** HEK293T cells were transfected with the proviral clone pNL4-3 PI952 (371) and anti-SRSF1 siRNA. 72 h post transfection, cells were harvested and RNA and viral supernatant isolated. Isolated RNA was subjected to RT-qPCR. **(A) – (B)** Relative mRNA expression levels of **(A)** *SRSF1* and **(B)** exon 1 and exon 7 containing mRNAs (total viral mRNA) normalized to GAPDH expression. **(C)** Analysis of viral splicing pattern upon SRSF1 knockdown. Isolated RNA was subjected to RT-PCR analysis using the indicated primer pairs for the 2 kb-, 4 kb- and *tat* mRNA-class (Table 2-4). HIV-1 transcript isoforms are depicted on the right according to (375). To compare total RNA amounts, separate RT-PCRs amplifying HIV-1 exon 7 containing transcripts as well as cellular GAPDH were performed. PCR amplicons were separated on a 12 % nondenaturing polyacrylamide gel. **(D) – (G)** Relative expression levels of **(D)** exon 2 and exon 3 containing, **(E)** *vif* and *vpr*, **(F)** *tat1*, *tat2* and *tat3* and **(G)** multiply spliced and unspliced mRNAs. HIV-1 mRNAs were analyzed using the indicated primers (Table 2-4 and Supplementary Figure 1). The mRNA expression of NL4-3 PI952 was set to 100% and the relative splice site

usage was normalized to total viral mRNA levels (exon 7 containing mRNAs). Unpaired two-tailed t-tests were calculated to determine whether the difference between the group of samples reached the level of statistical significance (\*  $p < 0.05$ , \*\*  $p < 0.01$ , \*\*\*  $p < 0.001$  and \*\*\*\*  $p < 0.0001$ ). Mean (+ SEM) of  $n = 4$  biological replicates is depicted for **(A)**, **(B)** and **(D) – (G)**.

Intracellular total viral mRNA levels were measured via RT-qPCR using primer pairs amplifying HIV-1 exon 1 or exon 7, which are present in all HIV-1 transcript variants (Figure 1-4 and Supplementary Figure 1). Exon 1 containing transcripts were significantly increased by 1.5-fold, while exon 7 containing transcripts were induced by 1.2-fold, albeit with no statistical significance (Figure 4-7 B). Hence, an effect of SRSF1 on LTR transcription was suggested. SRSF1 has previously been described to affect HIV-1 LTR transcription through the competitive binding with Tat for a TAR binding sequence (355; 356). Depleted levels of SRSF1 might thus lead to fewer competitive binding and enhance HIV-1 LTR promoter activity.

To investigate the impact of SRSF1 knockdown on HIV-1 alternative splicing, the viral splicing pattern was analyzed by semi-quantitative RT-PCR, using specific primer pairs to amplify intron-less (2 kb) and intron-containing (4 kb) HIV-1 mRNAs as well as the *tat* mRNA class. Both *vif1* and *tat2* levels were reduced in the *tat* mRNA-class, while no changes in splice site usage were observed within the 4 kb-class (Figure 4-7 C). In the 2 kb-class, *tat2* reduction was also detected, alongside a decrease in *nef3* mRNA expression (Figure 4-7 C). Splicing from splice donor (SD) 1 to splice acceptor (SA) 1 is required for the formation of *vif1*, *tat2* and *nef3* mRNAs, which all contain non-coding leader exon 2 (375). Thus, an effect of SRSF1 knockdown on the frequency of SA1 splice site usage was suggested. The observed changes in the viral splicing pattern were confirmed quantitatively via RT-qPCR using transcript specific primer pairs (Table 2-4 and Supplementary Figure 1). The inclusion of non-coding leader exons 2 and 3 in all viral transcripts were decreased, by 5- and 2-fold respectively (Figure 4-7 D). The inclusion of exon 2 requires splicing from SD1 to SA1 while inhibiting splicing at SD2/2b (375). The inclusion of exon 3 involves splicing from SD1 to SA2 while inhibiting splicing at SD3 (375). Furthermore, recognition of exon 2 and exon 3 is crucial for the generation of *vif* and *vpr* mRNAs and depends on cross-exon interactions between SA1 and SD2/2b, and SA2 and SD3 respectively (128; 410; 486). Vif plays a crucial role in HIV-1 replication in cells expressing APOBEC3G. The HIV-1 restriction factor APOBEC3G inserts G to A hypermutations into the viral genome during reverse transcription. Vif counteracts



APOBEC3G by inducing its ubiquitination and subsequent proteasomal degradation (115; 412; 436). A 3.6-fold downregulation in *vif* mRNA was measured upon SRSF1 knockdown (Figure 4-7 E), confirming the observed reduction in the semi-quantitative RT-PCR. As it has previously been shown that changes in Vif protein levels lead to a failure in viral replication (6; 310; 485), the strong repression of *vif* mRNA levels could potentially heavily affect HIV-1 replication. Splicing from SD1 to SA1 is required for the formation of *vif* mRNAs (375). The observed reduction in the formation of *vif* mRNA, as well as exon 2 including mRNAs, suggested a reduced usage of SA1. The splicing regulatory element (SRE) ESE M1/M2 regulates usage of SA1 and is a known target of SRSF1 (237). Thus, reduced levels of SRSF1 potentially led to a lower frequency in SA1 splice site usage, which resulted in decreased levels of *vif* and exon 2 containing mRNAs. Vpr counteracts several HRFs, such as the macrophage mannose receptor (MR), the lysosomal-associated transmembrane protein 5 (LAPTM5) or SAMHD1, and is thus also essential for HIV-1 replication, specifically in macrophages (132; 149; 302; 513). Knockdown of SRSF1 induced a 1.4-fold decrease in *vpr* mRNA levels (Figure 4-7 E). Generation of *vpr* mRNA requires splicing from SD1 to SA2 (375). Since both *vpr* mRNA expression levels and the inclusion of exon 3 were decreased, reduced splice site usage of SA2 was suggested. However, no SRE bound by SRSF1 has been described in this region of the viral pre-mRNA. Tat binds to the TAR sequence within the 5'-LTR promoter, recruiting the positive transcription elongation factor b (P-TEFb) complex and thus activating the efficient elongation of nascent viral transcripts (232; 233; 516). As depicted in Figure 4-7 F, depleted levels of SRSF1 resulted in unaltered expression of *tat1* mRNA levels, while *tat2* and *tat3* mRNA expression was reduced by 4- and 2-fold respectively (Figure 4-7 F). The formation of *tat1*, *tat2* and *tat3* mRNA requires splicing from SD4 to SA7. Furthermore, additional splicing needs to occur from SD1 to SA3 (*tat1*), from SD1 to SA1 and SD2 to SA3 (*tat2*) and from SD1 to SA2 and SD3 to SA3 (*tat3*) (375). Thus, reduced splice site usage of SA1 and SA2 was suggested, while the frequency of splicing events at SA3 seemed unaltered. As the levels of multiply spliced mRNAs (spliced from SD4 to SA7) were significantly decreased by 1.3-fold, and the levels of unspliced viral mRNAs (containing intron 1) simultaneously were significantly increased, it was suggested that SRSF1 knockdown shifts the ratio towards unspliced mRNAs (Figure 4-7 G). Unspliced mRNAs include the mRNA for the Gag-Pol precursor as well as the viral genome ready to be included into new virions. The presumed reduction in general splicing events at SA1

and SA2 matches the observed increase in unspliced mRNA transcripts. Since the expression levels of multiply spliced mRNAs were significantly decreased, a direct involvement of the SRSF1-bound SRE ESE3, which regulates splice site usage at SA7, was suggested (433).

The observed reduction in the splice site usage of SA1, SA2 and SA7 upon lower levels of SRSF1 was in accordance with the known role of SRSF1 as splicing enhancer upon binding to exonic splicing enhancers. While SRSF1-bound SREs have been shown to regulate splice site usage of SA1 and SA7 (237; 433), no known SRSF1-targeted SRE has been described in the proximity of SA2. However, the presence of an unidentified binding site of SRSF1 regulating SA2 or an indirect effect through the interaction with other splicing regulatory factors cannot be ruled out.

To evaluate whether SRSF1 knockdown, and the subsequent effects on HIV-1 LTR transcription and splice site usage, directly or indirectly affected viral infectivity, RPE-ISRE-luc cells were transiently co-transfected with the HIV-1 laboratory strain pNL4-3 (AD8) and a siRNA specifically targeting SRSF1 or a siRNA negative control. In contrast to HEK293T cells, RPE ISRE luc cell putatively express APOBEC3G and are thus a more suitable cell line to analyze the impact of reduced *vif* mRNA levels, as observed upon SRSF1 knockdown (Figure 4-7 E), on viral infectivity (293). After 72 h, the cellular supernatant was used to infect TZM-bl cells, which represent a reporter cell line to determine viral infectivity and contain reporter genes for firefly luciferase and  $\beta$ -galactosidase under the control of the HIV-1 LTR promoter (481). Luciferase activity was significantly increased by 1.9-fold (Figure 4-8 A). Hence, viral infectivity was suggested to be facilitated upon depleted levels of SRSF1 when compared to the negative control. X-Gal staining of infected TZM-bl cells confirmed the increase in viral infectivity (Figure 4-8 B). Thus, even though siRNA-induced knockdown of SRSF1 altered the delicate balance in the ratio of several HIV-1 mRNA transcripts, including a strong reduction in *vif* mRNA (3.6-fold) expression, higher levels of viral infectivity were observed.

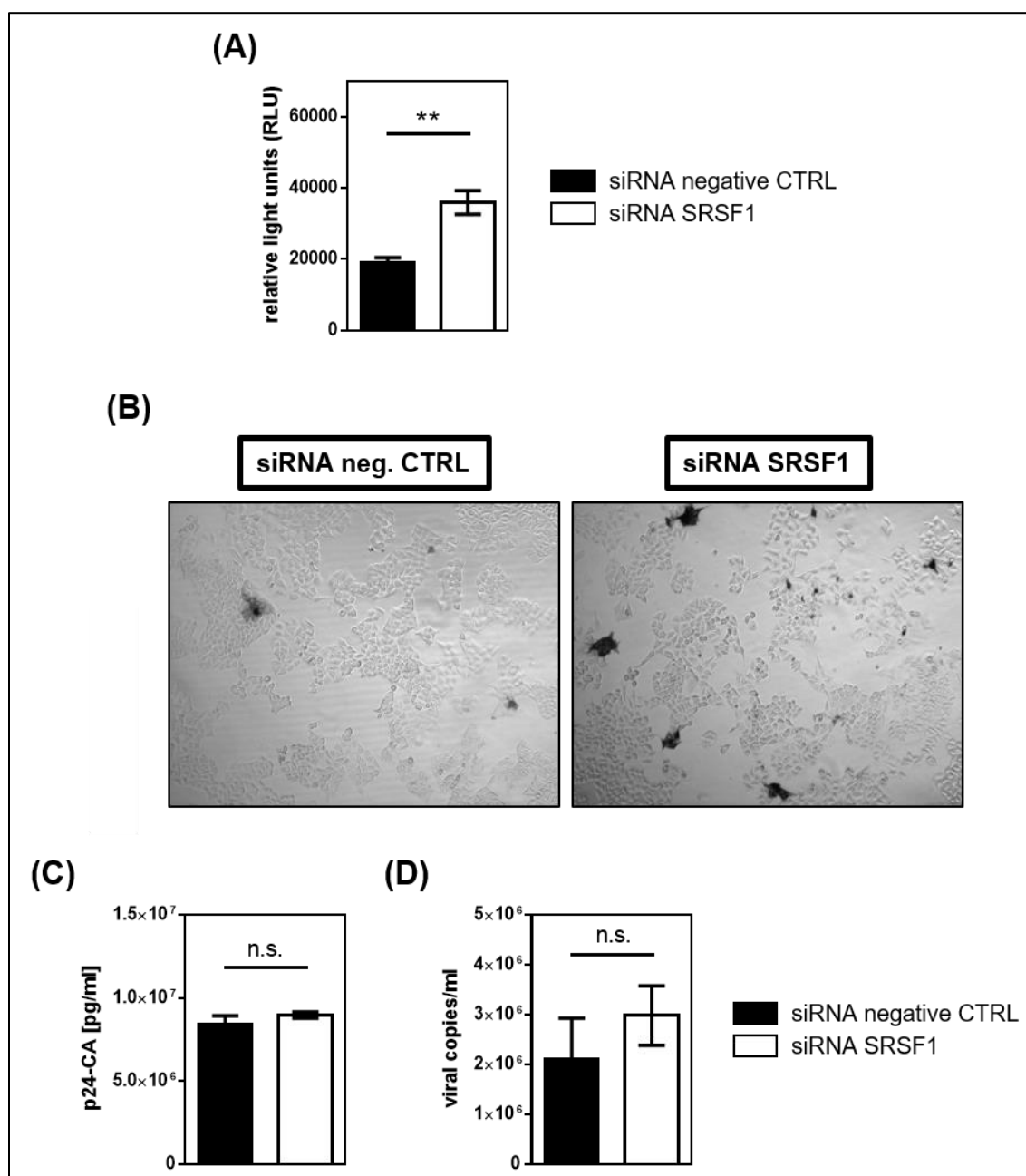


**Figure 4-8: Impact of siRNA-based knockdown of SRSF1 on HIV-1 infectivity and virus production.** RPE-ISRE luc cells were transfected with a plasmid coding for the proviral clone NL4-3 (AD8) (pNL4-3 AD8) (148) and the indicated siRNA. 72 h post transfection, cellular supernatant was harvested. **(A) – (B)** Viral infectivity was determined via TZM-bl assay. **(A)** Luciferase activity was determined measuring relative light units (RLUs). **(B)** Infected TZM-bl cells were stained with X-Gal. **(C)** p24-CA ELISA was performed to determine p24-CA levels in the cellular supernatant. **(D)** Cellular supernatant was used to determine viral copy number per ml. RT-qPCR was performed analyzing absolute expression levels of exon 7 containing transcripts (total viral mRNA). Statistical significance was determined using unpaired two-tailed t-tests (\*  $p < 0.05$  and \*\*  $p < 0.01$ ). Mean (+ SEM) of  $n = 4$  biological replicates is shown for **(A)**, **(C)** and **(D)**.

To assess whether the facilitated viral infectivity resulted from increased viral particle production, HIV-1 p24-CA protein levels in the cellular supernatant were monitored via twin-site sandwich ELISA. SRSF1 knockdown marginally induced p24-CA levels by 1.1-fold in the cellular supernatant, however, no statistical significance could be assigned (Figure 4-8 C). Furthermore, the number of viral copies in the cellular supernatant was monitored via RT-qPCR. An increase of 1.4-fold in viral copies was detected upon SRSF1 knockdown, albeit with no statistical significance (Figure 4-8 D). Thus, HIV-1 virus production was not significantly altered upon decreased levels of SRSF1.

Upon stimulation with IFN $\alpha$ 2 and IFN $\alpha$ 14 in THP-1 macrophages, strongly repressed levels of *SRSF1* mRNA expression were observed after an initial increase (Figure 4-4 A and B). The downregulation in SRSF1 levels might result from an autoregulatory negative feedback loop as a response to the early upregulation (111). The siRNA-mediated knockdown of SRSF1 was shown to alter HIV-1 alternative splice site usage, but also to facilitate viral infectivity, most likely due to enhanced LTR promoter activity. Thus, suppression of SRSF1 expression levels could potentially be beneficial for HIV-1 in terms of viral infectivity and subsequently to establish a systemic infection after viral entry to the host.

#### **4.1.6. Overexpression of SRSF1 levels affects HIV-1 post integration steps**

Upon IFN-stimulation in THP-1 macrophages, *SRSF1* mRNA expression was induced as an early response after 4 h (Figure 4-4). 4sU-tagging confirmed a strong upregulation in SRSF1 gene expression 4 h post treatment with IFN $\alpha$ 14 (Figure 4-6). Furthermore, increased levels of *SRSF1* mRNA were detected in THP-1 macrophages upon stimulation with IFN $\gamma$  (Figure 4-5).

Thus, to evaluate the effect of elevated levels of SRSF1 on HIV-1 RNA processing, HEK293T cells were transiently co-transfected with the a plasmid coding for the HIV-1 laboratory strain NL4-3 PI952 (pNL4-3 PI952) (371) and an expression vector coding for FLAG-tagged SRSF1 (pcDNA-FLAG-SF2) (206) or an empty vector (pcDNA3.1(+)) as mock control and incubated for 72 h. Total RNA was extracted from the cells and virus-containing supernatant was isolated. SRSF1 overexpression efficiency was verified via One-Step RT-qPCR, revealing enhanced levels of SRSF1 by multiple orders of magnitude (Figure 4-9 A).

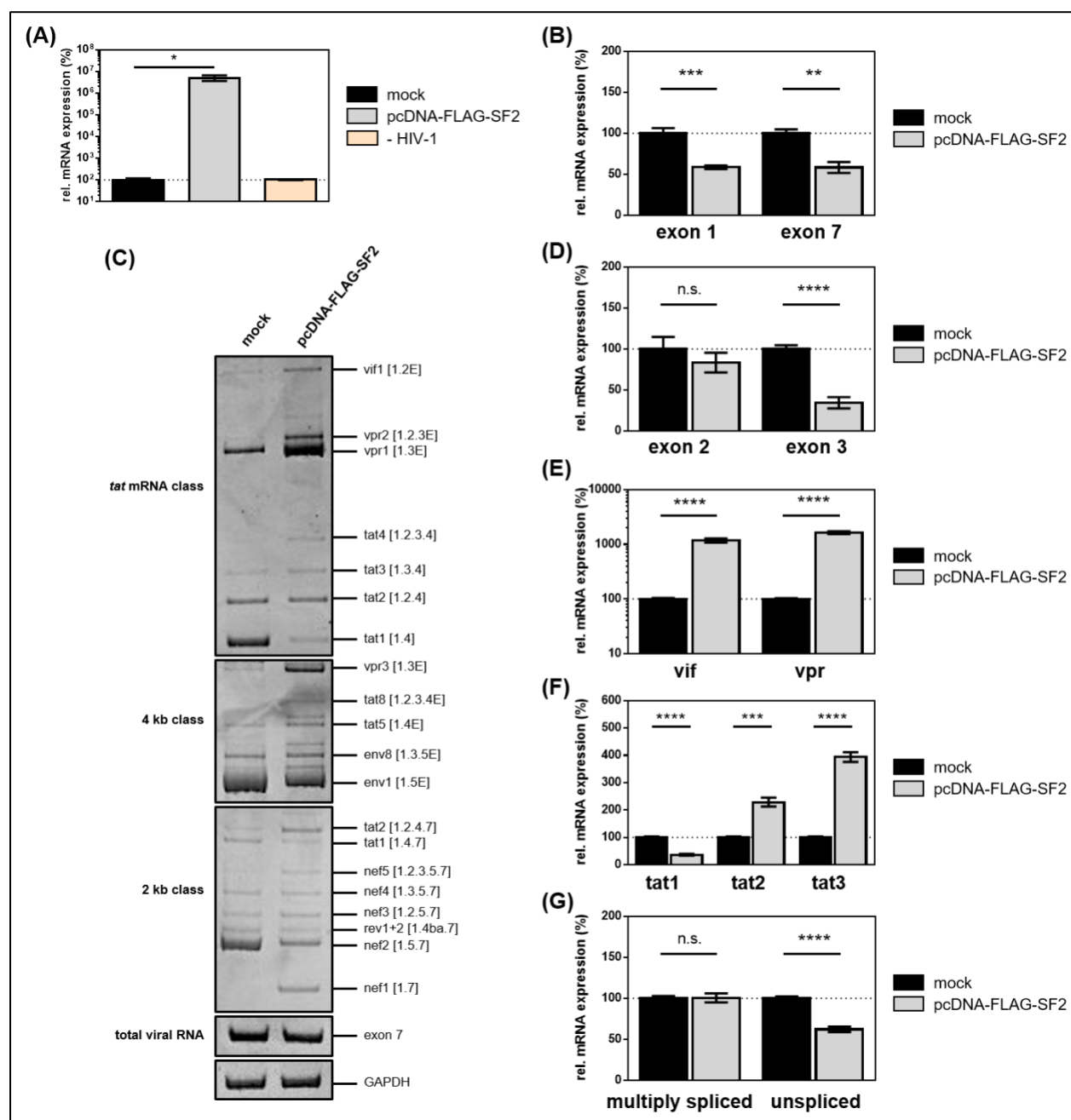


**Figure 4-9: Overexpression of SRSF1 affects HIV-1 LTR transcription and alternative splice site usage.** HEK293T cells were transiently transfected with a plasmid coding for the proviral clone NL4-3 PI952 (pNL4-3 PI952) (371) and a plasmid expressing FLAG-tagged SRSF1 (pcDNA-FLAG-SF2) (206). Cells were harvested 72 h post transfection and RNA and viral supernatant were extracted. **(A) – (B)** RT-qPCR was performed to determine relative mRNA expression levels of **(A)** *SRSF1* and **(B)** exon 1 and exon 7 containing mRNAs (total viral mRNA). GAPDH was used for normalization. **(C)** Viral splicing pattern upon SRSF1 overexpression. RT-PCR was performed using the indicated primer pairs for the 2 kb-, 4 kb- and *tat* mRNA-class (Table 2-4). HIV-1 transcript isoforms on the right are depicted according to (375). To normalize RNA amounts, separate RT-PCRs amplifying HIV-1 exon 7 containing transcripts as well as cellular GAPDH were performed. PCR amplicons were separated on a 12% nondenaturing polyacrylamide gel. **(D) – (G)** Total RNA was subjected to RT-qPCR to measure relative mRNA expression levels of **(D)**

exon 2 and exon 3 containing, **(E)** *vif* and *vpr*, **(F)** *tat1*, *tat2* and *tat3* and **(G)** multiply spliced and unspliced mRNAs using the indicated primers (Table 2-4). Splice site usage of NL4-3 PI952 was set to 100% and the relative splice site usage was normalized to exon 7-containing mRNAs (total viral RNA). Unpaired two-tailed t-tests were used to determine whether a statistical significance existed between the group of samples (\*  $p < 0.05$ , \*\*  $p < 0.01$ , \*\*\*  $p < 0.001$  and \*\*\*\*  $p < 0.0001$ ). Mean (+ SEM) of  $n = 4$  biological replicates is depicted for **(A)**, **(B)** and **(D)** – **(G)**.

RT-qPCR was performed to measure intracellular total viral mRNA using primer pairs amplifying HIV-1 exon 1 or exon 7 and normalized to GAPDH levels. Increased levels of SRSF1 led to a significant decrease of 1.7-fold in total viral mRNA levels determined by both exon 1 and exon 7 containing mRNAs (Figure 4-9 B). Thus an inhibitory effect on LTR transcription was suggested, which was in accordance with previous findings (63; 355). SRSF1 has been shown to compete with Tat for a binding sequence within TAR on the HIV-1 LTR promoter (355; 356). Accordingly, while overexpression of SRSF1 resulted in reduced HIV-1 LTR transcription (Figure 4-9 B), the siRNA-based knockdown of SRSF1 oppositely led to an increase in total viral RNA levels (Figure 4-7 B).

The effect of higher SRSF1 levels on the alternative splice site usage of HIV-1 was examined performing semi-quantitative RT-PCR. Viral splicing patterns of the intron-less 2 kb-, intron-containing 4 kb- and *tat* specific mRNA-classes were analyzed using specific primer pairs (Supplementary Figure 1). Analysis of both the *tat* mRNA and 2 kb-class revealed a reduction in *tat1* mRNA, while *tat2* mRNA expression was induced (Figure 4-9 C). Furthermore, increased levels of *vif1*, *vpr1-2* and *tat3-4* (*tat* mRNA class), *vpr3*, *tat5* and *tat8* (4-kb class) and *nef1* and *nef5* (2-kb class) were observed. The mRNA formation of *env1* and *nef2* was reduced in the 4 kb- and 2 kb-class respectively (Figure 4-9 C). Splicing from SD1 to SA1 is required for the formation of *vif1*, *tat2*, *tat4*, *tat8* and *vpr2*, while the formation of *vpr1*, *vpr3*, *tat3*, *tat4*, *tat8* mRNA involves splicing at SA2 (375). Since the expression of these mRNAs was increased, enhanced splice site usage of SA1 and SA2 was suggested. Decreased levels of *env1* and *nef2*, which are formed by splicing from SD1 to SA5, suggested an inhibited splice site usage at SA5. Thus, similar to the knockdown of SRSF1, elevated levels also considerably affected alternative splice site usage. Transcript specific primer pairs were used in RT-qPCR analysis to quantify the observed changes in mRNA expression upon SRSF1 overexpression. The inclusion of non-coding leader exons 2 and 3 is essential for the formation *vif* and *vpr* mRNAs, which have their start codon within the intron downstream of exon 2 and 3, respectively (270;

486). Upon SRSF1 overexpression, the inclusion of non-coding leader exon 2 was not significantly altered, whereas exon 3 inclusion was reduced by 3-fold (Figure 4-9 D). Elevated levels of SRSF1 induced a 12- and 16-fold increase in *vif* (spliced from SD1 to SA1) and *vpr* (spliced from SD1 to SA2) mRNA levels respectively (Figure 4-9 E). Thus, splicing events at SA1 and SA2 were likely enhanced, while splicing at SD2/2b and SD3 was repressed. Furthermore, elevated levels of SRSF1 might affect cross-exon interactions between SA1 and SD2/2b and SA2 and SD3, respectively. While an enhancing effect of elevated levels of SRSF1 on ESE M1/M2, which regulates splice site usage of SA1 (237), was suggested, no binding site of SRSF1 has been identified so far in the proximity of SA2. While *tat1* mRNA expression was repressed by 3-fold, both *tat2* and *tat3* mRNA levels were upregulated by 2.3- and 4-fold respectively (Figure 4-9 F). Formation of *tat1-3* mRNAs involves splicing from SD4 to SA7, while additional splicing is required for *tat1* (SD1 to SA3), *tat2* (SD1 to SA1 and SD2 to SA3) and *tat3* (SD1 to SA2 and SD3 to SA3) respectively (375). Thus, increased splice site usage of SA1 and SA2 was suggested, while splicing frequency at SA3 was likely inhibited. The suggested elevated splicing frequency at SA1 and SA2 was in accordance with the detected lower levels of unspliced mRNA transcripts by 1.6-fold (Figure 4-9 G). No alteration in multiply spliced mRNA levels (spliced from SD4 to SA7) was detected, thus an effect of SRSF1 overexpression on the frequency of SA7 splice site usage was unlikely (Figure 4-9 G). To assess, whether the induced changes in HIV-1 LTR transcription and alternative splicing upon overexpression of SRSF1 would affect viral infectivity, TZM-bl reporter cells were infected with virus-containing cellular supernatant. Overexpression of SRSF1 resulted in a strong and significant decrease of 4.1-fold in luciferase activity when compared to the mock transfected control, thus suggesting strongly reduced infectious virus titers (Figure 4-10 A). These results were confirmed by X-Gal staining of infected TZM-bl cells (Figure 4-10 B).

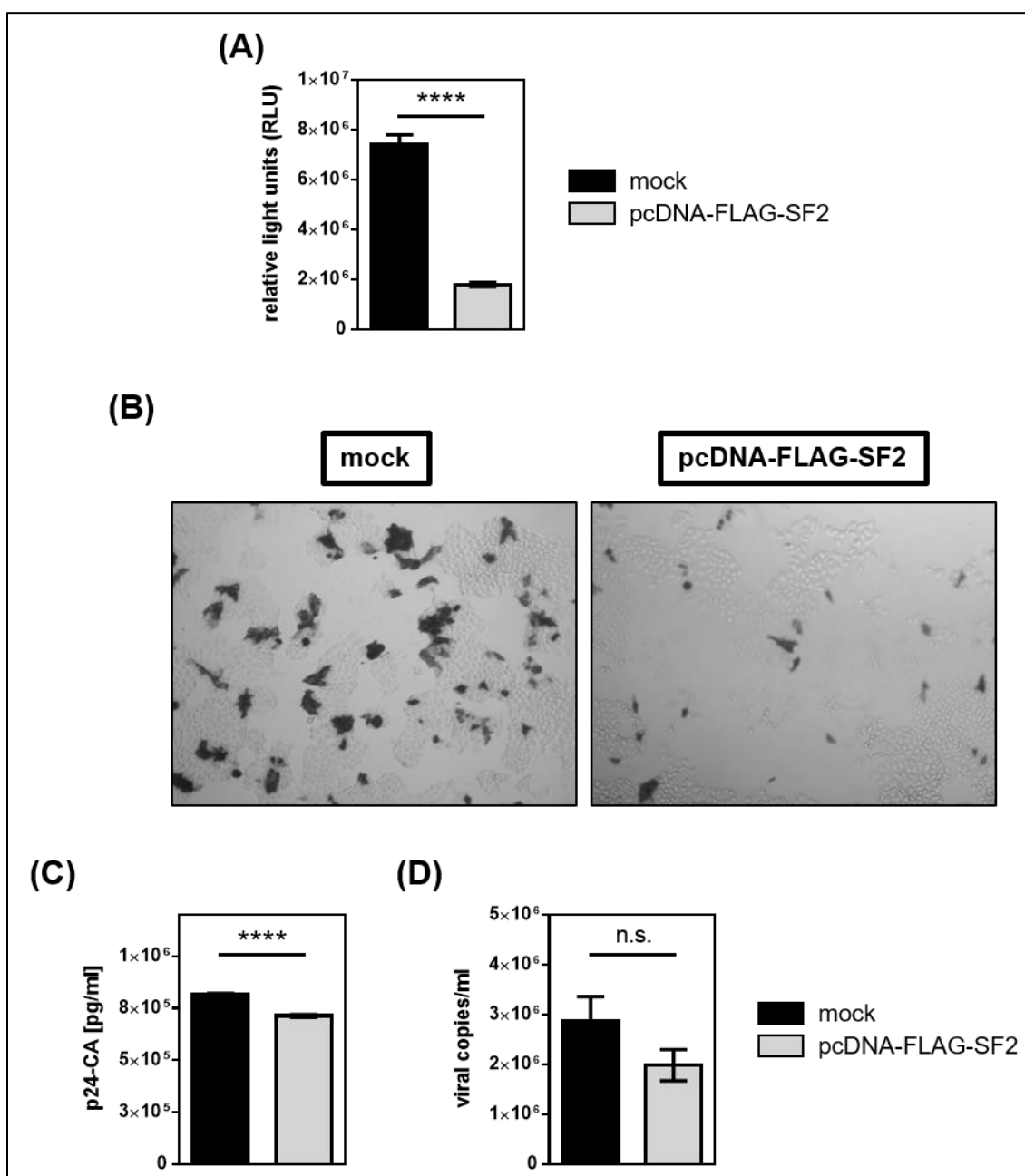


**Figure 4-10: Overexpression of SRSF1 affects HIV-1 infectivity and viral particle production.** HEK293T cells were co-transfected with a plasmid coding for the proviral clone NL4-3 PI952 (pNL4-3 PI952) (371) and a plasmid coding for FLAG-tagged SRSF1 (pcDNA-FLAG-SF2) (206). **(A) – (B)** 72 h post transfection, cell culture supernatant was used to determine viral infectious titers using TZM-bl reporter cells. **(A)** Measurement of luciferase activity. **(B)** X-Gal staining of TZM-bl cells incubated with cellular supernatant. **(C)** Viral RNA extracted from the supernatant was subjected to RT-qPCR to quantify absolute expression levels of exon 7-containing transcripts (total viral mRNA). **(D)** p24-CA ELISA was performed to determine viral particle production. Statistical significance was calculated using unpaired two-tailed t-tests (\*  $p < 0.05$ , \*\*  $p < 0.01$ , \*\*\*  $p < 0.001$  and  $p < 0.0001$ ). Mean (+ SEM) of  $n = 4$  biological replicates is depicted for **(A)**, **(C)** and **(D)**.



Interestingly, the detected higher expression of *vif* mRNA by 12-fold (Figure 4-9 E), which has been shown to be a crucial factor for HIV-1 infectivity and replication in non-permissive cells (436; 494), did not result in facilitated viral infectivity. Overexpression of SRSF1, and the subsequent alteration in HIV-1 LTR transcription and alternative splice site usage, resulted in significantly impaired viral infectivity, thus inducing opposite effects on HIV-1 infectious virus titers when compared to depleted levels of SRSF1 (Figure 4-8 A and B and 4-10 A and B).

To determine whether the impaired viral infectivity was due to altered HIV-1 particle production, p24-CA levels as well as viral copies in the cellular supernatant were determined. The levels of p24-CA protein were determined via p24-CA ELISA, revealing significantly lower levels of 1.2-fold in p24-CA levels upon elevated levels of SRSF1 (Figure 4-10 C). The number of viral copies extracted from the cellular supernatant was determined using RT-qPCR. A decrease of 1.4-fold in viral copies was detected upon overexpression of SRSF1, albeit with no statistical significance (Figure 4-10 D). Thus, in contrast to reduced levels of SRSF1, which had no significant effect on HIV-1 particle production (Figure 4-8), elevated levels resulted in a significant impairment of virus production.

Type I IFN-stimulation in THP-1 macrophages induced an upregulation of *SRSF1* mRNA expression after 4 h (Figure 4-4 A and B), while treatment with IFN $\gamma$  resulted in significantly increased *SRSF1* levels after 48 h (Figure 4-5 C). However, higher levels of SRSF1, which have been shown to be detrimental for HIV-1 particle production and infectivity, were potentially downregulated by the cellular autoregulation of SRSF1 (111). Thus, HIV-1 was suggested to have adapted to replicate efficiently under low levels of SRSF1, but not under elevated levels.

#### **4.1.7. HIV-1 affects the IFN-mediated repression of *SRSF1***

The expression levels of SRSF1 were significantly repressed upon HIV-1 infection and inversely correlated with the IFN signature in the acute phase of the viral infection (Chapter 4.1.1.). Stimulation of THP-1 macrophages and MDMs with IFN resulted in an immediate-early but transient upregulation of *SRSF1*, followed presumably by an autoregulatory repression (Chapter 4.1.3.). Furthermore, altered levels of SRSF1 were shown to substantially affect HIV-1 LTR transcription, alternative splicing, viral infectivity and viral particle production (Chapter 4.1.5. and 4.1.6.).

---

To assess, whether an acute HIV-1 infection would affect the IFN-mediated regulation of *SRSF1*, THP-1 macrophages were infected with the R5-tropic HIV-1 laboratory strain NL4-3 (AD8) 16 h prior to stimulation with IFN $\alpha$ 2 or IFN $\alpha$ 14. It has previously been shown that 16 h post HIV-1 infection the integration of the viral genome into the host cell genome was mostly complete (334). Thus, this time point was specifically chosen to focus on HIV-1 post integration steps.

Upon HIV-1 infection, stimulation with both subtypes resulted in a similar expression profile of *SRSF1* mRNA (Figure 4-11 A and B). Comparable to the expression profile of *SRSF1* in uninfected cells upon IFN-treatment, an initial upregulation after 4 h was observed by 1.7- and 1.4-fold for IFN $\alpha$ 2 and IFN $\alpha$ 14 respectively (Figure 4-11). 12 h post stimulation in HIV-1 infected cells, a 3.3-fold repression was observed for IFN $\alpha$ 2, while after 24 and 48 h a 1.9- and 1.5-fold increase in *SRSF1* mRNA expression was detected (Figure 4-11 A). IFN $\alpha$ 14 treatment resulted in a 5.9-fold downregulation after 12 h, while *SRSF1* mRNA levels were elevated by 1.8-fold upon IFN $\alpha$ 14 stimulation after 24 and 48 h (Figure 4-11 B).

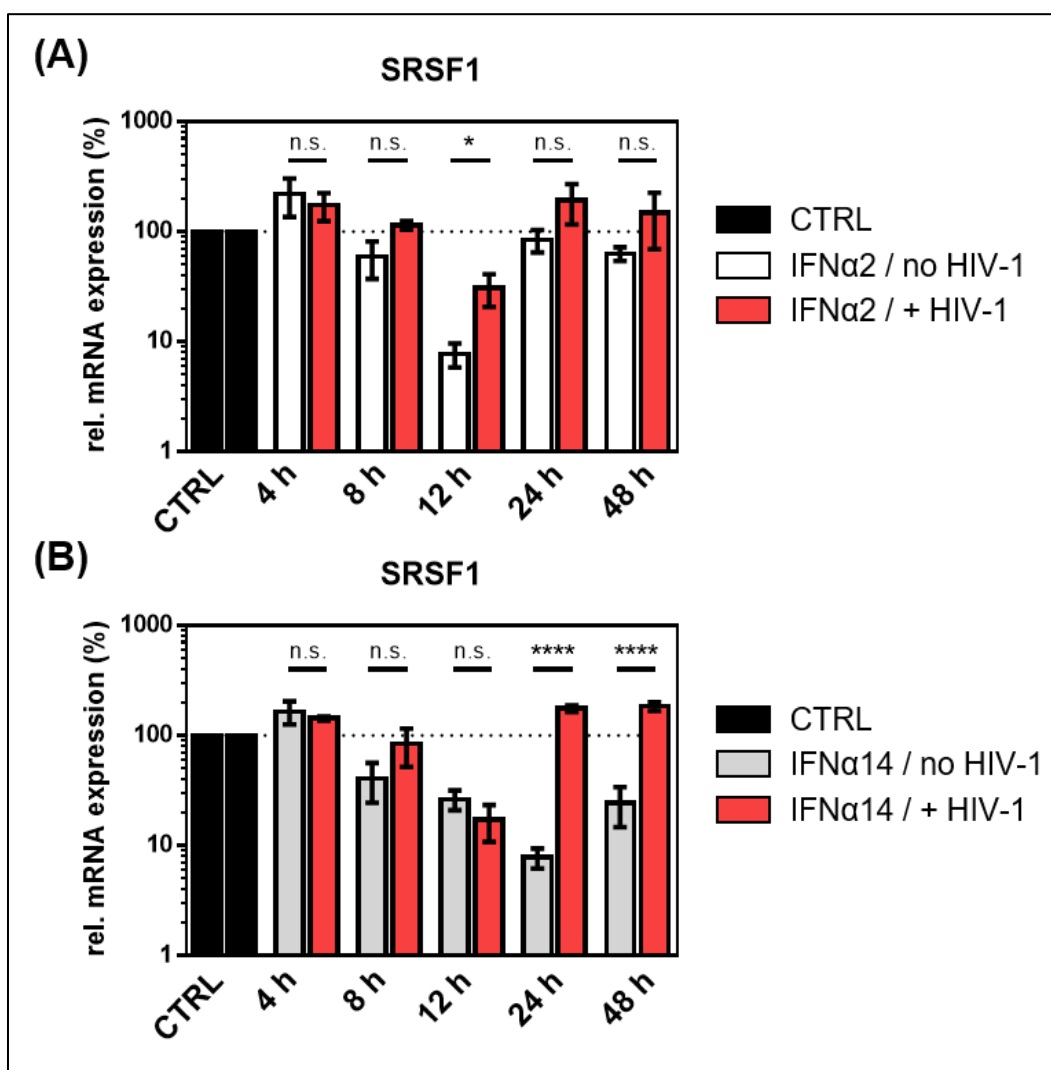


**Figure 4-11: HIV-1 affects IFN-mediated deregulation of *SRSF1*.** Differentiated THP-1 macrophages were infected with the R5-tropic NL4-3 (AD8) (148) at an MOI of 1. 16 h post infection, cells were treated with the indicated IFN subtype [10 ng/ml] over a period of 48 h. Cells were harvested at the indicated time points, RNA isolated and subjected to RT-qPCR. Relative mRNA expression levels of *SRSF1* in THP-1 cells after treatment with **(A)** IFNα2 or **(B)** IFNα14. GAPDH was used as house-keeping gene for normalization. Unpaired two-tailed t-tests were calculated to determine whether the difference between the group of samples reached the level of statistical significance (\*  $p < 0.05$ , \*\*  $p < 0.01$  and \*\*\*  $p < 0.001$ ). Mean (+ SEM) of  $n = 4$  biological replicates is shown.

In uninfected cells, the magnitude of the downregulation upon stimulation with both subtypes was stronger than in HIV-1 infected cells. While a 13-fold reduction in *SRSF1* mRNA expression was detected for IFNα2 and IFNα14 stimulation after 12 and 24 h respectively in uninfected cells, treatment of HIV-1 infected cells with both subtypes only resulted in a 3.3- (IFNα2) and 5.9-fold (IFNα14) *SRSF1* mRNA repression after 12 h (Figure 4-11). The expression profile of *SRSF1* mRNA strongly differed for IFNα2 and

IFN $\alpha$ 14 treatment in uninfected cells, whereas stimulation of HIV-1 infected cells with both subtypes resulted in a similar expression profile of *SRSF1* mRNA (Figure 4-11). Furthermore, the long-lasting repression of *SRSF1* mRNA expression, with a remaining 6-fold repression after 48 h of IFN $\alpha$ 14 treatment in uninfected cells was not observed in HIV-1 infected cells (Figure 4-11 B). Upon stimulation of HIV-1 infected cells with both subtypes, *SRSF1* expression levels were restored and even elevated 24 to 48 h post treatment (Figure 4-11). Thus, HIV-1 potentially directly or indirectly restored balanced levels of *SRSF1* for efficient HIV-1 RNA processing. However, a potential effect of the IFN-induction triggered upon the HIV-1 infection prior to the IFN treatment on the expression of *SRSF1* cannot be ruled out.

#### **4.2. *hnRNP* transcript levels are lower upon HIV-1 infection**

The protein family of hnRNPs consists of RNA-binding proteins with a wide range of functions in cellular splicing, RNA stability, translation or mRNA trafficking (162). Alongside the SRSF protein family, the hnRNP protein family is crucially involved in the regulation of HIV-1 alternative splicing (410). Thus, to investigate whether HIV-1 infection would, in addition to *SRSFs* (Chapter 4.1), also alter *hnRNP* gene expression, transcript levels of *hnRNPs* were analyzed in gut LPMCs of chronically HIV-1 infected individuals, either treatment naïve or under ART-treatment, and compared to healthy donors. LPMCs are mucosal immune cells from the lamina propria and are the first cells to be infected upon HIV-1 entry via the gastrointestinal tract (46; 427; 519).

In collaboration with Mario Santiago (Department of Medicine, University of Colorado Denver, USA), gene expression of all *hnRNP* family members was determined by reanalyzing RNA-sequencing data from a previous publication, as described in (Chapter 4.1.) (109). Similar to *SRSFs*, several *hnRNPs* were also differentially expressed upon chronic HIV-1 infection. Gene expression of *hnRNP A0* (1.3-fold), *hnRNP A1* (1.4-fold), *hnRNP A2B1* (1.3-fold), *hnRNP D* (1.3-fold), *hnRNP DL* (1.2-fold), *hnRNP F* (1.5-fold), *hnRNP H3* (1.6-fold), *hnRNP K* (1.3-fold), *hnRNP M* (1.3-fold), *hnRNP Q* (1.3-fold), *hnRNP R* (1.3-fold), *hnRNP U* (1.4-fold) and *hnRNP UL1* (1.2-fold) was significantly lower in treatment naïve chronically HIV-1 infected patients when compared to healthy donors (Figure 4-12 A).

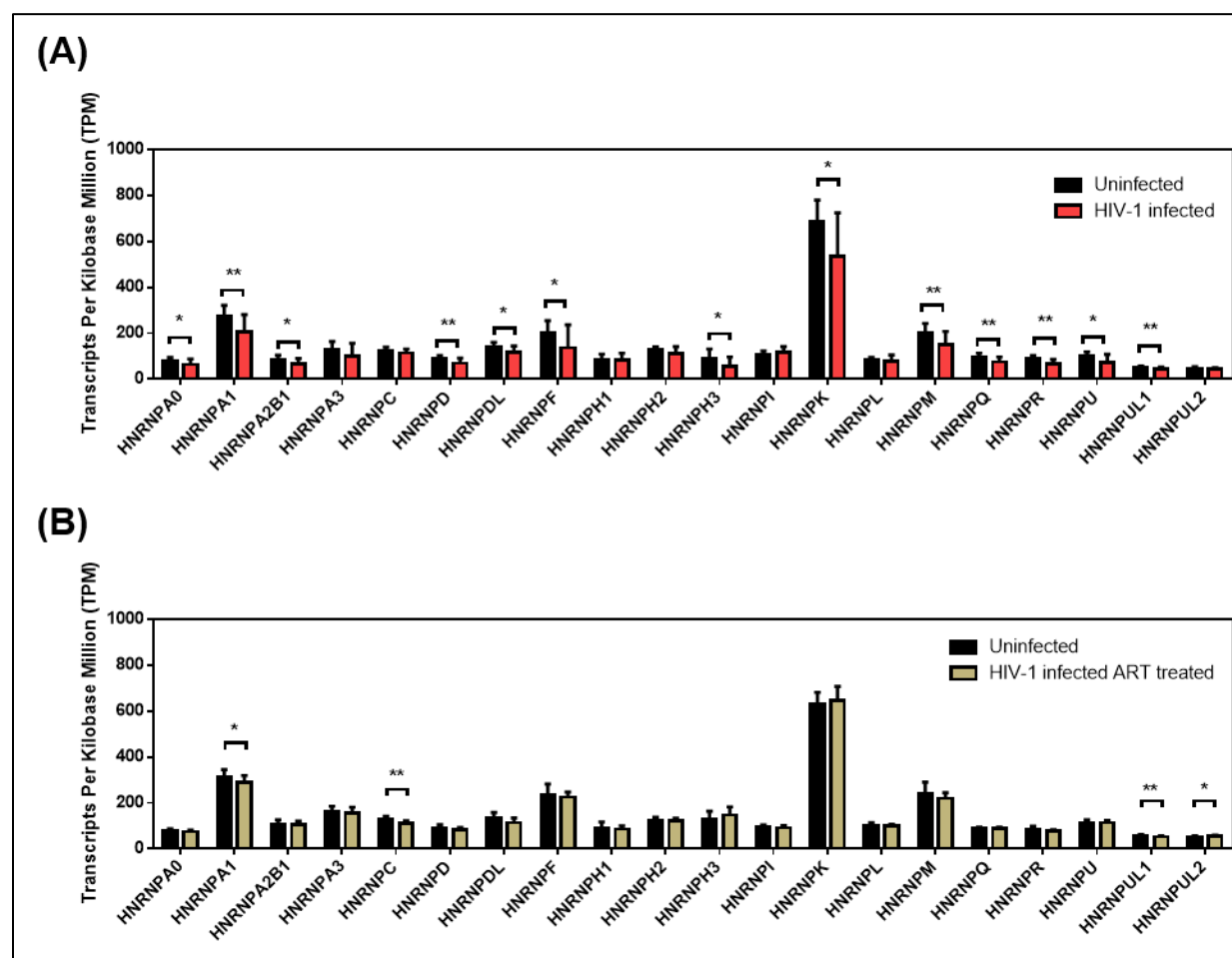


**Figure 4-12: Gene expression levels of *hnRNP* in treatment naïve or ART-treated HIV-1 infected individuals.** Expression of *hnRNP* genes was measured in gut LPMCs using RNA-sequencing analysis. Transcript levels of **(A)** treatment naïve HIV-1 infected and **(B)** ART-treated HIV-1 infected individuals compared to uninfected donors. TPM are depicted as mean (+ SD) for **(A)** 19 HIV-1 infected and 13 uninfected individuals and **(B)** 14 ART-treated and 11 uninfected individuals. Statistical significance in the differences between the group of samples was determined via unpaired two-tailed t-tests (\*  $p < 0.05$  and \*\*  $p < 0.01$ ).

Upon ART-treatment, however, comparable transcript levels were detected in comparison to uninfected donors for all *hnRNPs*, except for *hnRNP A1* and *hnRNP UL1*, which were expressed at lower levels (1.1-fold respectively) (Figure 4-12 B). Furthermore, gene expression of *hnRNP C* was lower (1.2-fold), while *hnRNP UL2* transcript levels were higher (1.1-fold) in HIV-1 infected patients under ART-treatment but not HIV-1 infected treatment naïve patients when compared to healthy donors (Figure 4-12). No significant differences in gene expression were observed for *hnRNP A3*, *hnRNP H1*, *hnRNP H2*, *hnRNP I* and *hnRNP L* upon HIV-1 infection, either treatment naïve or under ART-treatment (Figure 4-12).

HIV-1 infection thus affected the gene expression of distinct *hnRNPs* and *SRSFs*, as described above (Chapter 4.1.). This observation suggested an interaction between an HIV-1 infection and the regulation of the gene expression of these two families of cellular splicing factors, potentially due to the state of chronic inflammation induced upon HIV-1 infection.

#### **4.2.1. Specific *hnRNPs* are repressed upon IFN-stimulation in macrophages**

Several *hnRNPs* were expressed at a lower magnitude in chronically HIV-1 infected patients when compared to uninfected donors (Chapter 4.2.), potentially due to the induction of type I IFNs as a response to HIV-1 infection. Thus, to investigate whether *hnRNPs* are generally IRepGs, mRNA expression levels of relevant *hnRNPs* were analyzed in THP-1 cells upon IFN-stimulation. The subfamilies hnRNP A/B (hnRNP A0, hnRNP A1 and hnRNP A2/B1), hnRNP D and hnRNP F/H (hnRNP F and hnRNP H) were included, which have all been described to be involved in HIV-1 alternative splicing and RNA processing (54; 93; 114; 182; 196; 237; 410; 445; 457; 485; 486; 509). The IFN $\alpha$  subtype 14 was chosen, as it induced the strongest repression in *SRSF1* mRNA levels of all IFN $\alpha$  subtypes (Chapter 4.1.2.), as well as IFN $\alpha$ 2, which is the sole clinically approved IFN $\alpha$  subtype used to treat e.g. Hepatitis B infections (17).

THP-1 macrophages were stimulated with IFN $\alpha$ 2 or IFN $\alpha$ 14 for 12 h, before cells were harvested and total RNA was subjected to RT-qPCR analysis. Treatment with both subtypes induced a >2-fold significant downregulation in mRNA expression levels for *hnRNP A1*, *hnRNP A2/B1* and *hnRNP H* (Figure 4-13). Stimulation with IFN $\alpha$ 2 further induced a 2.4-fold reduction in *hnRNP D* mRNA (Figure 4-13 A), while IFN $\alpha$ 14 treatment also resulted in a 2.2-fold reduction of *hnRNP H* (Figure 4-13 B). Remarkably, the strongest repression upon stimulation with both subtypes was observed for *hnRNP A0*, with a 4.6-fold and 5.8-fold reduction for IFN $\alpha$ 2 and IFN $\alpha$ 14, respectively (Figure 4-13).

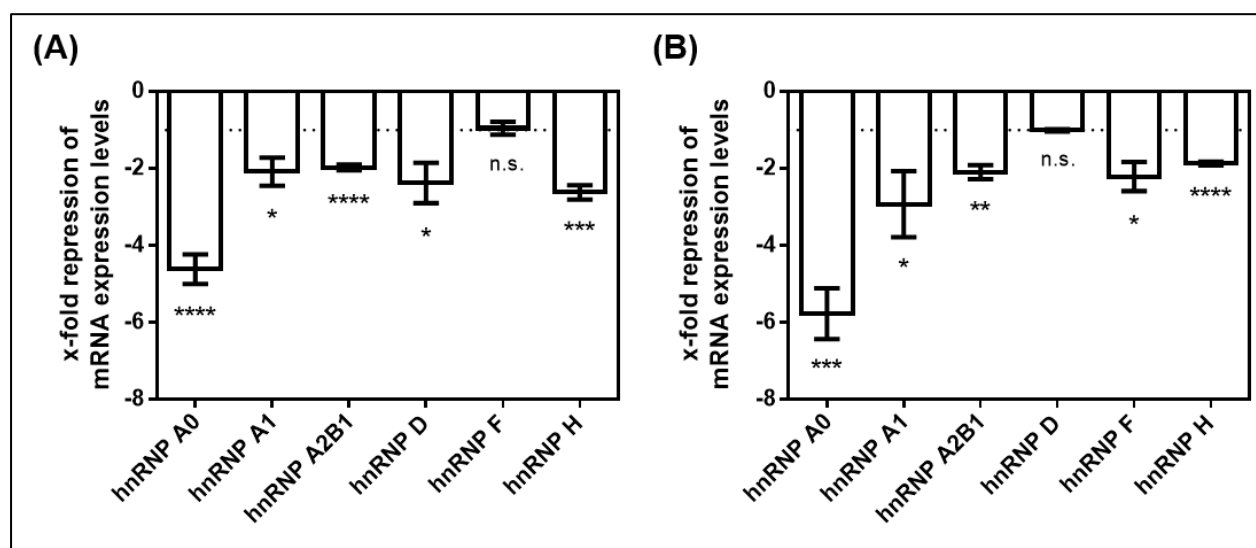


**Figure 4-13: Selected *hnRNP* mRNA levels upon stimulation with IFN $\alpha$ 2 or IFN $\alpha$ 14 in THP-1 cells.** Differentiated THP-1 cells were treated with IFN $\alpha$ 2 or IFN $\alpha$ 14 [10 ng/ml]. After 12 h, cells were harvested, total RNA isolated and subjected to RT-qPCR. mRNA expression levels of *hnRNP A0*, *hnRNP A1*, *hnRNP A2/B1*, *hnRNP D*, *hnRNP F* and *hnRNP H* upon stimulation with (A) IFN $\alpha$ 2 or (B) IFN $\alpha$ 14. Unpaired two-tailed t-tests were used to determine statistical significance (\*  $p < 0.05$ , \*\*  $p < 0.01$ , \*\*\*  $p < 0.001$  and \*\*\*\*  $p < 0.0001$ ). Mean (+ SEM) of  $n = 3$  biological replicates is depicted.

Since stimulation with IFN $\alpha$ 2 and IFN $\alpha$ 14 both revealed *hnRNP A0* to be the most significantly downregulated gene of all analyzed *hnRNPs*, the expression profile of this specific *hnRNP* was investigated in more detail. Although the *hnRNP A/B* family generally has been shown to be crucially involved in HIV-1 alternative splicing (410), *hnRNP A0* has not yet been described as a relevant splicing factor in HIV-1 RNA processing.

#### 4.2.2. *hnRNP A0* expression is lower in HIV-1 infected individuals

To further investigate the role of the so far poorly characterized *hnRNP A0* in the context of an HIV-1 infection, the mRNA expression profile of this factor was analyzed in PBMCs of HIV-1 positive individuals at different phases of infection. Therefore, PBMCs from HIV-1 infected patients during acute (Fiebig I-V) or chronic phase of infection (Fiebig VI) (138), treatment naïve or under ART-treatment, were isolated from whole blood samples as described above (Chapter 4.1.1.). PBMCs from HIV-1 negative donors served as control. ISG induction was measured using *ISG15* mRNA expression levels as surrogate marker, thus verifying IFN signature. Patients with no considerable induction in *ISG15* mRNA

expression were excluded from the statistical analysis and are depicted accordingly in (Figure 4-14).

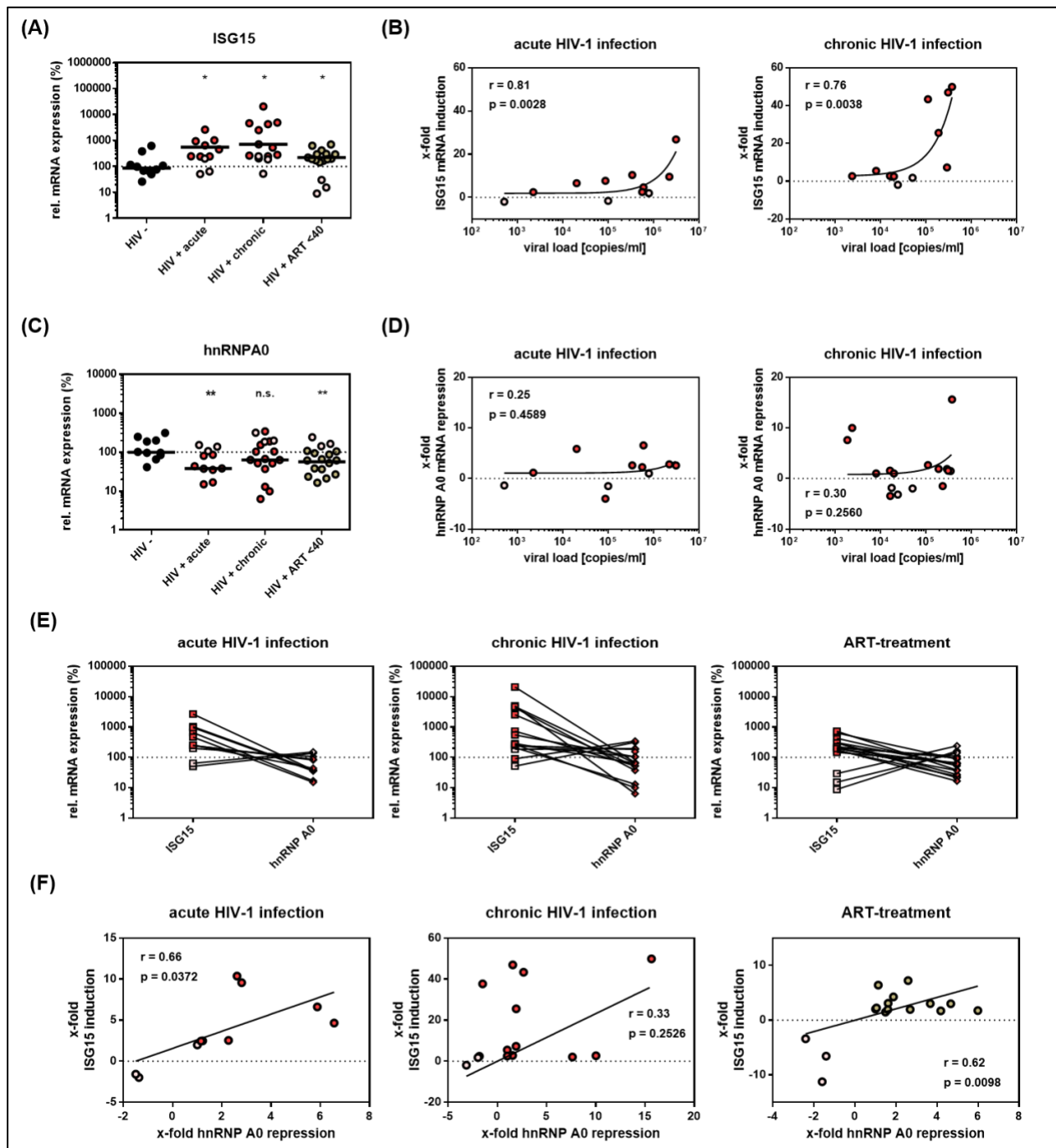


**Figure 4-14: *hnRNP A0* and *ISG15* mRNA levels inversely correlate upon HIV-1 infection.** (A) and (C) mRNA expression levels of (A) *ISG15* and (C) *hnRNP A0* measured via RT-qPCR analysis in PBMCs from acutely and chronically HIV-1 infected patients, treatment naïve or under ART-treatment, and healthy donors. The expression levels were normalized to ACTB expression. Statistical differences between two groups were calculated using the unpaired one-tailed t-tests (\*  $p < 0.05$  and \*\*  $p < 0.01$ ). (B) and (D) Plasma viral load of single patients was determined as



described in (Chapter 3.1.7.). After quantification of *ISG15* and *hnRNP A0* mRNA levels via qRT-PCR, correlation between plasma viral load and **(B)** *ISG15* or **(D)** *hnRNP A0* mRNA expression was calculated. Pearson correlation coefficient (r) and p-value (p) are indicated. **(E)** Relative *ISG15* and *hnRNP A0* mRNA expression levels for individual patients. **(F)** Correlation between x-fold repression of *hnRNP A0* mRNA levels and x-fold induction of *ISG15* mRNA levels for acutely and chronically HIV-1 infected patients, as well as HIV-1 infected individuals under ART-treatment. Pearson correlation coefficient (r) and p-value (p) are indicated. Low responders were defined as patients without *ISG15* mRNA induction upon HIV-1 infection and thus without IFN signature. These patients were excluded from statistical analysis. Data points of these patients are shown in light pink. For this patient cohort, samples from 10 uninfected donors, 8 acutely HIV-1 infected patients, 11 chronically HIV-1 infected patients and 13 HIV-1 infected patients under ART-treatment were analyzed.

*ISG15* mRNA expression was 5.6-, 7.3- and 2.2-fold higher in PBMCs of acutely, chronically and ART-treated HIV-1 infected patients when compared to healthy individuals (Figure 4-14 A). The induced IFN signature was proportional to the plasma viral load of acutely and chronically HIV-1 infected patients (Figure 4-14 B). When comparing acutely HIV-1 infected patients with healthy individuals, the expression of *SRSF1* mRNA was shown to inversely correlate with the induction of *ISG15* mRNA expression (Chapter 4.1.1). To investigate, whether the downregulation of *hnRNP A0* also correlated with the IFN signature in HIV-1 infected individuals, *hnRNP A0* mRNA expression levels were determined via RT-qPCR. When compared to HIV-1 negative donors, mRNA levels of *hnRNP A0* were lower in all groups of HIV-1 infected individuals (Figure 4-14 C). Acutely HIV-1 infected patients had 2.6-fold lower *hnRNP A0* expression levels, while chronically HIV-1 infected patients had 1.6-fold reduced mRNA expression levels and patients under ART-treatment had 1.8-fold lower expression levels when compared to uninfected individuals (Figure 4-14 C). A statistical significance in the differences of *hnRNP A0* mRNA expression levels, however, could only be determined for acutely HIV-1 infected patients, as well as patients under ART-treatment in comparison to healthy donors (Figure 4-14 C). No significant correlation could be determined between the expression levels of *hnRNP A0* and the plasma viral load of acutely or chronically HIV-1 infected patients (Figure 4-14 D). Similar to *SRSF1* (Figure 4-2 E), strongly induced levels of *ISG15* were generally concomitant with a strong repression in *hnRNP A0* expression (Figure 4-14 E). Patients with no or low *ISG15* induction, however, had no reduction in *hnRNP A0* mRNA expression and in some cases even a slight upregulation (Figure 4-14 E). Pearson correlation coefficients were determined to investigate, whether a direct correlation could

be observed between the downregulation of *hnRNP A0* mRNA and the induction of *ISG15* (Figure 4-14 F). Significant correlations were found for the groups of acutely HIV-1 infected and ART-treated patients (Figure 4-14 F). The expression of *hnRNP A0* mRNA levels was highly scattered for the group of chronically HIV-1 infected patients, which generally represent a more heterogeneous group concerning their stage of infection or co-morbidities.

The downregulation of *hnRNP A0* was generally concomitant with the induction of *ISG15* upon HIV-1 infection. Thus, a potential link between ISG induction and *hnRNP A0* repression was indicated, suggesting a potential role of *hnRNP A0* as IRepG.

#### **4.2.3. *hnRNP A0* is differentially regulated in HIV-1 target cells upon IFN-stimulation**

The expression levels of *SRSF1* and *hnRNP A0* mRNA were lower upon HIV-1 infection and a direct correlation was observed between the repression of these two factors and the IFN signature (Chapter 4.1.1. and 4.2.2.). Furthermore, *SRSF1* was shown to be deregulated upon stimulation with IFN $\alpha$ 2 and IFN $\alpha$ 14 (Chapter 4.1.3.). Thus, to investigate whether the repression of *hnRNP A0* mRNA expression was also a direct effect of the IFN-stimulation, the expression profile of *hnRNP A0* mRNA was analyzed upon IFN $\alpha$ 2 and IFN $\alpha$ 14 treatment in HIV-1 target cells in a time-course experiment. IFN signature was quantified via ISG induction, using *ISG15* as surrogate marker.

Upon stimulation of THP-1 macrophages with both IFN $\alpha$ 2 and IFN $\alpha$ 14, a 100- to 1,000-fold induction of *ISG15* mRNA expression levels was induced (Figure 4-15 A and B, left panel). Stimulation with IFN $\alpha$ 2 resulted in a significant downregulation in *hnRNP A0* mRNA expression of 2.8- and 4.6-fold after 8 and 12 h respectively, while gene expression was recovered to a less than 2-fold reduction after 24 and 48 h (Figure 4-15 A, right panel). Treatment with IFN $\alpha$ 14 induced a downregulation in *hnRNP A0* mRNA expression of 3.6- and 5.8-fold after 8 and 12 h respectively. The mRNA expression levels were still repressed by 2.9-fold after 24 h before reaching similar levels to the untreated control 48 h post stimulation (Figure 4-15 B, right panel). In contrast to the expression profile of *SRSF1* upon IFN treatment, no initial upregulation of *hnRNP A0* mRNA levels were observed.

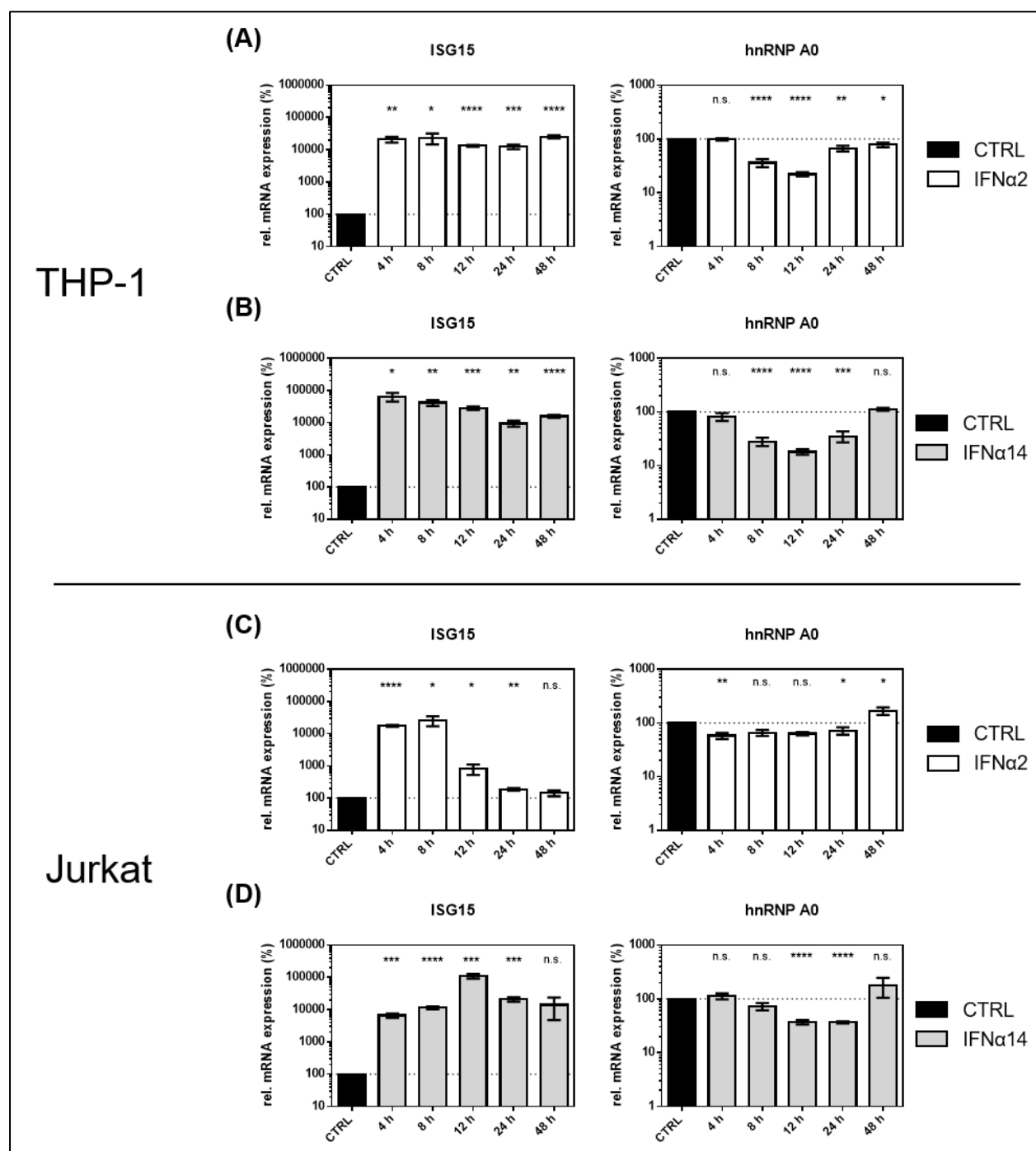


**Figure 4-15: *hnRNP A0* mRNA expression levels are differentially regulated upon stimulation of HIV-1 target cells with IFN $\alpha$ 2 or IFN $\alpha$ 14.** Stimulation of differentiated THP-1 macrophages and Jurkat T-cells with IFN $\alpha$ 2 (white) or IFN $\alpha$ 14 (grey) for 48 h [10 ng/ml]. Cells were harvested, RNA was extracted and subjected to RT-qPCR. **(A) – (B)** *ISG15* and *hnRNP A0* mRNA levels upon treatment with **(A)** IFN $\alpha$ 2 and **(B)** IFN $\alpha$ 14 in THP-1 macrophages. **(C) – (D)** *ISG15* and *hnRNP A0* mRNA levels upon treatment with **(C)** IFN $\alpha$ 2 and **(D)** IFN $\alpha$ 14 in Jurkat cells. ACTB expression was used for normalization. Statistical significance in the differences between the group of samples was calculated using unpaired two-tailed t-tests (\*  $p < 0.05$ , \*\*  $p < 0.01$ , \*\*\*  $p < 0.001$  and \*\*\*\*  $p < 0.0001$ ). Mean (+ SEM) of  $n = 4$  biological replicates is depicted.

In Jurkat T-cells, treatment with IFN $\alpha$ 2 induced *ISG15* mRNA levels by 100-fold after 4 and 8 h, before ISG-induction rapidly decreased and reached expression levels similar to the untreated control 24 to 48 h post stimulation (Figure 4-15 C, left panel). IFN $\alpha$ 14-treatment resulted in a 100- to 1,000-fold induction in *ISG15* mRNA levels through the course of the experiment (Figure 4-15 D, left panel). Generally, a less pronounced ISG induction was observed in Jurkat T-cells when compared to THP-1 macrophages. A less than 2-fold repression in *hnRNP A0* mRNA levels was detected after 4 to 24 h upon stimulation with IFN $\alpha$ 2 (Figure 4-15 C, right panel). Stimulation with IFN $\alpha$ 14 resulted in a significant 2.8-fold reduction in *hnRNP A0* mRNA levels after 12 and 24 h (Figure 4-15 D, right panel). However, 48 h post stimulation with both subtypes, *hnRNP A0* mRNA levels were elevated by 1.7- and 1.8-fold for IFN $\alpha$ 2 and IFN $\alpha$ 14 respectively when compared to the untreated control (Figure 4-15 C and D, right panel).

In conclusion, a time-dependent and significant downregulation of *hnRNP A0* mRNA expression was observed after stimulation with IFN $\alpha$ 2 and IFN $\alpha$ 14 in both THP-1 macrophages and Jurkat T-cells. Similar to the expression profile of *SRSF1*, the effect of IFN-stimulation on the repression of *hnRNP A0* mRNA expression was much more pronounced in macrophages when compared to T-cells, supporting the suggestion of a cell-type specific mechanism. However, while the expression profile of *SRSF1* was different upon stimulation with IFN $\alpha$ 2 and IFN $\alpha$ 14, the expression profile of *hnRNP A0* is largely similar upon treatment with both subtypes.

To verify, whether the IFN-mediated repression of *hnRNP A0* mRNA expression could be reproduced in primary human cells, primary human monocyte-derived macrophages (MDMs) were treated with IFN $\alpha$ 14 in collaboration with Fabian Roesmann (AG Widera, Institute for Medical Virology, University Hospital Frankfurt, Frankfurt am Main) as described above (Chapter 4.1.3.). ISG induction was measured using *ISG15* as surrogate marker. Levels of *ISG15* mRNA were induced by 50- to 500-fold upon stimulation with IFN $\alpha$ 14 (Figure 4-16 A, left panel).

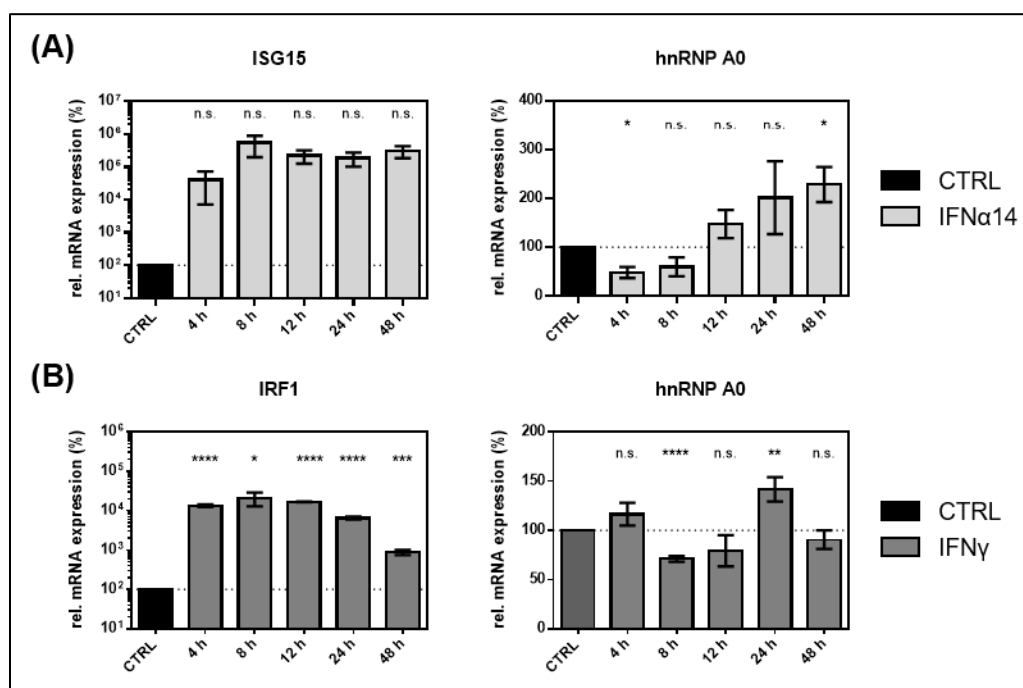


**Figure 4-16: *hnRNP A0* mRNA expression levels upon stimulation of HIV-1 target cells with type I and II IFNs. (A) – (B)** Monocyte-derived macrophages (MDMs) were stimulated with IFN $\alpha$ 14 [10 ng/ml] over a period of 48 h. Cells were harvested at the indicated time points and RNA was isolated. **(A)** *ISG15* and **(B)** *hnRNP A0* mRNA expression levels were measured via RT-qPCR. GAPDH was used for normalization. **(C) – (D)** Differentiated THP-1 cells were treated with IFN $\gamma$  at a concentration of 10 ng/ml. At the depicted time points, cells were harvested and RNA was extracted. Relative mRNA expression levels of **(C)** *IRF1* and **(D)** *hnRNP A0* were determined via RT-qPCR. Expression levels were normalized to GAPDH. Statistically significant difference between the group of samples was determined via unpaired two-tailed t-tests (\*  $p < 0.05$ , \*\*  $p < 0.01$ , \*\*\*  $p < 0.001$  and \*\*\*\*  $p < 0.0001$ ). Mean (+ SEM) of  $n = 4$  biological replicates is depicted. (Time points 24 h and 48 h for **(A)** only include two biological replicates.)

The mRNA expression levels of *hnRNP A0* were reduced by 2- and 1.7-fold after 4 and 8 h respectively upon IFN $\alpha$ 14 stimulation (Figure 4-16 A, right panel). Interestingly, *hnRNP A0* mRNA levels increased from 12 to 48 h, resulting in a significant, 2.3-fold induction after 48 h (Figure 4-16 A, right panel). Thus, *hnRNP A0* potentially represents an IRepG in primary human cells. However, an autoregulatory feedback loop might possibly recover *hnRNP A0* mRNA expression following the rapid IFN-induced repression. The repression of *hnRNP A0* mRNA levels upon stimulation with IFN $\alpha$ 14 occurred earlier, but to a lesser extent in MDMs when compared to THP-1 macrophages. Furthermore, the upregulation of *hnRNP A0* expression following the initial repression was observed in MDMs but not in THP-1 macrophages (Figure 4-15 A and B and 4-16 A).

To analyze, whether stimulation with type II IFN could also repress the expression of *hnRNP A0* mRNA, THP-1 macrophages were additionally treated with IFN $\gamma$ . As explained above (Chapter 4.1.3.), IFN $\gamma$  signals through a distinct signaling pathway and thus *IRF1* was used as surrogate marker for type II IFN specific ISG induction. When compared to the untreated control, stimulation with IFN $\gamma$  induced a 50- to 100-fold increase in *IRF1* mRNA expression 4 to 24 h post treatment, while after 48 h an induction of 9-fold was measured (Figure 4-16 B, left panel). The mRNA expression of *hnRNP A0* was significantly repressed by 1.4-fold after 8 h, before mRNA levels were recovered and significantly elevated by 1.4-fold after 24 h (Figure 4-16 B, right panel). The repression of *hnRNP A0* mRNA levels was much less pronounced and consistent for type II IFN than for type I IFNs. Thus, repression of *hnRNP A0* seems to be a preferentially type I IFN specific effect.

#### **4.2.4. Alteration in *hnRNP A0* gene expression occurs on transcriptional level**

IFN-stimulation altered the expression profile of *hnRNP A0* in HIV-1 target cells (Chapter 4.2.3.). To assess whether, similar to *SRSF1* gene expression, IFN-induced deregulation in *hnRNP A0* mRNA expression also occurred on the transcriptional level, 4sU-tagging was performed as described in (Chapter 4.1.4.). Briefly, newly synthesized RNA was metabolically labeled with 4sU, allowing the subsequent isolation and separation from pre-existing, untagged RNA (159; 377; 493). Stimulation of THP-1 macrophages with IFN $\alpha$ 14 induced an upregulation in 4sU-tagged *ISG15* mRNA levels by 50- to 500-fold, thus verifying IFN signature (Figure 4-17 A).

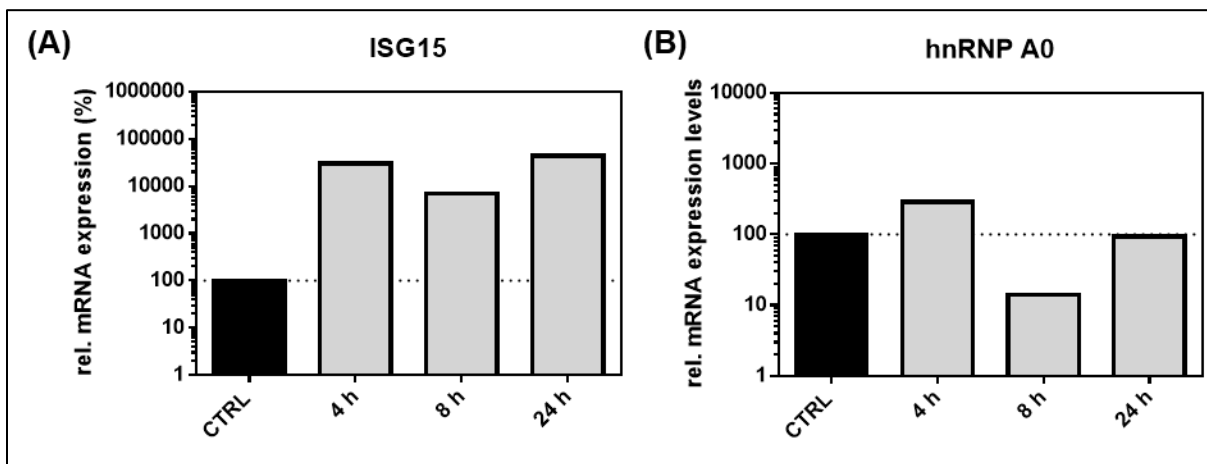


**Figure 4-17: IFN $\alpha$ 14-mediated changes in newly transcribed *hnRNP A0* mRNA.** Differentiated THP-1 macrophages were treated with 10 ng/ml of IFN $\alpha$ 14 for 4, 8 or 24 h. 4-thiouridine (4sU) was added 30 min before harvesting the cells and isolating total RNA. Newly synthesized, labeled RNA was then biotinylated and isolated from total RNA using streptavidin-coated magnetic beads. Relative mRNA expression was measured via RT-qPCR for (A) *ISG15* and (B) *hnRNP A0*. Expression was normalized to GAPDH. Due to the methodologically associated low yield, two biological replicates were pooled for RT-qPCR analysis.

The expression of *hnRNP A0* mRNA levels was induced by 3-fold after 4 h, followed by a 10-fold downregulation after 8 h. 24 h post stimulation, the mRNA expression levels of *hnRNP A0* were restored and reached the expression levels of the untreated control (Figure 4-17 B). Thus, a direct or indirect effect of IFN-stimulation on the transcriptional regulation of *hnRNP A0* was suggested. However, effects on mRNA stability or degradation cannot be excluded. While the expression profile of newly synthesized *hnRNP A0* mRNA was highly similar to the expression profile of *SRSF1*, the magnitude of the initial increase in mRNA expression varied greatly. 4 h post treatment with IFN $\alpha$ 14, a 16-fold increase in *SRSF1* mRNA was detected, while *hnRNP A0* mRNA levels were only increased by 3-fold. Both factors were repressed by 10-fold after 8 h. However, *SRSF1* mRNA expression was still reduced by 2-fold after 24 h, while *hnRNP A0* mRNA expression was fully restored when compared to the untreated control (Figure 4-6 B and 4-17 B). Furthermore, in contrast to *SRSF1*, the initial increase in *hnRNP A0* mRNA could not be observed analyzing *hnRNP A0* expression in THP-1 cells upon IFN-stimulation using total RNA. A potential explanation could be the existence of an autoregulatory mechanism maintaining homeostasis of *hnRNP A0* levels. Since the upregulation of newly synthesized mRNAs was much less pronounced for *hnRNP A0* when compared to *SRSF1* (3-fold compared to 16-fold), autoregulation might potentially be able to quickly restore

---

homeostatic levels of *hnRNP A0* mRNA, possibly through degradation of the newly synthesized mRNA.

#### **4.2.5. Knockdown of *hnRNP A0* levels affects HIV-1 post integration steps**

IFN-treatment of THP-1 and primary human macrophages resulted in the deregulation of *hnRNP A0* mRNA expression. A strong time-dependent downregulation of *hnRNP A0* was observed upon stimulation with IFN $\alpha$ 2 and IFN $\alpha$ 14 (Figure 4-15). Furthermore, the expression profile in MDMs showed a significant downregulation of *hnRNP A0* mRNA levels after 4 h (Figure 4-16.). Similar to *SRSF1*, the expression levels of *hnRNP A0* were also lower upon HIV-1 infection when compared to uninfected donors, correlating with ISG-induction during the acute phase of infection (Chapter 4.2.2.).

While many hnRNPs, especially the subfamily of hnRNP A/B, have been described to play a crucial role in HIV-1 RNA processing, hnRNP A0 has so far not been associated in this context. However, HIV-1 has many AU-rich elements (ARE) within its genome, which have been described to be the main targets of hnRNP A0 on RNAs (404). Thus, many potential binding sites for hnRNP A0 are dispersed throughout the HIV-1 mRNA. To mimic the repression of hnRNP A0 in the early phase after IFN-stimulation and to investigate whether the effect of decreased levels of hnRNP A0 affects HIV-1 RNA processing, HEK293T cells were transiently co-transfected with the HIV-1 laboratory strain pNL4-3 PI952 (371) and a siRNA specifically targeting hnRNP A0 or a siRNA negative control. 72 h post transfection, cells and virus-containing supernatant were harvested. Gene knockdown efficiency was verified via RT-qPCR, showing a knockdown efficiency of 90 % when compared to the negative control siRNA (Figure 4-18 A).



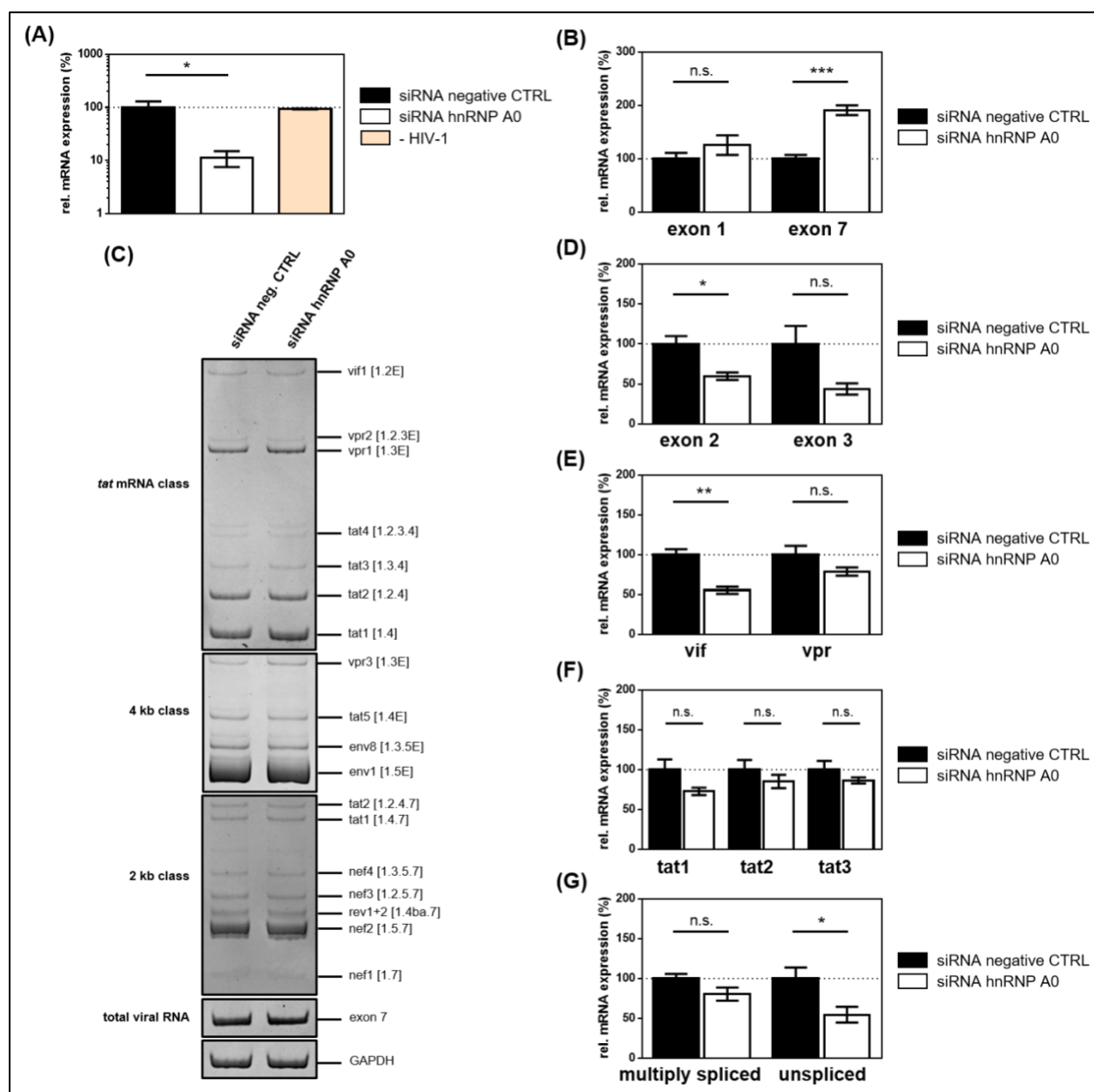


**Figure 4-18: siRNA-mediated knockdown of hnRNP A0 affects HIV-1 LTR transcription and splice site usage.** HEK293T cells were transfected with the proviral clone pNL4-3 PI952 (371) and a hnRNP A0 specific siRNA. After 72 h, cells were harvested and total RNA and viral supernatant isolated. **(A) – (B)** Relative mRNA expression levels of **(A)** *hnRNP A0* and **(B)** exon 1 and exon 7 containing mRNAs (total viral mRNA) were measured via RT-qPCR and normalized to GAPDH. **(C)** Viral splicing pattern upon hnRNP A0 knockdown was analyzed via RT-PCR using the indicated primer pairs for the 2 kb-, 4 kb- and *tat* mRNA-class (Table 2-4). HIV-1 transcript isoforms are depicted on the right according to (375). RT-PCRs amplifying HIV-1 exon 7 containing transcripts as well as cellular GAPDH were performed for RNA normalization. PCR products were separated on a 12% nondenaturing polyacrylamide gel. **(D) – (G)** RT-qPCR results for relative mRNA expression levels of **(D)** exon 2 and exon 3 containing, **(E)** *vif* and *vpr*, **(F)** *tat1*, *tat2* and *tat3* and **(G)** multiply spliced and unspliced mRNAs. Primer pairs used to determine HIV-1 mRNA levels are indicated in (Table 2-4 and Supplementary Figure 1). The splicing pattern of NL4-3 PI952 was set to 100% and relative usage of the splice sites was normalized to total viral

mRNA levels (exon 7 containing transcripts). Statistical significance in the differences between groups of samples were calculated via unpaired two-tailed t-test (\*  $p < 0.05$ , \*\*  $p < 0.01$ ,  $p < 0.001$  and \*\*\*\*  $p < 0.0001$ ). Mean (+ SEM) of  $n = 4$  biological replicates is depicted for **(A)**, **(B)** and **(D) – (G)**.

Intracellular total viral mRNA levels were measured using specific primer pairs amplifying HIV-1 exon 1 or exon 7, present in all viral mRNA transcripts (Figure 1-4 and Supplementary Figure 1), while GAPDH expression was used for normalization. Exon 1 containing mRNAs were slightly upregulated by 1.3-fold, albeit not significant, while mRNAs containing exon 7 were significantly upregulated by 1.9-fold upon hnRNP A0 knockdown (Figure 4-18 B). A direct or indirect impact of hnRNP A0 on HIV-1 LTR transcription was thus suggested.

To assess, whether depleted levels of hnRNP A0 would affect HIV-1 alternative splicing, viral splicing patterns were analyzed via RT-PCR. While no changes were observed in the viral splicing pattern of all HIV-1 mRNA-classes upon knockdown of hnRNP A0 with the semi-quantitative approach (Figure 4-18 C), RT-qPCR analysis revealed alterations in the expression of several HIV-1 mRNAs (Figure 4-18 D-G). Possibly, the semi-quantitative approach was not sensitive enough to detect the changes in viral splice site usage upon hnRNP A0 knockdown. The inclusion of non-coding leader exons 2 and 3 in all viral transcripts was reduced by 2- and 2.3-fold respectively (Figure 4-18 D). The inclusion of exon 2 requires splicing from SD1 to SA1 and inhibition of SD2/2b, while exon 3 inclusion results from splicing between SD1 to SA2 and inhibition of SD3 (375). The expression of both *vif* and *vpr* mRNAs, which strongly depend on the recognition of exon 2 and exon 3 respectively, was repressed by 2- and 1.3-fold upon knockdown of hnRNP A0 (Figure 4-18 E). Repressed levels of *vif* mRNA and exon 2 inclusion suggested reduced splicing events at SA1, while lower levels of *vpr* mRNA and exon 3 inclusion suggested reduced splicing frequency at SA2. Furthermore, cross-exon interactions between SA1 and SD2/2b and SA2 and SD3 were likely inhibited. *Tat1* mRNA levels were downregulated by 1.4-fold, while both *tat2* and *tat3* mRNA expression was only marginally reduced by 1.2-fold (Figure 4-18 F). Since the formation of *tat* mRNAs requires splicing between SD1 to SA3 and SD4 to SA7 (*tat1*), SD1 to SA1, SD2 to SA3 and SD4 to SA7 (*tat2*) and SD1 to SA2, SD3 to SA3 and SD4 to SA7 (*tat3*), reduced splice site usage at SA1, SA2 and SA3 was suggested. The levels of multiply spliced mRNAs (spliced from SD4 to SA7) were not significantly altered upon hnRNP A0 knockdown (Figure 4-18 G). Thus, an effect of depleted levels of hnRNP A0 on the splice site usage at SA7 was

unlikely. However, a significant downregulation of 2-fold was detected for unspliced mRNA levels (intron 1-containing) (Figure 4-18 G), which might possibly result from increased splicing efficiency at SA4 or SA5.

In contrast to the knockdown of SRSF1, which affected HIV-1 alternative splice site usage rather than LTR transcription, knockdown of hnRNP A0 resulted in a stronger increase in LTR transcription, while still considerably altering the HIV-1 splicing pattern. The mRNA levels of *vif* were reduced by 2-fold, which might substantially impede HIV-1 replication as a narrow range of Vif was shown to be crucial for efficient viral replication (6; 412; 486). While several targets on the HIV-1 pre-mRNA have been identified for SRSF1, no binding sites are known for hnRNP A0. Thus, the changes in LTR transcription or alternative splice site usage could not directly be linked to hnRNP A0. However, the HIV-1 genome is dispersed with AREs, thus representing a large number of potential binding site for hnRNP A0 on the viral pre-mRNA. Furthermore, indirect effects through the interaction with other cellular splicing factors cannot be ruled out.

To analyze whether a knockdown of hnRNP A0, and the resulting effects on HIV-1 LTR transcription and alternative splice site usage, including a 2-fold reduction in *vif* mRNA expression, would directly or indirectly affect HIV-1 infectious viral titers, the putatively APOBEC3G-expressing RPE-ISRE-luc cells (293) were co-transfected with the HIV-1 laboratory strain pNL4-3 (AD8) and a siRNA specifically targeting hnRNP A0 or a siRNA negative control. 72 h post transfection, TZM-bl reporter cells were infected with the virus-containing supernatant to determine viral infectivity. However, no effect on viral infectivity upon siRNA-mediated knockdown of hnRNP A0 on luciferase activity could be observed (Figure 4-19 A). X-Gal staining of TZM-bl cells infected with cellular supernatant confirmed those findings (Figure 4-19 B). Thus, at least in the RPE ISRE luc model cell line, depleted levels of hnRNP A0 and the concomitant reduction in *vif* mRNA expression did not negatively affect viral infectivity.

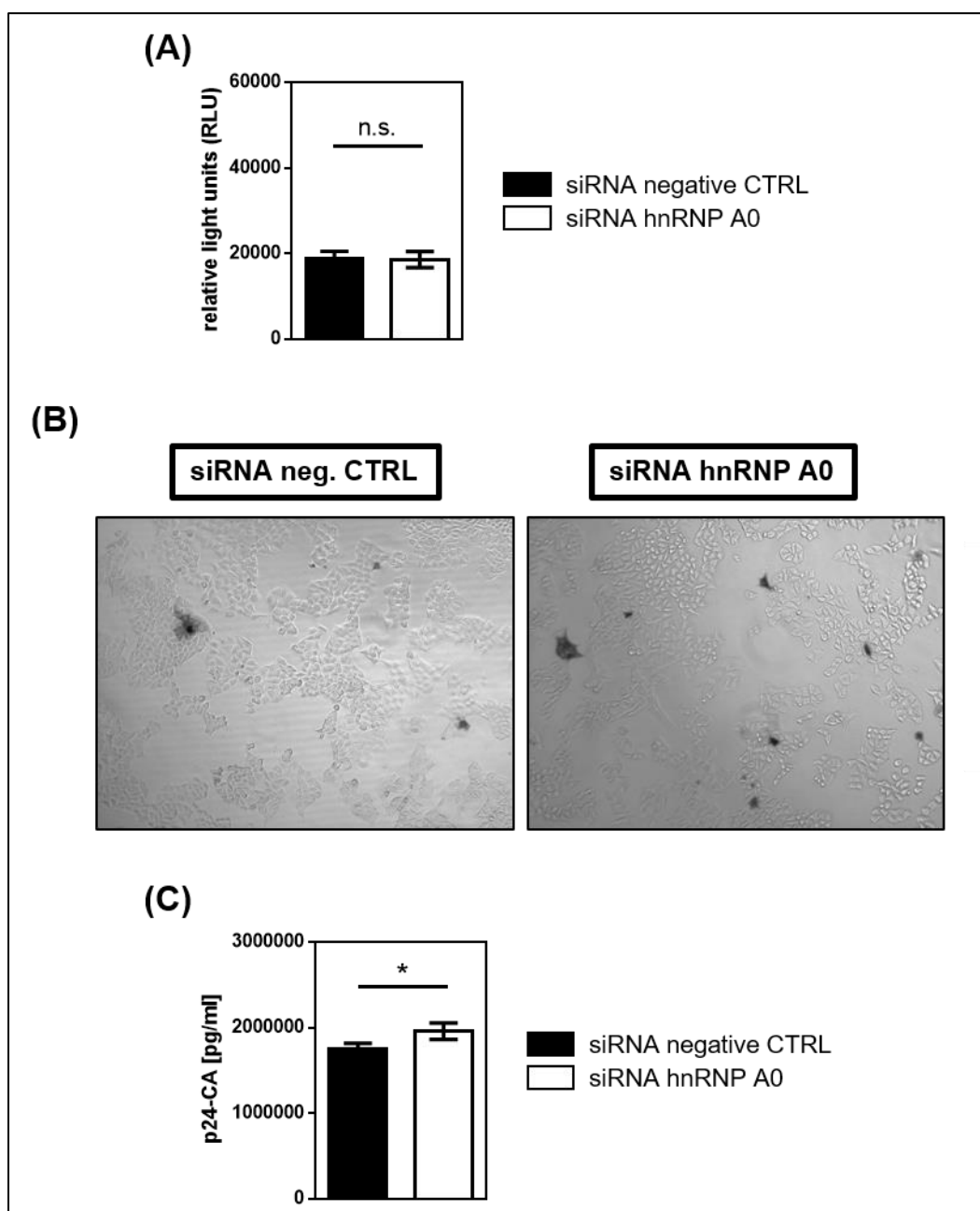


**Figure 4-19: Impact of siRNA-based knockdown of hnRNP A0 on HIV-1 infectivity and virus production.** RPE-ISRE luc cells were transfected with a plasmid coding for the HIV-1 proviral clone NL4-3 (AD8) (pNL4-3 AD8) (148) and the indicated siRNA. **(A) – (B)** After 72 h, TzM-bl cells were infected with cellular supernatant to determine viral infectivity. **(A)** Relative light units were measured to monitor luciferase activity. **(B)** X-Gal staining of TzM-bl cells infected with cellular supernatant. **(C)** Virus production was monitored via p24-CA ELISA of cellular supernatant. Unpaired two-tailed t-tests were calculated to determine whether the difference between the group of samples reached the level of statistical significance (\*  $p < 0.05$ ). Mean (+ SEM) of  $n = 4$  biological replicates is depicted for **(A)** and **(B)**.

p24-CA ELISA was performed to determine a potential effect of hnRNP A0-knockdown on virus production. A slight but significant increase of 1.1-fold in p24-CA-levels was detected (Figure 4-19 C). Thus, depleted levels of hnRNP A0 led to an increase in both HIV-1 LTR transcription and viral particle production.

In THP-1 and primary human macrophages, a significant downregulation in *hnRNP A0* mRNA expression was observed upon stimulation with IFN $\alpha$ 14 (Figure 4-15 B and 4-16 A). However, as indicated by the previous findings, depleted levels of hnRNP A0 altered HIV-1 LTR transcription and alternative splice site usage, but did not impede HIV-1 infectivity. Since knockdown of hnRNP A0 even significantly induced viral particle production, it is possible that HIV-1 has adapted to replicate efficiently under low levels of *hnRNP A0*, as induced by IFN-stimulation.

#### **4.2.6. Overexpression of hnRNP A0 levels affects HIV-1 post integration steps**

After an initial repression in *hnRNP A0* mRNA expression levels, stimulation with IFN $\alpha$ 14 induced an increase in *hnRNP A0* mRNA after 48 h in primary human macrophages as well as Jurkat T-cells (Figure 4-16 A and 4-15 C and D).

Thus, to evaluate the impact of hnRNP A0 overexpression on HIV-1 RNA post integration steps, a plasmid coding for FLAG-tagged hnRNP A0 (pcDNA-hnRNP A0) was generated (Chapter 3.2.8.8) and hnRNP A0 expression was verified (Supplementary Figure 2). HEK293T cells were then transiently co-transfected with the HIV-1 laboratory strain pNL4-3 PI952 (371) and pcDNA-hnRNP A0 or an empty vector (pcDNA3.1(+)) as mock control. Cells were incubated for 72 h, before cells and virus-containing supernatant were harvested. Overexpression efficiency was verified via RT-qPCR, revealing increased levels of *hnRNP A0* mRNA by multiple orders of magnitude (Figure 4-20 A).

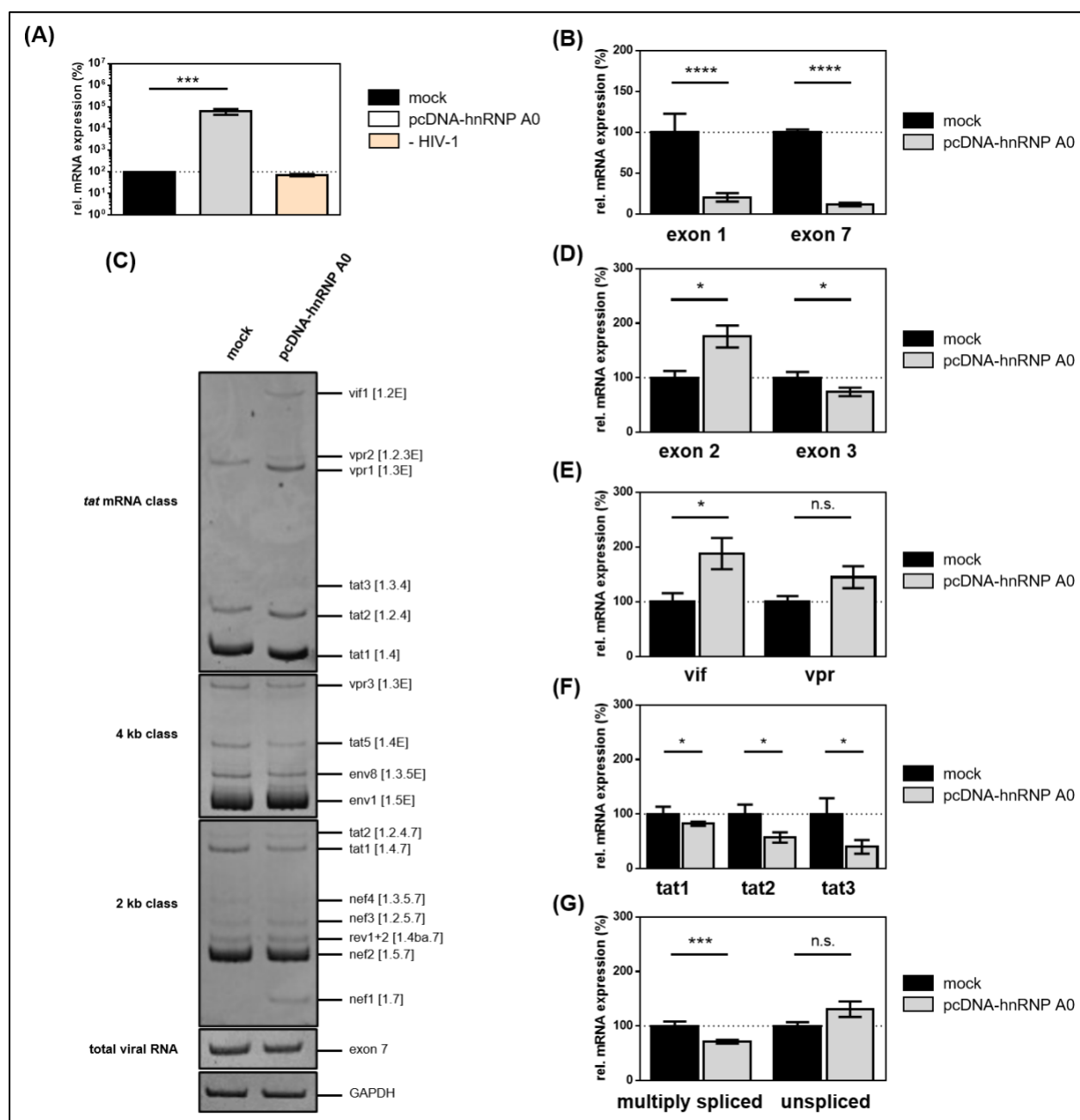


**Figure 4-20: Overexpression of hnRNP A0 affects HIV-1 LTR transcription and splice site usage.** HEK293T cells were transfected with the proviral clone pNL4-3 PI952 (371) and a plasmid coding for FLAG-tagged hnRNP A0 (pcDNA-hnRNP A0). 72 h following transfection, total RNA was harvested from the cells and viral supernatant was isolated. **(A) – (B)** RT-qPCR was performed to measure relative mRNA expression levels of **(A)** *hnRNP A0* and **(B)** exon 1 and exon 7 containing mRNAs (total viral mRNA). GAPDH expression levels were used for normalization. **(C)** Viral splicing pattern upon hnRNP A0 overexpression. RT-PCR was performed using the indicated primer pairs for the 2 kb-, 4 kb- and *tat* mRNA-class. HIV-1 transcript isoforms are shown on the right according to (375). RT-PCRs amplifying HIV-1 exon 7 containing transcripts as well as cellular GAPDH were performed for the normalization of RNA amounts. PCR amplicons were

separated on a 12% nondenaturing polyacrylamide gel. **(D) – (G)** RT-qPCR results for relative mRNA expression levels of **(D)** exon 2 and exon 3 containing, **(E)** *vif* and *vpr*, **(F)** *tat1*, *tat2* and *tat3* and **(G)** multiply spliced and unspliced mRNAs. Primers used for HIV-1 mRNA analysis are indicated in (Table 2-4). The splicing pattern of NL4-3 PI952 was set to 100% and the relative splice site usage was normalized to exon 7-containing mRNAs. Unpaired t tests were used for statistical analysis (\*  $p < 0.05$ , \*\*  $p < 0.01$ , \*\*\*  $p < 0.001$  and \*\*\*\*  $p < 0.0001$ ). Mean (+ SEM) of  $n = 4$  biological replicates is depicted for **(A)**, **(B)** and **(D) – (G)**.

Primer pairs amplifying HIV-1 exon 1 or exon 7 were used to determine intracellular total viral mRNA levels via RT-qPCR, while GAPDH levels were used for normalization. Overexpression of hnRNP A0 resulted in strongly reduced levels of total viral mRNA, with a reduction of 5- and 10-fold for exon 1- and exon 7-containing mRNAs respectively (Figure 4-20 B). These results suggested a direct or indirect inhibitory effect of hnRNP A0 on HIV-1 LTR transcription.

Depleted levels of hnRNP A0 affected both HIV-1 LTR transcription and alternative splicing. To assess, whether elevated levels of hnRNP A0 would, in addition to LTR transcription, also impact alternative splice site usage, viral splicing patterns were analyzed via semi-quantitative RT-PCR. Considerable changes were observed in the viral splicing patterns of the 2 kb-, 4 kb- and *tat*-specific mRNA classes, when compared to the mock-transfected control (Figure 4-20 C). Increased levels of *vif1*, *vpr1* and *vpr2* mRNA were detected in the *tat*-mRNA class. In the 2 kb- and 4 kb-mRNA class, an increase in *nef1* and *nef3* mRNA levels was observed, while levels of *tat1* and *tat5* mRNA were reduced (Figure 4-20 C). Splicing from SD1 to SA1 is required for the formation of *vif1*, *vpr2* and *nef3* mRNA, while splicing from SD1 to SA2 is essential for the generation of *vpr1* mRNA (375). Thus, increased splicing events at SA1 and SA2 were suggested. Since both *tat1* and *tat5* mRNA generation requires splicing from SD1 to SA3 (375), repressed splicing frequency at SA3 was likely. Transcript specific primers were used to quantify the observed alterations in splice site usage upon hnRNP A0 overexpression via RT-qPCR. While the inclusion of non-coding leader exon 2 was slightly upregulated by 1.8-fold, the inclusion non-coding leader exon 3 was slightly repressed by 1.4-fold (Figure 4-20 D). Both *vif* and *vpr* mRNAs were induced by 1.9- and 1.5-fold respectively upon elevated levels of hnRNP A0 (Figure 4-20 E). Thus, increased splicing events at SA1 and SA2, as well as promoted cross-exon interactions between SD2/2b and SA1 and SD3 and SA2,

---

were suggested. However, while splicing at SD2/2b was increased, splicing at SD3 was likely inhibited. *Tat1*, *tat2* and *tat3* mRNA levels were all significantly repressed by 1.2-, 1.8- and 2.5-fold respectively (Figure 4-20 F), which was likely due to an inhibiting effect of hnRNP A0 on the usage of SA3. The expression levels of multiply spliced mRNAs were significantly downregulated by 1.4-fold, whereas the expression levels of unspliced mRNAs were induced by 1.3-fold, albeit with no statistical significance (Figure 4-20 G). The suggested inhibition of splicing at SA3 might potentially be responsible for these findings. Thus, overexpression of hnRNP A0 shifted the ratio of multiply spliced / unspliced mRNAs towards unspliced mRNAs.

To investigate whether the alterations in HIV-1 LTR transcription and alternative splicing would affect viral infectivity, TZM-bl cells were infected with virus-containing cellular supernatant. A significant 2-fold decrease was observed in luciferase activity when compared to the mock-treated control (Figure 4-21 A) and confirmed via X-Gal staining (Figure 4-21 B). Thus, despite 1-9-fold higher *vif* mRNA levels (Figure 4-20 E), viral infectivity was significantly reduced upon elevated levels of hnRNP A0.



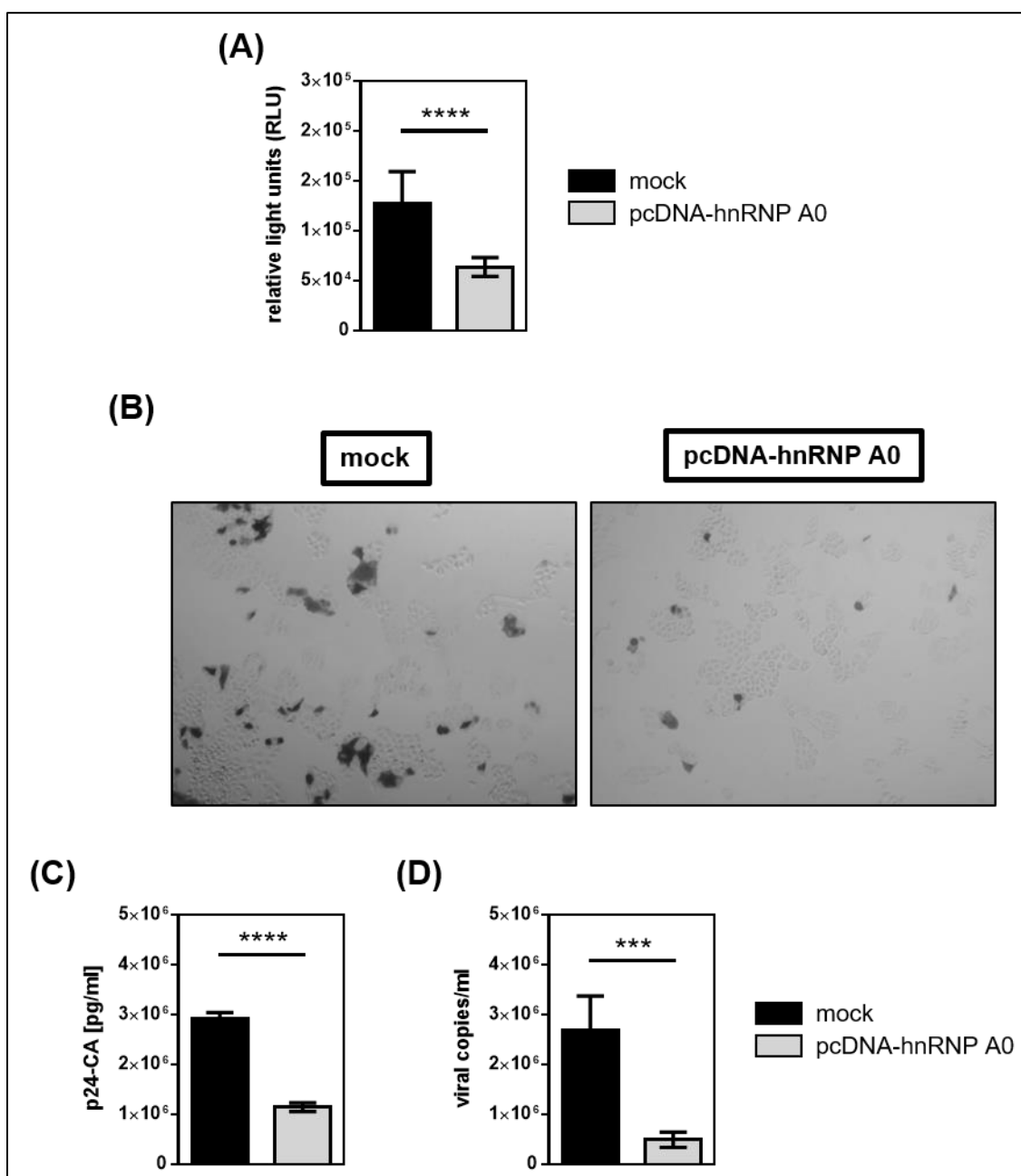


**Figure 4-21: Effect of hnRNP A0 overexpression on HIV-1 infectivity and viral particle production.** HEK293T cells were transiently transfected with a plasmid coding for the proviral clone NL4-3 PI952 (371) and a plasmid expressing FLAG-tagged hnRNP A0 (pcDNA-hnRNP A0). **(A) – (B)** After 72 h, TZM-bl cells were infected with cellular supernatant to determine viral infectious titers. **(A)** Luciferase activity measurement and **(B)** X-Gal staining of infected TZM-bl cells. **(C)** Virus production was measured performing p24-CA ELISA using cellular supernatant. **(D)** Viral RNA was extracted from the cellular supernatant and subjected to RT-qPCR to quantify the viral copies in the supernatant. Unpaired t tests were calculated to determine whether the difference between the group of samples reached the level of statistical significance (\*  $p < 0.05$ , \*\*  $p < 0.01$ , \*\*\*  $p < 0.001$  and \*\*\*\*  $p < 0.0001$ ). Mean (+ SEM) of  $n = 4$  biological replicates is depicted for **(A)**, **(C)** and **(D)**.

To assess, whether alterations in HIV-1 particle production might induce the impeded viral infectivity, the number of p24-CA levels in the cellular supernatant were analyzed via p24-CA ELISA. A significant decrease of 2.5-fold in p24-CA levels was observed upon *hnRNP A0* overexpression (Figure 4-21 C). Furthermore, a strong and significant decrease of 5.5-fold in viral copies per ml of supernatant was detected (Figure 4-21 D). Thus, in contrast to *hnRNP A0* knockdown (Figure 4-19), overexpression strongly inhibited viral particle production and infectivity.

After an initial downregulation 4 to 8 h post stimulation with IFN $\alpha$ 14 in MDMs, mRNA levels of *hnRNP A0* increased in a time-dependent manner from 12 to 48 h and were significantly upregulated after 48 h (Figure 4-16 A). Since elevated levels of *hnRNP A0* were shown to strongly inhibit virus production and viral infectivity, increase levels of *hnRNP A0* might potentially represent part of the IFN-mediated antiviral activity against HIV-1.

#### **4.2.7. HIV-1 affects the IFN-mediated regulation of *hnRNP A0***

HIV-1 infection was shown to induce lower expression levels of *hnRNP A0* (Figure 4-12 A and 4-14 C). In addition, a direct correlation was observed between the expression of *hnRNP A0* and ISG-induction in the early phase of an HIV-1 infection (Figure 4-14 F). IFN-stimulation was shown to repress the mRNA expression levels of *hnRNP A0* in HIV-1 target cells (Figure 4-15 and 4-16). Furthermore, *hnRNP A0* has been shown to affect HIV-1 replication at the level of LTR transcription, alternative splicing and virus production upon knockdown (Chapter 4.2.5.) and overexpression (Chapter 4.2.6.).

To analyze, whether an acute HIV-1 infection would affect the IFN-mediated deregulation of *hnRNP A0* mRNA, THP-1 macrophages were infected with the R5-tropic HIV-1 laboratory strain NL4-3 (AD8) 16 h prior to the stimulation with IFN $\alpha$ 2 or IFN $\alpha$ 14 as described above (Chapter 4.1.7.). The infection occurred 16 h prior to the IFN-treatment to focus on HIV-1 post integration steps. In HIV-1 infected THP-1 macrophages, IFN $\alpha$ 2 and IFN $\alpha$ 14 induced a similar response in the expression levels of *hnRNP A0* (Figure 4-22). Treatment with IFN $\alpha$ 2 led to a 1.7-, 2.4- and 2.4-fold repression in mRNA levels after 4, 8 and 12 h (Figure 4-22 A), while stimulation with IFN $\alpha$ 14 resulted in a 2.1-, 3- and 2.8-fold downregulation after 4, 8 and 12 h respectively (Figure 4-22 B). Gene expression was mostly recovered after 24 h, with a remaining repression in *hnRNP A0* mRNA expression of 1.3-fold upon stimulation with IFN $\alpha$ 14. 48 h post stimulation, a

1.4- and 2-fold increase in *hnRNP A0* mRNA levels was observed upon stimulation with IFN $\alpha$ 2 and IFN $\alpha$ 14 respectively (Figure 4-22 A and B).

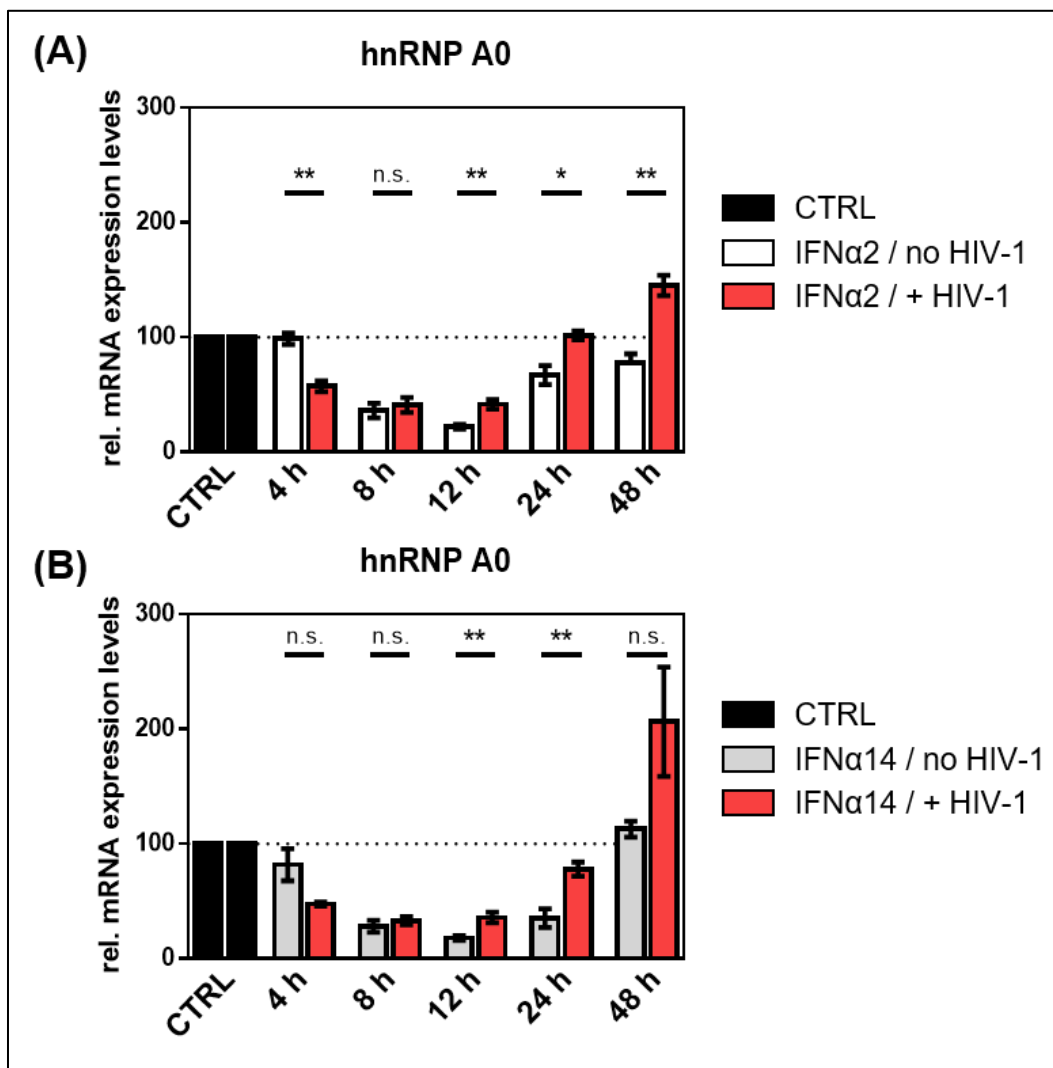


**Figure 4-22: HIV-1 affects IFN-mediated regulation of *hnRNP A0*.** (A) – (B) Differentiated THP-1 macrophages were infected with the R5-tropic NL4-3 (AD8) at an MOI of 1. 16 h post infection, cells were treated with the indicated IFN subtype over a period of 48 h at a concentration of 10 ng/ml. Cells were then harvested and RNA was isolated. RT-qPCR analysis revealed relative mRNA expression levels of *hnRNP A0* after treatment with (A) IFN $\alpha$ 2 or (B) IFN $\alpha$ 14. Statistical significance between the group of samples was determined via unpaired two-tailed t-tests (\*  $p < 0.05$ , \*\*  $p < 0.01$  and \*\*\*  $p < 0.001$ ). Mean (+ SEM) of  $n = 4$  biological replicates is depicted.

In uninfected cells, the downregulation of *hnRNP A0* mRNA levels occurred at a later time point of 8 to 12 h upon IFN-stimulation with both subtypes (Figure 4-22). However, the magnitude of the downregulation upon stimulation with IFN $\alpha$ 2 and IFN $\alpha$ 14 was stronger in uninfected cells (5- and 5.8-fold after 12 h respectively), than in acutely HIV-1 infected

---

cells (2.4- and 3-fold after 8 h respectively) (Figure 4-22). In contrast to uninfected cells, the expression levels of *hnRNP A0* were restored after 24 h upon a prevailing HIV-1 infection. Furthermore, an increase in *hnRNP A0* mRNA expression was observed in HIV-1 infected cells after 48 h (Figure 4-22).

Thus, similar to the expression of *SRSF1* (Figure 4-11), HIV-1 potentially restored balanced levels of *hnRNP A0*. The exact mechanism, however, remains unclear. Furthermore, a possible effect due to IFN induction upon the HIV-1 infection prior to the IFN treatment on the expression of *hnRNP A0* cannot be excluded.

## 5. Discussion

Type I IFNs play a key role in the early immune response upon viral infections, including HIV-1, by establishing an antiviral state in the host and bystander cells. Alongside the well-known induction of hundreds of IFN-stimulated genes (ISGs) and other immunomodulatory functions (247; 282), their mode of action also includes the downregulation of IFN-repressed genes (IRepGs), which include host dependency factors (HDFs) essential for viral replication (324; 455).

Upon HIV-1 infection, the viral genome is integrated irreversibly into the host cell genome. The provirus then acts as a transcriptional template under the control of the viral LTR promoter and exploits the cellular transcription and RNA processing apparatus for the regulation of its gene expression (386; 501). HIV-1 critically relies on alternative splicing for the production of balanced ratios of all HIV-1 mRNA transcripts (30; 244; 375; 386; 410; 435). Alongside the intrinsic strength of specific splice sites, a complex network of splicing regulatory elements (SREs) on the viral pre-mRNA, which are bound by cellular splicing factors, regulates the frequency of splicing events throughout the viral genome. These two levels of splicing regulatory mechanisms are referred to as the 'splicing code' (30; 31; 478).

Several SRSF and hnRNP proteins, which have been identified as HDFs in siRNA screenings (51; 260; 337; 515; 518), have largely been described as crucial regulators for cellular and HIV-1 RNA processing and particularly alternative splicing (27; 59; 410; 435). Through the specific binding to SREs on the viral pre-mRNA, they decisively influence splice site recognition and usage. As described in the following section, the cellular splicing factors *SRSF1* and *hnRNP A0* were identified as IFN-regulated genes, crucially affecting HIV-1 LTR transcription, alternative splicing and virus production.

### 5.1. *SRSF1* and *hnRNP A0* mRNA expression is predominantly type I IFN regulated

The stimulation of pattern recognition receptors (PRRs) upon HIV-1 infection leads to the production of type I IFNs (290; 322). In turn, IFNs trigger the expression of specific HIV-1 host restriction factors (HRFs), such as MX2, SAMHD1, TRIM22 or tetherin, which exert direct antiviral activity (277; 322). In this work, the induction of *IFN-stimulated gene 15* (*ISG15*) mRNA expression was measured as surrogate marker for ISG induction and thus IFN signature. ISG15 is one of the most abundantly expressed ISGs and was shown to impede HIV-1 replication during the process of budding (346; 365). When analyzing

PBMCs of acutely and chronically HIV-1 infected individuals, significantly higher levels of *ISG15* mRNA were observed when compared to healthy donors (Figure 4-2 A and 4-14 A). However, *ISG15* mRNA levels were lower in ART-treated patients, when compared to acutely or chronically HIV-1 infected individuals (Figure 4-2 A and 4-14 A). The expression of several HRFs, such as MX2, SAMHD1, TRIM22 or tetherin, was shown to be higher in LPMCs (109) and PBMCs (290) of chronically HIV-1 infected individuals when compared to uninfected donors. However, when analyzing gut LPMCs, patients under ART-treatment had low ISG levels comparable to HIV-1 uninfected individuals (109). Massanella and colleagues could show that the expression of over 4,000 genes was significantly altered when analyzing PBMCs of HIV-1 infected patients before and after ART-treatment (316). Several ISGs, such as *ISG15*, MX2, IFITM1 or IFI16 were repressed upon ART-treatment in comparison to chronic and untreated HIV-1 infections (316). However, whether the effect of ART-treatment on ISG expression occurred due to a decrease in inflammation or whether the administered drugs had a direct effect on the expression of these genes needs yet to be elucidated. The administration of a varying combination of antiretroviral drugs to the patients, including nucleoside reverse transcriptase inhibitors (NRTI), non-nucleoside reverse transcriptase inhibitors (NNRTI) and protease inhibitors, further represents a limiting factor of this study.

During this thesis, in collaboration with Mario Santiago (Department of Medicine, University of Colorado Denver, US), transcriptomic data of a previous study was reanalyzed and *SRSF* and *hnRNP* transcript levels were determined in gut LPMCs of chronically HIV-1 infected patients, either treatment naïve or under ART-treatment (109). Significantly altered levels of distinct *SRSF* and *hnRNP* members were observed upon chronic HIV-1 infection when compared to healthy individuals (Figure 4-1 A and 4-12 A). In particular, transcript levels of *SRSF1*, *SRSF3*, *SRSF7* and *SRSF10*, as well as *hnRNP A0*, *hnRNP A1*, *hnRNP A2B1*, *hnRNP D*, *hnRNP DL*, *hnRNP F*, *hnRNP H3*, *hnRNP K*, *hnRNP M*, *hnRNP Q*, *hnRNP R*, *hnRNP U* and *hnRNP UL1* were significantly lower in LPMCs of chronically HIV-1 infected patients when compared to uninfected donors. Thus, a direct or indirect effect of HIV-1 infection on the expression of *SRSF* and *hnRNP* transcript levels, possibly due to the infection induced IFN response, was suggested. Since the IFN signature in response to HIV-1 infection triggers the upregulation of hundreds of HRFs (322), the observed lower levels of HDFs upon chronic HIV-1 infection suggested a potential inverse correlation between ISG induction and the repression of

*SRSFs* and *hnRNPs*. Hence, distinct members of the *SRSF* and *hnRNP* family could potentially represent IRepGs.

Interestingly, no significant differences in the expression levels of the majority of *SRSFs* and *hnRNPs* were observed between HIV-1 infected individuals under ART treatment and uninfected donors (Figure 4-1 B and 4-12 B), suggesting restored ISG levels in the absence of viral replication. Lower levels were only determined for *SRSF3*, *SRSF9* and *SRSF10*, as well as *hnRNP A1*, *hnRNP C*, *hnRNP UL1* and *hnRNP UL2*. Transcript levels of *SRSF1*, which were expressed 2-fold lower upon chronic HIV-1 infection, were restored and even significantly higher by 1.2-fold in LPMCs of ART-treated HIV-1 infected patients in comparison to healthy individuals (Figure 4-1). While the alteration in the expression of *SRSF* and *hnRNP* transcripts was likely an IFN-induced effect, the possibility of ART-treatment affecting the expression of *SRSF* and *hnRNP* transcript levels cannot be excluded. The observed repression of ISG stimulation upon ART-treatment (109; 316), in addition to the observation of restored expression levels of *SRSF* and *hnRNP* upon ART-treatment when compared to healthy donors (Figure 4-1 and 4-12), thus supports the hypothesis of an inverse correlation between the induction of ISGs and the repression of *SRSFs* and *hnRNPs*.

Interestingly, while ART-treatment was suggested to restore the expression of *SRSF1* and *hnRNP A0* transcript levels in gut LPMCs (Figure 4-1 and 4-12), the same effect could not be observed in PBMCs (Figure 4-2 and 4-14). However, this discrepancy might be explained through the differences between the two immune cell populations as well as the drug availability in the corresponding tissue. Several studies could demonstrate a phenotypical and functional difference between LPMCs and PBMCs. Apart from the highly differing micro-environment, LPMCs have a different composition of immune cells (29; 47; 168; 400; 453; 454) and cytokine or receptor expression (47; 170; 425; 428). LPMCs are mucosal immune cells, including CD4<sup>+</sup> and CD8<sup>+</sup> T-cells, macrophages, DCs, NK cells and B-cells, which reside within the gastrointestinal lymphoid tissue (GALT). LPMCs are highly susceptible to both CCR5- and CXCR4-tropic HIV-1 strains and are used as *ex vivo* system to mirror the physiological background of an HIV-1 infection (276). Thus, infection of LPMCs is crucial for HIV-1 upon viral entry via the gastrointestinal tract (139; 224; 276). PBMCs include CD4<sup>+</sup> and CD8<sup>+</sup> T-cells, macrophages, monocytes, NK cells, DCs and B-cells. In contrast to LPMCs, PBMCs need an exogenous mitogen stimuli to render the cells susceptible to HIV-1 infection (176; 434). However, as PBMCs reside within the

peripheral blood, they are easier to collect as LPMCs and are thus more frequently used as *ex vivo* model to study HIV-1 infection.

Analysis of transcript levels in LPMCs of chronically HIV-1 infected patients in comparison to uninfected individuals revealed *SRSF1* to be the most differentially expressed gene of all *SRSFs*, with 2-fold lower mRNA levels upon HIV-1 infection (Figure 4-1 A). Since, in addition, *SRSF1* was previously shown to be involved in multiple steps of HIV-1 RNA processing, which will be discussed in more detail in (Chapter 5.3.), *SRSF1* was chosen from the subset of *SRSFs* for further analysis. Furthermore, *hnRNP A0* was chosen from the subset of *hnRNPs* for further investigation, as the low abundant member of the *hnRNP A/B* family was the most repressed gene of a distinct set of *hnRNP* family members upon IFN-stimulation in THP-1 macrophages (Figure 4-13).

Lower mRNA expression levels of both *SRSF1* and *hnRNP A0* were detected in PBMCs of acutely and chronically HIV-1 infected patients when compared to healthy individuals (Figure 4-2 C and 4-14 C). A statistical significance, however, could only be determined between the mRNA expression levels of *hnRNP A0* of acutely HIV-1 infected patients and uninfected individuals (Figure 4-14 C). The low number of study participants (10 uninfected donors, 8 acutely HIV-1 infected patients, 11 chronically HIV-1 infected patients and 13 HIV-1 infected patients under ART-treatment) and the heterogeneity of the respective patient groups presumably impeded further statistical significances between the patient groups. Especially chronically HIV-1 infected patients represent a heterogeneous cohort, since there can be large discrepancies between the stage of infection, general health or co-morbidities between the patients (300; 360). HIV-1 infected patients under ART-treatment represented a more homogeneous group with significantly lower levels of *SRSF1* and *hnRNP A0* mRNA when compared to healthy donors (Figure 4-2 C and 4-14 C).

Pearson correlation revealed an inverse correlation between the elevated expression of *ISG15* mRNA and the lower mRNA levels of both *SRSF1* and *hnRNP A0* in acutely HIV-1 infected patients (Figure 4-2 F and 4-14 F). Furthermore, an inverse correlation was observed between *ISG15* and *hnRNP A0* mRNA expression in ART-treated patients (Figure 4-14 F). It has previously been shown, that type I IFNs were strongly upregulated upon acute HIV-1 infection and subsequently induced the stimulation of ISGs (290). Thus, since an inverse correlation between ISG-induction and lower levels of *SRSF1* and *hnRNP A0* mRNA was observed upon acute HIV-1 infection, the early inflammation in



---

response to HIV-1 infection could possibly directly or indirectly lead to the repression of *SRSF1* and *hnRNP A0* mRNA expression. Thus, *SRSF1* and *hnRNP A0* represent potential IRepGs.

The 12 different subtypes, which belong to the IFN $\alpha$  subfamily, were shown to exert different antiviral functions such as the upregulation of distinct ISGs (165; 277; 287; 290). While several IFN $\alpha$  subtypes elicit antiviral activity inhibiting HIV-1 infection, the subtype IFN $\alpha$ 14 was the most potent subtype to inhibit HIV-1 replication both *ex vivo* and *in vivo* (187; 277). It was suggested, that the superior potency of IFN $\alpha$ 14 resulted from an increase in intrinsic and innate immunity, such as an upregulation of HRFs (MX2, tetherin, APOBEC3G) or NK cell activation (277). The subtype IFN $\alpha$ 2, which is the sole subtype currently used in clinical treatments, such as hepatitis B virus treatment (17), elicited weak antiviral activity in contrast to IFN $\alpha$ 14 (187; 277). IFN $\alpha$ 2 was the first subtype to be produced on a large-scale basis in the early 1980s and was thus chosen for clinical use with no prior evaluation of antiviral potencies in physiologically relevant target cells (362). However, clinical use of IFN $\alpha$ 2, which is administered in a PEGylated form to increase stability and *in vivo* activity (143), is limited by toxicity and severe side effects (424). The use of an *in vivo* humanized mouse model allowed the analysis of a combined treatment of ART and either IFN $\alpha$ 2 or IFN $\alpha$ 14. Concomitant administration of IFN $\alpha$ 14 and ART led to a much more efficient suppression in HIV-1 plasma viral load than the simultaneous administration of IFN $\alpha$ 2 and ART or ART-treatment alone (278; 440). A clinical study is currently carried out concomitantly administering ART and IFN $\alpha$ 2 (<https://clinicaltrials.gov/ct2/show/results/NCT02227277>). The use of subtype IFN $\alpha$ 14 instead of IFN $\alpha$ 2 could have a stronger antiviral effect in a clinical trial. Furthermore, the use of IFN $\alpha$ 14 could possibly avoid side effects, which occur upon IFN $\alpha$ 2 administration, such as nausea, fatigue or psychologic sequela (424). However, as IFN $\alpha$ 14 was shown to induce stronger intrinsic and innate immune responses (277), it cannot be excluded that administration of IFN $\alpha$ 14 might also potentially cause more severe side effects than IFN $\alpha$ 2.

Stimulation with both IFN $\alpha$ 2 and IFN $\alpha$ 14 resulted in the strong induction of *ISG15* mRNA levels in THP-1 macrophages, Jurkat T-cells and primary human macrophages (MDMs) (Figure 4-4, 4-5, 4-15 and 4-16). Generally, *ISG15*-induction was more pronounced in macrophages than in Jurkat T-cells. It was previously shown that absolute expression levels of *ISG15* in THP-1 cells are 2-fold lower when compared to Jurkat T-cells (460).

Increased levels of ISG15 have been observed in a variety of cancer diseases, such as breast, bladder, prostate or endometrium (14; 35; 106; 252; 399). *ISG15* expression was shown to be regulated by the tumor suppressor p53 (352). Enhanced ISGylation of p53 by ISG15 resulted in increased DNA damage and tumorigenesis (352). Thus, a regulatory feedback loop antagonizing *ISG15* expression in Jurkat T-cells, which have a higher endogenous *ISG15* expression than THP-1 macrophages, could possibly explain the difference in *ISG15* expression upon IFN-stimulation. The determination of absolute mRNA expression levels of *ISG15* upon IFN-stimulation could further elucidate the lower responsiveness of Jurkat T-cells in comparison to macrophages.

The mRNA expression levels of both *SRSF1* and *hnRNP A0* were significantly repressed upon IFN-stimulation in a time-dependent manner in THP-1 macrophages, Jurkat T-cells and MDMs (Figure 4-4, 4-5, 4-15 and 4-16). However, the effect on *SRSF1* and *hnRNP A0* mRNA expression varied greatly between different cell types and between transformed cell lines and primary cells. Thus, the IFN-mediated deregulation of HDFs seems to reflect cell type specific characteristics, such as the expression pattern of co-regulatory factors. Nevertheless, the physiological relevance of primary human cells is certainly higher than cell culture model systems. Apart from being genetically stable, the use of primary human cells includes donor-to-donor variations and maintains the characteristics and phenotype of the original cell type. Cell lines usually derive from cancerous tissue or from the immortalization of primary cells (344; 354). Differentiated THP-1 cells (456) and Jurkat T-cells (405) are commonly used as cell culture model systems for macrophages and T-cells. Cell lines typically contain upregulated signaling pathways such as cell cycle, oxidative phosphorylation or RNA metabolism, in comparison to primary cells (130; 349). Thus, IFN-stimulation of primary human cells provides a closer resemblance to physiological conditions.

Generally, stimulation with IFN $\alpha$ 14 induced stronger effects on both *ISG15* induction and *SRSF1* and *hnRNP A0* repression than stimulation with IFN $\alpha$ 2. Since *SRSF1* and *hnRNP A0* are not only essential factors in HIV-1 post integration steps, but are also crucially involved in a broad range of cellular mechanisms, longer periods of time with deregulated levels of both factors might potentially be detrimental to the cells. In particular, high levels of *ISG15* (14; 35; 106; 252; 399), as well as deregulation of *SRSF1* (98; 150; 245) and *hnRNP A0* (62; 262) have been shown to be involved in tumorigenesis. Hence, regarding a potential clinical administration, the longer-lasting and stronger effect of IFN $\alpha$ 14 on the

expression levels of ISGs and HDFs could possibly lead to even stronger side effects when compared to the administration of IFN $\alpha$ 2. Furthermore, since IFN $\gamma$  stimulation yielded negligible effects on the expression levels of *SRSF1* and *hnRNP A0* (Figure 4-5 C and 4-16 B) when compared to IFN $\alpha$ 2 or IFN $\alpha$ 14 stimulation, a preferentially type I IFN specific effect was suggested. While type I and type II IFNs bind different receptors and signal through different pathways (282; 368), cross-talk between the two cytokine families has been reported (87; 174; 442). Type I IFNs were shown to affect type II IFN mediated immune responses through the regulation of STAT1 expression (174). Thus, an overlap between the signaling cascades of both type I and type II IFNs regulating the expression of *SRSF1* and *hnRNP A0* expression cannot be excluded. Further experiments including type III IFNs would be of interest to analyze whether stimulation with IFN $\lambda$  results in the repression of *SRSF1* or *hnRNP A0*. Type I and III IFNs bind to different signaling receptors (264; 280; 474). However, the induced signaling pathways and transcriptional responses were shown to exhibit considerable overlap. While almost all cells respond to type I IFN stimulation, type III IFNs mainly target mucosal epithelial cells (323), which are often the first cells encountered by HIV-1 when entering via the vaginal or gastrointestinal tract (52; 70; 197).

Lower levels of *SRSF1* and *hnRNP A0* were detected in LPMCs (Figure 4-1 A and 4-12 A) and PBMCs (Figure 4-2 C and 4-14 C) of chronically HIV-1 infected patients when compared to healthy individuals. Furthermore, an inverse correlation between ISG induction and the reduced levels of *SRSF1* and *hnRNP A0* in acutely HIV-1 infected patients was observed (Figure 4-2 F and 4-14 F). Thus, *SRSF1* and *hnRNP A0* were suggested to represent IRepGs. However, stimulation with IFN $\alpha$ 2 and IFN $\alpha$ 14 of HIV-1 target cells did not solely result in a downregulation of *SRSF1* and *hnRNP A0*. Treatment of THP-1 macrophages with both subtypes induced an early increase in *SRSF1* mRNA expression before a strong 13-fold reduction was observed (Figure 4-4 A and B, right panel). Furthermore, after an initial downregulation of *hnRNP A0* mRNA upon treatment with IFN $\alpha$ 14 in MDMs, the expression levels were restored and even significantly increased at later time points (Figure 4-16 A, right panel). In conclusion, *SRSF1* and *hnRNP A0* seem to be IFN-regulated genes. However, whether they can explicitly be defined as IRepGs needs to be further elucidated in follow-up experiments. Whether or not *SRSF1* and *hnRNP A0* represent IRepGs, the alteration of their gene expression might

potentially be a part of the IFN-induced antiviral response in addition to the upregulation of ISGs.

## **5.2. *SRSF1* and *hnRNP A0* mRNA expression is regulated through an autoregulatory feedback loop**

While a deregulation in *SRSF1* and *hnRNP A0* mRNA expression levels upon IFN-stimulation was observed, the underlying mechanism remained unclear. The method of 4-thiouridine (4sU)-tagging was used to determine whether changes in *SRSF1* and *hnRNP A0* mRNA expression occurred on the transcriptional level. 4sU-tagging allows the metabolic labeling of newly synthesized mRNA and subsequent separation from pre-existing mRNAs (159; 493). Thus, this method enables the analysis of RNA stability, synthesis and degradation, as well as transcription factor functions (159; 377; 455; 493). In accordance to the observations made using total RNA, a strong induction in *ISG15* mRNA expression was detected in 4sU-labeled RNA upon treatment of THP-1 macrophages with IFN $\alpha$ 14 (Figure 4-6 A and 4-17 A). Furthermore, *SRSF1* and *hnRNP A0* mRNA expression was considerably repressed (Figure 4-6 B and 4-17 B). The observed changes in *SRSF1* and *hnRNP A0* mRNA expression upon IFN-stimulation were thus most likely due to a temporary transcriptional shutdown. Interestingly, a strong upregulation in *SRSF1* and *hnRNP A0* mRNA expression was observed upon stimulation with IFN $\alpha$ 14 in THP-1 prior to the strong downregulation (Figure 4-6 B and 4-17 B). These results were in agreement with the previous findings, which suggested *SRSF1* and *hnRNP A0* to be IFN-regulated genes (Chapter 5.1.). However, a role of other regulatory mechanisms in the biphasic expression of *SRSF1* and *hnRNP A0* mRNA upon IFN $\alpha$ 14 stimulation, such as mRNA decay or the effect of transcription factors, cannot be excluded.

*SRSF1* was described as a direct transcriptional target of the oncogenic transcription factor Myc (98; 314), while several potential Myc binding sites were also predicted on the *hnRNP A0* gene *in silico* using MotifMap (92; 504). Myc, including the three major family members c-myc, N-myc and L-myc, regulates gene expression through the binding of canonical or non-canonical E-box sequences (CACGTG/CANNTG) in the regulatory region of target genes (4; 41; 137; 305). Dimerization of Myc with the transcription factor myc-associated factor X (Max) is critical for the DNA-binding activity (10; 42). Aberrant expression of Myc contributes to a variety of human cancers (75; 155). Stimulation with

type I IFNs has previously been shown to decrease *Myc* expression levels via reduction in gene transcription (122), post-transcriptional destabilization (73) or reduction in mRNA half-life (95). In HeLa cells, the levels of *c-Myc* mRNA were decreased by two-fold upon treatment with IFN $\alpha$  (251). Thus, the observed reduction in *SRSF1* and *hnRNP A0* mRNA expression upon IFN $\alpha$  stimulation might derive from reduced levels of the transcription factor *Myc*. However, the exact regulatory mechanism of IFN-mediated reduction in *Myc* levels remains yet to be elucidated.

Since tight regulation of *SRSF1* expression is essential for normal cell physiology, *SRSF1* maintains homeostasis through negative splicing autoregulation (111; 439). Several potential splicing isoforms, resulting from the *SRSF1* pre-mRNA, have been detected. Isoform 1, the productively translated and functional intron-containing isoform, is by far the most abundant (439). However, elevated levels of *SRSF1* were shown to result in the removal of introns, which can lead to the degradation of these *SRSF1* isoforms through RNA surveillance pathways, such as nonsense-mediated mRNA decay (NMD) (99; 111; 169). This negative autoregulation might possibly explain the discrepancy between the magnitudes of the early upregulation in *SRSF1* mRNA after IFN $\alpha$ 14 stimulation in 4sU-labeled, freshly synthesized mRNA (Figure 4-6 B) and total RNA (Figure 4-4 B). Upon strongly elevated expression of *SRSF1* mRNA, the negative feedback loop could interfere by a higher frequency in intron-removal, thus resulting in the strongly reduced increase in *SRSF1* mRNA levels measured from total RNA as compared to freshly synthesized RNA. Furthermore, this mechanism is likely involved in the strong downregulation of *SRSF1* mRNA following the initial increase, which was observed at later time points. This mechanism potentially readjusts *SRSF1* mRNA levels to the levels of the untreated control with a timely delay. Hence, in future experiments it would be of interest to analyze time points later than 48 h after IFN-stimulation to monitor the timely progression of *SRSF1* mRNA levels until they are fully restored.

While a similar mechanism has been proposed for other hnRNP family members, such as hnRNP A1 (43) or hnRNP I (495), no autoregulatory feedback mechanism is so far known for hnRNP A0. Since hnRNP A0 has been described as important factor for several cellular functions, it is likely that the expression is tightly regulated. hnRNP A0 has been described to be involved in the post-transcriptional regulation of several transcription factors, such as TNF- $\alpha$ , COX-2 or MIP-2 (390), as well as the regulation of cancer cell growth in a variety of cancer diseases (62; 262). Since the mRNA of *hnRNP A0* only

contains a single exon, a mechanistically different regulation than the autoregulation of SRSF1 is likely. However, the exact mechanism of the regulation of *hnRNP A0* expression remains yet to be elucidated.

Furthermore, both SRSF1 and hnRNP A0 activity is regulated via phosphorylation. SRSF1 is phosphorylated at the Ser residues within the RS domain by SR specific protein kinases (SRPKs) 1 and 2 or CDC-like kinase 1 (Clk1). Dephosphorylation occurs via phosphatases PP1 and PP2A (99). The phosphorylation state of SRSF1 determines subcellular localization as well as cellular functions (99; 517). While partially phosphorylated SRSF1 was shown to bind with high affinity to RNA target sequences, unphosphorylated or fully phosphorylated SRSF1 did not have a high affinity for its target RNA sequence (76). Phosphorylation of hnRNP A0 occurs through MAPKAP-K2 at Ser84, thus regulating hnRNP A0 binding affinity (390). Since hnRNP A0 was identified to play a crucial role in the cell cycle, and dysregulation promoted diverse cancer diseases (262), it is suggested, that phosphorylation of hnRNP A0 is also tightly regulated. Thus, a direct or indirect interaction between IFNs and proteins involved in SRSF1 or hnRNP A0 phosphorylation, affecting subcellular localization and binding affinity of these two HDFs, cannot be ruled out. This question has to be addressed in future experiments.

In conclusion, the deregulation of *SRSF1* and *hnRNP A0* upon stimulation with IFN $\alpha$ 14 likely derives from the interaction of several regulatory mechanisms.

### **5.3. Altered expression levels of SRSF1 decisively affect HIV-1 post integration steps**

SRSF1 has been described to compete with the viral protein Tat for a binding sequence within the hairpin structure of TAR on the HIV-1 LTR promoter, thus inhibiting Tat transactivation. Furthermore, an overlapping binding sequence was found within the 5'-hairpin of 7SK RNA, which is a small nuclear RNA controlling P-TEFb, a factor regulating the elongation phase of transcription (356). Elevated levels of SRSF1 have been shown to significantly repress HIV-1 LTR transcription, while knockdown resulted in enhanced activation of the viral promoter (219; 356). In this work, it was demonstrated, that siRNA-mediated knockdown of SRSF1 in HEK293T cells induced a slight increase in HIV-1 LTR transcriptional activity, measured by exon 1 (1.5-fold) and exon 7 (1.2-fold) containing mRNAs, which are present in all viral transcripts (Figure 4-7 B). However, overexpression of SRSF1 had an inhibitory effect on viral transcription, resulting in a

1.7-fold significantly reduced total viral mRNA levels (Figure 4-9 B). Thus, competitive binding with Tat presumably resulted in lower HIV-1 LTR transcriptional activity upon elevated levels of SRSF1, while depleted levels of SRSF1 led to fewer competitive binding and thus higher transcriptional activity of the LTR promoter. Hence, a direct effect of SRSF1 on HIV-1 LTR transcription was likely, which was in accordance with previous findings as described above (219; 356).

Alternative splicing has been described as key factor for efficient viral replication and to extract the full genetic content of the short and compact HIV-1 genome (375; 410; 435). A complex network of splicing regulatory elements (SREs) is located on the viral pre-mRNA and bound by cellular splicing factors, which can inhibit or promote the recognition and usage of a splice site (162; 312). In combination with the intrinsic strength of the splice sites, these regulatory mechanisms are referred to as the 'splicing code' (31; 478). The splicing regulatory protein SRSF1 was shown to target several SREs on the HIV-1 pre-mRNA, which are ESE M1/M2 (237), GAR ESE (63) and ESE3 (433), thus promoting recognition of the respective splice sites (Figure 5-1). Binding of SRSF1 to the heptameric ESE M1/M2, which is located upstream of the 5'-SD2, results in enhanced recognition of the non-coding leader exon 2 via promoted cross-exon interactions between SD2 and SA1 (237). Targeting of GAR ESE by SRSF1 leads to the recruitment of U1 snRNP to the 5'-SD4 and thus increases splicing frequency at the upstream 3'-SA4cab and 3'-SA5 (63). ESE3, which is located downstream of 3'-SA7, promotes binding of U2AF65 to the splice acceptor upon binding of SRSF1, thus increasing splice site usage (433).

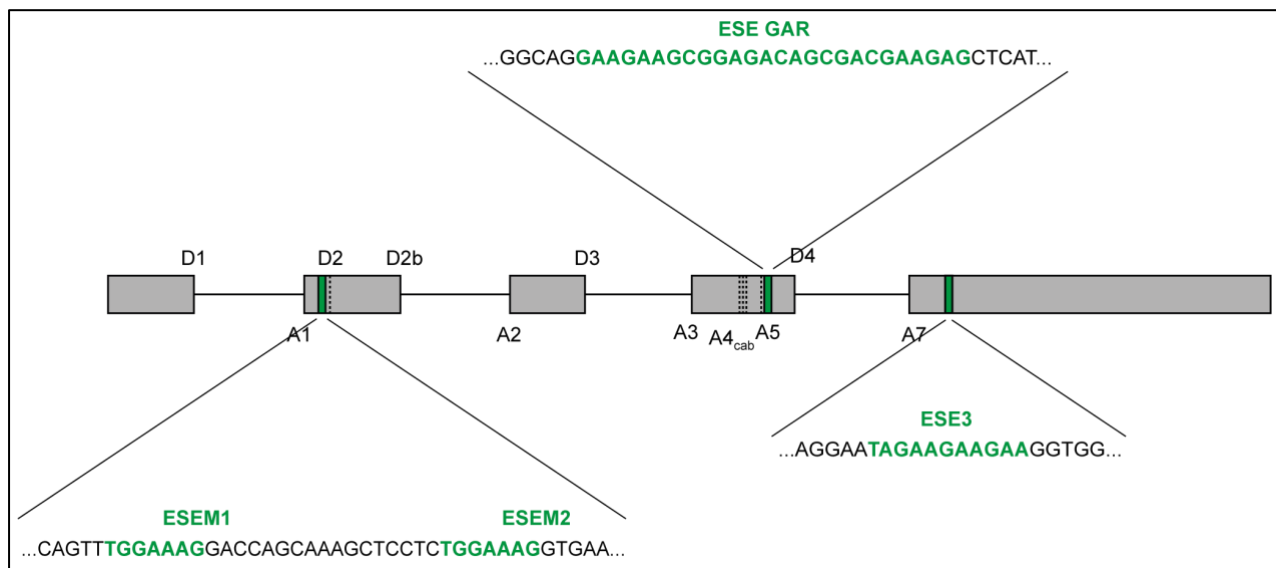


**Figure 5-1: Positions and sequences of SRSF1-bound SREs within the genome of HIV-1 (NL4-3).** Exons are depicted as grey boxes, while introns are shown as black lines. SRSF1-bound splicing enhancers ESEM1/M2 (237); GAR ESE (63); ESE3 (433) are colored in green and their respective sequence on the HIV-1 genome (NL4-3) is indicated.

SRSF1 contains 2 RRMs, which provide the RNA-binding specificity, and a short RS-domain (Figure 1-7) (414). The consensus motif of the SRSF1 binding site was identified via *in vivo* mapping to be the purine-rich pentamer GGAGA (71; 99). SRSF1 is known to primarily bind to ESE regions (414). Alongside the known ESE binding sites of SRSF1 on the HIV-1 pre-mRNA, further binding sites have been predicted *in silico* by the computational algorithm ESEfinder3.0 (69; 357). Since not all predicted binding sites represent SREs, binding of SRSF1 to a large number of the predicted binding sites will not result in the regulation of a splice site. Therefore, further empirical validation will be necessary to determine, which SRSF1-binding sites potentially represent SREs.

It was shown in this work that the ratio of multiply spliced to unspliced mRNAs was changed upon altered levels of SRSF1. While elevated levels resulted in a decreased expression of unspliced mRNAs without altering the expression of multiply spliced mRNAs (Figure 4-9 G), knockdown shifted the multiply spliced to unspliced mRNA ratio towards unspliced mRNAs (Figure 4-7 G). These findings are in accordance with the known role of SRSF1 acting as a splicing enhancer from an exonic position (127; 154; 294). Unspliced mRNAs include the *Gag-Pol* precursor as well as the viral genome which is incorporated into new virions, while multiply spliced mRNAs are characterized by splicing from SD4 to SA7. The SRE ESE3 is located downstream of SA7 and a known target of SRSF1 (433;



446). Binding of SRSF1 to ESE3 was shown to stabilize the binding of the U2 snRNP to the viral pre-mRNA (446), which is an important step in the assembly of the spliceosome (317). Mutation of ESE3 resulted in reduced splicing events at SA7 (446). Thus, the observed reduction in multiply spliced mRNAs upon knockdown of SRSF1 could be explained through a lower splicing frequency at SA7 due to the lack of SRSF1-mediated stabilization of the U2 snRNP binding to the SA (Figure 4-7 G). Overexpression of SRSF1 did not alter the expression levels of multiply spliced mRNAs (Figure 4-9 G), which was in accordance with previous findings showing that high levels of SRSF1 did not result in higher splicing efficiency at SA7, potentially due to low binding affinity (446). Furthermore, splicing at SA7 is regulated by ESS3 (12; 433) and ISS3 (445), which are both targeted by hnRNP A1. Since interactions between SRSF1 and hnRNP A1 have been described (82; 91; 402), altered levels of SRSF1 might indirectly impair the binding of hnRNP A1 to ESS3 and ISS3, thus further affecting splice site usage of SA7.

The HIV-1 accessory protein *Vif* plays a crucial role in the immune evasion of HIV-1 by counteracting the HRF APOBEC3G via targeting the protein for proteasomal degradation (383; 436; 494). The formation of *vif* mRNA results from splicing between SD1 and SA1. Since the *vif* AUG lies within intron 2, the intron downstream of the non-coding leader exon 2 must be retained (375). Thus, SA1 must be activated through cross-exon interactions with SD2 or SD2b, while splicing at SD2 and SD2b is inhibited. Cross-exon interactions play a crucial role in exon 2 recognition and *vif* mRNA formation by regulating exon definition between the 5'-SD and the upstream 3'-SA. Binding of the U1 snRNP to the SD activates the upstream SA, which results in the binding of U2 snRNP to the branch point sequence (BPS) and the formation of an exon recognition complex. The interaction between factors binding to U1 or U2 snRNP then induces the assembly of the spliceosome (100). The formation of *vif* mRNA is tightly regulated through six different SREs in addition to the intrinsic weakness of SD2 (Figure 5-2).

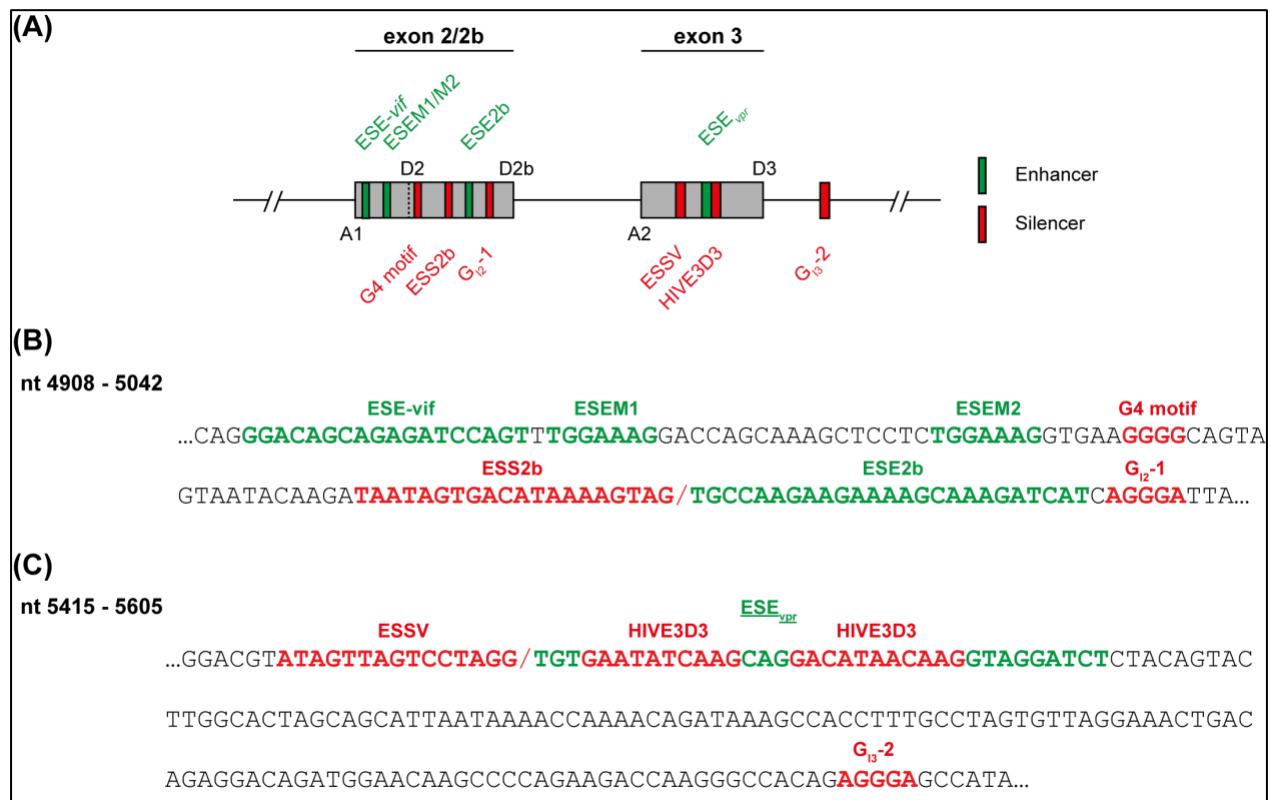


**Figure 5-2: SREs involved in the regulation of exon 2/2b and exon 3 splicing. (A)** Position of SREs within or in proximity of exon 2/2b and 3. **(B) – (C)** Sequence of SREs regulating exon 2/2b **(B)** or exon 3 **(C)** splicing (Sequence derived from viral laboratory clone NL4-3).

It was shown in this work that both elevated and reduced levels of SRSF1 led to significantly altered *vif* mRNA expression levels as well as the inclusion of non-coding leader exon 2. Knockdown of SRSF1 led to a 3.6-fold reduction in *vif* mRNA levels and a 5-fold decrease in exon 2 inclusion (Figure 4-7 D and F). Thus, splicing at SA1 was strongly inhibited. Elevated levels of SRSF1 resulted in a 12-fold increase in *vif* mRNA expression (Figure 4-9 D). However, no significant alteration in exon 2 inclusion was observed (Figure 4-9 F). Thus, it was suggested that usage of SA1 was strongly increased, while splicing frequency at SD2 and SD2b was blocked. A direct effect of SRSF1 on SA1 splice site usage was likely, since ESE M1/M2 was shown to be a direct target of SRSF1 (237). Reduced binding of SRSF1 to ESE M1/M2 was suggested to result in decreased recognition of SD2 and thus in reduced cross-exon interactions between SD2 and SA1. Subsequently, fewer splicing events occur at SA1, resulting in lower levels of *vif* and exon 2 containing mRNAs. Elevated levels of SRSF1 presumably resulted in increased binding events to ESE M1/M2, which led to increased recognition of SD2 and subsequently cross-exon interactions with SA1. However, while splice site usage at SA1

was strongly promoted, SD2 was recognized but not activated, thus resulting in unaltered levels in exon 2 containing mRNAs. Furthermore, a direct or indirect interaction between SRSF1 and other splicing regulatory factors binding to the SREs which regulate SD2 and SD2b recognition cannot be excluded. Protein-protein interactions between SRSF1 and Tra2- $\beta$ , which regulates the recognition of SD2b and SD2 through the binding of ESE2b (54), have been observed (189; 208; 303). Furthermore, SRSF1 was shown to interact with hnRNP A1 (82; 91; 402), which targets ESS2b (54). Tra2/SRSF10-binding to ESE2b was shown to activate recognition of SD2b while inhibiting splicing events at SD2 (54). ESS2b, however, counteracts the effects of ESE2b. Thus, altered levels of SRSF1 could possibly indirectly affect the regulation of ESE2b and ESS2b, and thus splice site recognition of SD2 and SD2b.

The viral protein Vpr is a multifunctional protein, which counteracts several HRFs, such as the macrophage mannose receptor (MR), SAMHD1 or the lysosomal-associated transmembrane protein 5 (LAPTM5) (132; 149; 302; 513). Generation of *vpr* mRNA requires splicing from SD1 to SA2 (375). U1 snRNP binding to SD3 is essential for the recognition of SA2 via cross-exon interactions. Similar to the *vif* mRNA, the translational AUG of *vpr* is located in the intron downstream of the non-coding leader exon. Therefore, splicing at SD3 must be repressed to retain intron 3 (128). While splice site SA2 is intrinsically strong, multiple SREs regulate splice site recognition (Figure 5-2). It has been suggested, that the two non-coding leader exons 2 and 3 are regulated in a mutually exclusive manner (486). Mutations in the intronic G-run G<sub>13-2</sub>, located downstream of SD3, were shown to increase exon 3 recognition, while exon 2 recognition as well as the formation of *vif* mRNA was reduced.

Altered levels of SRSF1 strongly affected *vpr* mRNA formation and the inclusion of non-coding leader exon 3. While knockdown of SRSF1 induced a significant repression in both *vpr* mRNA expression (1.4-fold) and exon 3 inclusion (2-fold) (Figure 4-7 D and F), overexpression resulted in strongly elevated mRNA expression of *vpr* (16-fold) but repressed inclusion of exon 3 (3-fold) (Figure 4-9 D and F). Reduced cross-exon interactions between SD3 and SA2 were suggested upon depleted levels of SRSF, possibly resulting from impeded binding of U1 snRNP to SD3. An increase in splicing events at SA2 was suggested upon elevated levels of SRSF1. Thus, recognition of SD3 was presumably increased, which resulted in elevated splice site usage of SA2, while simultaneously repressing splice site usage at SD3. No SRSF1-bound SREs have so far

been identified to regulate splice site recognition at SD3. Furthermore, no potential binding sites within this region could be detected using ESEfinder 3.0 (69). An indirect effect of SRSF1 on exon 3 recognition through the interaction with splicing factors directly binding to SREs which regulate *vpr* mRNA generation, however, cannot be ruled out. Interactions between SRSF1 and hnRNP A1 have been described previously (82; 91; 402), as well as interactions between SRSF1 and Tra2- $\beta$  (189; 208; 303). Thus, altered levels of SRSF1 could potentially affect binding of hnRNP A1 and Tra2- $\beta$  to ESSV and ESE<sub>*vpr*</sub> respectively, resulting in altered splice site recognition of SD3 and subsequently cross-exon interactions between SD3 and SA2. Competitive binding of hnRNP A1 with U2AF65 to the PPT inhibits splice site recognition of SA2 (114), while binding of Tra2- $\beta$  to ESE<sub>*vpr*</sub> resulted in increased inclusion of exon 3 (128). It was suggested that narrow levels of SRSF1 are necessary for balanced recognition of SD3 as well as cross-exon interactions between SD3 and SA2. The exact mechanism of the SRSF1-mediated regulation of SD3 splice site recognition, however, remains yet to be elucidated.

Upon SRSF1 knockdown, the levels of further exon 2 containing (*tat2* and *nef3*) and exon 3 containing mRNAs (*tat3* and *env8*), which require splicing between SD1 and SA1 or SD1 and SA2 respectively, were reduced (Figure 4-7 C). These observations were in accordance with the observed decrease in splicing events at SA1 and SA2 as described above, potentially due to reduced cross-exon interactions spanning exon 2 and exon 3. Elevated levels of SRSF1 resulted in increased mRNA expression of both exon 2 and exon 3 containing mRNAs (*vpr2*, *tat4*, *tat8* and *nef5*) (Figure 4-9 C). Thus, increased frequency of splicing at SA1, resulting from enhanced cross-exon interactions between SD2 and SA1 due to the binding of SRSF1 to ESE M1/M2, as well as SA2, was suggested. Moreover, repressed levels of mRNAs which are spliced from SD1 to SA4 were observed (*env1* and *nef2*) (Figure 4-9 C). The purine-rich bidirectional GAR ESE is located between SA5 and SD4 and has been described to regulate splice site usage at SA4 (19; 63). Binding of SRSF1 to GAR ESE was shown to promote binding of U1 snRNP to the 5'-SD4 and thus increases splicing frequency at the upstream 3'-SA4cab and 3'-SA5 (19; 63). However, elevated levels of SRSF1 resulted in reduced splicing events at SA4. Since regulation of splice site usage is a complex and dynamic process, which involves the interaction of a large number of proteins and splicing factors, it is possible that interactions of SRSF1 other factors impeded the stabilizing effect of SRSF1 on the binding of U1

snRNP to SD4. It was shown that binding of SRSF6 to ESE2 promotes splicing at SA3, while inhibiting splice site usage of SA4cab and SA5 (452).

Hence, the observed changes in splice site usage could most likely be linked to SREs which are known targets of SRSF1, or targeted by splicing factors interacting with SRSF1. Generally, knockdown and overexpression of SRSF1 induced strong, but opposing effects on the level of alternative splicing, which is in accordance with the role of SRSF1 acting as splicing enhancer when binding to exonic SREs. Since alternative splicing is a tightly regulated mechanism, unbalanced splicing of a specific splice site can substantially affect the splicing frequency of vicinal and competing splice sites.

Alteration of the balanced splicing of HIV-1 mRNAs was shown to impair viral replication and infectivity (219; 375). It has been shown, that particularly balanced levels of Vif are crucial for HIV-1 replication and viral infectivity in APOBEC3G-expressing cells (6; 436; 494). High levels of Vif drastically reduced viral infectivity through the inhibition of Gag processing at the nucleocapsid (6), while low levels of Vif led to a failure in viral replication due to the inability to evade APOBEC3G-mediated antiviral effects (486). Since HEK293T is a permissive cell line and lacks the expression of several host restriction factors including APOBEC3G (381), HEK293T was not a suitable cell line to analyze whether knockdown of SRSF1, and the subsequent repression of *vif* mRNA levels, would directly affect viral infectivity. Therefore, RPE-ISRE luc cells were chosen as cell culture model system, as they putatively express APOBEC3G (293) and showed a high transfection efficiency (data not shown).

Remarkably, despite a 3.6-fold reduction in *vif* mRNA expression, knockdown of SRSF1 resulted in significantly facilitated viral infectivity (Figure 4-8 A and B). One possible explanation might be that RPE-ISRE luc cells express APOBEC3G at low levels, which might not suffice to counteract the remaining expression of Vif. Immunoblot analysis to determine APOBEC3G protein expression levels in RPE-ISRE luc cells will need to be performed. The usage of high APOBEC3G expressing cell lines will be necessary to analyze the impact of reduced *vif* mRNA levels on viral infectivity in more detail. Elevated levels of SRSF1 resulted in drastically reduced viral infectivity (Figure 4-10 A and B). In accordance with previous findings (6), the observed increase in *vif* mRNA expression by 12-fold was concomitant with a 4.1-fold reduction in infectious viral titers (Figure 4-10 A). However, a Vif-independent mechanism of SRSF1 affecting virion infectivity directly or

indirectly through the interaction with cellular factors, such as post-translational modifications or viral packaging, cannot be excluded.

Knockdown of SRSF1 did not significantly alter virus production (Figure 4-8 C and D). However, the number of viral copies in the supernatant were marginally elevated by 1.4-fold, albeit with no statistical significance (Figure 4-8 C). This was in accordance with the observed increase in HIV-1 LTR promoter activity (Figure 4-7 B). Thus, increased HIV-1 LTR transcription might result in elevated infectious viral titers, despite reduced levels of *vif* mRNA. Overexpression of SRSF1 resulted in a significant reduction in viral copies (1.4-fold) and p24-levels (1.2-fold) in the cellular supernatant (Figure 4-10 C and D), which was in agreement with the strong inhibition in HIV-1 LTR promoter activity (Figure 4-9 B). Analyzing the level of encapsidated HIV-1 RNA copies could further be helpful to investigate, whether altered levels of SRSF1 might affect the efficiency of full length HIV-1 RNA encapsidation. Viral replication kinetics in APOBEC3G high and low expressing cells, such as CEM-SS or CEM-A cells (as performed in (486)), would ultimately reveal whether altered expression levels of SRSF1 and hnRNP A0, resulting in substantial changes in *vif* expression, affect HIV-1 replication.

In conclusion, knockdown and overexpression of SRSF1 crucially affected HIV-1 alternative splice site usage. Lower levels of SRSF1 increased viral LTR promoter activity and resulted in facilitated viral infectivity and particle production. Elevated levels, however, drastically reduced viral infectious titers and impeded virus production.

#### **5.4. Altered expression levels of hnRNP A0 decisively affect HIV-1 post integration steps**

In contrast to the well-known splicing factor SRSF1, relatively little is known so far about the characteristics of hnRNP A0 in cellular and HIV-1 alternative splicing. However, a role of hnRNP A0 as regulator of cellular RNA processing has been shown, such as the regulation of transcription factors (TNF- $\alpha$ , COX-2 or MIP-2) (390). Furthermore, hnRNP A0 was described to be the successor of tumor suppressor p53 upon silencing, which regulates cell cycle, genome stability or apoptosis (62). In this work, it was shown that IFN-stimulation of THP-1 macrophages resulted in the strongest repression of *hnRNP A0* mRNA levels out of all analyzed hnRNP members (Figure 4-13). Thus, to investigate a potential role of hnRNP A0 in the regulation of HIV-1 RNA processing, this factor was chosen for further experiments.

Contrary to the low abundant hnRNP A0, for which no direct target on the HIV-1 pre-mRNA has been identified so far, other hnRNP A/B members, including hnRNP A1 and hnRNP A2B1, have been widely described to regulate HIV-1 splice site usage. Several SREs, including ESS2b (54), G<sub>13</sub>-2 (486), ESSV (114; 196; 306), ESS2 (11; 64; 416), ESS3 (13; 417; 433) and ISS3 (445), are bound by hnRNP A/B proteins, as depicted in (Figure 5-3).

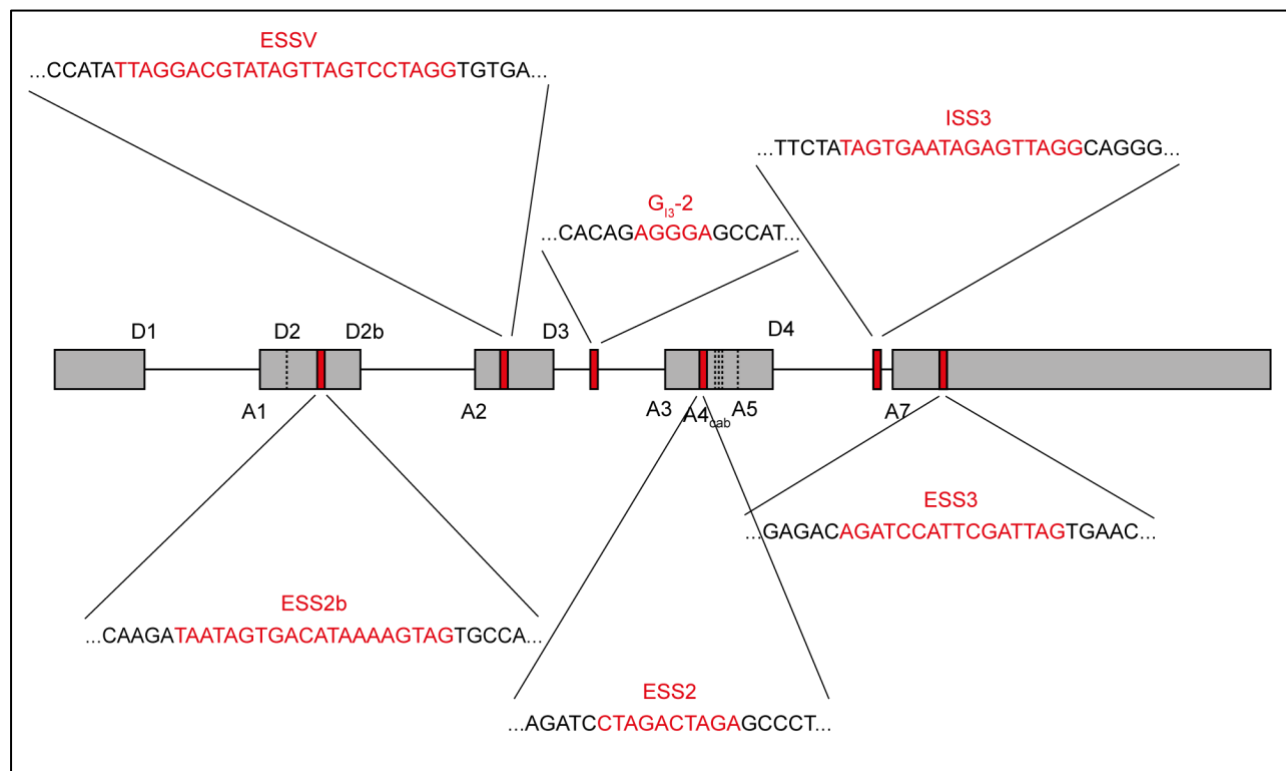


**Figure 5-3: Positions and sequences of hnRNP A/B-bound SREs within the genome of HIV-1 (NL4-3).** Exons are depicted as grey boxes, while introns are shown as black lines. Positions of the splicing regulatory elements ESS2b (54), ESSV (114; 196; 306), G<sub>13</sub>-2 (486), ESS2 (11; 64; 416), ISS3 (445) and ESS3 (12; 417; 433) are indicated as red boxes. The respective sequence on the HIV-1 genome (NL4-3) is indicated.

The complete structure of hnRNP A0 remains yet to be elucidated. However, the structure features 2 RRM (463), providing the RNA-binding specificity. AU-rich elements (AREs) were shown to be the target sequence of hnRNP A0 (338; 390; 507). The most common consensus motif of all ARE binding proteins is the pentamer AUUUA, which is often located in 3'-UTRs of mRNAs (74; 180). In addition to hnRNP A1 (183), which has several binding sites on within the viral genome, hnRNP A0 was also shown to bind to this sequence with high affinity (390). HIV-1 contains many AREs dispersed throughout its

genome, including its 3'-LTR (404). Further analysis, such as extensive mutagenesis or MS2 tagging, will be necessary to investigate, which ARE is targeted by hnRNP A0 and how the interaction of the potential hnRNP A0-bound SREs might regulate the fate of the HIV-1 pre-mRNA.

siRNA-mediated knockdown of hnRNP A0 in HEK293T cells induced a significant increase in total viral mRNA levels, measured by exon 1 (1.3-fold) and exon 7 (1.9-fold) containing mRNAs (Figure 4-18 B), while elevated levels led to a very strong reduction in exon 1 (5-fold) and exon 7 (10-fold) containing mRNA expression (Figure 420 B). Thus, overexpression of hnRNP A0 induced a pronounced inhibitory effect on HIV-1 LTR transcription. A direct or indirect effect of hnRNP A0 on the HIV-1 LTR transcriptional activity was suggested. Since many AREs are dispersed throughout the HIV-1 genome (404), direct binding of hnRNP A0 to a sequence within the 5'-LTR might possibly explain the substantial effect of altered hnRNP A0 levels on HIV-1 LTR transcription. hnRNP A0 was further shown to be involved in the transcriptional regulation of several transcription factors, such as TNF- $\alpha$ , COX-2, IL-6 and MIP-2 (390). Thus, an indirect effect of hnRNP A0 on HIV-1 LTR transcription through the regulation of a transcription factor directly binding to the viral LTR promoter cannot be excluded. Furthermore, analysis of interactions between spliceosomal proteins using the yeast two-hybrid system revealed protein-protein interactions between hnRNP A0 and SRSF1 (190). While the exact mechanism of interaction has not been elucidated yet, an indirect effect of altered hnRNP A0 levels on HIV-1 LTR transcription via interaction with SRSF1, which directly targets a region within TAR (356), cannot be ruled out.

To determine, whether the effect of hnRNP A0 on HIV-1 LTR transcription is Tat-dependent or -independent, analysis of LTR promoter activity in the presence of hnRNP A0 and either wt Tat and Tat Q35L mutant would be of interest. The Tat mutant Q35L was generated via single point mutation from glutamine to leucine at position 35 (107). This mutant lacks transcriptional activation capacity of the HIV-1 LTR due to impaired binding to P-TEFb (107). Thus, a potential binding of hnRNP A0 on to the HIV-1 5'-LTR in the presence and absence of Tat could be evaluated.

Knockdown of hnRNP A0 resulted in significantly reduced levels of unspliced mRNAs by 2-fold (Figure 4-18 G), while elevated levels of hnRNP A0 induced a 1.3-fold increase in unspliced mRNA (Figure 4-20 G). The expression levels of multiply spliced mRNAs (spliced from SD4 to SA7) were reduced by 1.3- and 1.4-fold upon knockdown and



overexpression of hnRNP A0, respectively (Figure 4-18 G and 4-20 G). Thus, splicing frequency at SA7 was reduced upon altered levels of hnRNP A0. SA7 splice site usage is regulated by ESE3 (433), ISS3 (445) and ESS3 (12; 417; 433). While ESE3 is bound by SRSF1 (433), ISS3 and ESS3 are targeted by hnRNP A1 (12; 417; 433; 445), which are known interaction partners of hnRNP A0. Thus, altered levels of hnRNP A0 could possibly indirectly affect splice site recognition and usage of SA7 via the interaction with SRSF1 or hnRNP A1. Similar to the effect of altered levels of SRSF1, both elevated and depleted levels of hnRNP A0 resulted in a decrease in multiply spliced mRNA levels. Thus, a direct interaction between the two RBPs cannot be ruled out.

Depleted levels of hnRNP A0 induced a 2- and 1.3-fold reduction in *vif* and *vpr* mRNA respectively (Figure 4-18 D). Concomitantly, non-coding leader exon 2 and exon 3 inclusion was repressed by 1.7- and 2.3-fold respectively (Figure 4-18 F). Thus, depleted levels of hnRNP A0 induced a decreased splicing frequency at SA1 and SA2, likely due to reduced splice site recognition at SD2, SD2b and SD3. Elevated levels of hnRNP A0 resulted in a 1.9- and 1.5-fold increase in *vif* and *vpr* mRNA expression (Figure 4-20 D). While exon 2 inclusion was induced by 1.8-fold, the inclusion of exon 3 was repressed by 1.4-fold (Figure 4-20 F). Increased levels of hnRNP A0 seemed to facilitate splice site recognition at SD2/2b and SD3, promoting cross-exon interactions spanning exon 2 and exon 3, thus resulting in elevated splice site usage at SA1 and SA2. However, while splicing at SD2/2b was increased, SD3 splice site usage was repressed. Since no known target SREs of hnRNP A0 have been identified so far, the impact of altered levels of hnRNP A0 on splice site usage cannot directly be linked to the regulation of specific splice sites.

Several of the SREs within exon 2 are targeted by known interaction partners of hnRNP A0, including SRSF1 (34; 190), hnRNP A1 (192; 391), hnRNP A2B1 (192; 503), hnRNP F (189; 190; 192) and hnRNP H (189; 192; 464). ESE M1/M2, which is targeted by SRSF1, directly affects splice site usage of SA1 (237). The G-runs G<sub>12</sub>-1 and G<sub>4</sub>, which regulate splice site recognition of SD2b and SD2, are bound by hnRNP F/H (131; 485). ESS2b, regulating splicing at SA1, SD2 and SD2b, is bound by hnRNP A/B (54). Furthermore, several SREs involved in the regulation of exon 3 recognition are also bound by interaction partners of hnRNP A0. The G-run G<sub>13</sub>-2, regulating splice site recognition at SD3, is bound by hnRNP F/H and hnRNP A2B1 (486). ESSV is bound by hnRNP A/B and involved in the regulation of SA2 recognition (114; 196; 306). Thus, altered levels of

hnRNP A0 might indirectly affect splice site recognition and usage, as well as exon 2 and exon 3 spanning cross-exon interactions, through PPI with other RNA-binding proteins. However, the large number of potential interaction partners of hnRNP A0 does not allow the identification of specific interactions affecting the regulation of a given splice site. The potential binding sites of hnRNP A0 on the viral pre-mRNA, in addition to the potential interactions with numerous other splicing factors, might be part of the complex regulatory network regulating HIV-1 alternative splice site usage.

To investigate a potential scaffold function of hnRNP A0 in the regulation of HIV-1 gene expression, the method of MS2 tethering could be performed (48; 83; 459). Therefore, hairpin-structures derived from the genome of the MS2 bacteriophage are inserted in proximity of splice sites on the HIV-1 genome. The MS2 coat protein, which binds the 21 nt long inserted hairpin with high affinity in the form of a dimer, is fused to a RBP of interest, thus bringing the RBP into proximity of different splice sites (48; 83; 459). Using different splicing reporters, potential binding sites involving protein-protein interactions of cellular splicing factors with hnRNP A0 could be identified. Furthermore, the use of truncated versions or deletion mutants of hnRNP A0, lacking distinct protein domains involved in RNA-binding or PPI might further elucidate, whether the observed alterations in HIV-1 LTR transcription and alternative splicing are due to a direct binding of hnRNP A0 on the viral genome or PPI with other splicing regulatory proteins.

As described in (Chapter 5.3.), RPE-ISRE luc cells were chosen as cell culture model systems to analyze the impact on altered levels of hnRNP A0 on viral infectivity due to their putative expression of APOBEC3G. Despite the observed 2-fold reduction in *vif* mRNA levels upon knockdown of hnRNP A0 (Figure 4-18 D), infectious viral titers were not altered (Figure 4-19 A and B). As discussed in (Chapter 5.3.), APOBEC3G levels might not be sufficiently high for a detectable impact on viral infectivity resulting from lower *vif* mRNA expression. Overexpression of hnRNP A0, however, resulted in substantially impaired viral infectivity (2-fold) (Figure 4-21 A and B), despite the 1.9-fold increase in *vif* mRNA levels (Figure 4-20 D). While elevated Vif levels were shown to be detrimental for HIV-1 replication (6), a further Vif-independent effect of hnRNP A0 on viral infectivity via the interaction with other cellular factors or an effect on viral packaging or post-transcriptional modifications cannot be ruled out.

A significant increase (1.1-fold) in virus production was observed upon hnRNP A0-knockdown (Figure 4-19 C), while overexpression led to strongly reduced viral copies

(2.5-fold) and p24-levels (5.5-fold) in the cellular supernatant (Figure 4-21 C and D). This was in accordance with the observed strong reduction in HIV-1 LTR transcription (10-fold for exon 7 containing mRNAs) upon elevated levels of hnRNP A0 (Figure 4-20 B), while depleted levels of hnRNP A0 resulted in a significant increase (1.9-fold for exon 7 containing mRNAs) in HIV-1 LTR promoter activity (Figure 4-18 B).

Thus, drastically reduced HIV-1 LTR transcription upon hnRNP A0 overexpression was suggested to result in impaired viral particle production as well as virus infectious titers, while knockdown of hnRNP A0 did not substantially alter HIV-1 LTR transcription and concomitantly virus production and infectivity.

### **5.5. Balanced levels of *SRSF1* and *hnRNP A0* are required for efficient HIV-1 LTR transcription, alternative splicing and virus production**

Overexpression and knockdown of SRSF1 and hnRNP A0 were shown to drastically affect HIV-1 post integration steps, as described in (Chapter 5.3. and 5.4.). While changes in SRSF1 expression resulted in strong alterations in the viral splicing pattern, changes in hnRNP A0 expression rather affected HIV-1 LTR transcription. Knockdown of both HDFs, in addition to increased LTR promoter activity, resulted in unaltered or marginally facilitated viral infectivity and viral particle production. However, overexpression of SRSF1 and hnRNP A0 resulted in drastically impaired viral infectivity and virus production. Hence, the IFN-induced repression of *SRSF1* and *hnRNP A0*, as described in (Chapter 5.1.), does not seem to have a direct and specific antiviral effect and might even be detrimental in the defense against HIV-1 infection. However, increased levels of *SRSF1* and *hnRNP A0*, which were observed at different time points upon IFN-stimulation in THP-1 macrophages and MDMs, might be part of the antiviral response in the early immune reaction due to IFN upregulation.

Since it was demonstrated that depleted levels of both HDFs did not negatively affect HIV-1 LTR transcription and even facilitated virus production and infectivity, it is possible, that HIV-1 has evolutionary adapted to the downregulation of these crucial regulators of LTR promoter activity and alternative splicing. Roughly 80 % of all HIV-1 infections are established by a single HIV-1 variant, the transmitted founder virus (TFV) (2; 218; 250). TFVs are adapted to the selective pressure exerted by type I IFNs during the early stage of infection. These viruses are generally R5-tropic and contain shorter variable regions, fewer *N*-linked glycosylation sites as well as amino acid signatures affecting env surface

expression (77; 90; 105; 167; 285; 298). However, the properties rendering TFVs relatively resistant against type I IFN antiviral activity are still not completely understood. Extending the infection experiments to TFVs could elucidate, whether viral alternative splicing might play a role in the relative resistance to type I IFNs and the IFN-induced repression of SRSF1 and hnRNP A0. Furthermore, primary viral isolates from chronically HIV-1 infected individuals should be included to rule out HIV-1 laboratory strain artifacts. Laboratory strains are generally less genetically variable than virus isolated from patients and are adapted to *in vitro* conditions.

The IFN-mediated knockdown of SRSF1 could be validated on the protein level with a timely delay of 12 to 24 h when compared to the mRNA levels (Figure 4-5 A). Since the protein levels were reduced after the repression in mRNA expression, protein degradation due to post-translational modifications was unlikely. A direct effect on the transcriptional level, however, was likely and was discussed in detail in (Chapter 5.2). Alternative splicing is regulated by SRSF1 and hnRNP A0 proteins, however, the correlation between mRNA expression and resulting protein levels has not yet been fully elucidated. Thus, detailed analysis of IFN-mediated deregulation of SRSF1 and hnRNP A0 on the protein level will be mandatory to evaluate the outcome of the alteration in gene expression and is currently a limiting factor of this work. Thus, it will be important to extend knockdown and overexpression experiments of SRSF1 and hnRNP A0 and analyze viral expression on the protein level.

Interestingly, a concomitant HIV-1 infection counteracted the IFN-mediated repression of both *SRSF1* and *hnRNP A0* mRNA levels in THP-1 macrophages when compared to uninfected cells (Figure 4-11 and 4-22). Thus, HIV-1 potentially restored balanced levels of both splicing factors, strengthening the hypothesis of SRSF1 and hnRNP A0 playing a crucial role in HIV-1 post integration steps and replication. However, whether the HIV-1 mediated changes in *SRSF1* and *hnRNP A0* expression are directed or undirected is not yet known. Furthermore, the mechanism of action remains unclear.

While 16 h post infection the process of integration is completed, the subsequent expression of viral proteins occurs in a timely regulated manner. Among the early expressed HIV-1 proteins are the accessory protein Nef (212), as well as Tat and Rev (234; 502). Expression of the accessory proteins Vif, Vpr and Vpu, however, occurs at a later stage of infection (212; 254; 334). While an involvement of Rev or Tat in the regulation of *SRSF1* and *hnRNP A0* expression seems unlikely, the involvement of the

early expressed accessory protein Nef should be investigated. Further experiments including HIV-1 virus mutants, which lack the expression of one of the viral accessory proteins Nef, Vif, Vpr and Vpu would be interesting to investigate the potential role of one of these viral accessory proteins in the regulation of SRSF1 and hnRNP A0 expression. HIV-1 accessory proteins act as adapter molecules by redirecting cellular host factor functions to virus-specific purposes and by counteracting antiviral activities of HRFs (437). Vif and Vpr induce the proteasomal degradation of HRFs such as APOBEC3G or SAMHD1, respectively (as reviewed in (84; 307; 437)). Vpu and Nef were also shown to counteract HRFs such as tetherin (341; 469) or serine incorporator 3 (SERINC3) and SERINC5 (465). Both Vpu and Nef, however, modulate additional functions such as the downregulation of cell surface receptors, signal transduction or antigen presentation (as reviewed in (255; 275; 437)). Thus, one possible connection could be the interaction of a viral protein with the autoregulatory feedback loop of SRSF1 and presumably hnRNP A0, thus inducing a quick recovery of the respective mRNA levels.

To further rule out a timely effect due to the early and late phase of HIV-1 replication, IFN-stimulation of latently HIV-1 infected cells could further be beneficial. The use of SupT1 cells will allow the uncoupling of the effects of HRFs from the SRSF1- and hnRNP A0-mediated effects. SupT1 cells are deficient for APOBEC3G, SAMHD1 and tetherin amongst other HRFs (381). Thus, SupT1 allow the replication of the HIV-1 minimal laboratory virus rtAde17, which is deficient for all viral accessory proteins (226).

Furthermore, it cannot be ruled out, that HIV-1 infection prior to IFN stimulation already induces the upregulation of IFN, thus affecting the expression levels of SRSF1 and hnRNP A0. Hence, viral sensing could be involved in the regulation of SRSF1 and hnRNP A0 expression. TLRs 7 and 8 recognize ssRNA molecules, such as the HIV-1 genome. Thus, investigating the effect of TLR 7/8 agonist Resiquimod on the expression of SRSF1 and hnRNP A0 could give further insight, whether viral sensing is involved in the downregulation of these two factors. Furthermore, agonists for RIG-I, TLR 3 or cGAS should also be included, since these PRRs are also involved in HIV-1 sensing. Generally, sensing through these PRRs induce the production of proinflammatory cytokines and IFNs. Thus, to rule out an eventual effect of viral sensing through the subsequent production of IFNs, an inhibitor of the JAK/STAT pathway should be included, such as ruxolitinib.

Ultimately, the effect of altered levels of SRSF1 and hnRNP A0 on HIV-1 post integration steps will need to be evaluated in more natural HIV-1 host cells, such as macrophages and T-cells. Since transient transfection efficiency of THP-1 and Jurkat cells is limited, stably transfected cells could be generated using the 'Sleeping Beauty' transposon system (265). This method allows the induction of a gene of interest either constitutively or in a doxycycline-dependent manner (265). Thus, the genes of *SRSF1* and *hnRNP A0*, or a target-specific shRNA, could be stably integrated into the host genome, allowing the analysis of altered expression of *SRSF1* and *hnRNP A0* on HIV-1 RNA processing and virus production in natural HIV-1 target cells.

### **5.6. SRSF1 and hnRNP A0 are potential targets for antiviral therapy**

SRSF1 and hnRNP A0 have been shown to be crucial regulators of HIV-1 post integration steps. However, both proteins have a much broader scope of action. SRSF1 is also an indispensable regulator in cellular splicing (517), genome stability (288), translation (396), nuclear export (202) and the nonsense-mediated mRNA decay (NMD) pathway (23; 512). While loss of function led to G2 cell cycle arrest and induced apoptosis (289), elevated levels of SRSF1 have been shown to be involved in a variety of cancers (98; 150; 245). Thus, SRSF1 is defined as a proto-oncogene. hnRNP A0 has also been linked to several cancer diseases, such as pancreatic, lung or gastric cancer (62; 262). Upon loss of function of p53, which is a crucial regulator of cell cycle, genome stability and apoptosis, hnRNP A0 can take over the checkpoint control of p53. Homeostatic levels of p53, however, have been shown to suppress hnRNP A0 expression (62). Furthermore, hnRNP A0 is involved in the post-transcriptional regulation of several transcription factors such as TNF- $\alpha$ , COX-2 and MIP-2 (390).

Thus, the IFN-mediated repression of *SRSF1* and *hnRNP A0* described in this work could, in addition to HIV-1 post integration steps, affect a broad range of other cellular functions. Restoring of the physiological levels of *SRSF1* and *hnRNP A0* mRNA levels after IFN-stimulation is indispensable for the cells, since unbalanced levels of these two HDFs for a longer period of time can have detrimental consequences. As discussed above, SRSF1 is auto-regulated by a negative feedback loop to ensure balanced levels. It is to be assumed, that hnRNP A0 is regulated by a similar mechanism, albeit without self-splicing, since the mRNA of *hnRNP A0* consists of a single exon with no introns (463).

---

Since alternative splice site usage is a crucial component of HIV-1 replication, this mechanism is a potential target for antiretroviral therapy as has been reviewed in (112; 448). Several small molecule compounds were shown to impede different stages of HIV-1 RNA processing, such as digoxin (499), chlorhexidine (497), 8-azaguanine (498) or ABX464 (61) with limited effects on the viability of the host cell. Different approaches include gene therapy based on RNA interference, where a target gene is silenced through the use of siRNAs (123; 184; 326) or the use of an antisense U7 snRNA, which is incorporated into U7 snRNP and induces exon skipping by masking of the splice site (21; 22).

An interesting question is whether drug targeting of SRSF1 or hnRNP A0 could result in HIV-1 replication inhibition. The drug IDC16 was described to inhibit the replication of CXCR4- and CCR5-tropic viruses, as well as multiple drug resistant virus isolates, via direct interaction with SRSF1 (26; 430). The indole derivative was suggested to bind to the RS domain of SRSF1, thereby preventing its phosphorylation and thus suppressing the exonic splicing enhancer activity of SRSF1. The formation of multiple spliced mRNA isoforms is restricted and thus the formation of early viral proteins like Tat, Rev and Nef (26; 430; 431). Current studies investigate potential deleterious side effects of IDC16 *in vivo*.

Current antiviral therapy is based on the inhibition of HIV-1 proteins such as integrase, reverse transcriptase or protease, which upon long-term use can result in the emergence of drug-resistant mutations and severe side effects (359). Thus, targeting cellular factors involved in the regulation of HIV-1 alternative splicing offers many new approaches for antiretroviral therapy circumventing HIV-1 drug resistance. However, the use of drugs targeting SRSF1 or hnRNP A0 should be approached cautiously, due to the numerous cellular processes which are directly affected by these two host cell proteins.

---

## 6. Conclusion

In this thesis, the cellular splicing factors *SRSF1* and *hnRNP A0* were identified as IFN-regulated genes. Analysis of two independent patient cohorts revealed an inverse correlation between ISG induction and the repression of both *SRSF1* and *hnRNP A0* expression in the early immune response upon HIV-1 infection, potentially due to IFN upregulation and the concomitant inflammation. Upon stimulation of HIV-1 target cells with IFN $\alpha$ 2 and IFN $\alpha$ 14, a strong and time-dependent repression in *SRSF1* and *hnRNP A0* mRNA expression was observed, which was likely induced by a temporary transcriptional shutdown. Following the initial downregulation, the expression of both genes was restored and at a later time point even significantly elevated, presumably through a mechanism of autoregulation. Both overexpression and knockdown of *SRSF1* and *hnRNP A0* substantially affected HIV-1 post integration steps, including LTR transcription, alternative splicing and virus production. While lower levels of both factors resulted in decreased *vif* mRNA expression levels, elevated *SRSF1* and *hnRNP A0* expression resulted in heavily impaired viral production and infectivity. These findings suggested that balanced levels of *SRSF1* and *hnRNP A0* are required for efficient HIV-1 replication. Thus, the IFN-mediated deregulation of the two HDFs might be part of the IFN-induced antiviral activity upon HIV-1 infection. Targeting cellular factors involved in the modulation of alternative splice site usage offers many new approaches for a potential antiviral therapy. However, due to the broad range of cellular processes in which *SRSF1* and *hnRNP A0* are involved, the use of drugs directly targeting *SRSF1* and *hnRNP A0* should be warily approached.



---

## 7. Summary

### 7.1. Summary

Type I interferons (IFNs) play a crucial role in the early innate immune defense against viral infections. In addition to their immunomodulatory function, they induce the transcription of hundreds of IFN-stimulated genes (ISGs), thereby establishing an antiviral state within the host cell and bystander cells. Furthermore, IFNs downregulate the expression of host dependency factors (HDFs), which are essential for viral replication. The human immunodeficiency virus type 1 (HIV-1) depends on the cellular transcription and RNA processing apparatus, including alternative splicing, to extract the full content of the short and compact genome. HIV-1 alternative splicing is regulated by a complex network of splicing regulatory elements (SREs), which are localized in close proximity to viral splice donor and acceptor sites and are bound by cellular splicing factors including members of the RNA-binding protein families serine/arginine-rich splicing factors (SRSFs) and heterogeneous nuclear ribonucleoproteins (hnRNPs).

In the present thesis, *SRSF1* and *hnRNP A0* were identified as IFN-regulated genes. Analyzing two independent patient cohorts, an inverse correlation was observed between ISG induction and the repression of *SRSF1* and *hnRNP A0*, since HIV-1 infection and apparently the concomitant inflammation during the acute and chronic phase resulted in decreased expression levels of *SRSF1* and *hnRNP A0*. Stimulation of HIV-1 target cells with IFN $\alpha$ 2 and IFN $\alpha$ 14 resulted in a strong and time-dependent downregulation of both genes either induced by a transcriptional shutdown or mRNA decay. However, expression levels of both genes were presumably restored by autoregulatory mechanisms and even significantly elevated 24-48 hours post IFN stimulation. Downregulation and overexpression of *SRSF1* and *hnRNP A0* crucially altered HIV-1 post integration steps at the level of LTR transcription, alternative splicing and virus production emphasizing the importance of balanced *SRSF1* and *hnRNP A0* levels for efficient HIV-1 replication. While lower levels of *SRSF1* and *hnRNP A0* resulted in low HIV-1 *vif* mRNA levels, elevated expression of both HDFs resulted in a particularly unfavorable condition for viral production and infectivity. This work highlights the so far undescribed role of *SRSF1* and *hnRNP A0* acting as IFN-regulated effector molecules, which decisively affect HIV-1 post integration steps and significantly contribute to the IFN-induced unfavorable cellular environment for HIV-1 replication.

## 7.2. Zusammenfassung

Die Ausschüttung von Typ I Interferonen (IFN) stellt einen frühen Abwehrmechanismus des angeborenen Immunsystems gegen eindringende Viren dar. Neben immunmodulatorischen Eigenschaften induzieren IFN die Expression hunderter IFN-stimulierter Gene (ISG), welche die infizierte Zelle sowie benachbarte Zellen in einen antiviralen Zustand versetzen. Des Weiteren wird die Expression von zellulären Wirtsabhängigkeitsfaktoren (HDF), welche essentiell für die virale Replikation sind, herunterreguliert. Das humane Immundefizienzvirus Typ 1 (HIV-1) nutzt den Replikations- und Spleißapparat der Wirtszelle um das volle genetische Kontingent des kurzen viralen Genoms auszuschöpfen. Die virale Genexpression wird von einem komplexen regulatorischen Netzwerk von Spleiß-regulatorischen Elementen (SRE) reguliert, welche sich in direkter Nachbarschaft zu viralen Spleißdonor- und Spleißakzeptorstellen befinden und von Mitgliedern der RNA-bindenden Proteinfamilien der Serin/Arginin-reichen Spleißfaktoren (SRSF) und der heterogenen nukleären Ribonukleoproteinen (hnRNP) gebunden werden.

In dieser Doktorarbeit wurden *SRSF1* und *hnRNP A0* als IFN-regulierte Gene identifiziert. Bei der Untersuchung von zwei unabhängigen Patientenkohorten wurde eine inverse Korrelation zwischen der Induktion von ISG und der Repression von *SRSF1* und *hnRNP A0* festgestellt. Eine HIV-1 Infektion und vermutlich die damit einhergehende Entzündungsreaktion resultierten in einer niedrigeren Expression von *SRSF1* und *hnRNP A0*. Die Stimulation von HIV-1 Zielzellen mit IFN $\alpha$ 2 und IFN $\alpha$ 14 führte zu einer ausgeprägten und zeitabhängigen Herunterregulation von beiden Genen, induziert durch einen transkriptionalen Shutdown oder durch mRNA Degradation. Die Expression beider Gene wurde nach der initialen Herunterregulierung wahrscheinlich durch autoregulatorische Mechanismen wiederhergestellt, was 24-48 h nach IFN Stimulation sogar zu einem signifikanten Anstieg führte. Herunterregulation sowie Überexpression von *SRSF1* und *hnRNP A0* beeinflussten HIV-1 Postintegrationsschritte wie die virale Transkription, alternatives Spleißen oder die Virusproduktion stark, was die Wichtigkeit von ausbalancierten Mengen an *SRSF1* und *hnRNP A0* für die HIV-1 Replikation hervorhob. Während niedrige Level an *SRSF1* und *hnRNP A0* in niedrigen *vif* mRNA Mengen resultierten, führten erhöhte Level beider Faktoren zu stark unvorteilhaften Bedingungen für die Virusproduktion und -replikation. Diese Arbeit hebt die bisher unbekannte Funktion von *SRSF1* und *hnRNP A0* als IFN-regulierte Effektormoleküle

---

hervor, welche entscheidenden Einfluss auf HIV-1 Postintegrationsschritte haben und zum IFN-induzierten antiviralen Zustand der Zelle beitragen.

## 8. References

1. Ablasser A, Goldeck M, Cavlar T, Deimling T, Witte G, et al. 2013. cGAS produces a 2'-5'-linked cyclic dinucleotide second messenger that activates STING. *Nature* 498:380-4
2. Abrahams MR, Anderson JA, Giorgi EE, Seoighe C, Mlisana K, et al. 2009. Quantitating the multiplicity of infection with human immunodeficiency virus type 1 subtype C reveals a non-poisson distribution of transmitted variants. *J Virol* 83:3556-67
3. Abram ME, Ferris AL, Shao W, Alvord WG, Hughes SH. 2010. Nature, position, and frequency of mutations made in a single cycle of HIV-1 replication. *J Virol* 84:9864-78
4. Adhikary S, Eilers M. 2005. Transcriptional regulation and transformation by Myc proteins. *Nat Rev Mol Cell Biol* 6:635-45
5. Ahn J, Hao C, Yan J, DeLucia M, Mehrens J, et al. 2012. HIV/simian immunodeficiency virus (SIV) accessory virulence factor Vpx loads the host cell restriction factor SAMHD1 onto the E3 ubiquitin ligase complex CRL4DCAF1. *J Biol Chem* 287:12550-8
6. Akari H, Fujita M, Kao S, Khan MA, Shehu-Xhilaga M, et al. 2004. High level expression of human immunodeficiency virus type-1 Vif inhibits viral infectivity by modulating proteolytic processing of the Gag precursor at the p2/nucleocapsid processing site. *J Biol Chem* 279:12355-62
7. Akira S, Takeda K. 2004. Toll-like receptor signalling. *Nat Rev Immunol* 4:499-511
8. Akira S, Uematsu S, Takeuchi O. 2006. Pathogen recognition and innate immunity. *Cell* 124:783-801
9. Alsayed Y, Uddin S, Ahmad S, Majchrzak B, Druker BJ, et al. 2000. IFN-gamma activates the C3G/Rap1 signaling pathway. *J Immunol* 164:1800-6
10. Amati B, Brooks MW, Levy N, Littlewood TD, Evan GI, Land H. 1993. Oncogenic activity of the c-Myc protein requires dimerization with Max. *Cell* 72:233-45
11. Amendt BA, Hesslein D, Chang LJ, Stoltzfus CM. 1994. Presence of negative and positive cis-acting RNA splicing elements within and flanking the first tat coding exon of human immunodeficiency virus type 1. *Mol Cell Biol* 14:3960-70
12. Amendt BA, Si ZH, Stoltzfus CM. 1995. Presence of exon splicing silencers within human immunodeficiency virus type 1 tat exon 2 and tat-rev exon 3: evidence for inhibition mediated by cellular factors. *Mol Cell Biol* 15:6480
13. Amendt BA, Si ZH, Stoltzfus CM. 1995. Presence of exon splicing silencers within human immunodeficiency virus type 1 tat exon 2 and tat-rev exon 3: evidence for inhibition mediated by cellular factors. *Mol Cell Biol* 15:4606-15
14. Andersen JB, Aaboe M, Borden EC, Goloubeva OG, Hassel BA, Orntoft TF. 2006. Stage-associated overexpression of the ubiquitin-like protein, ISG15, in bladder cancer. *Br J Cancer* 94:1465-71
15. Anderson JL, Johnson AT, Howard JL, Purcell DF. 2007. Both linear and discontinuous ribosome scanning are used for translation initiation from bicistronic human immunodeficiency virus type 1 env mRNAs. *J Virol* 81:4664-76
16. Anko ML. 2014. Regulation of gene expression programmes by serine-arginine rich splicing factors. *Semin Cell Dev Biol* 32:11-21

17. Antonelli G, Scagnolari C, Moschella F, Proietti E. 2015. Twenty-five years of type I interferon-based treatment: a critical analysis of its therapeutic use. *Cytokine Growth Factor Rev* 26:121-31
18. Arhel NJ, Souquere-Besse S, Munier S, Souque P, Guadagnini S, et al. 2007. HIV-1 DNA Flap formation promotes uncoating of the pre-integration complex at the nuclear pore. *EMBO J* 26:3025-37
19. Asang C, Hauber I, Schaal H. 2008. Insights into the selective activation of alternatively used splice acceptors by the human immunodeficiency virus type-1 bidirectional splicing enhancer. *Nucleic Acids Res* 36:1450-63
20. Ashokkumar M, Sonawane A, Sperk M, Tripathy SP, Neogi U, Hanna LE. 2020. In vitro replicative fitness of early Transmitted founder HIV-1 variants and sensitivity to Interferon alpha. *Sci Rep* 10:2747
21. Asparuhova MB, Barde I, Trono D, Schranz K, Schumperli D. 2008. Development and characterization of a triple combination gene therapy vector inhibiting HIV-1 multiplication. *J Gene Med* 10:1059-70
22. Asparuhova MB, Marti G, Liu S, Serhan F, Trono D, Schumperli D. 2007. Inhibition of HIV-1 multiplication by a modified U7 snRNA inducing Tat and Rev exon skipping. *J Gene Med* 9:323-34
23. Aznarez I, Nomakuchi TT, Tetenbaum-Novatt J, Rahman MA, Fregoso O, et al. 2018. Mechanism of Nonsense-Mediated mRNA Decay Stimulation by Splicing Factor SRSF1. *Cell Rep* 23:2186-98
24. Bach EA, Aguet M, Schreiber RD. 1997. The IFN gamma receptor: a paradigm for cytokine receptor signaling. *Annu Rev Immunol* 15:563-91
25. Baig E, Fish EN. 2008. Distinct signature type I interferon responses are determined by the infecting virus and the target cell. *Antivir Ther* 13:409-22
26. Bakkour N, Lin YL, Maire S, Ayadi L, Mahuteau-Betzer F, et al. 2007. Small-molecule inhibition of HIV pre-mRNA splicing as a novel antiretroviral therapy to overcome drug resistance. *PLoS Pathog* 3:1530-9
27. Balachandran AM, L.; Cochrane, A. 2018. Chapter 6 - Teetering on the Edge: The Critical Role of RNA Processing Control During HIV-1 Replication. *Retrovirus-Cell Interactions*:229-51
28. Baltimore D. 1971. Expression of animal virus genomes. *Bacteriol Rev* 35:235-41
29. Bamford KB, Fan X, Crowe SE, Leary JF, Gourley WK, et al. 1998. Lymphocytes in the human gastric mucosa during *Helicobacter pylori* have a T helper cell 1 phenotype. *Gastroenterology* 114:482-92
30. Baralle M, Baralle FE. 2018. The splicing code. *Biosystems* 164:39-48
31. Barash Y, Calarco JA, Gao W, Pan Q, Wang X, et al. 2010. Deciphering the splicing code. *Nature* 465:53-9
32. Barre-Sinoussi F, Chermann JC, Rey F, Nugeyre MT, Chamaret S, et al. 1983. Isolation of a T-lymphotropic retrovirus from a patient at risk for acquired immune deficiency syndrome (AIDS). *Science* 220:868-71
33. Barre-Sinoussi F, Ross AL, Delfraissy JF. 2013. Past, present and future: 30 years of HIV research. *Nat Rev Microbiol* 11:877-83
34. Behrends C, Sowa ME, Gygi SP, Harper JW. 2010. Network organization of the human autophagy system. *Nature* 466:68-76
35. Bektas N, Noetzel E, Veeck J, Press MF, Kristiansen G, et al. 2008. The ubiquitin-like molecule interferon-stimulated gene 15 (ISG15) is a potential prognostic marker in human breast cancer. *Breast Cancer Res* 10:R58

36. Bergantz L, Subra F, Deprez E, Delelis O, Richetta C. 2019. Interplay between Intrinsic and Innate Immunity during HIV Infection. *Cells* 8
37. Bhat MY, Solanki HS, Advani J, Khan AA, Keshava Prasad TS, et al. 2018. Comprehensive network map of interferon gamma signaling. *J Cell Commun Signal* 12:745-51
38. Biamonti G, Riva S. 1994. New insights into the auxiliary domains of eukaryotic RNA binding proteins. *FEBS Lett* 340:1-8
39. Billiau A, Matthys P. 2009. Interferon-gamma: a historical perspective. *Cytokine Growth Factor Rev* 20:97-113
40. Black DL. 2003. Mechanisms of alternative pre-messenger RNA splicing. *Annu Rev Biochem* 72:291-336
41. Blackwell TK, Huang J, Ma A, Kretzner L, Alt FW, et al. 1993. Binding of myc proteins to canonical and noncanonical DNA sequences. *Mol Cell Biol* 13:5216-24
42. Blackwood EM, Eisenman RN. 1991. Max: a helix-loop-helix zipper protein that forms a sequence-specific DNA-binding complex with Myc. *Science* 251:1211-7
43. Blanchette M, Chabot B. 1999. Modulation of exon skipping by high-affinity hnRNP A1-binding sites and by intron elements that repress splice site utilization. *EMBO J* 18:1939-52
44. Blencowe BJ. 2000. Exonic splicing enhancers: mechanism of action, diversity and role in human genetic diseases. *Trends Biochem Sci* 25:106-10
45. Blouin CM, Hamon Y, Gonnord P, Boularan C, Kagan J, et al. 2016. Glycosylation-Dependent IFN-gammaR Partitioning in Lipid and Actin Nanodomains Is Critical for JAK Activation. *Cell* 166:920-34
46. Bomsel M. 1997. Transcytosis of infectious human immunodeficiency virus across a tight human epithelial cell line barrier. *Nat Med* 3:42-7
47. Booth JS, Toapanta FR, Salerno-Goncalves R, Patil S, Kader HA, et al. 2014. Characterization and functional properties of gastric tissue-resident memory T cells from children, adults, and the elderly. *Front Immunol* 5:294
48. Bos TJ, Nussbacher JK, Aigner S, Yeo GW. 2016. Tethered Function Assays as Tools to Elucidate the Molecular Roles of RNA-Binding Proteins. *Adv Exp Med Biol* 907:61-88
49. Bourgeois CF, Lejeune F, Stevenin J. 2004. Broad specificity of SR (serine/arginine) proteins in the regulation of alternative splicing of pre-messenger RNA. *Prog Nucleic Acid Res Mol Biol* 78:37-88
50. Bradford MM. 1976. A rapid and sensitive method for the quantitation of microgram quantities of protein utilizing the principle of protein-dye binding. *Anal Biochem* 72:248-54
51. Brass AL, Dykxhoorn DM, Benita Y, Yan N, Engelman A, et al. 2008. Identification of host proteins required for HIV infection through a functional genomic screen. *Science* 319:921-6
52. Brenchley JM, Douek DC. 2008. HIV infection and the gastrointestinal immune system. *Mucosal Immunol* 1:23-30
53. Briggs JA, Wilk T, Welker R, Krausslich HG, Fuller SD. 2003. Structural organization of authentic, mature HIV-1 virions and cores. *EMBO J* 22:1707-15
54. Brillen AL, Walotka L, Hillebrand F, Muller L, Widera M, et al. 2017. Analysis of Competing HIV-1 Splice Donor Sites Uncovers a Tight Cluster of Splicing Regulatory Elements within Exon 2/2b. *J Virol* 91

55. Briscoe J, Rogers NC, Witthuhn BA, Watling D, Harpur AG, et al. 1996. Kinase-negative mutants of JAK1 can sustain interferon-gamma-inducible gene expression but not an antiviral state. *EMBO J* 15:799-809
56. Brown PO, Bowerman B, Varmus HE, Bishop JM. 1989. Retroviral integration: structure of the initial covalent product and its precursor, and a role for the viral IN protein. *Proc Natl Acad Sci U S A* 86:2525-9
57. Burd CG, Dreyfuss G. 1994. Conserved structures and diversity of functions of RNA-binding proteins. *Science* 265:615-21
58. Burdick RC, Li C, Munshi M, Rawson JMO, Nagashima K, et al. 2020. HIV-1 uncoats in the nucleus near sites of integration. *Proc Natl Acad Sci U S A* 117:5486-93
59. Busch A, Hertel KJ. 2012. Evolution of SR protein and hnRNP splicing regulatory factors. *Wiley Interdiscip Rev RNA* 3:1-12
60. Bushman FD, Malani N, Fernandes J, D'Orso I, Cagney G, et al. 2009. Host cell factors in HIV replication: meta-analysis of genome-wide studies. *PLoS Pathog* 5:e1000437
61. Campos N, Myburgh R, Garcel A, Vautrin A, Lapasset L, et al. 2015. Long lasting control of viral rebound with a new drug ABX464 targeting Rev - mediated viral RNA biogenesis. *Retrovirology* 12:30
62. Cannell IG, Merrick KA, Morandell S, Zhu CQ, Braun CJ, et al. 2015. A Pleiotropic RNA-Binding Protein Controls Distinct Cell Cycle Checkpoints to Drive Resistance of p53-Defective Tumors to Chemotherapy. *Cancer Cell* 28:831
63. Caputi M, Freund M, Kammler S, Asang C, Schaal H. 2004. A bidirectional SF2/ASF- and SRp40-dependent splicing enhancer regulates human immunodeficiency virus type 1 rev, env, vpu, and nef gene expression. *J Virol* 78:6517-26
64. Caputi M, Mayeda A, Krainer AR, Zahler AM. 1999. hnRNP A/B proteins are required for inhibition of HIV-1 pre-mRNA splicing. *EMBO J* 18:4060-7
65. Carlin AF, Plummer EM, Vizcarra EA, Sheets N, Joo Y, et al. 2017. An IRF-3-, IRF-5-, and IRF-7-Independent Pathway of Dengue Viral Resistance Utilizes IRF-1 to Stimulate Type I and II Interferon Responses. *Cell Rep* 21:1600-12
66. Carrera C, Pinilla M, Perez-Alvarez L, Thomson MM. 2010. Identification of unusual and novel HIV type 1 spliced transcripts generated in vivo. *AIDS Res Hum Retroviruses* 26:815-20
67. Cartegni L, Chew SL, Krainer AR. 2002. Listening to silence and understanding nonsense: exonic mutations that affect splicing. *Nat Rev Genet* 3:285-98
68. Cartegni L, Maconi M, Morandi E, Cobianchi F, Riva S, Biamonti G. 1996. hnRNP A1 selectively interacts through its Gly-rich domain with different RNA-binding proteins. *J Mol Biol* 259:337-48
69. Cartegni L, Wang J, Zhu Z, Zhang MQ, Krainer AR. 2003. ESEfinder: A web resource to identify exonic splicing enhancers. *Nucleic Acids Res* 31:3568-71
70. Cavarelli M, Scarlatti G. 2014. HIV-1 infection: the role of the gastrointestinal tract. *Am J Reprod Immunol* 71:537-42
71. Chang B, Levin J, Thompson WA, Fairbrother WG. 2010. High-throughput binding analysis determines the binding specificity of ASF/SF2 on alternatively spliced human pre-mRNAs. *Comb Chem High Throughput Screen* 13:242-52
72. Chatterjee A, Rathore A, Vidyant S, Kakkar K, Dhole TN. 2012. Chemokines and chemokine receptors in susceptibility to HIV-1 infection and progression to AIDS. *Dis Markers* 32:143-51

73. Chatterjee D, Savarese TM. 1992. Posttranscriptional regulation of c-myc proto-oncogene expression and growth inhibition by recombinant human interferon-beta ser17 in a human colon carcinoma cell line. *Cancer Chemother Pharmacol* 30:12-20
74. Chen CY, Shyu AB. 1995. AU-rich elements: characterization and importance in mRNA degradation. *Trends Biochem Sci* 20:465-70
75. Chen H, Liu H, Qing G. 2018. Targeting oncogenic Myc as a strategy for cancer treatment. *Signal Transduct Target Ther* 3:5
76. Cho S, Hoang A, Sinha R, Zhong XY, Fu XD, et al. 2011. Interaction between the RNA binding domains of Ser-Arg splicing factor 1 and U1-70K snRNP protein determines early spliceosome assembly. *Proc Natl Acad Sci U S A* 108:8233-8
77. Chohan B, Lang D, Sagar M, Korber B, Lavreys L, et al. 2005. Selection for human immunodeficiency virus type 1 envelope glycosylation variants with shorter V1-V2 loop sequences occurs during transmission of certain genetic subtypes and may impact viral RNA levels. *J Virol* 79:6528-31
78. Choudhary C, Kumar C, Gnad F, Nielsen ML, Rehman M, et al. 2009. Lysine acetylation targets protein complexes and co-regulates major cellular functions. *Science* 325:834-40
79. Chun TW, Moir S, Fauci AS. 2015. HIV reservoirs as obstacles and opportunities for an HIV cure. *Nat Immunol* 16:584-9
80. Clapham PR, McKnight A. 2001. HIV-1 receptors and cell tropism. *Br Med Bull* 58:43-59
81. Clifford DB, Ances BM. 2013. HIV-associated neurocognitive disorder. *Lancet Infect Dis* 13:976-86
82. Close P, East P, Dirac-Svejstrup AB, Hartmann H, Heron M, et al. 2012. DBIRD complex integrates alternative mRNA splicing with RNA polymerase II transcript elongation. *Nature* 484:386-9
83. Collier J, Wickens M. 2007. Tethered function assays: an adaptable approach to study RNA regulatory proteins. *Methods Enzymol* 429:299-321
84. Colomer-Lluch M, Ruiz A, Moris A, Prado JG. 2018. Restriction Factors: From Intrinsic Viral Restriction to Shaping Cellular Immunity Against HIV-1. *Front Immunol* 9:2876
85. Colwill K, Pawson T, Andrews B, Prasad J, Manley JL, et al. 1996. The Clk/Sty protein kinase phosphorylates SR splicing factors and regulates their intranuclear distribution. *EMBO J* 15:265-75
86. Corbeil J, Sheeter D, Genini D, Rought S, Leoni L, et al. 2001. Temporal gene regulation during HIV-1 infection of human CD4+ T cells. *Genome Res* 11:1198-204
87. Crisler WJ, Lenz LL. 2018. Crosstalk between type I and II interferons in regulation of myeloid cell responses during bacterial infection. *Curr Opin Immunol* 54:35-41
88. Cull VS, Tilbrook PA, Bartlett EJ, Brekalo NL, James CM. 2003. Type I interferon differential therapy for erythroleukemia: specificity of STAT activation. *Blood* 101:2727-35
89. Cullen BR. 2003. Nuclear RNA export. *J Cell Sci* 116:587-97
90. Curlin ME, Zioni R, Hawes SE, Liu Y, Deng W, et al. 2010. HIV-1 envelope subregion length variation during disease progression. *PLoS Pathog* 6:e1001228



91. Czuby A, Girstun A, Kowalska-Loth B, Trzcinska AM, Purta E, et al. 2005. Proteomic analysis of complexes formed by human topoisomerase I. *Biochim Biophys Acta* 1749:133-41
92. Daily K, Patel VR, Rigor P, Xie X, Baldi P. 2011. MotifMap: integrative genome-wide maps of regulatory motif sites for model species. *BMC Bioinformatics* 12:495
93. Damgaard CK, Tange TO, Kjems J. 2002. hnRNP A1 controls HIV-1 mRNA splicing through cooperative binding to intron and exon splicing silencers in the context of a conserved secondary structure. *RNA* 8:1401-15
94. Damier L, Domenjoud L, Branlant C. 1997. The D1-A2 and D2-A2 pairs of splice sites from human immunodeficiency virus type 1 are highly efficient in vitro, in spite of an unusual branch site. *Biochem Biophys Res Commun* 237:182-7
95. Dani C, Mechti N, Piechaczyk M, Lebleu B, Jeanteur P, Blanchard JM. 1985. Increased rate of degradation of c-myc mRNA in interferon-treated Daudi cells. *Proc Natl Acad Sci U S A* 82:4896-9
96. Darnell JE, Jr., Kerr IM, Stark GR. 1994. Jak-STAT pathways and transcriptional activation in response to IFNs and other extracellular signaling proteins. *Science* 264:1415-21
97. Das AT, Harwig A, Berkhout B. 2011. The HIV-1 Tat protein has a versatile role in activating viral transcription. *J Virol* 85:9506-16
98. Das S, Anczukow O, Akerman M, Krainer AR. 2012. Oncogenic splicing factor SRSF1 is a critical transcriptional target of MYC. *Cell Rep* 1:110-7
99. Das S, Krainer AR. 2014. Emerging functions of SRSF1, splicing factor and oncoprotein, in RNA metabolism and cancer. *Mol Cancer Res* 12:1195-204
100. De Conti L, Baralle M, Buratti E. 2013. Exon and intron definition in pre-mRNA splicing. *Wiley Interdiscip Rev RNA* 4:49-60
101. de Veer MJ, Holko M, Frevel M, Walker E, Der S, et al. 2001. Functional classification of interferon-stimulated genes identified using microarrays. *J Leukoc Biol* 69:912-20
102. de Weerd NA, Samarajiva SA, Hertzog PJ. 2007. Type I interferon receptors: biochemistry and biological functions. *J Biol Chem* 282:20053-7
103. Decker T, Kovarik P, Meinke A. 1997. GAS elements: a few nucleotides with a major impact on cytokine-induced gene expression. *J Interferon Cytokine Res* 17:121-34
104. Deeks SG, Overbaugh J, Phillips A, Buchbinder S. 2015. HIV infection. *Nat Rev Dis Primers* 1:15035
105. Derdeyn CA, Decker JM, Bibollet-Ruche F, Mokili JL, Muldoon M, et al. 2004. Envelope-constrained neutralization-sensitive HIV-1 after heterosexual transmission. *Science* 303:2019-22
106. Desai SD, Haas AL, Wood LM, Tsai YC, Pestka S, et al. 2006. Elevated expression of ISG15 in tumor cells interferes with the ubiquitin/26S proteasome pathway. *Cancer Res* 66:921-8
107. Dey SS, Xue Y, Joachimiak MP, Friedland GD, Burnett JC, et al. 2012. Mutual information analysis reveals coevolving residues in Tat that compensate for two distinct functions in HIV-1 gene expression. *J Biol Chem* 287:7945-55
108. Dharan A, Bachmann N, Talley S, Zwickelmaier V, Campbell EM. 2020. Nuclear pore blockade reveals that HIV-1 completes reverse transcription and uncoating in the nucleus. *Nat Microbiol* 5:1088-95

109. Dillon SM, Guo K, Austin GL, Gianella S, Engen PA, et al. 2018. A compartmentalized type I interferon response in the gut during chronic HIV-1 infection is associated with immunopathogenesis. *AIDS* 32:1599-611
110. Diner BA, Lum KK, Javitt A, Cristea IM. 2015. Interactions of the Antiviral Factor Interferon Gamma-Inducible Protein 16 (IFI16) Mediate Immune Signaling and Herpes Simplex Virus-1 Immunosuppression. *Mol Cell Proteomics* 14:2341-56
111. Ding FS, C.; Kuo Chow, K-H.; Elowitz, MB. 2020. Dynamics and functional roles of splicing factor autoregulation. *bioRxiv*
112. Dlamini Z, Hull R. 2017. Can the HIV-1 splicing machinery be targeted for drug discovery? *HIV AIDS (Auckl)* 9:63-75
113. Dominguez C, Fiset JF, Chabot B, Allain FH. 2010. Structural basis of G-tract recognition and encaging by hnRNP F quasi-RRMs. *Nat Struct Mol Biol* 17:853-61
114. Domsic JK, Wang Y, Mayeda A, Krainer AR, Stoltzfus CM. 2003. Human immunodeficiency virus type 1 hnRNP A/B-dependent exonic splicing silencer ESSV antagonizes binding of U2AF65 to viral polypyrimidine tracts. *Mol Cell Biol* 23:8762-72
115. Doyle T, Goujon C, Malim MH. 2015. HIV-1 and interferons: who's interfering with whom? *Nat Rev Microbiol* 13:403-13
116. Dreyfuss G, Kim VN, Kataoka N. 2002. Messenger-RNA-binding proteins and the messages they carry. *Nat Rev Mol Cell Biol* 3:195-205
117. Dreyfuss G, Matunis MJ, Pinol-Roma S, Burd CG. 1993. hnRNP proteins and the biogenesis of mRNA. *Annu Rev Biochem* 62:289-321
118. Dulbecco R, Vogt M. 1953. Some problems of animal virology as studied by the plaque technique. *Cold Spring Harb Symp Quant Biol* 18:273-9
119. Dyhr-Mikkelsen H, Kjems J. 1995. Inefficient spliceosome assembly and abnormal branch site selection in splicing of an HIV-1 transcript in vitro. *J Biol Chem* 270:24060-6
120. Ealick SE, Cook WJ, Vijay-Kumar S, Carson M, Nagabhushan TL, et al. 1991. Three-dimensional structure of recombinant human interferon-gamma. *Science* 252:698-702
121. Easlick J, Szubin R, Lantz S, Baumgarth N, Abel K. 2010. The early interferon alpha subtype response in infant macaques infected orally with SIV. *J Acquir Immune Defic Syndr* 55:14-28
122. Einat M, Resnitzky D, Kimchi A. 1985. Close link between reduction of c-myc expression by interferon and, G0/G1 arrest. *Nature* 313:597-600
123. Elbashir SM, Harborth J, Lendeckel W, Yalcin A, Weber K, Tuschl T. 2001. Duplexes of 21-nucleotide RNAs mediate RNA interference in cultured mammalian cells. *Nature* 411:494-8
124. Emerman M. 2006. How TRIM5alpha defends against retroviral invasions. *Proc Natl Acad Sci U S A* 103:5249-50
125. Engelman A, Cherepanov P. 2012. The structural biology of HIV-1: mechanistic and therapeutic insights. *Nat Rev Microbiol* 10:279-90
126. Erkelenz S, Hillebrand F, Widera M, Theiss S, Fayyaz A, et al. 2015. Balanced splicing at the Tat-specific HIV-1 3' splice site A3 is critical for HIV-1 replication. *Retrovirology* 12:29
127. Erkelenz S, Mueller WF, Evans MS, Busch A, Schoneweis K, et al. 2013. Position-dependent splicing activation and repression by SR and hnRNP proteins rely on common mechanisms. *RNA* 19:96-102

128. Erkelenz S, Poschmann G, Theiss S, Stefanski A, Hillebrand F, et al. 2013. Tra2-mediated recognition of HIV-1 5' splice site D3 as a key factor in the processing of vpr mRNA. *J Virol* 87:2721-34
129. Erkelenz S, Theiss S, Otte M, Widera M, Peter JO, Schaal H. 2014. Genomic HEXploring allows landscaping of novel potential splicing regulatory elements. *Nucleic Acids Res* 42:10681-97
130. Ertel A, Verghese A, Byers SW, Ochs M, Tozeren A. 2006. Pathway-specific differences between tumor cell lines and normal and tumor tissue cells. *Mol Cancer* 5:55
131. Exline CM, Feng Z, Stoltzfus CM. 2008. Negative and positive mRNA splicing elements act competitively to regulate human immunodeficiency virus type 1 vif gene expression. *J Virol* 82:3921-31
132. Fabryova H, Strebel K. 2019. Vpr and Its Cellular Interaction Partners: R We There Yet? *Cells* 8
133. Fassati A, Goff SP. 2001. Characterization of intracellular reverse transcription complexes of human immunodeficiency virus type 1. *J Virol* 75:3626-35
134. Feng H, Zhang YB, Gui JF, Lemon SM, Yamane D. 2021. Interferon regulatory factor 1 (IRF1) and anti-pathogen innate immune responses. *PLoS Pathog* 17:e1009220
135. Fenton-May AE, Dibben O, Emmerich T, Ding H, Pfafferott K, et al. 2013. Relative resistance of HIV-1 founder viruses to control by interferon-alpha. *Retrovirology* 10:146
136. Ferguson MR, Rojo DR, von Lindern JJ, O'Brien WA. 2002. HIV-1 replication cycle. *Clin Lab Med* 22:611-35
137. Fernandez PC, Frank SR, Wang L, Schroeder M, Liu S, et al. 2003. Genomic targets of the human c-Myc protein. *Genes Dev* 17:1115-29
138. Fiebig EW, Wright DJ, Rawal BD, Garrett PE, Schumacher RT, et al. 2003. Dynamics of HIV viremia and antibody seroconversion in plasma donors: implications for diagnosis and staging of primary HIV infection. *AIDS* 17:1871-9
139. Fleming SC, Kapembwa MS, MacDonald TT, Griffin GE. 1992. Direct in vitro infection of human intestine with HIV-1. *AIDS* 6:1099-104
140. Fonteneau JF, Larsson M, Beignon AS, McKenna K, Dasilva I, et al. 2004. Human immunodeficiency virus type 1 activates plasmacytoid dendritic cells and concomitantly induces the bystander maturation of myeloid dendritic cells. *J Virol* 78:5223-32
141. Forlani G, Shallak M, Ramia E, Tedeschi A, Accolla RS. 2019. Restriction factors in human retrovirus infections and the unprecedented case of CIITA as link of intrinsic and adaptive immunity against HTLV-1. *Retrovirology* 16:34
142. Forsbach A, Nemorin JG, Montino C, Muller C, Samulowitz U, et al. 2008. Identification of RNA sequence motifs stimulating sequence-specific TLR8-dependent immune responses. *J Immunol* 180:3729-38
143. Foster GR. 2010. Pegylated interferons for the treatment of chronic hepatitis C: pharmacological and clinical differences between peginterferon-alpha-2a and peginterferon-alpha-2b. *Drugs* 70:147-65
144. Francis AC, Melikyan GB. 2018. Single HIV-1 Imaging Reveals Progression of Infection through CA-Dependent Steps of Docking at the Nuclear Pore, Uncoating, and Nuclear Transport. *Cell Host Microbe* 23:536-48 e6
145. Frankel AD, Young JA. 1998. HIV-1: fifteen proteins and an RNA. *Annu Rev Biochem* 67:1-25

146. Freed EO. 2001. HIV-1 replication. *Somat Cell Mol Genet* 26:13-33
147. Freed EO. 2015. HIV-1 assembly, release and maturation. *Nat Rev Microbiol* 13:484-96
148. Freed EO, Englund G, Martin MA. 1995. Role of the basic domain of human immunodeficiency virus type 1 matrix in macrophage infection. *J Virol* 69:3949-54
149. Fregoso OI, Ahn J, Wang C, Mehrens J, Skowronski J, Emerman M. 2013. Evolutionary toggling of Vpx/Vpr specificity results in divergent recognition of the restriction factor SAMHD1. *PLoS Pathog* 9:e1003496
150. Fregoso OI, Das S, Akerman M, Krainer AR. 2013. Splicing-factor oncoprotein SRSF1 stabilizes p53 via RPL5 and induces cellular senescence. *Mol Cell* 50:56-66
151. Freund M, Asang C, Kammler S, Konermann C, Krummheuer J, et al. 2003. A novel approach to describe a U1 snRNA binding site. *Nucleic Acids Res* 31:6963-75
152. Fu XD. 1995. The superfamily of arginine/serine-rich splicing factors. *RNA* 1:663-80
153. Fu XD, Ares M, Jr. 2014. Context-dependent control of alternative splicing by RNA-binding proteins. *Nat Rev Genet* 15:689-701
154. Fu XD, Maniatis T. 1992. The 35-kDa mammalian splicing factor SC35 mediates specific interactions between U1 and U2 small nuclear ribonucleoprotein particles at the 3' splice site. *Proc Natl Acad Sci U S A* 89:1725-9
155. Gabay M, Li Y, Felsher DW. 2014. MYC activation is a hallmark of cancer initiation and maintenance. *Cold Spring Harb Perspect Med* 4
156. Gallo RC, Salahuddin SZ, Popovic M, Shearer GM, Kaplan M, et al. 1984. Frequent detection and isolation of cytopathic retroviruses (HTLV-III) from patients with AIDS and at risk for AIDS. *Science* 224:500-3
157. Gao D, Wu J, Wu YT, Du F, Aroh C, et al. 2013. Cyclic GMP-AMP synthase is an innate immune sensor of HIV and other retroviruses. *Science* 341:903-6
158. Gao F, Chen Y, Levy DN, Conway JA, Kepler TB, Hui H. 2004. Unselected mutations in the human immunodeficiency virus type 1 genome are mostly nonsynonymous and often deleterious. *J Virol* 78:2426-33
159. Garibaldi A, Carranza F, Hertel KJ. 2017. Isolation of Newly Transcribed RNA Using the Metabolic Label 4-Thiouridine. *Methods Mol Biol* 1648:169-76
160. Ge H, Manley JL. 1990. A protein factor, ASF, controls cell-specific alternative splicing of SV40 early pre-mRNA in vitro. *Cell* 62:25-34
161. Gelderblom HR, Ozel M, Pauli G. 1989. Morphogenesis and morphology of HIV. Structure-function relations. *Arch Virol* 106:1-13
162. Geuens T, Bouhy D, Timmerman V. 2016. The hnRNP family: insights into their role in health and disease. *Hum Genet* 135:851-67
163. Ghimire D, Rai M, Gaur R. 2018. Novel host restriction factors implicated in HIV-1 replication. *J Gen Virol* 99:435-46
164. Gibbert K, Dittmer U. 2011. Distinct antiviral activities of IFN-alpha subtypes. *Immunotherapy* 3:813-6
165. Gibbert K, Schlaak JF, Yang D, Dittmer U. 2013. IFN-alpha subtypes: distinct biological activities in anti-viral therapy. *Br J Pharmacol* 168:1048-58
166. Gill N, Chenoweth MJ, Verdu EF, Ashkar AA. 2011. NK cells require type I IFN receptor for antiviral responses during genital HSV-2 infection. *Cell Immunol* 269:29-37

167. Gnanakaran S, Bhattacharya T, Daniels M, Keele BF, Hraber PT, et al. 2011. Recurrent signature patterns in HIV-1 B clade envelope glycoproteins associated with either early or chronic infections. *PLoS Pathog* 7:e1002209
168. Goll R, Husebekk A, Isaksen V, Kauric G, Hansen T, Florholmen J. 2005. Increased frequency of antral CD4 T and CD19 B cells in patients with Helicobacter pylori-related peptic ulcer disease. *Scand J Immunol* 61:92-7
169. Goncalves V, Jordan P. 2015. Posttranscriptional Regulation of Splicing Factor SRSF1 and Its Role in Cancer Cell Biology. *Biomed Res Int* 2015:287048
170. Goode T, O'Connell J, Ho WZ, O'Sullivan GC, Collins JK, et al. 2000. Differential expression of neurokinin-1 receptor by human mucosal and peripheral lymphoid cells. *Clin Diagn Lab Immunol* 7:371-6
171. Goren A, Ram O, Amit M, Keren H, Lev-Maor G, et al. 2006. Comparative analysis identifies exonic splicing regulatory sequences--The complex definition of enhancers and silencers. *Mol Cell* 22:769-81
172. Gorlach M, Burd CG, Portman DS, Dreyfuss G. 1993. The hnRNP proteins. *Mol Biol Rep* 18:73-8
173. Gorlach M, Wittekind M, Beckman RA, Mueller L, Dreyfuss G. 1992. Interaction of the RNA-binding domain of the hnRNP C proteins with RNA. *EMBO J* 11:3289-95
174. Gough DJ, Messina NL, Hii L, Gould JA, Sabapathy K, et al. 2010. Functional crosstalk between type I and II interferon through the regulated expression of STAT1. *PLoS Biol* 8:e1000361
175. Goujon C, Moncorge O, Bauby H, Doyle T, Ward CC, et al. 2013. Human MX2 is an interferon-induced post-entry inhibitor of HIV-1 infection. *Nature* 502:559-62
176. Gowda SD, Stein BS, Mohaghehpour N, Benike CJ, Engleman EG. 1989. Evidence that T cell activation is required for HIV-1 entry in CD4+ lymphocytes. *J Immunol* 142:773-80
177. Graveley BR. 2000. Sorting out the complexity of SR protein functions. *RNA* 6:1197-211
178. Green DS, Young HA, Valencia JC. 2017. Current prospects of type II interferon gamma signaling and autoimmunity. *J Biol Chem* 292:13925-33
179. Greenlund AC, Morales MO, Viviano BL, Yan H, Krolewski J, Schreiber RD. 1995. Stat recruitment by tyrosine-phosphorylated cytokine receptors: an ordered reversible affinity-driven process. *Immunity* 2:677-87
180. Gruber AR, Fallmann J, Kratochvill F, Kovarik P, Hofacker IL. 2011. AREsite: a database for the comprehensive investigation of AU-rich elements. *Nucleic Acids Res* 39:D66-9
181. Gui JF, Lane WS, Fu XD. 1994. A serine kinase regulates intracellular localization of splicing factors in the cell cycle. *Nature* 369:678-82
182. Hallay H, Locker N, Ayadi L, Ropers D, Guittet E, Branlant C. 2006. Biochemical and NMR study on the competition between proteins SC35, SRp40, and heterogeneous nuclear ribonucleoprotein A1 at the HIV-1 Tat exon 2 splicing site. *J Biol Chem* 281:37159-74
183. Hamilton BJ, Burns CM, Nichols RC, Rigby WF. 1997. Modulation of AUUUA response element binding by heterogeneous nuclear ribonucleoprotein A1 in human T lymphocytes. The roles of cytoplasmic location, transcription, and phosphorylation. *J Biol Chem* 272:28732-41
184. Hammond SM, Caudy AA, Hannon GJ. 2001. Post-transcriptional gene silencing by double-stranded RNA. *Nat Rev Genet* 2:110-9

185. Han SP, Tang YH, Smith R. 2010. Functional diversity of the hnRNPs: past, present and perspectives. *Biochem J* 430:379-92
186. Hardy MP, Owczarek CM, Jermini LS, Ejdeback M, Hertzog PJ. 2004. Characterization of the type I interferon locus and identification of novel genes. *Genomics* 84:331-45
187. Harper MS, Guo K, Gibbert K, Lee EJ, Dillon SM, et al. 2015. Interferon-alpha Subtypes in an Ex Vivo Model of Acute HIV-1 Infection: Expression, Potency and Effector Mechanisms. *PLoS Pathog* 11:e1005254
188. Harris RS, Hultquist JF, Evans DT. 2012. The restriction factors of human immunodeficiency virus. *J Biol Chem* 287:40875-83
189. Havugimana PC, Hart GT, Nepusz T, Yang H, Turinsky AL, et al. 2012. A census of human soluble protein complexes. *Cell* 150:1068-81
190. Hegele A, Kamburov A, Grossmann A, Sourlis C, Wowro S, et al. 2012. Dynamic protein-protein interaction wiring of the human spliceosome. *Mol Cell* 45:567-80
191. Heil F, Hemmi H, Hochrein H, Ampenberger F, Kirschning C, et al. 2004. Species-specific recognition of single-stranded RNA via toll-like receptor 7 and 8. *Science* 303:1526-9
192. Hein MY, Hubner NC, Poser I, Cox J, Nagaraj N, et al. 2015. A human interactome in three quantitative dimensions organized by stoichiometries and abundances. *Cell* 163:712-23
193. Hervas-Stubbs S, Perez-Gracia JL, Rouzaut A, Sanmamed MF, Le Bon A, Melero I. 2011. Direct effects of type I interferons on cells of the immune system. *Clin Cancer Res* 17:2619-27
194. Hicks MJ, Mueller WF, Shepard PJ, Hertel KJ. 2010. Competing upstream 5' splice sites enhance the rate of proximal splicing. *Mol Cell Biol* 30:1878-86
195. Hilditch L, Towers GJ. 2014. A model for cofactor use during HIV-1 reverse transcription and nuclear entry. *Curr Opin Virol* 4:32-6
196. Hillebrand F, Peter JO, Brillen AL, Otte M, Schaal H, Erkelenz S. 2017. Differential hnRNP D isoform incorporation may confer plasticity to the ESSV-mediated repressive state across HIV-1 exon 3. *Biochim Biophys Acta Gene Regul Mech* 1860:205-17
197. Hladik F, McElrath MJ. 2008. Setting the stage: host invasion by HIV. *Nat Rev Immunol* 8:447-57
198. Hong X, Scofield DG, Lynch M. 2006. Intron size, abundance, and distribution within untranslated regions of genes. *Mol Biol Evol* 23:2392-404
199. Hotter D, Bosso M, Jonsson KL, Krapp C, Sturzel CM, et al. 2019. IFI16 Targets the Transcription Factor Sp1 to Suppress HIV-1 Transcription and Latency Reactivation. *Cell Host Microbe* 25:858-72 e13
200. Hrecka K, Hao C, Gierszewska M, Swanson SK, Kesik-Brodacka M, et al. 2011. Vpx relieves inhibition of HIV-1 infection of macrophages mediated by the SAMHD1 protein. *Nature* 474:658-61
201. Hu WS, Hughes SH. 2012. HIV-1 reverse transcription. *Cold Spring Harb Perspect Med* 2
202. Huang Y, Gattoni R, Stevenin J, Steitz JA. 2003. SR splicing factors serve as adapter proteins for TAP-dependent mRNA export. *Mol Cell* 11:837-43
203. Huang Y, Steitz JA. 2001. Splicing factors SRp20 and 9G8 promote the nucleocytoplasmic export of mRNA. *Mol Cell* 7:899-905
204. Huang Y, Steitz JA. 2005. SRprizes along a messenger's journey. *Mol Cell* 17:613-5

205. Huang Y, Yario TA, Steitz JA. 2004. A molecular link between SR protein dephosphorylation and mRNA export. *Proc Natl Acad Sci U S A* 101:9666-70
206. Huang YQ, Ling XH, Yuan RQ, Chen ZY, Yang SB, et al. 2017. miR30c suppresses prostate cancer survival by targeting the ASF/SF2 splicing factor oncoprotein. *Mol Med Rep* 16:2431-8
207. Huelga SC, Vu AQ, Arnold JD, Liang TY, Liu PP, et al. 2012. Integrative genome-wide analysis reveals cooperative regulation of alternative splicing by hnRNP proteins. *Cell Rep* 1:167-78
208. Huttlin EL, Bruckner RJ, Paulo JA, Cannon JR, Ting L, et al. 2017. Architecture of the human interactome defines protein communities and disease networks. *Nature* 545:505-9
209. Ibrahim EC, Schaal TD, Hertel KJ, Reed R, Maniatis T. 2005. Serine/arginine-rich protein-dependent suppression of exon skipping by exonic splicing enhancers. *Proc Natl Acad Sci U S A* 102:5002-7
210. Igarashi K, Garotta G, Ozmen L, Ziemiecki A, Wilks AF, et al. 1994. Interferon-gamma induces tyrosine phosphorylation of interferon-gamma receptor and regulated association of protein tyrosine kinases, Jak1 and Jak2, with its receptor. *J Biol Chem* 269:14333-6
211. Iijima N, Mattei LM, Iwasaki A. 2011. Recruited inflammatory monocytes stimulate antiviral Th1 immunity in infected tissue. *Proc Natl Acad Sci U S A* 108:284-9
212. Imam H, Bano AS, Patel P, Holla P, Jameel S. 2015. The lncRNA NRON modulates HIV-1 replication in a NFAT-dependent manner and is differentially regulated by early and late viral proteins. *Sci Rep* 5:8639
213. Isaacs A, Lindenmann J. 1957. Virus interference. I. The interferon. *Proc R Soc Lond B Biol Sci* 147:258-67
214. Ivashkiv LB, Donlin LT. 2014. Regulation of type I interferon responses. *Nat Rev Immunol* 14:36-49
215. Iwabu Y, Fujita H, Kinomoto M, Kaneko K, Ishizaka Y, et al. 2009. HIV-1 accessory protein Vpu internalizes cell-surface BST-2/tetherin through transmembrane interactions leading to lysosomes. *J Biol Chem* 284:35060-72
216. Iwasaki A. 2012. A virological view of innate immune recognition. *Annu Rev Microbiol* 66:177-96
217. Iwasaki A, Medzhitov R. 2004. Toll-like receptor control of the adaptive immune responses. *Nat Immunol* 5:987-95
218. Iyer SS, Bibollet-Ruche F, Sherrill-Mix S, Learn GH, Plenderleith L, et al. 2017. Resistance to type 1 interferons is a major determinant of HIV-1 transmission fitness. *Proc Natl Acad Sci U S A* 114:E590-E9
219. Jablonski JA, Caputi M. 2009. Role of cellular RNA processing factors in human immunodeficiency virus type 1 mRNA metabolism, replication, and infectivity. *J Virol* 83:981-92
220. Jackson RJ, Hellen CU, Pestova TV. 2010. The mechanism of eukaryotic translation initiation and principles of its regulation. *Nat Rev Mol Cell Biol* 11:113-27
221. Jacquenet S, Decimo D, Muriaux D, Darlix JL. 2005. Dual effect of the SR proteins ASF/SF2, SC35 and 9G8 on HIV-1 RNA splicing and virion production. *Retrovirology* 2:33
222. Jakobsen MR, Mogensen TH, Paludan SR. 2013. Caught in translation: innate restriction of HIV mRNA translation by a schlafen family protein. *Cell Res* 23:320-2

- 
223. Jaks E, Gavutis M, Uze G, Martal J, Piehler J. 2007. Differential receptor subunit affinities of type I interferons govern differential signal activation. *J Mol Biol* 366:525-39
224. Jarry A, Cortez A, Rene E, Muzeau F, Brousse N. 1990. Infected cells and immune cells in the gastrointestinal tract of AIDS patients. An immunohistochemical study of 127 cases. *Histopathology* 16:133-40
225. Jean-Philippe J, Paz S, Caputi M. 2013. hnRNP A1: the Swiss army knife of gene expression. *Int J Mol Sci* 14:18999-9024
226. Jeeninga RE, Jan B, van den Berg H, Berkhout B. 2006. Construction of doxycycline-dependent mini-HIV-1 variants for the development of a virotherapy against leukemias. *Retrovirology* 3:64
227. Jensen KB, Dredge BK, Stefani G, Zhong R, Buckanovich RJ, et al. 2000. Nova-1 regulates neuron-specific alternative splicing and is essential for neuronal viability. *Neuron* 25:359-71
228. Jeong S. 2017. SR Proteins: Binders, Regulators, and Connectors of RNA. *Mol Cells* 40:1-9
229. Ji X, Zhou Y, Pandit S, Huang J, Li H, et al. 2013. SR proteins collaborate with 7SK and promoter-associated nascent RNA to release paused polymerase. *Cell* 153:855-68
230. Jiang L, Huang J, Higgs BW, Hu Z, Xiao Z, et al. 2016. Genomic Landscape Survey Identifies SRSF1 as a Key Oncodriver in Small Cell Lung Cancer. *PLoS Genet* 12:e1005895
231. Jiang Z, Wei F, Zhang Y, Wang T, Gao W, et al. 2021. IFI16 directly senses viral RNA and enhances RIG-I transcription and activation to restrict influenza virus infection. *Nat Microbiol* 6:932-45
232. Jones KA. 1997. Taking a new TAK on tat transactivation. *Genes Dev* 11:2593-9
233. Jones KA, Peterlin BM. 1994. Control of RNA initiation and elongation at the HIV-1 promoter. *Annu Rev Biochem* 63:717-43
234. Jordan A, Bisgrove D, Verdin E. 2003. HIV reproducibly establishes a latent infection after acute infection of T cells in vitro. *EMBO J* 22:1868-77
235. Joseph SB, Swanstrom R, Kashuba AD, Cohen MS. 2015. Bottlenecks in HIV-1 transmission: insights from the study of founder viruses. *Nat Rev Microbiol* 13:414-25
236. Kammler S, Leurs C, Freund M, Krummheuer J, Seidel K, et al. 2001. The sequence complementarity between HIV-1 5' splice site SD4 and U1 snRNA determines the steady-state level of an unstable env pre-mRNA. *RNA* 7:421-34
237. Kammler S, Otte M, Hauber I, Kjems J, Hauber J, Schaal H. 2006. The strength of the HIV-1 3' splice sites affects Rev function. *Retrovirology* 3:89
238. Kane M, Case LK, Wang C, Yurkovetskiy L, Dikiy S, Golovkina TV. 2011. Innate immune sensing of retroviral infection via Toll-like receptor 7 occurs upon viral entry. *Immunity* 35:135-45
239. Kane M, Yadav SS, Bitzegeio J, Kutluay SB, Zang T, et al. 2013. MX2 is an interferon-induced inhibitor of HIV-1 infection. *Nature* 502:563-6
240. Kannan N, Neuwald AF. 2004. Evolutionary constraints associated with functional specificity of the CMGC protein kinases MAPK, CDK, GSK, SRPK, DYRK, and CK2alpha. *Protein Sci* 13:2059-77
241. Kanopka A, Muhlemann O, Akusjarvi G. 1996. Inhibition by SR proteins of splicing of a regulated adenovirus pre-mRNA. *Nature* 381:535-8



242. Kärber G. 1931. Beitrag zur kollektiven Behandlung pharmakologischer Reihenversuche. *Naunyn-Schmiedebergs Archiv für experimentelle Pathologie und Pharmakologie* 162:480-3
243. Kariuki SM, Selhorst P, Arien KK, Dorfman JR. 2017. The HIV-1 transmission bottleneck. *Retrovirology* 14:22
244. Karn J, Stoltzfus CM. 2012. Transcriptional and posttranscriptional regulation of HIV-1 gene expression. *Cold Spring Harb Perspect Med* 2:a006916
245. Karni R, de Stanchina E, Lowe SW, Sinha R, Mu D, Krainer AR. 2007. The gene encoding the splicing factor SF2/ASF is a proto-oncogene. *Nat Struct Mol Biol* 14:185-93
246. Kato H, Takeuchi O, Mikamo-Satoh E, Hirai R, Kawai T, et al. 2008. Length-dependent recognition of double-stranded ribonucleic acids by retinoic acid-inducible gene-I and melanoma differentiation-associated gene 5. *J Exp Med* 205:1601-10
247. Katze MG, He Y, Gale M, Jr. 2002. Viruses and interferon: a fight for supremacy. *Nat Rev Immunol* 2:675-87
248. Kaul M, Garden GA, Lipton SA. 2001. Pathways to neuronal injury and apoptosis in HIV-associated dementia. *Nature* 410:988-94
249. Kawai T, Akira S. 2007. Signaling to NF-kappaB by Toll-like receptors. *Trends Mol Med* 13:460-9
250. Keele BF, Giorgi EE, Salazar-Gonzalez JF, Decker JM, Pham KT, et al. 2008. Identification and characterization of transmitted and early founder virus envelopes in primary HIV-1 infection. *Proc Natl Acad Sci U S A* 105:7552-7
251. Kelly JM, Gilbert CS, Stark GR, Kerr IM. 1985. Differential regulation of interferon-induced mRNAs and c-myc mRNA by alpha- and gamma-interferons. *Eur J Biochem* 153:367-71
252. Kiessling A, Hogrefe C, Erb S, Bobach C, Fuessel S, et al. 2009. Expression, regulation and function of the ISGylation system in prostate cancer. *Oncogene* 28:2606-20
253. Kim JH, Hahm B, Kim YK, Choi M, Jang SK. 2000. Protein-protein interaction among hnRNPs shuttling between nucleus and cytoplasm. *J Mol Biol* 298:395-405
254. Kim SY, Byrn R, Groopman J, Baltimore D. 1989. Temporal aspects of DNA and RNA synthesis during human immunodeficiency virus infection: evidence for differential gene expression. *J Virol* 63:3708-13
255. Kirchhoff F. 2010. Immune evasion and counteraction of restriction factors by HIV-1 and other primate lentiviruses. *Cell Host Microbe* 8:55-67
256. Kitamura A, Takahashi K, Okajima A, Kitamura N. 1994. Induction of the human gene for p44, a hepatitis-C-associated microtubular aggregate protein, by interferon-alpha/beta. *Eur J Biochem* 224:877-83
257. Klotman ME, Kim S, Buchbinder A, DeRossi A, Baltimore D, Wong-Staal F. 1991. Kinetics of expression of multiply spliced RNA in early human immunodeficiency virus type 1 infection of lymphocytes and monocytes. *Proc Natl Acad Sci U S A* 88:5011-5
258. Kogan M, Rappaport J. 2011. HIV-1 accessory protein Vpr: relevance in the pathogenesis of HIV and potential for therapeutic intervention. *Retrovirology* 8:25
259. Koizumi J, Okamoto Y, Onogi H, Mayeda A, Krainer AR, Hagiwara M. 1999. The subcellular localization of SF2/ASF is regulated by direct interaction with SR protein kinases (SRPKs). *J Biol Chem* 274:11125-31

260. Konig R, Zhou Y, Elleder D, Diamond TL, Bonamy GM, et al. 2008. Global analysis of host-pathogen interactions that regulate early-stage HIV-1 replication. *Cell* 135:49-60
261. Koning FA, Newman EN, Kim EY, Kunstman KJ, Wolinsky SM, Malim MH. 2009. Defining APOBEC3 expression patterns in human tissues and hematopoietic cell subsets. *J Virol* 83:9474-85
262. Konishi H, Fujiya M, Kashima S, Sakatani A, Dokoshi T, et al. 2020. A tumor-specific modulation of heterogeneous ribonucleoprotein A0 promotes excessive mitosis and growth in colorectal cancer cells. *Cell Death Dis* 11:245
263. Konopka K, Pretzer E, Plowman B, Duzgunes N. 1993. Long-term noncytopathic productive infection of the human monocytic leukemia cell line THP-1 by human immunodeficiency virus type 1 (HIV-1IIIB). *Virology* 193:877-87
264. Kotenko SV, Durbin JE. 2017. Contribution of type III interferons to antiviral immunity: location, location, location. *J Biol Chem* 292:7295-303
265. Kowarz E, Loscher D, Marschalek R. 2015. Optimized Sleeping Beauty transposons rapidly generate stable transgenic cell lines. *Biotechnol J* 10:647-53
266. Krainer AR, Conway GC, Kozak D. 1990. The essential pre-mRNA splicing factor SF2 influences 5' splice site selection by activating proximal sites. *Cell* 62:35-42
267. Krecic AM, Swanson MS. 1999. hnRNP complexes: composition, structure, and function. *Curr Opin Cell Biol* 11:363-71
268. Kruize Z, Kootstra NA. 2019. The Role of Macrophages in HIV-1 Persistence and Pathogenesis. *Front Microbiol* 10:2828
269. Krummheuer J, Johnson AT, Hauber I, Kammler S, Anderson JL, et al. 2007. A minimal uORF within the HIV-1 vpu leader allows efficient translation initiation at the downstream env AUG. *Virology* 363:261-71
270. Krummheuer J, Lenz C, Kammler S, Scheid A, Schaal H. 2001. Influence of the small leader exons 2 and 3 on human immunodeficiency virus type 1 gene expression. *Virology* 286:276-89
271. Kumar H, Kawai T, Akira S. 2011. Pathogen recognition by the innate immune system. *Int Rev Immunol* 30:16-34
272. Laemmli UK. 1970. Cleavage of structural proteins during the assembly of the head of bacteriophage T4. *Nature* 227:680-5
273. Laguette N, Sobhian B, Casartelli N, Ringeard M, Chable-Bessia C, et al. 2011. SAMHD1 is the dendritic- and myeloid-cell-specific HIV-1 restriction factor counteracted by Vpx. *Nature* 474:654-7
274. Lahouassa H, Daddacha W, Hofmann H, Ayinde D, Logue EC, et al. 2012. SAMHD1 restricts the replication of human immunodeficiency virus type 1 by depleting the intracellular pool of deoxynucleoside triphosphates. *Nat Immunol* 13:223-8
275. Landi A, Iannucci V, Nuffel AV, Meuwissen P, Verhasselt B. 2011. One protein to rule them all: modulation of cell surface receptors and molecules by HIV Nef. *Curr HIV Res* 9:496-504
276. Lapenta C, Boirivant M, Marini M, Santini SM, Logozzi M, et al. 1999. Human intestinal lamina propria lymphocytes are naturally permissive to HIV-1 infection. *Eur J Immunol* 29:1202-8
277. Lavender KJ, Gibbert K, Peterson KE, Van Dis E, Francois S, et al. 2016. Interferon Alpha Subtype-Specific Suppression of HIV-1 Infection In Vivo. *J Virol* 90:6001-13

278. Lavender KJ, Pace C, Sutter K, Messer RJ, Pouncey DL, et al. 2018. An advanced BLT-humanized mouse model for extended HIV-1 cure studies. *AIDS* 32:1-10
279. Lavoie TB, Kalie E, Crisafulli-Cabatu S, Abramovich R, DiGioia G, et al. 2011. Binding and activity of all human alpha interferon subtypes. *Cytokine* 56:282-9
280. Lazear HM, Schoggins JW, Diamond MS. 2019. Shared and Distinct Functions of Type I and Type III Interferons. *Immunity* 50:907-23
281. Leblanc J, Weil J, Beemon K. 2013. Posttranscriptional regulation of retroviral gene expression: primary RNA transcripts play three roles as pre-mRNA, mRNA, and genomic RNA. *Wiley Interdiscip Rev RNA* 4:567-80
282. Lee AJ, Ashkar AA. 2018. The Dual Nature of Type I and Type II Interferons. *Front Immunol* 9:2061
283. Lee AJ, Chen B, Chew MV, Barra NG, Shenouda MM, et al. 2017. Inflammatory monocytes require type I interferon receptor signaling to activate NK cells via IL-18 during a mucosal viral infection. *J Exp Med* 214:1153-67
284. Lee WJ, Fu RM, Liang C, Sloan RD. 2018. IFITM proteins inhibit HIV-1 protein synthesis. *Sci Rep* 8:14551
285. Li B, Decker JM, Johnson RW, Bibollet-Ruche F, Wei X, et al. 2006. Evidence for potent autologous neutralizing antibody titers and compact envelopes in early infection with subtype C human immunodeficiency virus type 1. *J Virol* 80:5211-8
286. Li M, Kao E, Gao X, Sandig H, Limmer K, et al. 2012. Codon-usage-based inhibition of HIV protein synthesis by human schlafen 11. *Nature* 491:125-8
287. Li SF, Gong MJ, Zhao FR, Shao JJ, Xie YL, et al. 2018. Type I Interferons: Distinct Biological Activities and Current Applications for Viral Infection. *Cell Physiol Biochem* 51:2377-96
288. Li X, Manley JL. 2005. Inactivation of the SR protein splicing factor ASF/SF2 results in genomic instability. *Cell* 122:365-78
289. Li X, Wang J, Manley JL. 2005. Loss of splicing factor ASF/SF2 induces G2 cell cycle arrest and apoptosis, but inhibits internucleosomal DNA fragmentation. *Genes Dev* 19:2705-14
290. Li Y, Sun B, Esser S, Jessen H, Streeck H, et al. 2017. Expression Pattern of Individual IFNA Subtypes in Chronic HIV Infection. *J Interferon Cytokine Res* 37:541-9
291. Liang S, Wei H, Sun R, Tian Z. 2003. IFNalpha regulates NK cell cytotoxicity through STAT1 pathway. *Cytokine* 23:190-9
292. Lim ES, Fregoso OI, McCoy CO, Matsen FA, Malik HS, Emerman M. 2012. The ability of primate lentiviruses to degrade the monocyte restriction factor SAMHD1 preceded the birth of the viral accessory protein Vpx. *Cell Host Microbe* 11:194-204
293. Lin H, Zhang Z, Zhang H, Yan P, Wang Q, Bai L. 2009. Primary culture of human blood-retinal barrier cells and preliminary study of APOBEC3 expression: an in vitro study. *Invest Ophthalmol Vis Sci* 50:4436-43
294. Lin S, Fu XD. 2007. SR proteins and related factors in alternative splicing. *Adv Exp Med Biol* 623:107-22
295. Little SJ, Holte S, Routy JP, Daar ES, Markowitz M, et al. 2002. Antiretroviral-drug resistance among patients recently infected with HIV. *N Engl J Med* 347:385-94
296. Liu Q, Dreyfuss G. 1995. In vivo and in vitro arginine methylation of RNA-binding proteins. *Mol Cell Biol* 15:2800-8

297. Liu SY, Sanchez DJ, Aliyari R, Lu S, Cheng G. 2012. Systematic identification of type I and type II interferon-induced antiviral factors. *Proc Natl Acad Sci U S A* 109:4239-44
298. Liu Y, Curlin ME, Diem K, Zhao H, Ghosh AK, et al. 2008. Env length and N-linked glycosylation following transmission of human immunodeficiency virus Type 1 subtype B viruses. *Virology* 374:229-33
299. Loomis RJ, Naoe Y, Parker JB, Savic V, Bozovsky MR, et al. 2009. Chromatin binding of SRp20 and ASF/SF2 and dissociation from mitotic chromosomes is modulated by histone H3 serine 10 phosphorylation. *Mol Cell* 33:450-61
300. Lourenco L, Colley G, Nosyk B, Shopin D, Montaner JS, et al. 2014. High levels of heterogeneity in the HIV cascade of care across different population subgroups in British Columbia, Canada. *PLoS One* 9:e115277
301. Lu J, Pan Q, Rong L, He W, Liu SL, Liang C. 2011. The IFITM proteins inhibit HIV-1 infection. *J Virol* 85:2126-37
302. Lubow J, Collins KL. 2020. Vpr Is a VIP: HIV Vpr and Infected Macrophages Promote Viral Pathogenesis. *Viruses* 12
303. Luck K, Kim DK, Lambourne L, Spirohn K, Begg BE, et al. 2020. A reference map of the human binary protein interactome. *Nature* 580:402-8
304. Lund JM, Alexopoulou L, Sato A, Karow M, Adams NC, et al. 2004. Recognition of single-stranded RNA viruses by Toll-like receptor 7. *Proc Natl Acad Sci U S A* 101:5598-603
305. Luscher B, Larsson LG. 1999. The basic region/helix-loop-helix/leucine zipper domain of Myc proto-oncoproteins: function and regulation. *Oncogene* 18:2955-66
306. Madsen JM, Stoltzfus CM. 2005. An exonic splicing silencer downstream of the 3' splice site A2 is required for efficient human immunodeficiency virus type 1 replication. *J Virol* 79:10478-86
307. Malim MH, Bieniasz PD. 2012. HIV Restriction Factors and Mechanisms of Evasion. *Cold Spring Harb Perspect Med* 2:a006940
308. Malim MH, Cullen BR. 1991. HIV-1 structural gene expression requires the binding of multiple Rev monomers to the viral RRE: implications for HIV-1 latency. *Cell* 65:241-8
309. Mamede JI, Cianci GC, Anderson MR, Hope TJ. 2017. Early cytoplasmic uncoating is associated with infectivity of HIV-1. *Proc Natl Acad Sci U S A* 114:E7169-E78
310. Mandal D, Feng Z, Stoltzfus CM. 2010. Excessive RNA splicing and inhibition of HIV-1 replication induced by modified U1 small nuclear RNAs. *J Virol* 84:12790-800
311. Manley JL, Krainer AR. 2010. A rational nomenclature for serine/arginine-rich protein splicing factors (SR proteins). *Genes Dev* 24:1073-4
312. Manley JL, Tacke R. 1996. SR proteins and splicing control. *Genes Dev* 10:1569-79
313. Mansky LM, Temin HM. 1995. Lower in vivo mutation rate of human immunodeficiency virus type 1 than that predicted from the fidelity of purified reverse transcriptase. *J Virol* 69:5087-94
314. Mao DY, Watson JD, Yan PS, Baryshte-Lovejoy D, Khosravi F, et al. 2003. Analysis of Myc bound loci identified by CpG island arrays shows that Max is essential for Myc-dependent repression. *Curr Biol* 13:882-6

315. Martinez-Contreras R, Cloutier P, Shkreta L, Fiset JF, Revil T, Chabot B. 2007. hnRNP proteins and splicing control. *Adv Exp Med Biol* 623:123-47
316. Massanella M, Singhania A, Beliakova-Bethell N, Pier R, Lada SM, et al. 2013. Differential gene expression in HIV-infected individuals following ART. *Antiviral Res* 100:420-8
317. Matera AG, Wang Z. 2014. A day in the life of the spliceosome. *Nat Rev Mol Cell Biol* 15:108-21
318. Matlin AJ, Clark F, Smith CW. 2005. Understanding alternative splicing: towards a cellular code. *Nat Rev Mol Cell Biol* 6:386-98
319. Mattei S, Glass B, Hagen WJ, Krausslich HG, Briggs JA. 2016. The structure and flexibility of conical HIV-1 capsids determined within intact virions. *Science* 354:1434-7
320. Mbisa JL, Barr R, Thomas JA, Vandegraaff N, Dorweiler IJ, et al. 2007. Human immunodeficiency virus type 1 cDNAs produced in the presence of APOBEC3G exhibit defects in plus-strand DNA transfer and integration. *J Virol* 81:7099-110
321. Mbisa JL, Bu W, Pathak VK. 2010. APOBEC3F and APOBEC3G inhibit HIV-1 DNA integration by different mechanisms. *J Virol* 84:5250-9
322. McNab F, Mayer-Barber K, Sher A, Wack A, O'Garra A. 2015. Type I interferons in infectious disease. *Nat Rev Immunol* 15:87-103
323. Meager A, Visvalingam K, Dilger P, Bryan D, Wadhwa M. 2005. Biological activity of interleukins-28 and -29: comparison with type I interferons. *Cytokine* 31:109-18
324. Megger DA, Philipp J, Le-Trilling VTK, Sitek B, Trilling M. 2017. Deciphering of the Human Interferon-Regulated Proteome by Mass Spectrometry-Based Quantitative Analysis Reveals Extent and Dynamics of Protein Induction and Repression. *Front Immunol* 8:1139
325. Meier A, Alter G, Frahm N, Sidhu H, Li B, et al. 2007. MyD88-dependent immune activation mediated by human immunodeficiency virus type 1-encoded Toll-like receptor ligands. *J Virol* 81:8180-91
326. Meister G, Tuschl T. 2004. Mechanisms of gene silencing by double-stranded RNA. *Nature* 431:343-9
327. Meylan PR, Spina CA, Richman DD, Kornbluth RS. 1993. In vitro differentiation of monocytoid THP-1 cells affects their permissiveness for HIV strains: a model system for studying the cellular basis of HIV differential tropism. *Virology* 193:256-67
328. Michlewski G, Sanford JR, Caceres JF. 2008. The splicing factor SF2/ASF regulates translation initiation by enhancing phosphorylation of 4E-BP1. *Mol Cell* 30:179-89
329. Miller MD, Farnet CM, Bushman FD. 1997. Human immunodeficiency virus type 1 preintegration complexes: studies of organization and composition. *J Virol* 71:5382-90
330. Misteli T, Spector DL. 1996. Serine/threonine phosphatase 1 modulates the subnuclear distribution of pre-mRNA splicing factors. *Mol Biol Cell* 7:1559-72
331. Mitchell RS, Katsura C, Skasko MA, Fitzpatrick K, Lau D, et al. 2009. Vpu antagonizes BST-2-mediated restriction of HIV-1 release via beta-TrCP and endo-lysosomal trafficking. *PLoS Pathog* 5:e1000450
332. Miyauchi K, Kim Y, Latinovic O, Morozov V, Melikyan GB. 2009. HIV enters cells via endocytosis and dynamin-dependent fusion with endosomes. *Cell* 137:433-44
333. Mogensen TH. 2009. Pathogen recognition and inflammatory signaling in innate immune defenses. *Clin Microbiol Rev* 22:240-73, Table of Contents

334. Mohammadi P, Desfarges S, Bartha I, Joos B, Zangger N, et al. 2013. 24 hours in the life of HIV-1 in a T cell line. *PLoS Pathog* 9:e1003161
335. Moll HP, Maier T, Zommer A, Lavoie T, Brostjan C. 2011. The differential activity of interferon-alpha subtypes is consistent among distinct target genes and cell types. *Cytokine* 53:52-9
336. Morales DJ, Lenschow DJ. 2013. The antiviral activities of ISG15. *J Mol Biol* 425:4995-5008
337. Murali TM, Dyer MD, Badger D, Tyler BM, Katze MG. 2011. Network-based prediction and analysis of HIV dependency factors. *PLoS Comput Biol* 7:e1002164
338. Myer VE, Steitz JA. 1995. Isolation and characterization of a novel, low abundance hnRNP protein: A0. *RNA* 1:171-82
339. Nayler O, Stamm S, Ullrich A. 1997. Characterization and comparison of four serine- and arginine-rich (SR) protein kinases. *Biochem J* 326 ( Pt 3):693-700
340. Naylor SL, Sakaguchi AY, Shows TB, Law ML, Goeddel DV, Gray PW. 1983. Human immune interferon gene is located on chromosome 12. *J Exp Med* 157:1020-7
341. Neil SJ, Zang T, Bieniasz PD. 2008. Tetherin inhibits retrovirus release and is antagonized by HIV-1 Vpu. *Nature* 451:425-30
342. Nilsen TW, Graveley BR. 2010. Expansion of the eukaryotic proteome by alternative splicing. *Nature* 463:457-63
343. Novoyatleva T, Heinrich B, Tang Y, Benderska N, Butchbach ME, et al. 2008. Protein phosphatase 1 binds to the RNA recognition motif of several splicing factors and regulates alternative pre-mRNA processing. *Hum Mol Genet* 17:52-70
344. O'Hare MJ, Bond J, Clarke C, Takeuchi Y, Atherton AJ, et al. 2001. Conditional immortalization of freshly isolated human mammary fibroblasts and endothelial cells. *Proc Natl Acad Sci U S A* 98:646-51
345. Ocwieja KE, Sherrill-Mix S, Mukherjee R, Custers-Allen R, David P, et al. 2012. Dynamic regulation of HIV-1 mRNA populations analyzed by single-molecule enrichment and long-read sequencing. *Nucleic Acids Res* 40:10345-55
346. Okumura A, Lu G, Pitha-Rowe I, Pitha PM. 2006. Innate antiviral response targets HIV-1 release by the induction of ubiquitin-like protein ISG15. *Proc Natl Acad Sci U S A* 103:1440-5
347. Ott M, Geyer M, Zhou Q. 2011. The control of HIV transcription: keeping RNA polymerase II on track. *Cell Host Microbe* 10:426-35
348. Pace C, Keller J, Nolan D, James I, Gaudieri S, et al. 2006. Population level analysis of human immunodeficiency virus type 1 hypermutation and its relationship with APOBEC3G and vif genetic variation. *J Virol* 80:9259-69
349. Pan C, Kumar C, Bohl S, Klingmueller U, Mann M. 2009. Comparative proteomic phenotyping of cell lines and primary cells to assess preservation of cell type-specific functions. *Mol Cell Proteomics* 8:443-50
350. Pan Q, Shai O, Lee LJ, Frey BJ, Blencowe BJ. 2008. Deep surveying of alternative splicing complexity in the human transcriptome by high-throughput sequencing. *Nat Genet* 40:1413-5
351. Pandey S, Kawai T, Akira S. 2014. Microbial sensing by Toll-like receptors and intracellular nucleic acid sensors. *Cold Spring Harb Perspect Biol* 7:a016246
352. Park JH, Yang SW, Park JM, Ka SH, Kim JH, et al. 2016. Positive feedback regulation of p53 transactivity by DNA damage-induced ISG15 modification. *Nat Commun* 7:12513

353. Parrish NF, Gao F, Li H, Giorgi EE, Barbian HJ, et al. 2013. Phenotypic properties of transmitted founder HIV-1. *Proc Natl Acad Sci U S A* 110:6626-33
354. Pastor DM, Poritz LS, Olson TL, Kline CL, Harris LR, et al. 2010. Primary cell lines: false representation or model system? a comparison of four human colorectal tumors and their coordinately established cell lines. *Int J Clin Exp Med* 3:69-83
355. Paz S, Caputi M. 2015. SRSF1 inhibition of HIV-1 gene expression. *Oncotarget* 6:19362-3
356. Paz S, Krainer AR, Caputi M. 2014. HIV-1 transcription is regulated by splicing factor SRSF1. *Nucleic Acids Res* 42:13812-23
357. Paz S, Lu ML, Takata H, Trautmann L, Caputi M. 2015. SRSF1 RNA Recognition Motifs Are Strong Inhibitors of HIV-1 Replication. *J Virol* 89:6275-86
358. Pegram HJ, Andrews DM, Smyth MJ, Darcy PK, Kershaw MH. 2011. Activating and inhibitory receptors of natural killer cells. *Immunol Cell Biol* 89:216-24
359. Pennings PS. 2013. HIV Drug Resistance: Problems and Perspectives. *Infect Dis Rep* 5:e5
360. Pereyra F, Addo MM, Kaufmann DE, Liu Y, Miura T, et al. 2008. Genetic and immunologic heterogeneity among persons who control HIV infection in the absence of therapy. *J Infect Dis* 197:563-71
361. Perez-Caballero D, Zang T, Ebrahimi A, McNatt MW, Gregory DA, et al. 2009. Tetherin inhibits HIV-1 release by directly tethering virions to cells. *Cell* 139:499-511
362. Pestka S. 2007. The interferons: 50 years after their discovery, there is much more to learn. *J Biol Chem* 282:20047-51
363. Pestka S, Krause CD, Walter MR. 2004. Interferons, interferon-like cytokines, and their receptors. *Immunol Rev* 202:8-32
364. Pfaffl MW. 2001. A new mathematical model for relative quantification in real-time RT-PCR. *Nucleic Acids Res* 29:e45
365. Pincetic A, Kuang Z, Seo EJ, Leis J. 2010. The interferon-induced gene ISG15 blocks retrovirus release from cells late in the budding process. *J Virol* 84:4725-36
366. Pine R, Decker T, Kessler DS, Levy DE, Darnell JE, Jr. 1990. Purification and cloning of interferon-stimulated gene factor 2 (ISGF2): ISGF2 (IRF-1) can bind to the promoters of both beta interferon- and interferon-stimulated genes but is not a primary transcriptional activator of either. *Mol Cell Biol* 10:2448-57
367. Pinol-Roma S, Dreyfuss G. 1992. Shuttling of pre-mRNA binding proteins between nucleus and cytoplasm. *Nature* 355:730-2
368. Plataniias LC. 2005. Mechanisms of type-I- and type-II-interferon-mediated signalling. *Nat Rev Immunol* 5:375-86
369. Pollard VW, Malim MH. 1998. The HIV-1 Rev protein. *Annu Rev Microbiol* 52:491-532
370. Polzer S, Dittmar MT, Schmitz H, Schreiber M. 2002. The N-linked glycan g15 within the V3 loop of the HIV-1 external glycoprotein gp120 affects coreceptor usage, cellular tropism, and neutralization. *Virology* 304:70-80
371. Polzer S, van Yperen M, Kirst M, Schwalbe B, Schaal H, Schreiber M. 2010. Neutralization of X4- and R5-tropic HIV-1 NL4-3 variants by HOCl-modified serum albumins. *BMC Res Notes* 3:155

372. Popov S, Rexach M, Ratner L, Blobel G, Bukrinsky M. 1998. Viral protein R regulates docking of the HIV-1 preintegration complex to the nuclear pore complex. *J Biol Chem* 273:13347-52
373. Popp MW, Maquat LE. 2014. The dharmas of nonsense-mediated mRNA decay in mammalian cells. *Mol Cells* 37:1-8
374. Power D, Santoso N, Dieringer M, Yu J, Huang H, et al. 2015. IFI44 suppresses HIV-1 LTR promoter activity and facilitates its latency. *Virology* 481:142-50
375. Purcell DF, Martin MA. 1993. Alternative splicing of human immunodeficiency virus type 1 mRNA modulates viral protein expression, replication, and infectivity. *J Virol* 67:6365-78
376. Qing Y, Stark GR. 2004. Alternative activation of STAT1 and STAT3 in response to interferon-gamma. *J Biol Chem* 279:41679-85
377. Radle B, Rutkowski AJ, Ruzsics Z, Friedel CC, Koszinowski UH, Dolken L. 2013. Metabolic labeling of newly transcribed RNA for high resolution gene expression profiling of RNA synthesis, processing and decay in cell culture. *J Vis Exp*
378. Rahm N, Telenti A. 2012. The role of tripartite motif family members in mediating susceptibility to HIV-1 infection. *Curr Opin HIV AIDS* 7:180-6
379. Ramakrishnan MA. 2016. Determination of 50% endpoint titer using a simple formula. *World J Virol* 5:85-6
380. Rasaiyaah J, Tan CP, Fletcher AJ, Price AJ, Blondeau C, et al. 2013. HIV-1 evades innate immune recognition through specific cofactor recruitment. *Nature* 503:402-5
381. Rausell A, Munoz M, Martinez R, Roger T, Telenti A, Ciuffi A. 2016. Innate immune defects in HIV permissive cell lines. *Retrovirology* 13:43
382. Razzak M. 2012. Genetics: Schlafen 11 naturally blocks HIV. *Nat Rev Urol* 9:605
383. Refsland EW, Harris RS. 2013. The APOBEC3 family of retroelement restriction factors. *Curr Top Microbiol Immunol* 371:1-27
384. Refsland EW, Stenglein MD, Shindo K, Albin JS, Brown WL, Harris RS. 2010. Quantitative profiling of the full APOBEC3 mRNA repertoire in lymphocytes and tissues: implications for HIV-1 restriction. *Nucleic Acids Res* 38:4274-84
385. Robberson BL, Cote GJ, Berget SM. 1990. Exon definition may facilitate splice site selection in RNAs with multiple exons. *Mol Cell Biol* 10:84-94
386. Roebuck KA, Saifuddin M. 1999. Regulation of HIV-1 transcription. *Gene Expr* 8:67-84
387. Ropers D, Ayadi L, Gattoni R, Jacquenet S, Damier L, et al. 2004. Differential effects of the SR proteins 9G8, SC35, ASF/SF2, and SRp40 on the utilization of the A1 to A5 splicing sites of HIV-1 RNA. *J Biol Chem* 279:29963-73
388. Roth MB, Murphy C, Gall JG. 1990. A monoclonal antibody that recognizes a phosphorylated epitope stains lampbrush chromosome loops and small granules in the amphibian germinal vesicle. *J Cell Biol* 111:2217-23
389. Rousseau MN, Vergne L, Montes B, Peeters M, Reynes J, et al. 2001. Patterns of resistance mutations to antiretroviral drugs in extensively treated HIV-1-infected patients with failure of highly active antiretroviral therapy. *J Acquir Immune Defic Syndr* 26:36-43
390. Rousseau S, Morrice N, Peggie M, Campbell DG, Gaestel M, Cohen P. 2002. Inhibition of SAPK2a/p38 prevents hnRNP A0 phosphorylation by MAPKAP-K2 and its interaction with cytokine mRNAs. *EMBO J* 21:6505-14



391. Roy R, Durie D, Li H, Liu BQ, Skehel JM, et al. 2014. hnRNPA1 couples nuclear export and translation of specific mRNAs downstream of FGF-2/S6K2 signalling. *Nucleic Acids Res* 42:12483-97
392. Sadler AJ, Williams BR. 2008. Interferon-inducible antiviral effectors. *Nat Rev Immunol* 8:559-68
393. Samatanga B, Dominguez C, Jelesarov I, Allain FH. 2013. The high kinetic stability of a G-quadruplex limits hnRNP F qRRM3 binding to G-tract RNA. *Nucleic Acids Res* 41:2505-16
394. Samuel CE. 2001. Antiviral actions of interferons. *Clin Microbiol Rev* 14:778-809, table of contents
395. Sanford JR, Ellis JD, Cazalla D, Caceres JF. 2005. Reversible phosphorylation differentially affects nuclear and cytoplasmic functions of splicing factor 2/alternative splicing factor. *Proc Natl Acad Sci U S A* 102:15042-7
396. Sanford JR, Gray NK, Beckmann K, Caceres JF. 2004. A novel role for shuttling SR proteins in mRNA translation. *Genes Dev* 18:755-68
397. Sanford JR, Wang X, Mort M, Vanduy N, Cooper DN, et al. 2009. Splicing factor SFRS1 recognizes a functionally diverse landscape of RNA transcripts. *Genome Res* 19:381-94
398. Sapa AK, Anko ML, Grishina I, Lorenz M, Pabis M, et al. 2009. SR protein family members display diverse activities in the formation of nascent and mature mRNPs in vivo. *Mol Cell* 34:179-90
399. Satake H, Tamura K, Furihata M, Anchi T, Sakoda H, et al. 2010. The ubiquitin-like molecule interferon-stimulated gene 15 is overexpressed in human prostate cancer. *Oncol Rep* 23:11-6
400. Satoh Y, Ogawara H, Kawamura O, Kusano M, Murakami H. 2012. Clinical Significance of Peripheral Blood T Lymphocyte Subsets in Helicobacter pylori-Infected Patients. *Gastroenterol Res Pract* 2012:819842
401. Sattentau QJ, Stevenson M. 2016. Macrophages and HIV-1: An Unhealthy Constellation. *Cell Host Microbe* 19:304-10
402. Sauliere J, Murigneux V, Wang Z, Marquet E, Barbosa I, et al. 2012. CLIP-seq of eIF4AIII reveals transcriptome-wide mapping of the human exon junction complex. *Nat Struct Mol Biol* 19:1124-31
403. Schafer A, Bogerd HP, Cullen BR. 2004. Specific packaging of APOBEC3G into HIV-1 virions is mediated by the nucleocapsid domain of the gag polyprotein precursor. *Virology* 328:163-8
404. Schneider R, Campbell M, Nasioulas G, Felber BK, Pavlakis GN. 1997. Inactivation of the human immunodeficiency virus type 1 inhibitory elements allows Rev-independent expression of Gag and Gag/protease and particle formation. *J Virol* 71:4892-903
405. Schneider U, Schwenk HU, Bornkamm G. 1977. Characterization of EBV-genome negative "null" and "T" cell lines derived from children with acute lymphoblastic leukemia and leukemic transformed non-Hodgkin lymphoma. *Int J Cancer* 19:621-6
406. Schoggins JW, Wilson SJ, Panis M, Murphy MY, Jones CT, et al. 2011. A diverse range of gene products are effectors of the type I interferon antiviral response. *Nature* 472:481-5
407. Schroder K, Hertzog PJ, Ravasi T, Hume DA. 2004. Interferon-gamma: an overview of signals, mechanisms and functions. *J Leukoc Biol* 75:163-89

408. Schulze-Gahmen U, Hurley JH. 2018. Structural mechanism for HIV-1 TAR loop recognition by Tat and the super elongation complex. *Proc Natl Acad Sci U S A* 115:12973-8
409. Schwartz S, Felber BK, Benko DM, Fenyo EM, Pavlakis GN. 1990. Cloning and functional analysis of multiply spliced mRNA species of human immunodeficiency virus type 1. *J Virol* 64:2519-29
410. Sertznig H, Hillebrand F, Erkelenz S, Schaal H, Widera M. 2018. Behind the scenes of HIV-1 replication: Alternative splicing as the dependency factor on the quiet. *Virology* 516:176-88
411. Shattock RJ, Moore JP. 2003. Inhibiting sexual transmission of HIV-1 infection. *Nat Rev Microbiol* 1:25-34
412. Sheehy AM, Gaddis NC, Choi JD, Malim MH. 2002. Isolation of a human gene that inhibits HIV-1 infection and is suppressed by the viral Vif protein. *Nature* 418:646-50
413. Shen R, Richter HE, Smith PD. 2011. Early HIV-1 target cells in human vaginal and ectocervical mucosa. *Am J Reprod Immunol* 65:261-7
414. Shepard PJ, Hertel KJ. 2009. The SR protein family. *Genome Biol* 10:242
415. Sheth N, Roca X, Hastings ML, Roeder T, Krainer AR, Sachidanandam R. 2006. Comprehensive splice-site analysis using comparative genomics. *Nucleic Acids Res* 34:3955-67
416. Si Z, Amendt BA, Stoltzfus CM. 1997. Splicing efficiency of human immunodeficiency virus type 1 tat RNA is determined by both a suboptimal 3' splice site and a 10 nucleotide exon splicing silencer element located within tat exon 2. *Nucleic Acids Res* 25:861-7
417. Si ZH, Rauch D, Stoltzfus CM. 1998. The exon splicing silencer in human immunodeficiency virus type 1 Tat exon 3 is bipartite and acts early in spliceosome assembly. *Mol Cell Biol* 18:5404-13
418. Siebel CW, Guthrie C. 1996. The essential yeast RNA binding protein Np13p is methylated. *Proc Natl Acad Sci U S A* 93:13641-6
419. Siegal FP, Kadowaki N, Shodell M, Fitzgerald-Bocarsly PA, Shah K, et al. 1999. The nature of the principal type 1 interferon-producing cells in human blood. *Science* 284:1835-7
420. Silverman RH. 2007. Viral encounters with 2',5'-oligoadenylate synthetase and RNase L during the interferon antiviral response. *J Virol* 81:12720-9
421. Silvin A, Manel N. 2015. Innate immune sensing of HIV infection. *Curr Opin Immunol* 32:54-60
422. Simon V, Bloch N, Landau NR. 2015. Intrinsic host restrictions to HIV-1 and mechanisms of viral escape. *Nat Immunol* 16:546-53
423. Sinha R, Allemand E, Zhang Z, Karni R, Myers MP, Krainer AR. 2010. Arginine methylation controls the subcellular localization and functions of the oncoprotein splicing factor SF2/ASF. *Mol Cell Biol* 30:2762-74
424. Sleijfer S, Bannink M, Van Gool AR, Kruit WH, Stoter G. 2005. Side effects of interferon-alpha therapy. *Pharm World Sci* 27:423-31
425. Smart CJ, Trejdosiewicz LK, Badr-el-Din S, Heatley RV. 1988. T lymphocytes of the human colonic mucosa: functional and phenotypic analysis. *Clin Exp Immunol* 73:63-9
426. Smith CW, Chu TT, Nadal-Ginard B. 1993. Scanning and competition between AGs are involved in 3' splice site selection in mammalian introns. *Mol Cell Biol* 13:4939-52

427. Smith PD, Meng G, Sellers MT, Rogers TS, Shaw GM. 2000. Biological parameters of HIV-1 infection in primary intestinal lymphocytes and macrophages. *J Leukoc Biol* 68:360-5
428. Smythies LE, Sellers M, Clements RH, Mosteller-Barnum M, Meng G, et al. 2005. Human intestinal macrophages display profound inflammatory anergy despite avid phagocytic and bacteriocidal activity. *J Clin Invest* 115:66-75
429. Song JH, Wang CX, Song DK, Wang P, Shuaib A, Hao C. 2005. Interferon gamma induces neurite outgrowth by up-regulation of p35 neuron-specific cyclin-dependent kinase 5 activator via activation of ERK1/2 pathway. *J Biol Chem* 280:12896-901
430. Soret J, Bakkour N, Maire S, Durand S, Zekri L, et al. 2005. Selective modification of alternative splicing by indole derivatives that target serine-arginine-rich protein splicing factors. *Proc Natl Acad Sci U S A* 102:8764-9
431. Soret J, Gabut M, Tazi J. 2006. SR proteins as potential targets for therapy. *Prog Mol Subcell Biol* 44:65-87
432. Spearman C. 1908. The Method of 'Right and Wrong Cases' (Constant Stimuli) without Gauss's Formulae. *British Journal of Psychology* 2:227-42
433. Staffa A, Cochrane A. 1995. Identification of positive and negative splicing regulatory elements within the terminal tat-rev exon of human immunodeficiency virus type 1. *Mol Cell Biol* 15:4597-605
434. Stevenson M, Stanwick TL, Dempsey MP, Lamonica CA. 1990. HIV-1 replication is controlled at the level of T cell activation and proviral integration. *EMBO J* 9:1551-60
435. Stoltzfus CM. 2009. Chapter 1. Regulation of HIV-1 alternative RNA splicing and its role in virus replication. *Adv Virus Res* 74:1-40
436. Stopak K, de Noronha C, Yonemoto W, Greene WC. 2003. HIV-1 Vif blocks the antiviral activity of APOBEC3G by impairing both its translation and intracellular stability. *Mol Cell* 12:591-601
437. Strebel K. 2013. HIV accessory proteins versus host restriction factors. *Curr Opin Virol* 3:692-9
438. Suhasini M, Reddy TR. 2009. Cellular proteins and HIV-1 Rev function. *Curr HIV Res* 7:91-100
439. Sun S, Zhang Z, Sinha R, Karni R, Krainer AR. 2010. SF2/ASF autoregulation involves multiple layers of post-transcriptional and translational control. *Nat Struct Mol Biol* 17:306-12
440. Sutter K, Lavender KJ, Messer RJ, Widera M, Williams K, et al. 2019. Concurrent administration of IFNalpha14 and cART in TKO-BLT mice enhances suppression of HIV-1 viremia but does not eliminate the latent reservoir. *Sci Rep* 9:18089
441. Tacke R, Manley JL. 1995. The human splicing factors ASF/SF2 and SC35 possess distinct, functionally significant RNA binding specificities. *EMBO J* 14:3540-51
442. Takaoka A, Mitani Y, Suemori H, Sato M, Yokochi T, et al. 2000. Cross talk between interferon-gamma and -alpha/beta signaling components in caveolar membrane domains. *Science* 288:2357-60
443. Takaoka A, Yanai H. 2006. Interferon signalling network in innate defence. *Cell Microbiol* 8:907-22
444. Takeuchi O, Akira S. 2010. Pattern recognition receptors and inflammation. *Cell* 140:805-20

445. Tange TO, Damgaard CK, Guth S, Valcarcel J, Kjems J. 2001. The hnRNP A1 protein regulates HIV-1 tat splicing via a novel intron silencer element. *EMBO J* 20:5748-58
446. Tange TO, Kjems J. 2001. SF2/ASF binds to a splicing enhancer in the third HIV-1 tat exon and stimulates U2AF binding independently of the RS domain. *J Mol Biol* 312:649-62
447. Tauzin A, Espinosa Ortiz A, Blake O, Soundaramourty C, Joly-Beauparlant C, et al. 2021. Differential Inhibition of HIV Replication by the 12 Interferon Alpha Subtypes. *J Virol* 95:e0231120
448. Tazi J, Bakkour N, Marchand V, Ayadi L, Aboufirassi A, Branlant C. 2010. Alternative splicing: regulation of HIV-1 multiplication as a target for therapeutic action. *FEBS J* 277:867-76
449. Thompson MR, Kaminski JJ, Kurt-Jones EA, Fitzgerald KA. 2011. Pattern recognition receptors and the innate immune response to viral infection. *Viruses* 3:920-40
450. Tian M, Maniatis T. 1993. A splicing enhancer complex controls alternative splicing of doublesex pre-mRNA. *Cell* 74:105-14
451. Toccafondi E, Lener D, Negroni M. 2021. HIV-1 Capsid Core: A Bullet to the Heart of the Target Cell. *Front Microbiol* 12:652486
452. Tranell A, Tingsborg S, Fenyo EM, Schwartz S. 2011. Inhibition of splicing by serine-arginine rich protein 55 (SRp55) causes the appearance of partially spliced HIV-1 mRNAs in the cytoplasm. *Virus Res* 157:82-91
453. Trejdosiewicz LK, Badr-el-Din S, Smart CJ, Malizia G, Oakes DJ, et al. 1989. Colonic mucosal T lymphocytes in ulcerative colitis: expression of CD7 antigen in relation to MHC class II (HLA-D) antigens. *Dig Dis Sci* 34:1449-56
454. Trejdosiewicz LK, Smart CJ, Oakes DJ, Howdle PD, Malizia G, et al. 1989. Expression of T-cell receptors TcR1 (gamma/delta) and TcR2 (alpha/beta) in the human intestinal mucosa. *Immunology* 68:7-12
455. Trilling M, Bellora N, Rutkowski AJ, de Graaf M, Dickinson P, et al. 2013. Deciphering the modulation of gene expression by type I and II interferons combining 4sU-tagging, translational arrest and in silico promoter analysis. *Nucleic Acids Res* 41:8107-25
456. Tsuchiya S, Yamabe M, Yamaguchi Y, Kobayashi Y, Konno T, Tada K. 1980. Establishment and characterization of a human acute monocytic leukemia cell line (THP-1). *Int J Cancer* 26:171-6
457. Tsuruno C, Ohe K, Kuramitsu M, Kohma T, Takahama Y, et al. 2011. HMGA1a is involved in specific splice site regulation of human immunodeficiency virus type 1. *Biochem Biophys Res Commun* 406:512-7
458. Tuerk C, Eddy S, Parma D, Gold L. 1990. Autogenous translational operator recognized by bacteriophage T4 DNA polymerase. *J Mol Biol* 213:749-61
459. Tutucci E, Vera M, Biswas J, Garcia J, Parker R, Singer RH. 2018. An improved MS2 system for accurate reporting of the mRNA life cycle. *Nat Methods* 15:81-9
460. Uhlen M, Fagerberg L, Hallstrom BM, Lindskog C, Oksvold P, et al. 2015. Proteomics. Tissue-based map of the human proteome. *Science* 347:1260419
461. Ule J, Blencowe BJ. 2019. Alternative Splicing Regulatory Networks: Functions, Mechanisms, and Evolution. *Mol Cell* 76:329-45
462. UNAIDS UN. 2021. Global HIV & AIDS statistics - Fact sheet.
463. UniProt C. 2021. UniProt: the universal protein knowledgebase in 2021. *Nucleic Acids Res* 49:D480-D9

- 
464. Uren PJ, Bahrami-Samani E, de Araujo PR, Vogel C, Qiao M, et al. 2016. High-throughput analyses of hnRNP H1 dissects its multi-functional aspect. *RNA Biol* 13:400-11
  465. Usami Y, Wu Y, Gottlinger HG. 2015. SERINC3 and SERINC5 restrict HIV-1 infectivity and are counteracted by Nef. *Nature* 526:218-23
  466. Uyangaa E, Kim JH, Patil AM, Choi JY, Kim SB, Eo SK. 2015. Distinct Upstream Role of Type I IFN Signaling in Hematopoietic Stem Cell-Derived and Epithelial Resident Cells for Concerted Recruitment of Ly-6Chi Monocytes and NK Cells via CCL2-CCL3 Cascade. *PLoS Pathog* 11:e1005256
  467. Uze G, Schreiber G, Piehler J, Pellegrini S. 2007. The receptor of the type I interferon family. *Curr Top Microbiol Immunol* 316:71-95
  468. van Boxel-Dezaire AH, Stark GR. 2007. Cell type-specific signaling in response to interferon-gamma. *Curr Top Microbiol Immunol* 316:119-54
  469. Van Damme N, Goff D, Katsura C, Jorgenson RL, Mitchell R, et al. 2008. The interferon-induced protein BST-2 restricts HIV-1 release and is downregulated from the cell surface by the viral Vpu protein. *Cell Host Microbe* 3:245-52
  470. Verhoef K, Tijms M, Berkhout B. 1997. Optimal Tat-mediated activation of the HIV-1 LTR promoter requires a full-length TAR RNA hairpin. *Nucleic Acids Res* 25:496-502
  471. Vivier E, Tomasello E, Baratin M, Walzer T, Ugolini S. 2008. Functions of natural killer cells. *Nat Immunol* 9:503-10
  472. Volberding PA, Deeks SG. 2010. Antiretroviral therapy and management of HIV infection. *Lancet* 376:49-62
  473. von Appen A, Kosinski J, Sparks L, Ori A, DiGuilio AL, et al. 2015. In situ structural analysis of the human nuclear pore complex. *Nature* 526:140-3
  474. Wack A, Terczynska-Dyla E, Hartmann R. 2015. Guarding the frontiers: the biology of type III interferons. *Nat Immunol* 16:802-9
  475. Wahl MC, Will CL, Luhrmann R. 2009. The spliceosome: design principles of a dynamic RNP machine. *Cell* 136:701-18
  476. Wang ET, Sandberg R, Luo S, Khrebtkova I, Zhang L, et al. 2008. Alternative isoform regulation in human tissue transcriptomes. *Nature* 456:470-6
  477. Wang Y, Xiao X, Zhang J, Choudhury R, Robertson A, et al. 2013. A complex network of factors with overlapping affinities represses splicing through intronic elements. *Nat Struct Mol Biol* 20:36-45
  478. Wang Z, Burge CB. 2008. Splicing regulation: from a parts list of regulatory elements to an integrated splicing code. *RNA* 14:802-13
  479. Wang Z, Hoffmann HM, Grabowski PJ. 1995. Intrinsic U2AF binding is modulated by exon enhancer signals in parallel with changes in splicing activity. *RNA* 1:21-35
  480. Watts JM, Dang KK, Gorelick RJ, Leonard CW, Bess JW, Jr., et al. 2009. Architecture and secondary structure of an entire HIV-1 RNA genome. *Nature* 460:711-6
  481. Wei X, Decker JM, Liu H, Zhang Z, Arani RB, et al. 2002. Emergence of resistant human immunodeficiency virus type 1 in patients receiving fusion inhibitor (T-20) monotherapy. *Antimicrob Agents Chemother* 46:1896-905
  482. Weissmann C, Weber H. 1986. The interferon genes. *Prog Nucleic Acid Res Mol Biol* 33:251-300
  483. Wentz MP, Moore BE, Cloyd MW, Berget SM, Donehower LA. 1997. A naturally arising mutation of a potential silencer of exon splicing in human

- immunodeficiency virus type 1 induces dominant aberrant splicing and arrests virus production. *J Virol* 71:8542-51
484. Wheelock EF. 1965. Interferon-Like Virus-Inhibitor Induced in Human Leukocytes by Phytohemagglutinin. *Science* 149:310-1
485. Widera M, Erkelenz S, Hillebrand F, Krikoni A, Widera D, et al. 2013. An intronic G run within HIV-1 intron 2 is critical for splicing regulation of vif mRNA. *J Virol* 87:2707-20
486. Widera M, Hillebrand F, Erkelenz S, Vasudevan AA, Munk C, Schaal H. 2014. A functional conserved intronic G run in HIV-1 intron 3 is critical to counteract APOBEC3G-mediated host restriction. *Retrovirology* 11:72
487. Widera M, Klein AN, Cinar Y, Funke SA, Willbold D, Schaal H. 2014. The D-amino acid peptide D3 reduces amyloid fibril boosted HIV-1 infectivity. *AIDS Res Ther* 11:1
488. Wilen CB, Tilton JC, Doms RW. 2012. HIV: cell binding and entry. *Cold Spring Harb Perspect Med* 2
489. Wilk T, Gross I, Gowen BE, Rutten T, de Haas F, et al. 2001. Organization of immature human immunodeficiency virus type 1. *J Virol* 75:759-71
490. Wilkinson ME, Charenton C, Nagai K. 2020. RNA Splicing by the Spliceosome. *Annu Rev Biochem* 89:359-88
491. Will CL, Luhrmann R. 2011. Spliceosome structure and function. *Cold Spring Harb Perspect Biol* 3
492. Williams BR. 2001. Signal integration via PKR. *Sci STKE* 2001:re2
493. Windhager L, Bonfert T, Burger K, Ruzsics Z, Krebs S, et al. 2012. Ultrashort and progressive 4sU-tagging reveals key characteristics of RNA processing at nucleotide resolution. *Genome Res* 22:2031-42
494. Wissing S, Galloway NL, Greene WC. 2010. HIV-1 Vif versus the APOBEC3 cytidine deaminases: an intracellular duel between pathogen and host restriction factors. *Mol Aspects Med* 31:383-97
495. Wollerton MC, Gooding C, Wagner EJ, Garcia-Blanco MA, Smith CW. 2004. Autoregulation of polypyrimidine tract binding protein by alternative splicing leading to nonsense-mediated decay. *Mol Cell* 13:91-100
496. Wonderlich ER, Leonard JA, Collins KL. 2011. HIV immune evasion disruption of antigen presentation by the HIV Nef protein. *Adv Virus Res* 80:103-27
497. Wong R, Balachandran A, Mao AY, Dobson W, Gray-Owen S, Cochrane A. 2011. Differential effect of CLK SR Kinases on HIV-1 gene expression: potential novel targets for therapy. *Retrovirology* 8:47
498. Wong RW, Balachandran A, Haaland M, Stoilov P, Cochrane A. 2013. Characterization of novel inhibitors of HIV-1 replication that function via alteration of viral RNA processing and rev function. *Nucleic Acids Res* 41:9471-83
499. Wong RW, Balachandran A, Ostrowski MA, Cochrane A. 2013. Digoxin suppresses HIV-1 replication by altering viral RNA processing. *PLoS Pathog* 9:e1003241
500. Wu JY, Maniatis T. 1993. Specific interactions between proteins implicated in splice site selection and regulated alternative splicing. *Cell* 75:1061-70
501. Wu Y. 2004. HIV-1 gene expression: lessons from provirus and non-integrated DNA. *Retrovirology* 1:13
502. Wu Y, Marsh JW. 2001. Selective transcription and modulation of resting T cell activity by preintegrated HIV DNA. *Science* 293:1503-6

503. Xiao K, McClatchy DB, Shukla AK, Zhao Y, Chen M, et al. 2007. Functional specialization of beta-arrestin interactions revealed by proteomic analysis. *Proc Natl Acad Sci U S A* 104:12011-6
504. Xie X, Rigor P, Baldi P. 2009. MotifMap: a human genome-wide map of candidate regulatory motif sites. *Bioinformatics* 25:167-74
505. Xing L, Wang S, Hu Q, Li J, Zeng Y. 2016. Comparison of three quantification methods for the TZM-bl pseudovirus assay for screening of anti-HIV-1 agents. *J Virol Methods* 233:56-61
506. Yamamoto M, Sato S, Hemmi H, Hoshino K, Kaisho T, et al. 2003. Role of adaptor TRIF in the MyD88-independent toll-like receptor signaling pathway. *Science* 301:640-3
507. Young DJ, Stoddart A, Nakitandwe J, Chen SC, Qian Z, et al. 2014. Knockdown of Hnrnpa0, a del(5q) gene, alters myeloid cell fate in murine cells through regulation of AU-rich transcripts. *Haematologica* 99:1032-40
508. Yun CY, Fu XD. 2000. Conserved SR protein kinase functions in nuclear import and its action is counteracted by arginine methylation in *Saccharomyces cerevisiae*. *J Cell Biol* 150:707-18
509. Zahler AM, Damgaard CK, Kjems J, Caputi M. 2004. SC35 and heterogeneous nuclear ribonucleoprotein A/B proteins bind to a juxtaposed exonic splicing enhancer/exonic splicing silencer element to regulate HIV-1 tat exon 2 splicing. *J Biol Chem* 279:10077-84
510. Zennou V, Perez-Caballero D, Gottlinger H, Bieniasz PD. 2004. APOBEC3G incorporation into human immunodeficiency virus type 1 particles. *J Virol* 78:12058-61
511. Zhang D, Zhang DE. 2011. Interferon-stimulated gene 15 and the protein ISGylation system. *J Interferon Cytokine Res* 31:119-30
512. Zhang Z, Krainer AR. 2004. Involvement of SR proteins in mRNA surveillance. *Mol Cell* 16:597-607
513. Zhao L, Wang S, Xu M, He Y, Zhang X, et al. 2021. Vpr counteracts the restriction of LAPTM5 to promote HIV-1 infection in macrophages. *Nat Commun* 12:3691
514. Zheng ZM. 2004. Regulation of alternative RNA splicing by exon definition and exon sequences in viral and mammalian gene expression. *J Biomed Sci* 11:278-94
515. Zhou H, Xu M, Huang Q, Gates AT, Zhang XD, et al. 2008. Genome-scale RNAi screen for host factors required for HIV replication. *Cell Host Microbe* 4:495-504
516. Zhou Q, Chen D, Pierstorff E, Luo K. 1998. Transcription elongation factor P-TEFb mediates Tat activation of HIV-1 transcription at multiple stages. *EMBO J* 17:3681-91
517. Zhou Z, Fu XD. 2013. Regulation of splicing by SR proteins and SR protein-specific kinases. *Chromosoma* 122:191-207
518. Zhu J, Davoli T, Perriera JM, Chin CR, Gaiha GD, et al. 2014. Comprehensive identification of host modulators of HIV-1 replication using multiple orthologous RNAi reagents. *Cell Rep* 9:752-66
519. Zhu T, Mo H, Wang N, Nam DS, Cao Y, et al. 1993. Genotypic and phenotypic characterization of HIV-1 patients with primary infection. *Science* 261:1179-81
520. Zila V, Margiotta E, Turonova B, Muller TG, Zimmerli CE, et al. 2021. Cone-shaped HIV-1 capsids are transported through intact nuclear pores. *Cell* 184:1032-46 e18

- 
521. Zotova AA, Atemasova AA, Filatov AV, Mazurov DV. 2019. [HIV Restriction Factors and Their Ambiguous Role during Infection]. *Mol Biol (Mosk)* 53:240-55
  522. Zuniga EI, McGavern DB, Pruneda-Paz JL, Teng C, Oldstone MB. 2004. Bone marrow plasmacytoid dendritic cells can differentiate into myeloid dendritic cells upon virus infection. *Nat Immunol* 5:1227-34



---

## 9. Appendix

### 9.1. List of abbreviations

4sU	4-thiouridine
ψ	RNA packaging signal

#### A

AIDS	acquired immunodeficiency syndrome
Akt	protein kinase B (PKB)
APC	antigen-presenting cells
APOBEC3G	apolipoprotein B mRNA editing enzyme 3G
APS	ammonium persulfate
ARE	AU-rich elements
Arg	arginine
ART	antiretroviral therapy
AU	adenylate-uridylate

#### B

BGH	bovine growth hormone
BPS	branch point sequence

#### C

°C	degree Celsius
CA	capsid
CBF-β	core binding factor subunit β
CCL2	CC-chemokine ligand 2
CCR5	C-C chemokine receptor type 5
CD4	cluster of differentiation 4
cDNA	complementary DNA
CDS	coding sequence
cGAS	cyclic GMP-AMP synthase
cGAMP	cyclic GMP-AMP
CLIP-seq	cross-linking immunoprecipitation and high-throughput sequencing

---

Clk1	CDC-like kinase 1
CMV	cytomegalovirus
COX-2	cyclooxygenase-2
cPPT	central polypurine tract
CRM1	Chromosomal Maintenance 1
CRKL	v-crk sarcoma virus CT10 oncogene homolog (avian)-like
CXCR4	C-X-C chemokine receptor type 4

**D**

DC	dendritic cell
DMEM	Dulbecco's Modified Eagle Medium
DNA	deoxyribonucleic acid
dNTPs	deoxynucleotide triphosphates
dsDNA	double-stranded DNA
DTT	dithiothreitol

**E**

eIF2a	transcription initiation factor 2a
EDTA	ethylenediaminetetraacetic acid
eGFP	enhanced green fluorescent protein
ELISA	enzyme-linked immunosorbent assay
Env	envelope glycoprotein
ERK1/2	extracellular-signal regulated kinase 1/2
ESE	exonic splice enhancer
ESS	exonic splice silencer

**F**

FCS	fetal calf serum
fwd	forward

**G**

Gag	Group-specific antigen
GAR	guanosine-adenosine-rich

---

GAS	IFN $\beta$ -activated sites
gp	glycoprotein
GTPase	guanosine triphosphatase
<b>H</b>	
h	hour
HDF	host dependency factor
HIV-1	human immunodeficiency virus type 1
HIV-2	human immunodeficiency virus type 2
hnRNP	heterogeneous nuclear ribonucleoproteins
HRF	host restriction factor

**I**

IFI16	$\gamma$ -IFN inducible protein 16
IFI44	IFN-induced protein 44
IFITM1-3	interferon-induced transmembrane protein 1-3
IFN	interferon
IFNAR	IFN $\alpha$ / $\beta$ receptor
IFNGR	IFN $\gamma$ receptor
IL	interleukin
IMDM	Iscove's Modified Dulbecco's Medium
IN	integrase
IRepG	IFN repressed gene
IRF	IFN regulatory factor
ISE	intronic splice enhancer
ISG	IFN stimulated gene
ISG15	IFN stimulated gene 15
ISGF3	IFN stimulated gene factor 3
ISRE	IFN stimulated response element
ISS	intronic splice silencer

**J**

JAK1	janus kinase 1
------	----------------

**K**

kb	kilobase
kDa	kilodalton
KH	K-homology domain

**L**

L	leucine
LAPTM5	lysosomal-associated transmembrane protein 5
LB	lysogeny broth
LP	lamina propria
LPMCs	lamina propria mononuclear cells
LTR	long terminal repeat

**M**

MAPK	mitogen activated protein kinase
MAPKAP-K2	MAP kinase activated protein kinase 2
MDA-5	melanoma differentiation-associated gene 5
MDMs	monocyte-derived macrophages
min	minute
MIP-2	macrophage inflammatory protein 2
MK-2	mitogen-activated protein kinase 2
MOI	multiplicity of infection
MR	mannose receptor
mRNA	messenger RNA
MX2	myxovirus resistance 2
MyD88	myeloid differentiation primary response 88

**N**

N	purine or pyrimidine
Nef	negative effector
NF- $\kappa$ B	nuclear factor ' $\kappa$ -light-chain-enhancer' of activated B-cells
NGS	next generation sequencing
NK cells	natural killer cells

---

NLR	nucleotide-binding oligomerization domain-like receptor
NLS	nuclear localization signal
nm	nanometer
NMD	nonsense-mediated mRNA decay
NNRTI	non-nucleoside reverse transcriptase inhibitor
NRTI	nucleoside reverse transcriptase inhibitor
nt	nucleotide

**O**

OAS1	2'-5'-oligoadenylate-synthetase 1
ORF	open reading frame

**P**

p	protein
PAA	polyacrylamide
PAMP	pathogen-associated molecular pattern
PBMCs	peripheral blood mononuclear cells
PBS	phosphate buffered saline
PBS	primer binding site
PCR	polymerase chain reaction
pDC	plasmacytoid dendritic cell
PFU	plaque forming units
PI	protease inhibitor
PI3K	phosphoinositide 3-kinase
PIC	pre-integration complex
PKR	protein kinase R
Pol	polymerase
PP1	protein phosphatase 1
PP2a	protein phosphatase 2a
PPT	poly-purine tract
PPT	poly-pyrimidine tract
PR	protease
pre-mRNA	precursor mRNA

---

PRR	pattern recognition receptor
P/S	Penicillin/Streptomycin
P-TEFb	positive transcription elongation factor b
<b>Q</b>	
Q	glutamine
qRRM	quasi RNA recognition motif
<b>R</b>	
R	Repeated or purine
RBP	RNA-binding protein
rcf	relative centrifugal force
rev	reverse
Rev	regulator of expression of virion proteins
RGG	glycine-rich box
RIG-I	retinoic acid-inducible gene I
RLU	relative light units
RNA	ribonucleic acid
RNAPII	RNA polymerase II
RPMI	Roswell Park Memorial Institute 1640 Medium
RRE	Rev-responsive element
RRM	RNA recognition motif
RRMH	RRM homology domain
RS	arginine/serine-rich domain
RT	reverse transcriptase
RT-PCR	semi-quantitative PCR analysis
RT-qPCR	quantitative real-time PCR analysis
<b>S</b>	
SA	splice acceptor
SAMHD1	sterile $\alpha$ -motif and histidine aspartate domain-containing protein 1
SD	splice donor
SD	standard deviation

---

SDS	sodium dodecyl sulfate
SELEX	selected evolution of ligands through exponential enrichment
SEM	standard error of the mean
Ser	serine
SERINC3	serine incorporator 3
SERINC5	serine incorporator 5
SIN3A	SIN3 transcription regulator homologue A
siRNA	small interfering RNA
SIV	simian immunodeficiency virus
SLFN11	Schlafen 11
SRE	splicing regulatory element
SRPK	SR specific protein kinases
SRSF	serine/arginine-rich splicing factors
s	second
ss	splice site
ssRNA	single-stranded RNA
STAT	signal transducer and activator of transcription
STING	stimulator of IFN genes

**T**

TAR	trans-activation response element
Tat	trans-activator of transcription
TBS	tris-buffered saline
TBS-T	TBS with Tween-20
TCE	2,2,2-trichloroethanol
TCID <sub>50</sub>	tissue culture infectious dose 50
TEMED	tetramethylethylenediamine
TFV	transmitted founder virus
Th1	T-helper cell type 1
TLR	toll like receptor
TNF- $\alpha$	tumor necrosis factor $\alpha$
TPA	12- O-tetradecaoylphorbol-13-acetate
TPM	transcript per million

---

Tra2	transformer 2 protein
TRIF	TIR-domain-containing adapter-inducing IFN $\beta$
TRIM5 $\alpha$	tripartite motif-containing protein 5 $\alpha$
TRIM22	tripartite motif-containing 22
tRNA	transfer RNA
TYK2	tyrosine kinase 2

**U**

U1 snRNP	U1 small nuclear ribonucleoprotein
U2AF65	U2 auxiliary factor 65 kDa subunit
U2 snRNP	U2 small nuclear ribonucleoprotein
U3	Unique 3
U5	Unique 5

**V**

V3 loop	variable loop 3
Vif	viral infectivity factor
Vpr	viral protein R
Vpu	viral protein U
Vpx	viral protein X

**W**

wt	wild type
----	-----------

**Y**

Y	pyrimidine
---	------------

**Z**

Zn	Zinc knuckle
----	--------------



## 9.2. List of figures

Figure 1-1	Structure of a mature HIV-1 particle.....	2
Figure 1-2	Illustration of the HIV-1 genomic structure.....	3
Figure 1-3	Schematic and simplified drawing of the HIV-1 replication cycle.....	5
Figure 1-4	Schematic representation of the HIV-1 mRNA classes.....	7
Figure 1-5	Schematic representation of splice site recognition and alternatively spliced transcripts.....	9
Figure 1-6	Splicing regulatory elements (SREs) regulate cellular and viral splice site usage.....	11
Figure 1-7	Structural organization of the SRSF proteins.....	12
Figure 1-8	Structural organization of the hnRNP proteins.....	16
Figure 1-9	Type I IFN signaling pathway.....	22
Figure 1-10	Type II IFN signaling pathway.....	24
Figure 1-11	IFN-induced HIV-1 restriction factors.....	27
Figure 3-1	Differentiation of THP-1 monocytic cells.....	44
Figure 3-2	Expression vector pcDNA3.1-hnRNP A0.....	55
Figure 4-1	Gene expression levels of <i>SRSFs</i> in treatment naïve or ART-treated HIV-1 infected individuals.....	65
Figure 4-2	<i>SRSF1</i> and <i>ISG15</i> expression levels inversely correlate upon HIV-1 infection.....	67
Figure 4-3	<i>SRSF1</i> expression upon stimulation with IFN $\alpha$ subtypes.....	70
Figure 4-4	<i>SRSF1</i> mRNA levels are differentially regulated upon stimulation of HIV-1 target cells with IFN $\alpha$ 2 or IFN $\alpha$ 14.....	73
Figure 4-5	<i>SRSF1</i> mRNA and protein levels are differentially regulated upon treatment of macrophages with IFNs.....	75
Figure 4-6	IFN $\alpha$ 14-mediated changes in newly transcribed <i>SRSF1</i> mRNA.....	77
Figure 4-7	siRNA-mediated knockdown of <i>SRSF1</i> affects HIV-1 LTR transcription and splice site usage.....	79
Figure 4-8	Impact of siRNA-based knockdown of <i>SRSF1</i> on HIV-1 infectivity and virus production.....	83
Figure 4-9	Overexpression of <i>SRSF1</i> affects HIV-1 LTR transcription and splice site usage.....	85

---

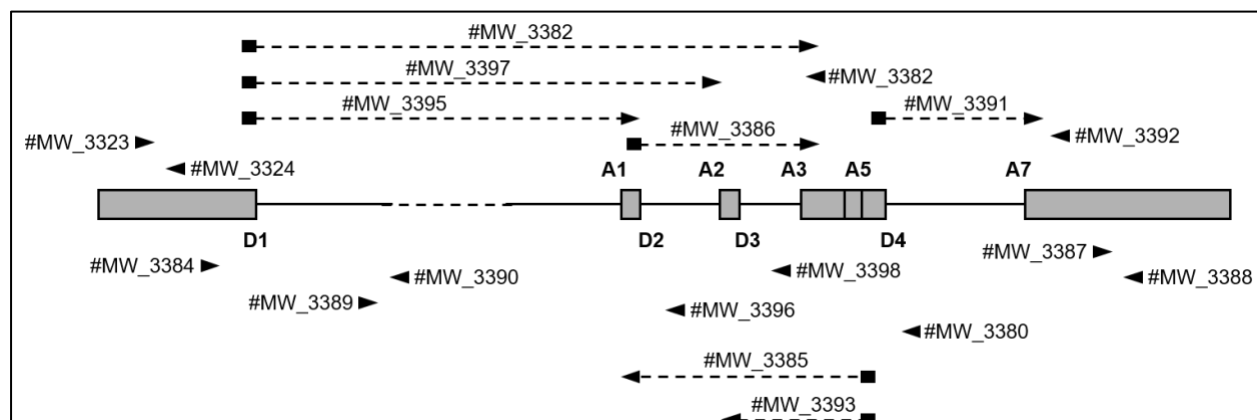
Figure 4-10	Overexpression of SRSF1 affects HIV-1 infectivity and viral particle production.....	88
Figure 4-11	HIV-1 affects IFN-mediated regulation of <i>SRSF1</i> .....	91
Figure 4-12	Gene expression levels of <i>hnRNP</i> in treatment naïve or ART-treated HIV-1 infected individuals.....	93
Figure 4-13	Selected <i>hnRNP</i> mRNA expression levels upon stimulation with IFN $\alpha$ 2 or IFN $\alpha$ 14 in THP-1 cells.....	95
Figure 4-14	<i>hnRNP A0</i> and <i>ISG15</i> mRNA levels inversely correlate upon HIV-1 infection .....	96
Figure 4-15	<i>hnRNP A0</i> mRNA expression levels are differentially regulated upon stimulation of HIV-1 target cells with IFN $\alpha$ 2 or IFN $\alpha$ 14 .....	99
Figure 4-16	<i>hnRNP A0</i> mRNA expression levels upon stimulation of HIV-1 target cells with type I and II IFNs .....	101
Figure 4-17	IFN $\alpha$ 14-mediated changes in newly transcribed <i>hnRNP A0</i> mRNA. ....	103
Figure 4-18	siRNA-mediated knockdown of <i>hnRNP A0</i> affects HIV-1 LTR transcription and splice site usage .....	105
Figure 4-19	Impact of siRNA-based knockdown of <i>hnRNP A0</i> on HIV-1 infectivity and virus production.....	108
Figure 4-20	Overexpression of <i>hnRNP A0</i> affects HIV-1 LTR transcription and splice site usage.....	110
Figure 4-21	Effect of <i>hnRNP A0</i> overexpression on HIV-1 infectivity and viral particle production.....	113
Figure 4-22	HIV-1 affects IFN-mediated regulation of <i>hnRNP A0</i> .....	115
Figure 5-1	Positions and sequences of SRSF1-bound SREs within the genome of HIV-1 (NL4-3).....	128
Figure 5-2	SREs involved in the regulation of exon 2/2b and exon 3 splicing.....	130
Figure 5-3	Positions and sequences of <i>hnRNP A/B</i> -bound SREs within the genome of HIV-1 (NL4-3).....	135

---

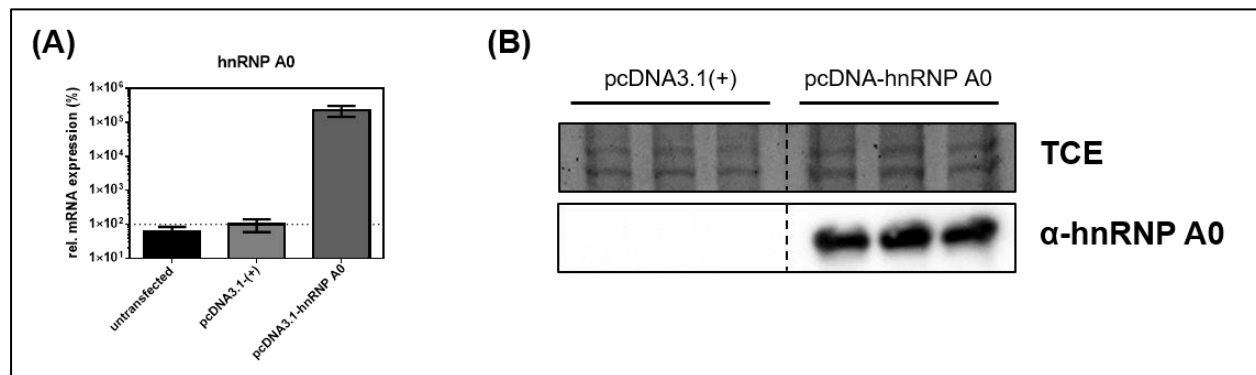
### 9.3. List of tables

Table 2-1	Chemicals and reagents .....	30
Table 2-2	Commercially available kits .....	33
Table 2-3	Cell lines.....	33
Table 2-4	Oligonucleotides used for cloning, RT-qPCR and RT-PCR .....	34
Table 2-5	Plasmids used for transfection or cloning .....	35
Table 2-6	Antibodies used for Western Blot or ELISA .....	37
Table 2-7	Enzymes used for restriction digest, DNA digest, RT-PCR, RT or ligation... .....	37
Table 2-8	Buffers and solution .....	38
Table 2-9	Material.....	40
Table 2-10	Instruments.....	41
Table 2-11	Software .....	42
Table 3-1	Recipe for one 12 % polyacrylamide (PAA) gel used for DNA separation ... .....	48
Table 3-2	Recipe for four 12 % SDS-polyacrylamide gels used for protein separation .....	50

## 9.4. Supplementary Figures



**Supplementary Figure 1: Schematic representation of the primer positions on the viral pre-mRNA.** HIV-1 exons are depicted as grey boxes, while introns are depicted as straight lines. Splice donor (SD) and splice acceptor (SA) positions are indicated. Positions of the respective primers used for RT-PCR and RT-qPCR are shown as arrowheads. Exon-junction primers are indicated via dashed lines connecting arrowhead and rectangle.



**Supplementary Figure 2: Validation of pcDNA-hnRNP A0 expression vector.** HEK293T cells were transiently transfected with pcDNA-hnRNP A0 or pcDNA3.1(+) as mock control. 24 h post transfection, RNA or proteins were isolated. (A) RT-qPCR was performed to determine mRNA expression levels of *hnRNP A0*. (B) Western Blot analysis was performed to verify protein expression of *hnRNP A0*. TCE staining was used for protein normalization. Western Blot analysis was performed by Fabian Roesmann (Institute for Medical Virology, University Hospital Frankfurt, Frankfurt am Main).

## 9.5. Acknowledgements

An dieser Stelle möchte ich mich zuerst bei Ulf und Marek für die Möglichkeit bedanken, an diesem spannenden Projekt zu arbeiten und am Institut für Virologie zu promovieren. Vielen Dank für eure stetige Unterstützung und die Vielzahl an wissenschaftlichen Anregungen. Insbesondere geht mein Dank an Marek, für die vielen Denkanregungen und Hilfestellungen, aber auch für den gewährten wissenschaftlichen und experimentellen Freiraum.

Ein herzlicher Dank geht auch an Kathrin für die vielen nützlichen Ratschläge und die stetige Unterstützung. Danke für dein immer offenes Ohr!

Ein besonderer Dank geht an Carina und an Barbara, die den Laboralltag angenehm gestaltet haben, viele praktische Tipps parat hatten und mich auch in stressigen Zeiten immer unterstützt haben.

Mein Dank gilt ebenfalls der Jürgen-Manchot Stiftung sowie der Medizinischen Fakultät der Universität Duisburg-Essen für das jeweilige Gewähren eines Stipendiums, ohne welche die Ausführung dieser Doktorarbeit nicht möglich gewesen wäre.

Des Weiteren möchte ich Prof. Mirko Trilling und Prof. Sandra Ciesek danken für die konstruktiven Gespräche und anregenden wissenschaftlichen Diskussionen.

Ein Dank geht auch an Prof. Mario Santiago für die konstruktive Zusammenarbeit, sowie an Fabian für die Unterstützung bei einigen experimentellen Ausführungen.

Vielen Dank auch an meine Freunde und an meine Familie, die immer zur Stelle waren und mich zu jeder Zeit unterstützt haben. Besonders hervorheben möchte ich meine Eltern, ohne deren bedingungsloser Rückhalt diese Arbeit nicht möglich gewesen wäre. Ein großer Dank geht auch an Mandy für die vielen Aufmunterungen und das Erleichtern des Alltags neben der Arbeit.

## **9.6. Curriculum Vitae**

Der Lebenslauf ist aus datenschutzrechtlichen Gründen nicht in der Online-Version enthalten.

## **9.6. Curriculum Vitae**

Der Lebenslauf ist aus datenschutzrechtlichen Gründen nicht in der Online-Version enthalten.



## 9.7. Declarations

Erklärung:

Hiermit erkläre ich, gem. § 6 Abs. (2) g) der Promotionsordnung der Fakultät für Biologie zur Erlangung des Dr. rer. nat., dass ich das Arbeitsgebiet, dem das Thema „Durch Interferone hervorgerufene Änderung des zellulären Spleißapparates und der Einfluss auf die Replikation von HIV-1“ zuzuordnen ist, in Forschung und Lehre vertrete und den Antrag von Helene Sertznig befürworte und die Betreuung auch im Falle eines Weggangs, wenn nicht wichtige Gründe dem entgegenstehen, weiterführen werde.

Essen, den \_\_\_\_\_  
Ulf Dittmer

Erklärung:

Hiermit erkläre ich, gem. § 7 Abs. (2) d) + f) der Promotionsordnung der Fakultät für Biologie zur Erlangung des Dr. rer. nat., dass ich die vorliegende Dissertation selbstständig verfasst und mich keiner anderen als der angegebenen Hilfsmittel bedient, bei der Abfassung der Dissertation nur die angegebenen Hilfsmittel benutzt und alle wörtlich oder inhaltlich übernommenen Stellen als solche gekennzeichnet habe.

Essen, den \_\_\_\_\_  
Helene Sertznig

Erklärung:

Hiermit erkläre ich, gem. § 7 Abs. (2) e) + g) der Promotionsordnung der Fakultät für Biologie zur Erlangung des Dr. rer. nat., dass ich keine anderen Promotionen bzw. Promotionsversuche in der Vergangenheit durchgeführt habe und dass diese Arbeit von keiner anderen Fakultät/Fachbereich abgelehnt worden ist.

Essen, den \_\_\_\_\_  
Helene Sertznig